HEAT PUMP DRYERS

Theory, Design and Industrial Applications

HEAT PUMP DRYERS

Theory, Design and Industrial Applications

Odilio Alves-Filho

CRC Press
Taylor & Francis Group
Boca Raton London New York

CRC Press is an imprint of the
Taylor & Francis Group, an **informa** business

CRC Press
Taylor & Francis Group
6000 Broken Sound Parkway NW, Suite 300
Boca Raton, FL 33487-2742

Version Date: 20150708

International Standard Book Number-13: 978-1-4987-1134-0 (eBook - PDF)

Contents

Preface

Although classical refrigeration and heat pumps have been around for several decades, the research and development of modern heat pump drying technology has only recently advanced from pilot to industrial applications.

The novel heat pump drying technology has social–technological impact and cost-efficiency advantages compared to conventional drying. The worldwide trend and progress in computerised data acquisition systems, electromechanics and controlling devices are all contributing to further improvements and creating new topics for research in heat pump drying. Allied to this progress, advances in new metals and materials allow for building lighter, stronger and more compact heat pump drying systems.

The future is for heat pump dryers operating with natural fluids because this technology is in full harmony with the Kyoto and Montreal protocols. Favourably, after careful design and extensive tests at the Norwegian University of Science and Technology, Trondheim, Norway, the heat pump dryers were scaled up from bench to pilot plants. After industrial plant refinements, this technology effectively reached commercial applications. These steps entail process sustainability and techno-economic problems that are solved only after extensive experimentation with the products of commercial interest and processes operating with environment-friendly fluids. These steps are followed by optimisation of drying operating conditions for high product quality, low-energy use and viable cost.

The literature in drying is scattered with separate coverage of drying fundamentals, design, experiments, modelling and simulations. Also, no account is available explaining the drying-dependent and -independent variables' intricate relationships or how theory, design and experiments form the basis for acceptable scaling up, refining the operation of pilot and full industrial plants. There is no comprehensive reference on heat pump dryer design for a given product considering the process conditions, refrigerant and moist air properties as well as the relationship to energy demand, climate change and environmental impact.

Heat pump drying allows processing heat-sensitive materials and manufacturing high quality dried products at competitive cost. Also, it operates in atmospheric freeze drying and evaporative drying modes for processing materials that are difficult to handle in conventional dryers. It allows manufacturing dried products with similar quality but at lower cost than those produced by conventional dryers.

This book covers in a single volume the underlying essentials and theory required for design and application of heat pump dryers. It includes comprehensive layout of heat pump dryers for diverse applications and products with enhanced market value. The equations, diagrams and procedures are explained for building up the basis for heat pump dryer design and dimensioning. Considering the operating conditions, refrigerant, moist air and product properties, heat pump dryers and conventional dryers are compared in terms of performance, removal rate and energy utilisation. The solutions to the techno-economics issues are approached by establishing the drying conditions for enhanced product properties.

This book explores the suitable paths and steps for process–product decision making based on measurable coefficients of performance, thermal efficiency and specific moisture extraction ratio of the heat pump dryer. It provides detailed descriptions of heat pump dryers operating with natural fluids with benefits in components with reduced size,

climate stability and low environmental impact. Several arrangements of heat pump dryers are illustrated and problems are solved for cases ranging from bench scale to pilot and industrial plants.

Thus, heat pump drying is among the best currently available green technologies for superior-quality products while fully complying with the energy, quality and environmental concerns. It has advanced from pioneering research and demonstration work to an applied technology that progresses toward a greater applicability by modern industries.

The shared faith in the present and future potential of this technology inspired me to write this book, and I hope that it will be useful for readers in the years to come.

Odilio Alves-Filho
Trondheim, Norway

Acknowledgements

I am glad to acknowledge the relevant R&D conditions provided by the Center of Excellence in Dewatering at the Department of Energy and Process Engineering, where my experiments have been conducted as well as my colleagues working in the field of heat pump drying technology.

I express my appreciation to the Faculty of Engineering Science and Technology, Norwegian University of Science and Technology, Trondheim, Norway, which is involved with green drying technologies. It provided an inspiring environment and excellent research facilities that enabled me to make this publication a reality.

I thank my wife, Dr. Svetlana Alves, for her constructive thoughts, encouragement, and motivation during my long working hours writing this book.

Nomenclature

a	constant	
AZB	azeotropic blend	
b	constant	
CIP	cleaning in place system	
COP	coefficient of performance	
c_p	specific heat at constant pressure	kJ/kg·K
c_v	specific heat at constant volume	kJ/kg·K
D	effective mass diffusivity	m^2/s
d	diameter	m
DOD	detectable odour	
dW	differential work	kJ
e	the base of natural logarithms equals 2.71828…	
E_e	evaporation specific energy	kJ/kg
FER	fire and explosion risks	
GHG	greenhouse gas	
GWP	global warming potential	
h	convective heat transfer coefficient	$W/m^2·K$
h	specific enthalpy	kJ/kg
HCFC	hydrochlorofluorocarbon	
HFC	hydrofluorocarbon	
J	mass flux	$kg/m^2·s$
K	correlation slope	
M	molecular mass (weight)	kg/kmol
m	mass	kg
$\dot{m}$	mass flow rate	kg/s
$\dot{m}_W$	water removal rate	kg/s
n_h	number of hours	h/day, h/yr
ODP	ozone depletion potential	
p	pressure	Pa, bar
p_r	pressure ratio	
Q_H	condensing capacity	kW
q_H	specific condensing capacity	kJ/kg
Q_L	cooling capacity	kW
q_L	specific evaporating capacity	kJ/kg
R	universal gas constant equal to 8.31441	kJ/mol·K
r	mass recirculation ratio	
r	mass ratio	kg/kg
r	mixing ratio	kg/kg
r	percent change	%
r	radius	m
R_{me}	ratio of moisture removal to energy	kg/kJ
s	specific entropy	kJ/kg·K
SAG	safety class-group	
S_{ec}	specific energy consumption	kJ/kg

SIN	single substance	
SMER	specific moisture extraction ratio	kg/KWh
SUR	suffocation risk	
T	absolute temperature	K
t	temperature	°C
TXR	toxicity risk	
u	specific internal energy	kJ/kg
u	velocity	m/s
V	total volume of mixture	m^3
$\dot{V}$	volumetric flow rate	m^3/s
v	specific volume	m^3/kg
VCE	volumetric cooling effect	kJ/m^3
W	compressor shaft work	kW
w	specific work	kJ/kg
X	moisture content	%wb, %db
x	absolute humidity	kg/kg
ZEB	zeotropic blend	

Greek letters

Δ	difference	
$\Delta h/\Delta X$	slope of the line of enthalpy versus absolute humidity	kJ/kg
$\Delta h/\Delta X$	ratio of enthalpy to absolute humidity difference	kJ/kg
ε_D	dryer effectiveness	kg/kWh
η_i	isentropic efficiency	
η_t	dryer thermal efficiency	
ϕ	relative humidity	%, decimal
λ	volumetric efficiency	
μ	absolute or dynamic viscosity	Pa·s
μ	degree of saturation	
ν	kinematic viscosity	m^2/s
ρ	density	kg/m^3
τ	time	s

Superscript

*	at equilibrium, at wet-bulb temperature

Subscripts

0	initial, reference, state points and properties at 0°C
a	air
b	blower
bub	refrigerant bubble point
c	condenser, compression, critical point
con	condensing
db	moist air dry-bulb, dry-weight basis
dew	refrigerant dew point
dm	dry-matter
dp	moist air dew point
ev	evaporating, even

gc	gas cooler
H	high, condenser
L	low, evaporator
i	isentropic, intermediate
in	inlet
int	intermediate
m	mixture of moist air
ma	mixture of exhaust and ambient air
mol	molar
od	odd
out	outlet
p	dried product
r	refrigerant
sat	saturation
sc	subcooled
sh	superheated
t	total
tr	trolley
v	water vapour
w	water
wb	moist air wet-bulb, wet-weight basis

Author

Prof. Odilio Alves-Filho earned his master and PhD degrees in mechanical engineering from the University of California, Davis, and the Norwegian University of Science and Technology, Trondheim, Norway, where he is a professor and chair for the advanced PhD course in heat and mass transport in porous media. He is a former dean of the Faculty of Mechanical-Electrical Engineering, head of the Center of Excellence in Dewatering and CEO of Innovative Drying Technology, Trondheim, Norway. He has developed the Ramalho and Alves-Filho Model, which is applied for the systematic analysis, evaluation and formulation of instructional objectives in engineering teaching and learning. His efforts have stretched the known borders of R&D in the field of engineered learning, besides contributing to the design of modern drying processes for a sustainable society. Prof. Odilio Alves-Filho has received more than 10 awards in R&D innovation and engineering from recognized institutions in Europe, Asia and the Americas, including 'Excellence in Drying of 2000' in the Netherlands and 'Distinguished Professor Award of 2011' in Russia. He has authored around 300 journal and conference articles, several book chapters and two books, has edited ten academic proceedings and holds 16 patents on new drying systems that are applied to industry with the vision to enhance the product–process quality, to benefit the environment and to save energy. Prof. Alves-Filho is a co-founder of the successful Nordic Drying Conference series in 2001 and is credited with expanding it to Nordic Baltic Drying Conference series in 2015.

1

Conventional and Heat Pump Drying: Benefits and Drawbacks

Conventional drying is a common process, which has benefits, limitations and drawbacks. The key problems that recently appeared in conventional dryers can be solved using heat pump dryers. This chapter compares conventional and heat pump drying. It describes the product quality, energy and environmental aspects of both drying processes as well as the principles of operation of heat pump dryers.

1.1 Classification of Conventional Dryers

Conventional dryers applied in the manufacturing of dried products consume a large amount of energy. The energy use is related to the mechanism governing mass and heat transfer between the drying medium and the wet material (Keey 1972). This energy use depends on the type of conventional dryer, classified as shown in Figure 1.1 (Alves-Filho and Mujumdar 2002). The vacuum freeze and rotary dryers are classified as contact or conductive types, whereas the spray, tunnel, band and fluidised bed dryers are classified as convective dryers. Radiation is often the governing mechanism of heat transport in other types of dryers. The most common conventional dryers operate either at high temperatures or very low temperatures under vacuum pressure. These dryers have both advantages and drawbacks. For example, the high temperature and short time dryer is useful for specific materials, but there is a limitation with regard to converting thermally sensitive materials into high-quality dried products. Conversely, the long time and low temperature vacuum freeze dryer applies for heat-sensitive materials into high-quality, but comes with high production costs. The ranges of energy utilisation by common types of commercial dryers are presented in Table 1.1 (Alves-Filho and Mujumdar 2002).

The specific moisture extraction ratio (SMER) indicates the energy utilisation by a dryer. SMER is defined as the mass of water removed per unit of energy consumed in the drying process, as given in Table 1.1. Conventional dryers have SMERs ranging between 0.1 and 0.7, indicating a low thermal efficiency. Therefore, the challenge is to design dryers that are thermally efficient aiming to reduce energy.

1.2 Energy Aspects in Conventional Drying

Drying is a highly intensive energy process, and it is essential to understand the aspects of energy development because the energy cost directly affects the cost of the dried product (Mujumdar 2007). Energy cost is dependent on the current price of fossil fuels. These fuels

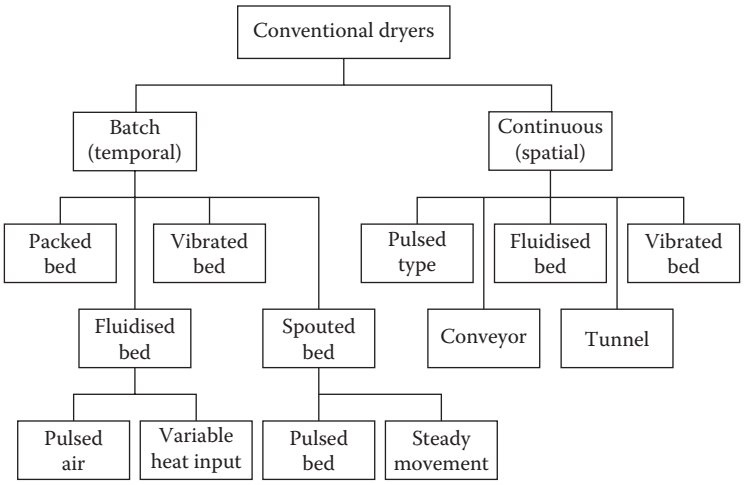

FIGURE 1.1
Classification of conventional dryers. (From Alves-Filho, O. and Mujumdar, A.S. 2002, *Proceedings of the 1st International Conference "Energy-Saving Technologies for Drying and Hygrothermal Processing,"* Moscow, Russia, 28–30 May, Vol. 1, pp. 36–51.)

TABLE 1.1

Main Types of Commercial Dryers with Energy Utilisation and SMER

Conventional Dryers	Minimum Energy, kJ/kg	Maximum Energy, kJ/kg	Average SMER, kg/kWh
Vacuum freeze	45,000	115,000	0.08
Rotary	4600	9200	0.52
Spray	4500	11,500	0.45
Tunnel	5500	6000	0.63
Band	4000	6000	0.72
Fluidised bed	4000	6000	0.72

Source: Alves-Filho, O. and Mujumdar, A.S. (2002), *Proceedings of the 1st International Conference "Energy-Saving Technologies for Drying and Hygrothermal Processing,"* Moscow, Russia, 28–30 May, Vol. 1, pp. 36–51.

(e.g., oil, diesel and charcoal) are the sources to generate steam in thermal power plants. The development of this sector increases the demand for fossil fuels and contributes to increased release of large amounts of greenhouse gases (GHGs) into the atmosphere.

Fossil fuel has been the prime mover for industrialisation and transportation, but the world's oil production has reached a limit. The price of oil and its derivatives fluctuates, with an upward trend. The consumption of fossil fuel has increased in the recent past and is expected to increase in the future, as indicated in Figure 1.2 (IEA 2013).

The fluctuation in oil price depends on many factors and greatly affects the processing industry. The rate of economic growth is, among other variables, a function of real gross domestic product (GDP) and aggregate demand, which depends on multiple factors related to supply and demand. The oil price, GDP and this aggregate are interrelated and have an effect on consumption, export, investment, expenditure, inflation, interest and exchange rate as also investor–consumer confidence, wages and jobs. Thus, there are effects on the processing industry, banking, construction and similar sectors. The GDP and aggregate demand quickly respond to the changes in oil and energy prices, with a simultaneous rise and drop of positive (demand–supply) and negative factors (e.g., inflation), respectively.

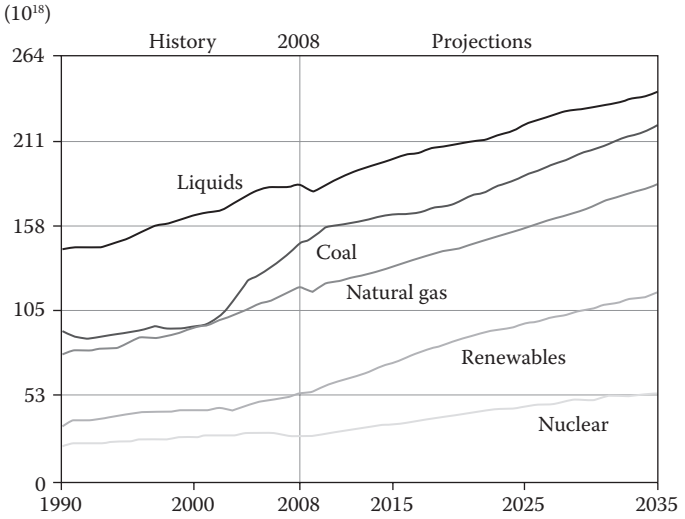

FIGURE 1.2
Fossil fuel consumption in the past and in the future. (Based on IEA. 2013, *Energy Efficiency*, Market Report, IEA, Paris.)

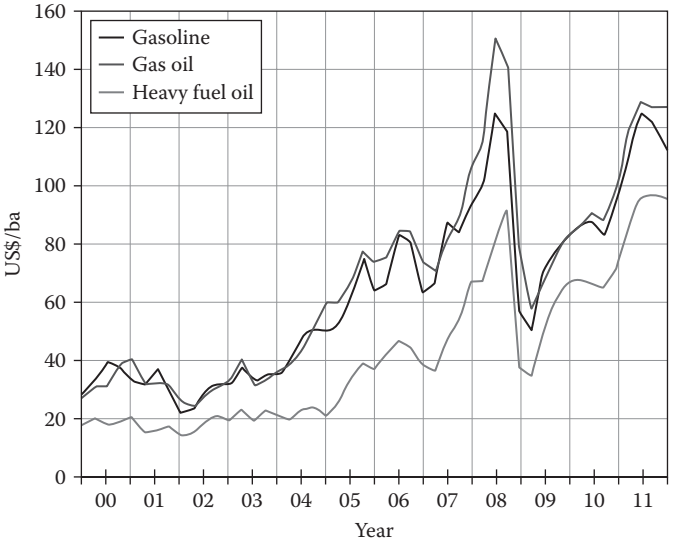

FIGURE 1.3
Oil prices from 2000 to 2011, showing a peak collapse in 2008. (Based on IEA. 2013, *Energy Efficiency*, Market Report, IEA, Paris.)

In 2000, with the average price of oil below US$30 per barrel, there was little to no concern about the impact of price of oil on the product cost. As indicated in Figure 1.3 (IEA 2013), an illustrative event occurred in 2008 when the oil price increased to US$147 per barrel, causing a crisis felt worldwide. This increase produced a series of undesired peaks and cliffs as shown in Figure 1.4 (IEA 2013). An immediate consequence was the drop in demand for

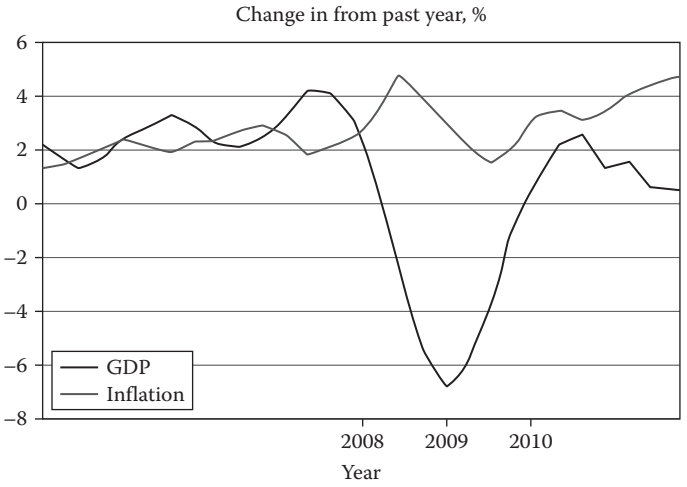

FIGURE 1.4
Economic decline, GDP cliff and inflation peak overlapping with oil price in 2008–2010. (Modified from IEA. 2013, *Energy Efficiency*, Market Report, IEA, Paris.)

dried products because consumers were unable to buy these products. Furthermore, there was a depressive resonance in the processing industries and many failed to deliver dried products at previous contract prices and ran into losses; others barely survived and are still unstable to sustain or are suffering from that impact.

Currently, the process of drying consumes up to 50% of the total energy in the industrial sector. Therefore, considering the past and future trends of energy cost and availability, the success of the drying industry depends on the design of improved and efficient processes that are capable of reducing energy consumption while manufacturing superior quality dried products at competitive costs.

1.3 Environment and Climate Aspects Related to Drying

Conventional dryers consume large amounts of energy and have an equivalent contribution to GHG emission into the atmosphere. Another significant contributor to GHG emission is the artificially produced chemical refrigerants and foam-blowing agents.

The living space of our planet is confined to the gaseous envelope in the atmosphere, the hydrosphere and the crust. The temperature and related conditions in this living space depend on two delicate net balances. The first balance is based on the energy received from the sun's radiation and the energy rejected as infrared radiation in longer wavelengths. A disturbance of this net energy balance causes an increasing warming of the biosphere as a result of gases blocking the rejection of infrared radiation to outer space. These gases, known as GHGs, include carbon dioxide, chlorofluorocarbons (CFCs), hydrochlorofluorocarbons (HCFCs), hydrofluorocarbons (HFCs), hydrocarbons, methane, nitrous oxide and others.

The second balance is the net mass balance of oxygen and carbon dioxide as GHGs. This mass balance is engaged by the sun's radiation, the plants covering nearly all greenish

crust still untouched by humans and the GHGs emitted by natural and artificial processes. The synopsis of this principle is that the sun's photons successfully penetrate the atmosphere and strike forests and green leaves of plants, triggering photosynthesis, which combines carbon dioxide with water to produce carbohydrates (e.g., sugars, cellulose) and oxygen (a by-product). This principle of photosynthesis must be sustained because it removes GHGs and manufactures substances essential for life and respiration. It produces the building blocks of the trees and the plants, which form the base of the food chain, thereby supplying nourishment to herbivores, which subsequently are consumed by carnivores, including humans.

Furthermore, this photon–leaf release of oxygen and capture of carbon dioxide maintains a balanced and tolerable concentration of GHGs and oxygen for a life-supporting biosphere.

This photosynthetic phenomenon is in equilibrium with the carbon dioxide released by natural processes, including, for example, cellulose decomposition and volcanism. Thus, any disturbance of the net oxygen–GHG mass balance results in an overheating of the biosphere and many appalling effects in the hydrological and carbon dioxide–air cycles. However, GHGs are still being produced and released in increased concentrations, mainly by energy-dependent industries; direct combustion users; transport and agriculture sectors; and wastes, chemicals, and solvents processing plants.

Although the photon–leaf mass balance is still a colossal phenomenon, it may eventually be unable to cope with the ever-increasing carbon dioxide concentration in the living space.

The most extensive initiative to reduce the GHG emission is occurring in Europe through proposals and incentives. However, the set targets are difficult to reach due to the varying resources and priorities of the countries involved. The progress of the GHG reduction initiative looks promising in Scandinavia, but the achievement reached varies across countries. Of course, if all nations are considered, the target problems are magnified and an overall reduction of GHG emission is unreachable.

The estimated artificial emission of GHGs in 2011 was about 33.4 Gt, a quantity that is difficult to grasp. A familiar geometrical shape should give a better sense of the magnitude involved. Imagine an equivalent carbon dioxide sphere with a density of 1.98 kg/m^3. This results in an emission equivalent of a carbon dioxide satellite-like sphere with a 32-km diameter.

Note that gradually smaller spheres have been emitted in the near past, and if the current negative target outcome remains, progressively larger satellite-like spheres will be emitted in the future. This statement is reinforced by the estimated 50-Gt GHGs emission for 2050 when nearly 100 of these satellite-like spheres would occupy the stratosphere and disrupt our planet's thermal and hydrological cycles as well as life on Earth.

Another consideration is the effect of chemical substance degradation on the living space stratosphere. The indicator is the ozone depletion potential (ODP).

The early twentieth century conception of the CFCs and HCFCs contributed to the widespread use of commercial refrigeration and aerosol agents. However, no concern existed on the long-term effect of these chlorinated substances on the environment, health and safety. Although they were considered initially safe, these fluids were reported to cause accidents in low-level spaces, such as the machinery room in ships, because the gaseous forms of these substances are colourless and odourless, and these denser gases displace breathable air in confined spaces.

The most striking observations made at the end of the past century, indicated that the highly stable chlorine molecule in CFCs and HCFCs causes severe damage to the stratospheric ozone layer.

As a consequence of the Montreal Protocol, these refrigerants were phased out and replaced by HFCs that have zero ODP and global warming potential (GWP).

The Kyoto Protocol laid out the next set of protection rules, which dealt with GHG emissions and their outcome on climate change. The protocol demands reduction of GHGs and the GWP, which has become an essential parameter in the selection of refrigerants. Therefore, HFCs are to be reduced gradually by replacement, low charge, containment, recycling, and destruction of the fluid at the end of life of the equipment. This also implies that HFCs will eventually be phased out. Therefore, the natural structure involved in energy and mass net balances must be preserved by selecting the most appropriate refrigerants and heat pump fluids with near zero GWP and zero ODP.

Heat pump drying can be designed to operate with natural fluids, resulting in a significant drop in GHG emissions. In particular, when electricity is generated in fossil-fuelled thermal power plants, the heat pump technology provides a reduction in energy consumption, with an equivalent drop in GHG emissions. Furthermore, the heat pump dryers operate in closed cycles both in the refrigerant and drying air loops. This means that it is a green technology without ambient pollution by emission of fine particles or thermal pollution by hot exhaust air.

1.4 Benefits and Principle of Operation of Heat Pump Drying

As mentioned in Sections 1.1 and 1.2, conventional dryers have problems and limitations, such as a low-quality dried product, negative environmental impact and high-energy consumption, which results in high product costs. A proposed solution to these problems is to apply heat pump drying because it is a ready-to-use technology. It operates well at medium-to-low temperatures (below the material's initial freezing point) as well as in high-temperature applications for preheating. It can also combine low and medium temperatures in one heat pump dryer, with the aim of saving energy while producing superior-quality products (Alves-Filho et al. 2003).

Figure 1.5 shows the range of operating pressures and temperatures in heat pumps and conventional dryers. A properly designed heat pump dryer uses only a fraction of the energy required by conventional dryers. It is several orders of magnitude more energy efficient and less expensive than conventional dryers (Table 1.2).

Table 1.2 shows that adiabatic and polytropic heat pump dryers have SMERs similar to or slightly higher than those of superheated steam dryers. Let me now describe what a heat pump dryer is and how it operates. This drying technology is designed to operate at atmospheric pressure, in single or multiple stages, in batch or continuous modes, with a moving or fluidised bed for further enhancement of energy use and water removal rate. It can also operate in a stationary bed with lower rates.

The heat pump dryer recovers heat from the drying exhaust vapour that is lost in open conventional dryers. A properly designed heat pump dryer has a closed loop and fully recovers energy that is distributed for both the heating and cooling required in a drying process. The refrigerant flows through the evaporator where it absorbs latent heat from the exhaust vapour and recycles it through the condenser (Lock 1996). In a similar way, valuable volatiles can be recovered and harmful condensable vapours can be separated and discarded.

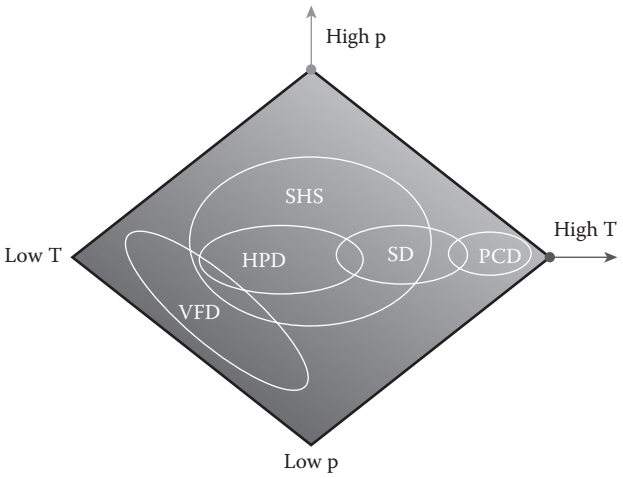

FIGURE 1.5
Range of operating pressures and temperatures in heat pump and conventional dryers.

TABLE 1.2

Energy Utilisation by Main Conventional and Heat Pump Dryers

Conventional Dryers	SMER, kg/kWh	Specific Energy, kJ/kg
Rotary, spray, tunnel and fluid bed	0.5–0.75	7200–4800
Vacuum freeze	0.08	–
Adiabatic heat pump fluidised bed dryer	2–3	1800–1200
Polytropic heat pump fluidised bed dryer	3–5	1200–720
Superheated steam dryer	2.4–3.6	1500–1000

The magnitude of heat recovery in a heat pump dryer depends on the area available for heat transfer and on the properties of the refrigerant and moist air. It also depends on the moist air and evaporating refrigerant temperatures as well as on the difference between evaporating and condensing temperature. The last condition is highly dependent on the number of stages of the heat pump dryer (Alves-Filho 2011).

The single-stage vapour compression is a commonly applied heat pump cycle. In this case, only one evaporator cools the moist air, condenses the water vapour fraction and absorbs (for boiling the refrigerant) the corresponding latent heat of vapour condensation.

Figure 1.6 illustrates a simplified single-stage heat pump system. The main components are the expansion valve, evaporator, internal and external condensers and the compressor. After flowing through the heat pump evaporator and the condenser, the dry and warm air is ready to flow into the drying chamber. The simplified heat pump dryer has two separated loops with common heat exchangers. The drying air loop (abca) contains the air cooler (EVA), heater (CON), blower and the drying chamber. The main components of the refrigerant loop (12341) are the expansion valve (THR), evaporator (EVA), condenser (CON) and compressor (COM). The heat pump fluid and drying air loops are coupled through the common evaporator and condenser to recover the exhaust energy.

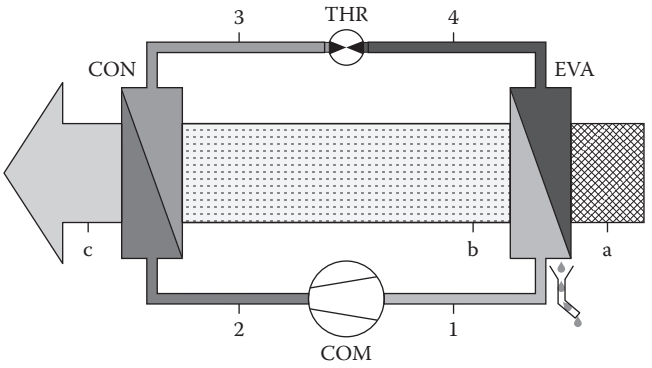

FIGURE 1.6
Principle of operation in a simplified heat pump dryer.

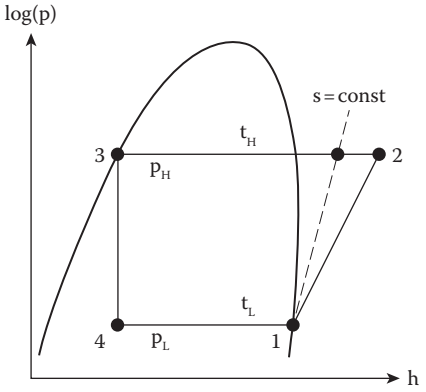

FIGURE 1.7
Simplified heat pump cycle on the log pressure–enthalpy diagram.

The refrigerant closed cycle is composed of four processes as shown in Figure 1.7.

1–2: Non-isentropic compression. Here, the saturated vapour is compressed from the evaporating pressure to condensing pressure and temperature and becomes superheated vapour.

2–3: Isobaric condensation. The superheated vapour rejects superheat in the first section of the condenser and becomes saturated vapour. Then, the vapour rejects further heat as it flows through the last section of the condenser, changes phase to saturated liquid, and is collected in the receiver.

3–4: Adiabatic expansion. Here, the saturated or subcooled liquid at high pressure enters the expansion valve and is throttled adiabatically to the lower pressure. At the exit of the valve, it becomes a vapour–liquid mixture and flows into the evaporator.

4–1: Isobaric evaporation. The refrigerant mixture flows through the evaporator, takes up heat from the moist air and changes phase to saturated vapour at the exit of the evaporator. This saturated vapour flows into the compressor to restart the cycle.

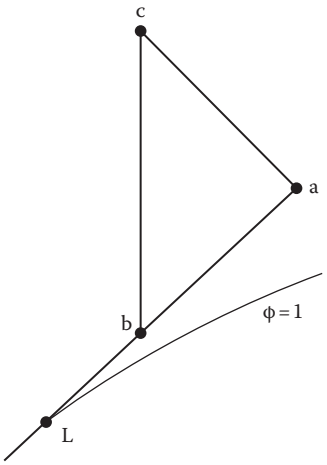

FIGURE 1.8
Drying air cycle on the Mollier diagram.

The closed heat pump drying air cycle is composed of three processes as shown in the Mollier diagram in Figure 1.8:

c–a: Adiabatic drying process where the drying air at the set temperature flows through the drying chamber and removes moisture from the bed of wet material.

a–b: Cooling the moist air and water vapour condensation with liquid drainage. As the moist air flows through the evaporator, the vapour condenses to liquid and is drained out of the drying loop. To perform this step, the evaporator surface is kept at state point L with a temperature below the dew-point temperature in the air at the inlet drying chamber (point c).

b–c: Heating of the moist air by the condenser using the energy recovered by the evaporator. The low-temperature energy absorbed in the evaporator promotes boiling of the refrigerant, and then it is compressed to high-temperature energy and reused by the condenser to heat the drying air. This completes the cycle of energy recovery in the heat pump dryer.

Although a single-stage heat pump drying system is advantageously and widely applied, it cannot provide several streams of drying air with different conditions and operate with a large evaporating and condensing temperature difference. For this latter case, the solution is a multistage heat pump drying.

Figure 1.9 shows the two-stage heat pump dryer that operates with a large evaporating and condensing temperature difference and provides two airstreams with different conditions. The refrigerant liquid from the condenser D is collected in the receiver E, flows into the expansion valve F and is collected in the intermediate pressure tank G. Simultaneously, this tank receives intermediate pressurised superheated vapour from the first stage compressor A1. In the tank G, the refrigerant is separated into two phases. One phase is saturated liquid that enters the expansion valve H connected to the evaporator I and the low-stage compressor A1. The other phase is saturated vapour that flows to the suction line of the high-stage compressor A2. This compressor discharges superheated

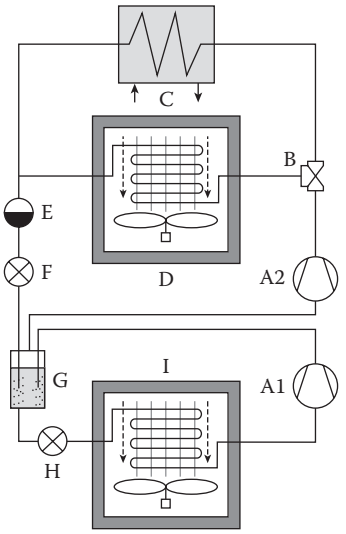

FIGURE 1.9
Two-stage heat pump dryer.

vapour to the three-way valve B, which directs the vapour to the external and internal condensers C and D, respectively.

The second stage drying involves moisture removal by evaporation at higher rates. The two-stage heat pump dryer operates with energy recovery for high efficiency (superior-quality dried product), resulting in reduced energy use and costs.

Currently, heat pump drying is commercially and industrially applied for processing fish and vegetables. Extensive research is ongoing for the development of new dried products and process improvements (Alves-Filho and Strømmen 1996).

This chapter shows that heat pump drying is a novel technology that offers major benefits in terms of product quality, energy savings and environmental emission minimisation. Heat pump dryers can operate in single or combined evaporation or atmospheric freeze sublimation modes for drying of foods, fruits, berries, vegetables and other heat-sensitive products (Alves-Filho and Roos 2006). Heat pump dryers are up to five times more efficient than conventional dryers, with potential for implementation by modern industries.

2

Single-Stage Vapour Compression Heat Pumps for Drying

A vapour compression heat pump system can be designed as single vapour compression system with a throttling valve or similar device separating the low- and high-pressure sides. Heat exchangers, mainly called condensers and evaporators, are applied to transfer energy between the heat pump system working fluid and the surroundings. The working fluid changes phase from vapour to liquid as it flows through the condenser and releases energy to the heat sink. This direction of energy transfer requires a higher temperature in the heat pump fluid than in the heat sink. Simultaneously, the working fluid changes phase from a liquid and vapour mixture to vapour by boiling in the evaporator while receiving energy from the heat source. This direction of energy transfer also requires lower temperature in the evaporating fluid than in the heat source. These processes take place in a closed cycle as the working fluid flows through condensers, evaporators, compressors and throttling devices. The energy transfer obeys the statements of the first and the second laws of thermodynamics. In addition, the energy exchange occurs in accordance with the mechanisms of heat conduction, convection, sublimation, condensation and evaporation.

The fluid properties in the inlet and outlet of each heat pump component characterise the state points, processes and thermodynamic cycle. The performances of heat pumps operating with different fluids can be compared subsequent to the determination of the fluid properties in the mentioned state points (ASHRAE Handbook of Fundamentals 2009).

This chapter covers the principle of operation and the equations to compare performances and capacities of single vapour compression heat pump systems with drying channels. The calculations and comparisons are based on operating conditions and working fluid properties at the state points of the heat pump cycle. Problems are solved for a variety of heat pump systems with natural and conventional fluids. The required fluid properties for the problems are given in tables and graphs in Chapter 7.

2.1 Laws of Thermodynamics and the Heat Pump Cycles

A heat pump system is applied to transport energy from a low-temperature medium surrounding the evaporator to the higher temperature medium surrounding the condenser. This energy exchange occurs as the working fluid flows through the heat pump components and changes phase in the cycle. This energy exchange complies with the laws of thermodynamics and the mechanisms of heat transfer.

The first law of thermodynamics states that energy is conserved and remains constant in an isolated system and ideal closed cycle. The second law establishes the direction of energy flow by stating that, in the absence of other effects, heat transfers occur from regions of high-to-low temperature. The first law of thermodynamics is applied to a closed

heat pump cycle and allows accounting of the energy exchange between the components and the surrounding media. It provides the energy balance in the working fluid in the evaporator, condenser, compressor, throttling valve and the surrounding media. This requires a temperature difference to drive energy transfer between the components and the heat sink or source in conformity with the laws of thermodynamics (Holman 1988).

In the case of a single-stage vapour compression system, the first law of thermodynamics establishes that the heat rejected by the condensing fluid to the heat sink must be equal to the sum of the energy absorbed by the evaporating fluid from the heat source and the work input to the compressor. The application of the second law in to the same system indicates the direction of energy flow between the components and surrounding media. Then, this law determines that energy transfers from a cold media or heat source to the evaporator only if the evaporator temperature is below the heat source temperature. Likewise, energy transfers from the condenser to the warm side media or heat sink only if the condenser temperature is higher than the heat sink temperature. These statements occur consistently in appropriately designed vapour compression heat pump systems.

An analysis of heat pump performance requires knowledge of the layout and function of each component in the system. The components are responsible for the processes and cycles that govern energy transfer according to the laws of thermodynamics. For instance, the evaporator, compressor, condensation and expansion valve are responsible for the processes of evaporation, compression, condensation and throttling comprising the heat pump cycle.

Figure 2.1 illustrates a simple vapour compression heat pump system exchanging energy with the surrounding media. The energy transfer depends on the layout of the system and on the temperature difference between the working refrigerant flowing inside the components, the heat source or heat sink, and the compressor shaft work. By operating between the limiting temperatures t_H and t_L, this cycle is able to absorb the energy q_L from the heat source and reject the energy q_H to the heat sink with the specific work w.

The processes in this heat pump system are as follows:

1–2: Vapour compression and discharge of superheated vapour at condensing pressure.

2–3: Condensation at constant pressure and change of state from superheated vapour to saturated liquid. This condensation leads to release energy to the heat sink.

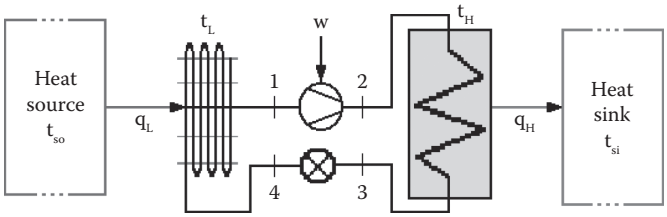

FIGURE 2.1
Compression heat pump system operating between the heat source and sink limiting temperatures according to the statements of the first and second laws of thermodynamics. The main processes are as follows: 1 to 2 – vapour compression from saturated to superheated vapour at condensing pressure, 2 to 3 – condensation with heat rejected by the condenser fluid and phase changes from vapour to saturated liquid, 3 to 4 – throttling from saturated liquid to vapour and liquid mixture at evaporating pressure, 4 to 1 – evaporation with heat absorption by the fluid in the evaporator and change of phase from liquid–vapour mixture to saturated vapour.

3–4: Throttling of saturated liquid to a liquid–vapour mixture at evaporating pressure.

4–1: Evaporation at constant temperature and change of state from liquid–vapour mixture to saturated vapour. This evaporation energy is supplied by the heat source.

This heat pump system complies with the first law of thermodynamics because energy is preserved and also with the second law of thermodynamics because energy flows from higher to lower temperature regions. The laws of energy transfer require a difference between condensing fluid temperature t_H and the heat sink temperature t_{si}, and a temperature difference between the evaporating fluid temperature t_L and the heat source t_{so}. Furthermore, the evaporating temperature t_L must be lower than the heat source t_{so}, and the fluid condensing temperature t_H must be lower than the heat sink temperature t_{si}.

The analysis of a heat pump system requires identification of the thermodynamic state points of the cycle and calculation or determination of the fluid properties at each of these points.

The heat pump fluid properties are obtained in refrigerant tables and diagrams (see Chapter 7) that are available for most pure fluids and refrigerant blends commonly used in heat pump systems. The diagrams are made by plotting the pressure versus enthalpy and temperature versus entropy, and they show typical dome-shaped curves separating the refrigerant phases and states. The plotting of the system cycle on this diagram leads to the location of the state points and identification of the phases involved in the heat pump processes. This is particularly important for calculation because it allows determination of required fluid properties on each state point of the processes composing the heat pump cycle.

Figure 2.2 shows the typical dome-shaped curve in the pressure versus enthalpy diagram for heat pump fluids. Saturation occurs on the curve ABC, and the peak is fluid critical point B that defines both the critical temperature and pressure. The curves

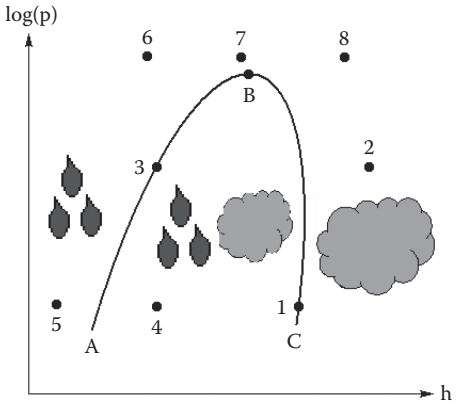

FIGURE 2.2
Saturation dome-shaped curve and the thermodynamic state points with phase regions for a heat pump fluid in the pressure versus enthalpy diagram. AB – liquid saturation line, B – critical point, BC – vapour saturation line, 1 – saturated vapour state, 2 – superheated vapour, 3 – saturated liquid state, 4 – liquid–vapour mixture, 5, 6 – sub-cooled liquid state, 7, 8 – state where liquid is undistinguishable from vapour or vice versa.

to the right and left of the critical point are the saturated vapour and saturated liquid lines, respectively. The region of superheated vapour is located to the right side of the saturated vapour line, whereas the region of sub-cooled liquid is on the left side of the saturated liquid line. The region of vapour and liquid mixture or two-phase region is enclosed by the dome-shaped curve. At temperatures and pressures above the critical point, there is no distinction between liquid and vapour. Figure 2.2 illustrates the following states points: 1 – saturated vapour, 2 – superheated vapour, 3 – saturated liquid, 4 – liquid–vapour mixture, 5 and 6 – sub-cooled liquid and 7 and 8 – state no distinction between vapour from liquid.

Notice that point 6 is a sub-cooled liquid state because it is at temperature below the critical value, whereas points 7 and 8 are indistinguishable liquid or vapour states because their temperatures or pressures are above the critical values.

Moreover, from the pressure versus enthalpy diagrams, the thermodynamic properties of the heat pump fluid can be determined from the temperature versus entropy diagrams. Figure 2.3a and 2.3b presents these diagrams that have also saturation dome-shaped curves. The diagrams show the constant curves or lines: A to B is saturated liquid, B to C is saturated vapour, 1 to 2 is constant temperature, 3 to 4 is constant pressure, 5 to 6 is constant specific enthalpy, 7 to 8 is constant specific entropy, 9 to 10 is constant specific volume and B to 11 is the constant quality. Notice the change in curvature, slope and position of the same curve or line representing the property in the diagrams. Moreover, both diagrams indicate that pressure and temperature follow constant lines only inside the wet-mixture regions.

Then, the analysis of performance and comparison of heat pump systems requires knowledge of the energy exchanged between the heat pump components and surroundings. It also involves determination of refrigerant properties in cycle by using equations, diagrams and tables. The comparison is generally made based upon a reference thermodynamic cycle. A common reference is the Carnot cycle that is described in the next section.

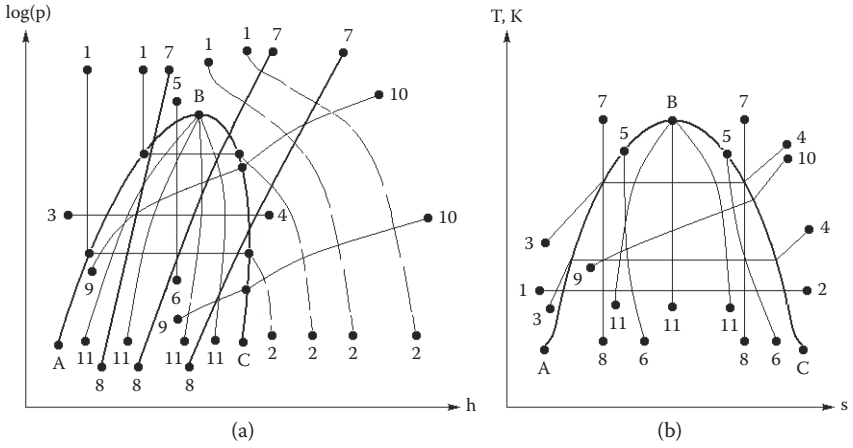

FIGURE 2.3
Saturation dome-shaped curve and constant thermodynamic properties of refrigerants (a) in the pressure versus enthalpy diagram and (b) in the temperature versus entropy diagram. A to B – saturated liquid lines, B to C – saturated vapour lines, 1 to 2 – constant temperature lines, 3 to 4 – constant pressure lines, 5 to 6 – constant specific enthalpy lines, 7 to 8 – constant specific entropy lines, 9 to 10 – constant specific volume lines, B to 11 – constant quality lines.

2.2 Carnot Cycle

The Carnot cycle has a perfect efficiency that is unsurpassed by any other real cycle operating between two temperature levels. Figure 2.4 illustrates the wet vapour compression ideal Carnot cycle plotted in the temperature versus entropy and pressure versus enthalpy diagrams. The diagrams indicate the state points at the inlet and outlet of the heat pump components shown in Figure 2.1.

The Carnot cycle consists of the following thermodynamically reversible processes:

1–2: Isentropic compression where wet vapour is compressed to saturated vapour.

2–3: Isothermal–isobaric condensation and heat release where saturated vapour changes phase to saturated liquid.

3–4: Isentropic throttling where the saturated liquid at condensing pressure is expanded to liquid–vapour mixture at evaporating pressure.

4–1: Isothermal–isobaric evaporation where the fluid mixture receives heat and becomes wet vapour at the initial state point 1 to restart the Carnot cycle.

The reversibility of the Carnot implies no temperature difference between the evaporator and condenser surface and the heat source and sink, respectively. In addition, the reversible Carnot cycle has no energy loss and functions as a heat pump by taking shaft work for energy exchange between low- and high-temperature sources. Theoretically, it operates like a reversed heat engine cycle, i.e., it generates shaft power by exchanging energy with the high- and low-temperature sources.

As a consequence, the Carnot cycle is theoretical because the perfect efficient and reversible processes are unattainable. The reason it is a reference cycle is because it measures of how close to ideal cycle is the actual coefficient of performance (COP) of a heat pump system.

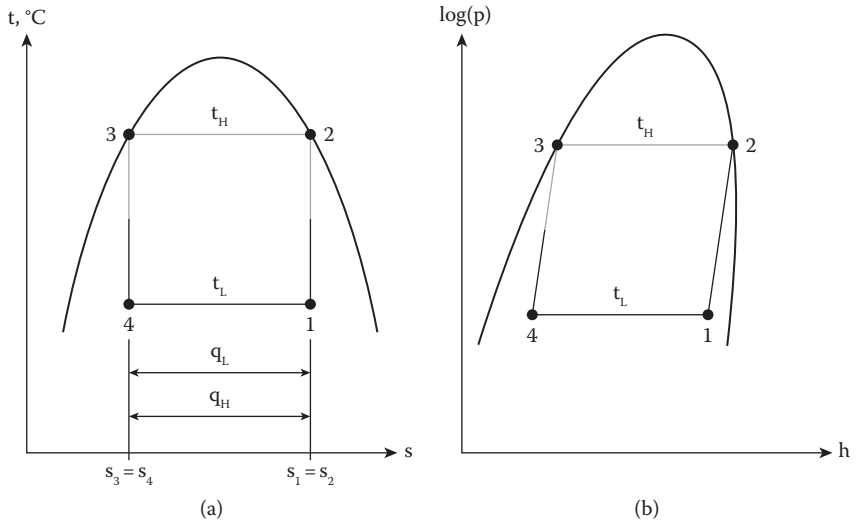

FIGURE 2.4
Ideal Carnot cycle. (a) Cycle in the temperature versus entropy diagram. (b) Cycle in the pressure versus enthalpy diagram.

The importance of this relation is that the COP indicates the heat pump ability to release and absorb energy in exchange for shaft work.

The Carnot cycle sketched in Figure 2.4 operates between temperatures t_L and t_H and has maximum coefficients of performance that can be expressed, in terms of the corresponding absolute temperatures T_L and T_H, by

$$COP_H = \frac{q_H}{w} = \frac{T_H}{T_H - T_L}\frac{s_2 - s_4}{s_2 - s_4} = \frac{T_H}{T_H - T_L} \tag{2.1}$$

$$COP_L = \frac{q_L}{w} = \frac{T_L}{T_H - T_L}\frac{s_2 - s_4}{s_2 - s_4} = \frac{T_L}{T_H - T_L} \tag{2.2}$$

$$COP_L = \frac{q_L}{w} = \frac{q_H - w}{w} = COP_H - 1 \quad \therefore COP_H = \frac{q_H}{w} = \frac{q_L + w}{w} = COP_L + 1 \tag{2.3}$$

where s is specific entropy in kJ/kg K, w is specific work in kJ/kg, q_H is the specific energy rejected by the condenser to the heat sink in kJ/kg and q_L is the specific energy absorbed by the evaporator from the heat source in kJ/kg.

The first law of thermodynamics states that the energy rejected to the heat sink by the condenser is equal to the sum of the energy transferred from the heat source to the evaporator and the compressor work, as follows:

$$q_H = q_L + w \tag{2.4}$$

Introducing the mass flow rate in each component leads to

$$\dot{m}_H q_H = \dot{m}_L q_L + \dot{m}_L w \quad \therefore Q_H = Q_L + W \tag{2.5}$$

where Q_H, Q_L and W are the condensing capacity, cooling capacity and compressor work, respectively, and $\dot{m}_H$ and $\dot{m}_L$ are the mass flow rates in the condenser and evaporator or compressor, respectively.

The laws of thermodynamics and heat transfer are the basis to quantify a heat pump COP that approaches but never reaches the value of the ideal Carnot cycle. The deviation from the ideal cycle are due to the actual temperature differences required for energy transport between the fluid in the heat exchangers and surrounding media and the unavoidable energy losses in the heat pump components.

Aside from operating pressure and temperature, the COP depends on the type of working fluid and heat pump, compression stages, and design and layout of evaporator, condenser and auxiliary components. Once the type of heat pump system and fluid are selected, the laws of thermodynamics and heat and mass balance equations are applied with proper boundary conditions to establish the heat pump coefficients of performance and capacity.

The components and respective layout of the system will have a considerable effect on coefficients' performances and energy exchange. Now, we progress with an examination and evaluation of single vapour compression heat pumps with different layouts and arrangements of the components in the system.

2.3 Single-Stage Vapour Compression Heat Pump as a Modified Carnot Cycle

Vapour compression heat pump systems are among the most widely applied technologies at the present time. This section describes the vapour compression systems, component arrangements and calculations of capacities and performances based on shaft work to compressor and energy transfer between the evaporator or condenser and the surroundings. The calculations are based on the thermodynamic state points of the cycle created as the fluid flows through the heat pump components and drying channels. A single-stage vapour compression heat pump can be designed with different layouts and arrangements according to different applications.

A single-stage dry vapour compression heat pump system may be developed from a slight modification of the ideal Carnot cycle.

Figure 2.5a and 2.5b shows the cycles for the Carnot modified heat pump system in temperature versus entropy and pressure versus enthalpy diagrams, respectively. From point 1, the saturated vapour is compressed to superheated vapour at point 2. Then, the superheated vapour is cooled (or desuperheated) to saturation to point 3 and enters the condensers, kept at constant temperature, changing phase to saturated liquid at point 4. Then, this liquid flows through the throttling valve and becomes a liquid–vapour mixture at point 5. After that, the mixture flows through the evaporator at constant temperature and changes phase to saturated vapour at point 1 and re-enters the cycle.

The COP of this system is lower than that of the Carnot cycle because the superheated vapour at point 2 requires isothermal instead of non-isentropic compression to reach point 3.

This heat pump cycle has the following processes:

1–2: Isentropic compression
2–3: Isothermal and non-isentropic compression
3–4: Isothermal condensation
4–5: Isentropic expansion
5–6: Isothermal and isobaric evaporation.

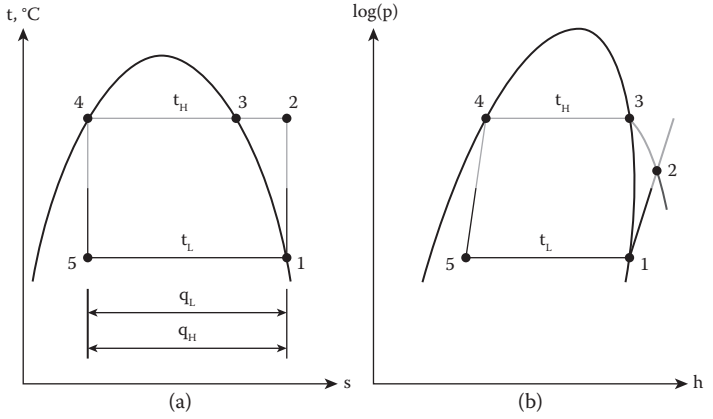

FIGURE 2.5
Carnot cycle modified to dry compression heat pump. (a) Cycle in the temperature versus entropy diagram. (b) Cycle in the pressure versus enthalpy diagram.

However, this system has the limitation of an unpractical isothermal compression process from state points 2 to 3. This problem is solved by several single-stage vapour compression systems. Some options are the non-isentropic and isentropic vapour compression heat pumps with dry-expansion evaporator, flooded evaporator and internal heat exchanger. The non-isentropic and isentropic vapour compression heat pump system with drying channels is examined next.

2.4 Isentropic and Non-Isentropic Saturated Vapour Compression Heat Pump with Dry-Expansion Evaporator

Figure 2.6 illustrates the isentropic and non-isentropic saturated vapour compression heat pumps with dry-expansion evaporator and drying channels.

Figure 2.6a and 2.6b shows the layout and the state points in the cycles in a pressure versus enthalpy diagram, respectively. From state point 1, the saturated vapour is isentropic and non-isentropic compressed to superheated vapour to points 2_i and 2, respectively. Then, the vapour flows through the condenser, changes phase to saturated liquid and is collected in the receiver. The saturated liquid leaves the receiver at point 3, and it is throttled to a liquid and vapour mixture at point 4. Then, the mixture flows through the evaporator and becomes saturated vapour at point 1 to be compressed again.

The equations are developed for non-isentropic vapour compression heat pump considering the state points in the cycle shown in Figure 2.6b.

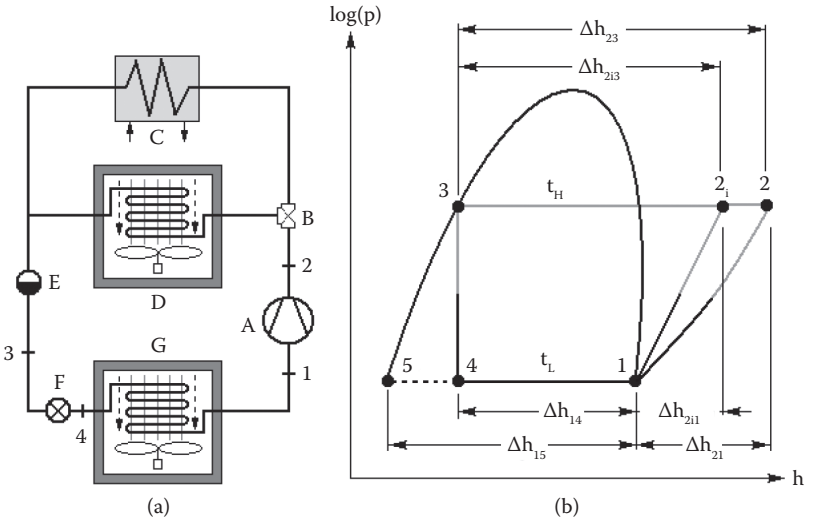

FIGURE 2.6
Isentropic and non-isentropic saturated vapour compression heat pumps, indicating the corresponding specific enthalpy differences in each process. (a) Main components: A – compressor, B – three-way valve, C – external condenser, D – drying channel with air heater, E – liquid receiver, F – expansion valve, G – drying channel with air cooler. (b) Schematic of the cycle in the pressure versus enthalpy diagram.

The isentropic efficiency is the ratio of the isentropic to non-isentropic enthalpy differences during compression, expressed by

$$\eta_i = \frac{h_{2i} - h_1}{h_2 - h_1} = \frac{\Delta h_{2i1}}{\Delta h_{21}} \tag{2.6}$$

The total mass flow rate of heat pump fluid is the ratio of cooling capacity to the specific enthalpy difference of the working fluid in the evaporator. Thus, for the isentropic and non-isentropic processes, the total mass flow rate is

$$\dot{m} = \frac{Q_L}{h_1 - h_4} \tag{2.7}$$

The quality of the mixture at the exit of the throttling valve or at inlet of the evaporator at state point 4 is expressed by

$$x_4 = \frac{h_4 - h_1}{h_1 - h_5} = \frac{\Delta h_{41}}{\Delta h_{15}} \tag{2.8}$$

Then, the mass flow rates of vapour and liquid are

$$\dot{m}_{v4} = x_4 \frac{Q_L}{h_1 - h_4} = x_4 \cdot \dot{m} \tag{2.9}$$

$$\dot{m}_{\ell 4} = (1 - x_4) \frac{Q_L}{h_1 - h_4} = (1 - x_4) \cdot \dot{m} \tag{2.10}$$

The mass flow rates must balance as follows:

$$\dot{m} = \left[x_4 + (1 - x_4)\right] \frac{Q_L}{h_1 - h_4} = \frac{Q_L}{h_1 - h_4} = \dot{m}_{v4} + \dot{m}_{\ell 4} \tag{2.11}$$

The cooling capacity is

$$Q_L = \dot{m} \cdot (h_1 - h_4) = \dot{m} \cdot \Delta h_{14} \tag{2.12}$$

For the heat pump with isentropic process the work input and condensing capacity are

$$W_i = \dot{m} \cdot (h_{2i} - h_1) = \dot{m} \cdot \Delta h_{2i1} \tag{2.13}$$

$$Q_{Hi} = \dot{m} \cdot (h_{2i} - h_3) = \dot{m} \cdot \Delta h_{2i3} \tag{2.14}$$

For the heat pump with non-isentropic process the work and condensing capacity are

$$W = \dot{m} \cdot (h_2 - h_1) = \dot{m} \cdot \Delta h_{21} \tag{2.15}$$

$$Q_H = \dot{m} \cdot (h_2 - h_3) = \dot{m} \cdot \Delta h_{23} \tag{2.16}$$

The equations for coefficients of performance on the low- and high-pressure sides of the isentropic heat pump are as follows:

$$COP_L = \frac{h_1 - h_4}{h_{2i} - h_1} = \frac{\Delta h_{14}}{\Delta h_{2i1}} = \frac{Q_L}{W_i} \tag{2.17}$$

$$COP_H = \frac{h_{2i} - h_3}{h_{2i} - h_1} = \frac{\Delta h_{2i3}}{\Delta h_{2i1}} = \frac{Q_{Hi}}{W_i} \tag{2.18}$$

The equations for coefficients of performance of the non-isentropic heat pump are as follows:

$$COP_L = \frac{h_1 - h_4}{h_2 - h_1} = \frac{\Delta h_{14}}{\Delta h_{21}} = \frac{Q_L}{W} \tag{2.19}$$

$$COP_H = \frac{h_2 - h_3}{h_2 - h_1} = \frac{\Delta h_{23}}{\Delta h_{21}} = \frac{Q_H}{W} \tag{2.20}$$

2.5 Basic Vapour Compression Heat Pump with Dry-Expansion Evaporator and Drying Channels

The main feature of the basic heat pump with dry evaporator is that only saturated vapour enters the suction line and that only saturated liquid goes into the throttling valve. This cycle is an alternative to the modified Carnot cycle and also the basic reference cycle to compare performances of single vapour compression heat pumps.

Figure 2.7 presents the details of the basic vapour compression heat pump system with dry-expansion evaporator. Figure 2.7a shows the layout and main components: A – compressor, B – three-way valve, C – external condenser, D – drying channel with air heater, E – liquid receiver, F – expansion valve and G – drying channel with air cooler.

Figure 2.7b illustrates the cycle and processes with the state points in the pressure versus enthalpy diagram. Point 1 is saturated vapour that undergoes isentropic compression

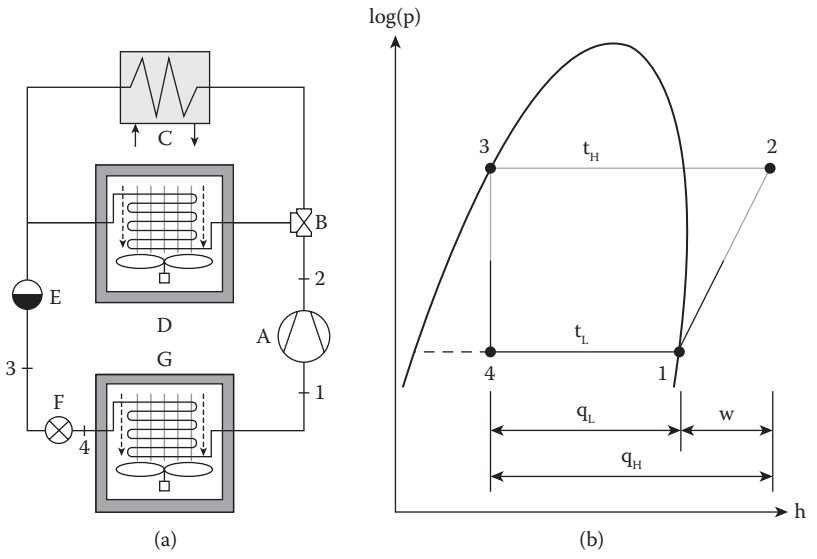

FIGURE 2.7
Basic vapour compression heat pump system. (a) Main components: A – compressor, B – three-way valve, C – external condenser, D – drying channel with air heater, E – liquid receiver, F – expansion valve, G – drying channel with air cooler. (b) Schematic of the cycle in the pressure versus enthalpy diagram.

to superheated vapour at point 2. Then, the fluid enters the condensers and change phase to saturated liquid at point 3. From this point, the saturated liquid is throttled to a liquid and vapour mixture at point 4. After evaporation, the mixture becomes saturated vapour at point 1 to be compressed again.

The processes in this cycle are as follows:

1–2: Isentropic compression of the saturated vapour to superheated vapour
2–3: Isobaric condensation of the superheated vapour to saturated liquid
3–4: Adiabatic expansion of the saturated liquid to vapour–liquid mixture
4–1: Isothermal–isobaric evaporation of the mixture to saturated vapour.

The heat pump fluid changes phase from 1 to 2 by compression with shaft work given by

$$w = \frac{q_L}{COP_L} = h_2 - h_1 \quad \therefore W = \frac{Q_L}{COP_L} = \dot{m}\left(h_2 - h_1\right) \tag{2.21}$$

The heat released to the surroundings by the condensers occurs as the fluid changes state from 2 to 3 and it is expressed by

$$q_H = w \cdot COP_H = h_2 - h_3 \quad \therefore Q_H = W \cdot COP_H = \dot{m}\left(h_2 - h_3\right) \tag{2.22}$$

The adiabatic or constant enthalpy throttling process occurs as fluid state points change from 3 to 4. The energy involved in an adiabatic process is

$$q_{ex} = h_3 - h_4 = 0 \quad \therefore Q_{ex} = \dot{m}(h_3 - h_4) = 0 \tag{2.23}$$

The heat absorbed by the evaporator from the surroundings results in the change of state from vapour–liquid mixture to saturated vapour and it is expresses by

$$q_L = w \cdot COP_L = h_1 - h_4 \quad \therefore Q_L = W \cdot COP = \dot{m}\left(h_1 - h_4\right) \tag{2.24}$$

The heat pump COP is expressed by

$$COP_H = \frac{q_H}{w} = \frac{h_2 - h_3}{h_2 - h_1} = \frac{Q_H}{W} \tag{2.25}$$

The COP based on the evaporation and cooling is given by

$$COP_L = \frac{q_L}{w} = \frac{h_1 - h_4}{h_2 - h_1} = \frac{Q_L}{W} \tag{2.26}$$

2.6 Vapour Compression Heat Pump with Flooded Evaporator

The vapour compression heat pump with flooded evaporator is an alternative the previous system. It has an additional accumulator and a float-controlled valve that improves the cooling effect and protects the compressor from damage.

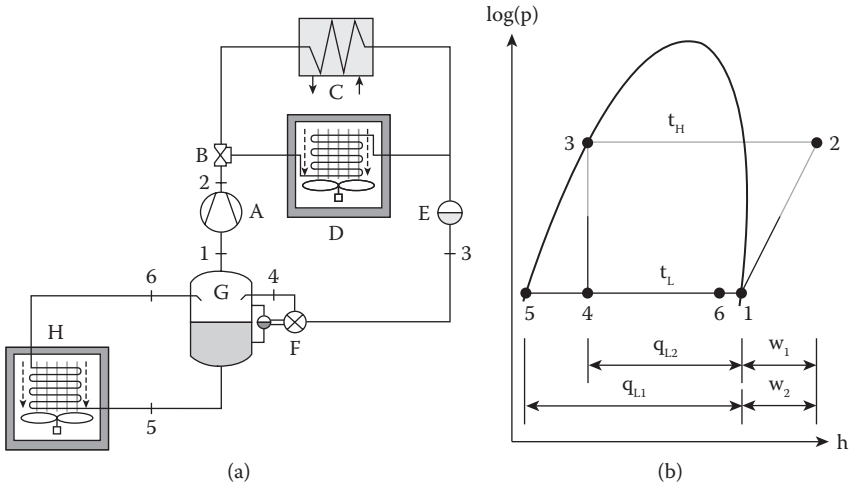

FIGURE 2.8
Vapour compression heat pump system with flooded evaporator. (a) Main components: A – compressor, B – three-way valve, C – external condenser, D – drying channel with air heater (internal condenser), E – liquid receiver, F – float-controlled valve, G – accumulator, H – drying channel with air cooler (evaporator). (b) Cycle with flooded evaporator in the pressure and enthalpy diagram.

Figure 2.8a presents the flooded evaporator heat pump system. It shows the main components that are similar to the previous basic heat pump system except that the dry-expansion evaporator and expansion valve are replaced by a flooded evaporator, accumulator vessel and float-controlled valve.

Figure 2.8b illustrates the heat pump cycle in the pressure versus enthalpy diagram. The cycle starts at point 1 where saturated vapour at evaporating temperature enters the compressor A and is discharged as superheated vapour in point 2. This vapour is directed by the three-way valve B to condensers C and D where it changes phase to saturated liquid at point 3 and it is collected by the liquid receiver E. From point 3, the liquid is throttled by the float-controlled valve F to vapour–liquid mixture at point 4 and enters the accumulator G where it is separated into liquid and vapour fractions. The saturated liquid fraction leaves the bottom of the accumulator at point 5 and flows through evaporator H, changes phase to nearly saturated mixture at point 6 and flows into the accumulator G. From the top of the accumulator G, saturated vapour at point 1 enters the suction line of the compressor A to complete the cycle.

The main processes in this cycle are as follows:

1–2: Isentropic compression
2–3: Isobaric condensation
3–4: Adiabatic expansion followed by vapour–liquid separation
4–5: Isobaric cooling
5–6: Isothermal and isobaric evaporation.

Notice that the stable saturated conditions of state points 1 and 5 depend on the accumulator's ability to separate the vapour and liquid fractions in state points 4 and 6. This process is readily achieved in a properly designed heat pump and accumulator.

The compressor shaft work is expressed by

$$w = \frac{q_L}{COP_L} = \frac{q_H}{COP_H} = h_2 - h_1 \quad \therefore W = \frac{Q_L}{COP_L} = \frac{Q_H}{COP_H} = \dot{m}(h_2 - h_1) \tag{2.27}$$

The condensing capacity is

$$q_H = w \cdot COP_H = h_2 - h_3 = (h_2 - h_1) \cdot COP_H \quad \therefore Q_H = W \cdot COP_H = \dot{m}(h_2 - h_3) \tag{2.28}$$

The throttling is an adiabatic process, hence

$$q_{ex} = h_3 - h_4 = 0 \quad \therefore Q_{ex} = \dot{m}(h_3 - h_4) = 0 \tag{2.29}$$

The evaporation or cooling capacity is

$$q_L = w \cdot COP_L = h_1 - h_5 \quad \therefore Q_L = W \cdot COP_L = \dot{m}(h_1 - h_5) \tag{2.30}$$

The heat pump COP is

$$COP_H = \frac{q_H}{w} = \frac{h_2 - h_3}{h_2 - h_1} = \frac{Q_H}{W} \tag{2.31}$$

The COP based on evaporation or cooling is

$$COP_L = \frac{q_L}{w} = \frac{h_5 - h_1}{h_2 - h_1} = \frac{Q_L}{W} \tag{2.32}$$

2.7 Vapour Compression Heat Pump with Internal Heat Exchanger

The problems of the previously described dry-expansion system are also solved by the vapour compression heat pump with internal heat exchanger illustrated in Figure 2.9. This is done by adding an internal heat exchanger. The objectives are to slightly superheat the vapour and avoid liquid droplets entering the compressor and to sub-cool the liquid before throttling to enhance the cooling effect.

Figure 2.9a illustrates the heat pump system with an internal heat exchanger and the main components. Figure 2.9b shows this heat pump cycle in the pressure versus enthalpy diagram. The cycle starts with slightly superheated vapour at point 1 that flows through the compressor A and becomes superheated vapour at point 2. The vapour is directed by the three-way valve B to the condensers C and D, and becomes saturated liquid at point 3. After collection in the liquid receiver E, it flows through the internal heat exchanger F and becomes sub-cooled liquid at point 4, where it is throttled by the expansion valve G to become a liquid–vapour mixture at point 5. The mixture flows through the evaporator H and changes phase to saturated vapour at point 6. This vapour flows through the internal heat exchanger F and becomes slightly superheated at point 1 to be compressed once more.

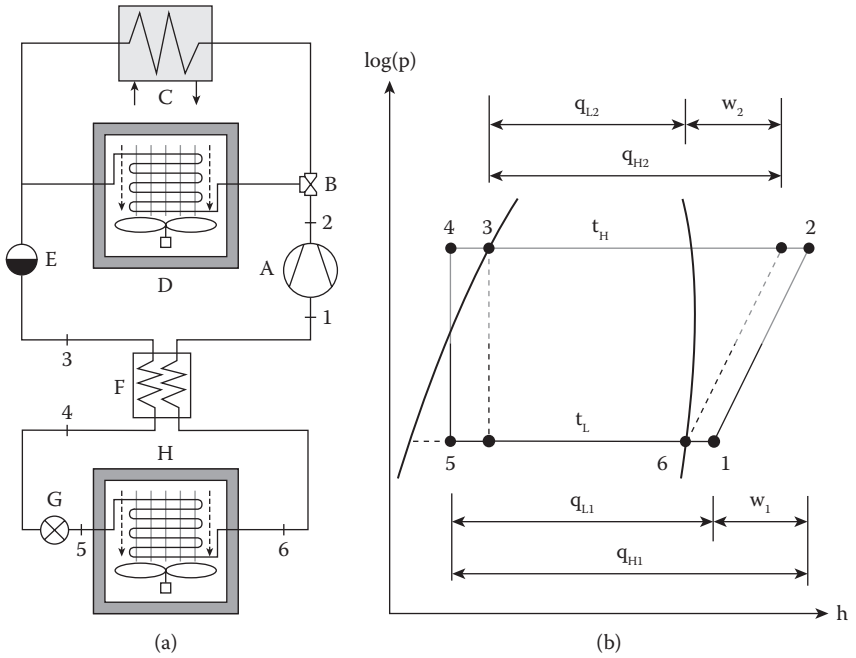

FIGURE 2.9
Vapour compression heat pump system with internal heat exchanger. (a) Main components: A – compressor, B – three-way valve, C – external condenser, D – drying channel with air heater (internal condenser), E – liquid receiver, F – internal heat exchanger, G – expansion valve, H – drying channel with air cooler (evaporator). (b) Schematic of the cycle with internal heat exchanger in the pressure versus enthalpy diagram.

The main processes in the cycle are as follows:

1–2: Isentropic compression
2–3: Isobaric condensation
4–5: Adiabatic expansion
5–6: Isobaric and isothermal evaporation.

Note that the additional processes of isobaric sub-cooling from 3 to 4 and vapour superheating from 6 to 1 are performed simultaneously by the internal heat exchanger.
The shaft work for this system is expressed by

$$w = h_2 - h_1 = \frac{q_L}{COP_L} = \frac{h_6 - h_5}{COP_L} \quad \therefore W = \dot{m}(h_2 - h_1) = \frac{Q_L}{COP_L} = \frac{\dot{m}}{COP_L}(h_6 - h_5) \quad (2.33)$$

The heat released by the condenser to the surrounding media is

$$q_H = w \cdot COP_H = h_2 - h_3 \quad \therefore Q_H = W \cdot COP_H = \dot{m}(h_2 - h_1) \cdot COP_H = \dot{m}(h_2 - h_3) \quad (2.34)$$

The throttling process is adiabatic, thus

$$q_{ex} = h_4 - h_5 = 0 \quad \therefore Q_{ex} = \dot{m}(h_4 - h_5) = 0 \quad (2.35)$$

The cooling or evaporation capacity is

$$q_L = \frac{w}{COP_L} = \frac{h_2 - h_1}{COP_L} = h_6 - h_5 \quad \therefore Q_L = \frac{W}{COP_L} = \frac{\dot{m}\cdot(h_2 - h_1)}{COP_L} = \dot{m}(h_6 - h_5) \tag{2.36}$$

The COP on the high-pressure side is expressed by

$$COP_H = \frac{q_H}{w} = \frac{h_2 - h_3}{h_2 - h_1} = \frac{Q_H}{W} \tag{2.37}$$

The COP on the low-pressure side is given by

$$COP_L = \frac{q_L}{w} = \frac{h_6 - h_5}{h_2 - h_1} = \frac{Q_L}{W} \tag{2.38}$$

2.8 Comparison and Limitations of the Single-Stage Vapour Compression Systems

A performance comparison is made for basic, flooded evaporator and internal heat exchanger single-stage vapour compression heat pump systems. The three systems operate with R717, cooling capacity of 100 kW, evaporating temperature at 5°C and condensing temperature at 40°C.

The performances were calculated for the three single vapour compression heat pump systems, and the results are given in Table 2.1. The volumetric cooling effect (VCE) indicates the R717 refrigeration effect per unit compressor swept volume of vapour. The highest COP_L is the heat pump with flooded evaporator, with a value 16% above the value of the basic system. The COP_L is similar for the basic and internal heat exchanger systems. The COP_H is similar for the basic and flooded systems and slightly lower for the heat pump with internal heat exchanger.

The single-stage compression systems are unsuitable for applications with large temperature difference between evaporating and condensing temperatures, which is

TABLE 2.1

Characteristics and Performances of the Three Types of Vapour Compression Heat Pump Systems Operating with R717

System	VCE, kJ/m³	w, kJ/kg	q_L, kJ/kg	q_H, kJ/kg	COP_L	COP_H
Basic	4427.3	156.6	1076.5	1233.1	6.87	7.87
Flooded	5115.0	156.6	1243.7	1233.1	7.94	7.87
Internal heat exchanger	4488.0	161.3	1091.3	1254.2	6.77	7.78
Ratio						
Basic	1.00	1.00	1.00	1.00	1.00	1.00
Flooded	1.16	1.00	1.16	1.00	1.16	1.00
Internal heat exchanger	1.01	1.03	1.01	1.02	0.98	0.99

known as temperature lift. In such cases the setbacks of single-stage systems are low efficiency and high compressor discharge temperature at the condensing pressure. The large temperature lift in a single vapour compression heat pump system results in increased specific work because the compressor's isentropic efficiency is highly dependent on pressure ratio or temperature lift. The isentropic efficiency increases sharply to a maximum value and quickly drops as the pressure and ratio increases.

The problems of single compression systems are solved by applying multistage vapour compression systems that are covered in Chapter 3.

2.9 Problems and Solutions

PROBLEM 2.1

Comparison of Isentropic and Non-Isentropic Saturated Vapour Compression Heat Pump with Dry-Expansion Evaporator

The non-isentropic (with isentropic efficiency 0.8) and isentropic saturated vapour compression heat pump and cycles are illustrated in Figure 2.6. Compare both systems with R717 based on the mass flow rate, specific cooling effect, shaft work, condensing capacity and coefficients of performance. Both systems operate with constant cooling capacity of 100 kW, evaporating temperature at 5°C, condensing temperature at 40°C and adiabatic throttling.

Given:

$Q_o = 100$ kW	$\eta_i = 0.8$
$t_L = 5°C$	$h_3 = h_4$
$t_H = 40°C$	

Solution:

1. Determination of the required properties for refrigerant R717

   The properties for commonly used refrigerants are obtained from the tables and diagrams given in Chapter 7. Table 2.2 gives the properties for refrigerant R717 for isentropic and non-isentropic processes in the heat pump cycle with evaporating

TABLE 2.2

Properties in the Cycle State Points for Non-Isentropic and Isentropic Vapour Compression Heat Pumps with R717

	State Point							
	Basic Isentropic				Basic Non-Isentropic			
Property	**1**	**2**	**3**	**4**	**1**	**2i**	**2**	**4**
t, °C	5.0	84.4	40.0	5.0	5.0	84.4	103.9	5.0
p, bar	5.16	15.55	15.55	5.16	5.16	15.55	15.55	5.16
h, kJ/kg	1628.9	1785.5	552.4	552.4	1628.9	1785.5	1837.7	552.4
s, kJ/kg·K	6.1188	6.1188	—	—	6.1188	6.2610	—	—

temperature at 5°C and condensing temperature at 40°C for the state points shown in Figure 2.6.

2. Calculation of specific enthalpy at point 2 in the isentropic compression cycle

$$h_2 = h_1 + \frac{h_{2i} - h_1}{\eta_i} = 1837.7 \text{ kJ/kg}$$

3. Calculation of specific enthalpy differences

   For the isentropic compression cycle, the enthalpy differences between the state points are as follows:

$$\Delta h_{21} = h_{2i} - h_1 = 1785.5 - 1628.9 = 156.6 \text{ kJ/kg}$$

$$\Delta h_{14} = h_1 - h_4 = 1628.9 - 552.4 = 1076.5 \text{ kJ/kg}$$

$$\Delta h_{2i3} = h_{2i} - h_3 = 1785.5 - 552.4 = 1233.1 \text{ kJ/kg}$$

   For the isentropic compression cycle, the enthalpy differences are as follows:

$$\Delta h_{21} = h_2 - h_1 = 1837.7 - 1628.9 = 208.8 \text{ kJ/kg}$$

$$\Delta h_{14} = h_1 - h_4 = 1628.9 - 552.4 = 1076.5 \text{ kJ/kg}$$

$$\Delta h_{23} = h_2 - h_3 = 1837.7 - 552.4 = 1285.3 \text{ kJ/kg}$$

4. Calculation of mass flow rates of circulating refrigerant

   Considering a cooling capacity of 100 kW, the mass flow rate for both cycles is as follows:

$$\dot{m} = \frac{Q_L}{h_1 - h_4} = \frac{100}{1076.5} = 0.0929 \text{ kg/s}$$

5. Calculation of the work and condensing capacity

   The work and condensing capacity for the isentropic compression cycle are as follows:

$$W_i = \dot{m}(h_{2i} - h_1) = 0.0929 \cdot 156.6 = 14.6 \text{ kW}$$

$$Q_{Hi} = \dot{m}(h_{2i} - h_3) = 0.0929 \cdot 1233.1 = 114.6 \text{ kW}$$

   The work and condensing heat for non-isentropic compression cycle are as follows:

$$W = \dot{m}(h_2 - h_1) = 0.0929 \cdot 208.8 = 19.4 \text{ kW}$$

$$Q_H = \dot{m}(h_2 - h_3) = 0.0929 \cdot 1285.8 = 119.4 \text{ kW}$$

TABLE 2.3

Summary of Characteristics and Performances for the Isentropic and Non-Isentropic Saturated Vapour Compression Heat Pumps

	Characteristics and COP					
Compression	**$\dot{m}$, kg/s**	**s_{2i} or s_2, kJ/kg·K**	**W, kW**	**Q_H, kW**	**COP_L**	**COP_H**
Isentropic	0.0929	6.1188	14.6	114.6	6.87	7.87
Non-isentropic	0.0929	6.2610	19.4	119.4	5.15	6.15

6. Calculation of coefficients of performance

   For the isentropic compression cycle, the coefficients are as follows:

$$COP_{Li} = \frac{q_{Li}}{w_i} = \frac{1076.5}{156.6} = 6.87$$

$$COP_{Hi} = \frac{q_{Hi}}{w_i} = \frac{1233.1}{156.6} = 7.87$$

   For the non-isentropic compression cycle, the coefficients are as follows:

$$COP_L = \frac{q_L}{w} = \frac{1076.5}{208.8} = 5.15$$

$$COP_H = \frac{q_H}{w} = \frac{1285.4}{208.8} = 6.15$$

7. Summarised table and comparison of performances

   Table 2.3 lists the main parameters to compare characteristics and performances of the isentropic and non-isentropic heat pump system operating with R717.

The COPs for the isentropic and non-isentropic saturated vapour compression heat pumps are calculated and compared for the evaporating and condensing temperature at 5°C and 40°C, respectively.

The non-isentropic process corresponds to the real-world (practical) heat pump system. It differs from the isentropic process by having higher specific entropy and temperature at the superheated vapour discharged by the compressor. As a consequence, the non-isentropic heat pump system has higher mass flow rate and lower COPs than the isentropic cycle.

PROBLEM 2.2

Performances of Basic Vapour Compression Heat Pump with Dry-Expansion Evaporator Operating with R717 and R22

A basic vapour compression heat pump with dry-expansion evaporator and drying channels and the cycle are presented in Figure 2.7. Considering that system, make a summarised table comparing the systems operating with R717 and R22 based on mass flow rate, specific cooling effect, shaft work, condensing capacity and coefficients of performance.

Both systems operate with constant cooling capacity of 100 kW, evaporating temperature at 5°C, condensing temperature at 40°C, isentropic compression and adiabatic throttling.

Given:

$Q_o = 100$ kW	$\eta_i = 1$
$t_L = 5°C$	$h_3 = h_4$
$t_H = 40°C$	

Solution:

1. Determination of the required properties for refrigerants R717 and R22

   The properties for commonly used refrigerants are obtained from the tables and diagrams given in Chapter 7.

   Table 2.4 gives the properties for refrigerants R717 and R22 for the evaporating and condensing temperatures of 5°C and 40°C, respectively. The heat pump cycle and state points are specified in Figure 2.7b.

2. Calculation of specific enthalpy differences in the compressor, evaporator and condenser

   For the refrigerant R717, the enthalpy differences between the state points are as follows:

$$\Delta h_{21} = h_2 - h_1 = 1785.5 - 1628.9 = 156.6 \text{ kJ/kg}$$

$$\Delta h_{14} = h_1 - h_4 = 1628.9 - 552.4 = 1076.5 \text{ kJ/kg}$$

$$\Delta h_{23} = h_2 - h_3 = 1785.5 - 552.4 = 1233.1 \text{ kJ/kg}$$

   For the refrigerant R22, the values are as follows:

$$\Delta h_{21} = h_2 - h_1 = 431.1 - 407.2 = 23.9 \text{ kJ/kg}$$

$$\Delta h_{14} = h_1 - h_4 = 407.2 - 249.7 = 157.5 \text{ kJ/kg}$$

$$\Delta h_{23} = h_2 - h_3 = 431.1 - 249.7 = 181.4 \text{ kJ/kg}$$

TABLE 2.4

Properties of Refrigerants R717 and R22 in the Cycle State Points of the Basic Vapour Compression Heat Pump with Dry-Expansion Evaporator

	Refrigerant and State Point							
	R717				**R22**			
Property	**1**	**2**	**3**	**4**	**1**	**2**	**3**	**4**
t, °C	5.0	84.4	40.0	5.0	5.0	55.8	40.0	5.0
p, bar	5.16	15.55	15.55	5.16	5.84	15.33	15.33	5.84
h, kJ/kg	1628.9	1785.5	552.4	552.4	407.2	431.13	249.8	249.8
s, kJ/kg·K	6.1188	6.1188	—	—	1.7451	1.7451	—	—

3. Calculation of mass flow rates of circulating refrigerant
   Considering a cooling capacity of 100 kW, the mass flow rate for the R717 system is as follows:

$$\dot{m} = \frac{Q_L}{h_1 - h_4} = \frac{100}{1076.5} = 0.0929 \text{ kg/s}$$

   The mass flow rate for the R22 system is as follows:

$$\dot{m} = \frac{Q_L}{h_1 - h_4} = \frac{100}{157.5} = 0.6349 \text{ kg/s}$$

4. Calculation of the work and condensing capacity
   The work and condensing capacity for the R717 system are as follows:

$$W = \dot{m}(h_2 - h_1) = 0.0929 \cdot 156.6 = 14.6 \text{ kW}$$

$$Q_H = \dot{m}(h_2 - h_3) = 0.0929 \cdot 1233.1 = 114.6 \text{ kW}$$

   The work and condensing capacity for the R22 system are as follows:

$$W = \dot{m}(h_2 - h_1) = 0.6349 \cdot 23.9 = 15.2 \text{ kW}$$

$$Q_H = \dot{m}(h_2 - h_3) = 0.6349 \cdot 181.4 = 115.2 \text{ kW}$$

5. Calculation of coefficients of performance
   For the heat pump system with R717, the coefficients are as follows:

$$COP_L = \frac{q_L}{w} = \frac{1076.5}{156.6} = 6.87$$

$$COP_H = \frac{q_H}{w} = \frac{1233.1}{156.6} = 7.87$$

   For the heat pump system with R22, the coefficients are as follows:

$$COP_L = \frac{q_L}{w} = \frac{157.5}{23.9} = 6.58$$

$$COP_H = \frac{q_H}{w} = \frac{181.4}{23.9} = 7.58$$

6. Summarised table and comparison of performances
   Table 2.5 shows the main parameters to compare characteristics and performances of the basic vapour compression heat pump with dry-expansion evaporator operating with R717 and R22.

TABLE 2.5

Summary of Characteristics and Performances of the Basic Vapour Compression Heat Pump with Dry-Expansion Evaporator

	Characteristics and COP					
Refrigerant	**$\dot{m}$, kg/s**	**Δh_{14}, kJ/kg**	**W, kW**	**Q_H, kW**	**COP_L**	**COP_H**
R717	0.0929	1076.5	14.6	114.6	6.87	7.87
R22	0.6349	157.5	15.2	115.2	6.58	7.58

The basic vapour compression heat pump with dry-expansion evaporator has high coefficients of performance for evaporating and condensing temperatures of 5°C and 40°C. The system with R717 has the benefits of lower mass flow rate, higher cooling effect and slightly higher coefficients of performance compared to the R22 system.

However, this system has two major problems. The first problem is transport of liquid droplets into the compressor, with consequent damage in case of suction occurring prior to the state point 1. The second problem is that after expansion, the mixture of vapour–liquid at point 4 causes a drop in the cooling effect or the enthalpy difference $h_1 - h_4$. For clear visualisation and better understanding of these limitations, refer to Tables 2.4 and 2.5 and in the cycle plotted in Figure 2.7b. These problems are solved either by the vapour compression heat pump with flooded evaporator or with internal heat exchanger, which are described in sequence in Problems 2.3 and 2.4.

PROBLEM 2.3

Comparison of Vapour Compression Heat Pump with Flooded Evaporator Operating with R717 and R22

A heat pump system with flooded evaporator and the cycle are presented in Figure 2.8. Make a summarised table comparing the systems with R717 and R22 based on mass flow rate, specific cooling effect, shaft work, condensing capacity and coefficients of performance. The systems operate with constant cooling capacity of 100 kW, evaporating temperature at 5°C, condensing temperature at 40°C, isentropic compression and adiabatic throttling.

Given:

$Q_o = 100$ kW	$\eta_i = 1$
$t_L = 5$°C	$h_3 = h_4$
$t_H = 40$°C	

Solution:

1. Determination of the required properties for refrigerants R717 and R22

   Table 2.6 gives the properties for refrigerants R717 and R22 for heat pump cycle with evaporating and condensing temperatures 5°C and 40°C.
2. Calculation of specific enthalpy differences in the compressor, evaporator and condenser

TABLE 2.6

Properties of Refrigerants R717 and R22 in the Cycle State Points for the Heat Pump with Flooded Evaporator

	Refrigerant and State Point							
	R717				R22			
Property	**1**	**2**	**3**	**5**	**1**	**2**	**3**	**5**
t, °C	5.0	84.4	40.0	5.0	5.0	55.8	40.0	5.0
p, bar	5.16	15.55	15.55	5.16	5.84	15.33	15.33	5.84
h, kJ/kg	1628.9	1785.5	552.4	385.2	407.2	431.13	249.8	205.9
s, kJ/kg·K	6.1188	6.1188	—	—	1.7451	1.7451	—	—

For the refrigerant R717, the values in the enthalpy difference between the state points are as follows:

$$\Delta h_{21} = h_2 - h_1 = 1785.5 - 1628.9 = 156.6 \text{ kJ/kg}$$

$$\Delta h_{15} = h_1 - h_5 = 1628.9 - 385.2 = 1243.7 \text{ kJ/kg}$$

$$\Delta h_{23} = h_2 - h_3 = 1785.5 - 552.4 = 1233.1 \text{ kJ/kg}$$

For the refrigerant R22 the values are as follows:

$$\Delta h_{21} = h_2 - h_1 = 431.1 - 407.2 = 23.9 \text{ kJ/kg}$$

$$\Delta h_{15} = h_1 - h_5 = 407.2 - 205.9 = 201.3 \text{ kJ/kg}$$

$$\Delta h_{23} = h_2 - h_3 = 431.1 - 249.7 = 181.4 \text{ kJ/kg}$$

3. Calculation of mass flow rates of circulating refrigerant in the evaporator and condenser

   Considering a cooling capacity of 100 kW, the mass flow rate in the evaporator for R717 is as follows:

$$\dot{m}_e = \frac{Q_L}{h_1 - h_5} = \frac{100}{1243.7} = 0.0804 \text{ kg/s}$$

From mass balance in the accumulator, the R717 mass flow rate of refrigerant circulating in the compressor and condenser is as follows:

$$\dot{m}_c = \dot{m}_e \frac{h_1 - h_5}{h_1 - h_4} = \frac{1243.7}{1076.5} = 0.0929 \text{ kg/s}$$

The R22 mass flow rate in the evaporator is as follows:

$$\dot{m}_e = \frac{Q_L}{h_1 - h_5} = \frac{100}{201.3} = 0.4969 \text{ kg/s}$$

The R22 mass flow rate in the compressor and condenser is as follows:

$$\dot{m}_c = \dot{m}_e \frac{h_1 - h_5}{h_1 - h_4} = 0.4969 \frac{201.3}{157.5} = 0.6350 \text{ kg/s}$$

4. Calculation of the work and condensing capacity
   The work and condensing capacity for the R717 system are as follows:

$$W = \dot{m}_c (h_2 - h_1) = 0.0929 \cdot 156.6 = 14.5 \text{ kW}$$

$$Q_H = \dot{m}_c (h_2 - h_3) = 0.0929 \cdot 1233.1 = 114.5 \text{ kW}$$

   The work and condensing capacity for the R22 system are as follows:

$$W = \dot{m}_c (h_2 - h_1) = 0.6350 \cdot 23.9 = 15.2 \text{ kW}$$

$$Q_H = \dot{m}_c (h_2 - h_3) = 0.6350 \cdot 181.4 = 115.2 \text{ kW}$$

5. Calculation of coefficients of performance
   For the system with R717, the coefficients are as follows:

$$COP_L = \frac{Q_L}{W} = \frac{100}{14.5} = 6.87$$

$$COP_H = \frac{Q_H}{W} = \frac{114.5}{14.5} = 7.87$$

   For the system with R22, the coefficients are as follows:

$$COP_L = \frac{Q_L}{W} = \frac{100}{15.2} = 6.58$$

$$COP_H = \frac{Q_H}{W} = \frac{115.2}{15.2} = 7.58$$

6. Summarised table and comparison of performances
   Table 2.7 lists the main parameters to compare characteristics and performances of the heat pump system with flooded evaporator operating with R717 and R22.

TABLE 2.7

Summary of Characteristics and Performances of the Heat Pump System with Flooded Evaporator

	Characteristics and COP					
Refrigerant	**$\dot{m}$, kg/s**	**Δh_{15}, kJ/kg**	**W, kW**	**Q_H, kW**	**COP_L**	**COP_H**
R717	0.0804	1243.7	14.5	114.5	6.87	7.87
R22	0.4968	201.3	15.2	115.2	6.58	7.58

The heat pump system with flooded evaporator has excellent coefficients of performances for evaporating and condensing temperature at 5°C and 40°C. Compared with the R22 system, the R717 system has lower mass flow rate, higher cooling effect and higher coefficients of performance.

In addition, for both R717 and R22, the systems with flooded evaporator have lower mass flow rate, higher cooling effect and higher coefficients of performances compared to values for basic heat pump with dry-expansion evaporator.

This section closes with Problem 2.4 to highlight that the main tasks of the vapour compression heat pump system with flooded evaporator with additional accumulator and float-controlled valve are separation of saturated liquid and vapour the main tasks. This leads the benefits of improvement in the cooling effect indicated by $h_1 - h_5$ in Figure 2.8b and of compressor protection from liquid droplets.

PROBLEM 2.4

Performances of Vapour Compression Heat Pump with Internal Heat Exchanger Operating with R717 and R22

A vapour compression heat pump with internal heat exchanger operates in a cycle is presented in Figure 2.9. Make a summarised table comparing the systems operating with R717 and R22 based on mass flow rate, specific cooling effect, shaft work, condensing capacity and coefficients of performance. The systems operate with constant cooling capacity of 100 kW, evaporating temperature at 5°C, condensing temperature at 40°C, isentropic compression and adiabatic throttling.

Given:

$Q_o = 100$ kW	$\eta_i = 1$
$t_L = 5$°C	$h_3 = h_4$
$t_H = 40$°C	

Solution:

1. Determination of the required properties for refrigerants R717 and R22

   Table 2.8 shows the properties for refrigerants R717 and R22 for heat pump cycle with evaporating and condensing temperatures of 5°C and 40°C.

2. Calculation of specific enthalpy differences in the compressor, evaporator and condenser

   For the system with R717, the enthalpy differences between the state points are as follows:

$$\Delta h_{21} = h_2 - h_1 = 1806.6 - 1645.3 = 161.3 \text{ kJ/kg}$$

$$\Delta h_{65} = h_6 - h_5 = 1628.9 - 537.6 = 1091.3 \text{ kJ/kg}$$

$$\Delta h_{23} = h_2 - h_3 = 1806.6 - 552.4 = 1254.2 \text{ kJ/kg}$$

   For the refrigerant R22, the values are as follows:

$$\Delta h_{21} = h_2 - h_1 = 436.4 - 411.7 = 24.7 \text{ kJ/kg}$$

TABLE 2.8

Properties of Refrigerants R717 and R22 in the Cycle State Points for the Heat Pump with Internal Heat Exchanger

	Refrigerant and State Point					
	R717					
Property	**1**	**2**	**3**	**4**	**5**	**6**
t, °C	11	92.2	40.0	37.0	5.0	5.0
p, bar	5.16	15.55	15.55	15.55	5.16	5.16
h, kJ/kg	1645.3	1806.6	552.4	537.6	537.6	1628.9
s, kJ/kg·K	6.1771	6.1771	—	—	—	6.1188
R22						
t, °C	11	61.7	40	37	5	5
p, bar	5.84	15.33	15.33	15.33	5.84	5.84
h, kJ/kg	411.7	436.4	249.8	245.8	245.8	407.2
s, kJ/kg·K	1.7609	1.7609	—	—	—	1.7451

$$\Delta h_{65} = h_6 - h_5 = 407.2 - 245.8 = 161.4 \text{ kJ/kg}$$

$$\Delta h_{23} = h_2 - h_3 = 436.4 - 249.8 = 186.6 \text{ kJ/kg}$$

3. Calculation of mass flow rates of circulating refrigerant
   Considering a cooling capacity of 100 kW, the mass flow rate for R717 is as follows:

$$\dot{m} = \frac{Q_L}{h_6 - h_5} = \frac{100}{1091.3} = 0.0916 \text{ kg/s}$$

   The R22 mass flow rate is as follows:

$$\dot{m} = \frac{Q_L}{h_6 - h_5} = \frac{100}{161.4} = 0.6195 \text{ kg/s}$$

4. Calculation of the work and condensing capacity
   The work and condensing capacity for the R717 system are as follows:

$$W = \dot{m}(h_2 - h_1) = 0.0916 \cdot 161.3 = 14.8 \text{ kW}$$

$$Q_H = \dot{m}(h_2 - h_3) = 0.0916 \cdot 1254.2 = 114.9 \text{ kW}$$

   The work and condensing capacity for the R22 system are as follows:

$$W = \dot{m}(h_2 - h_1) = 0.6195 \cdot 24.7 = 15.3 \text{ kW}$$

$$Q_H = \dot{m}(h_2 - h_3) = 0.6195 \cdot 186.6 = 115.6 \text{ kW}$$

TABLE 2.9

Summary of Characteristics and Performances of the Vapour Compression Heat Pump with Internal Heat Exchanger

	Characteristics and COP					
Refrigerant	$\dot{m}$, **kg/s**	Δh_{65}, **kJ/kg**	**W, kW**	Q_H, **kW**	COP_L	COP_H
R717	0.0916	1091.3	14.8	114.9	6.77	7.78
R22	0.6195	161.4	15.3	115.6	6.53	7.55

5. Calculation of coefficients of performance

   For the system with R717, the coefficients are as follows:

$$COP_L = \frac{\Delta h_{65}}{\Delta h_{21}} = \frac{1091.3}{161.3} = 6.77$$

$$COP_H = \frac{\Delta h_{23}}{\Delta h_{21}} = \frac{1254.2}{161.3} = 7.78$$

   For the system with R22, the coefficients are as follows:

$$COP_L = \frac{\Delta h_{65}}{\Delta h_{21}} = \frac{161.4}{24.7} = 6.53$$

$$COP_H = \frac{\Delta h_{23}}{\Delta h_{21}} = \frac{186.6}{24.7} = 7.55$$

6. Summarised table and comparison of performances

   Table 2.9 lists the main parameters to compare characteristics and performances of the vapour compression heat pump with internal heat exchanger and operating with R717 and R22.

The heat pump system with internal heat exchanger has excellent coefficients of performance for the given evaporating and condensing temperatures. Compared to the R22 system, the R717 system has lower mass flow rate, lower work, higher cooling effect and higher coefficients of performance.

The solution of this problem revealed that the addition of an internal heat exchanger in this heat pump system produced the benefits of assuring that

- Slightly superheated vapour occurs at point 1 protecting the compressor from damage by liquid droplets
- Sub-cooled liquid is available at point 4 to enhance the cooling effect from $h_6 - h_3$ to $h_1 - h_5$ as indicated in Figure 2.9a and 2.9b

3

Multistage Vapour Compression Heat Pumps for Drying

The multistage vapour compression heat pump system has more components, but has the benefit of superior performance in a wider pressure range and temperature lift than single-stage vapour compression. A particular difference is that the multistage heat pump has two or more compressors and throttling devices operating at three or more temperature and pressure levels.

For large temperature lifts or pressure ranges, a single-stage compression system has the limitations of high compressor work and discharge temperature and low isentropic efficiency. The multistage vapour compression systems split the large pressure difference into smaller intervals, each driven by a compressor and auxiliary devices. A properly designed multistage heat pump system combined with the drying channel operates reliably in temperature ranges of −30°C to 40°C or wider (Granryd et al. 2009).

This chapter describes the multistage vapour compression heat pumps and the processes of the thermodynamic heat pump cycles. It also covers the principles of operation, the working fluid properties at each state point of the cycle and the equations to compare performances of the heat pump systems.

The properties of the working fluid at the inlet and outlet of each component characterise the state points, processes and thermodynamic heat pump cycle. The properties are calculated by equations, by correlations, or are determined from tables and graphs given in Chapter 7 or by using a variety of computer software.

Problems are solved for a variety of multistage vapour compression heat pumps with drying channels and operating with natural and conventional fluids.

3.1 Two-Stage Compression Heat Pump with Gas Intercooler

Figure 3.1 shows the layout of a two-stage vapour compression heat pump system with gas cooler, the cycle and main components.

Figure 3.1a illustrates the layout of the components of the heat pump system, where the numbers for the state points in the inlet and outlet of each component are similar to the numbers for the state points in the cycle.

Figure 3.1b presents the processes in the cycle of the heat pump with intercooler in the pressure versus enthalpy diagram. The saturated vapour at point 1 enters the first-stage compressor A1 and leaves as superheated vapour at point 2. Then, it flows through the gas cooler B, and it is isobarically cooled to point 3 where it enters the second-stage compressor A2 and becomes superheated vapour at point 4. After that, the vapour flows through the condensers D and E, changes phase and is collected in the liquid receiver F. The saturated liquid at point 5 enters the expansion valve G to be adiabatically throttled to a liquid–vapour mixture at point 6. The mixture flows through the evaporator H,

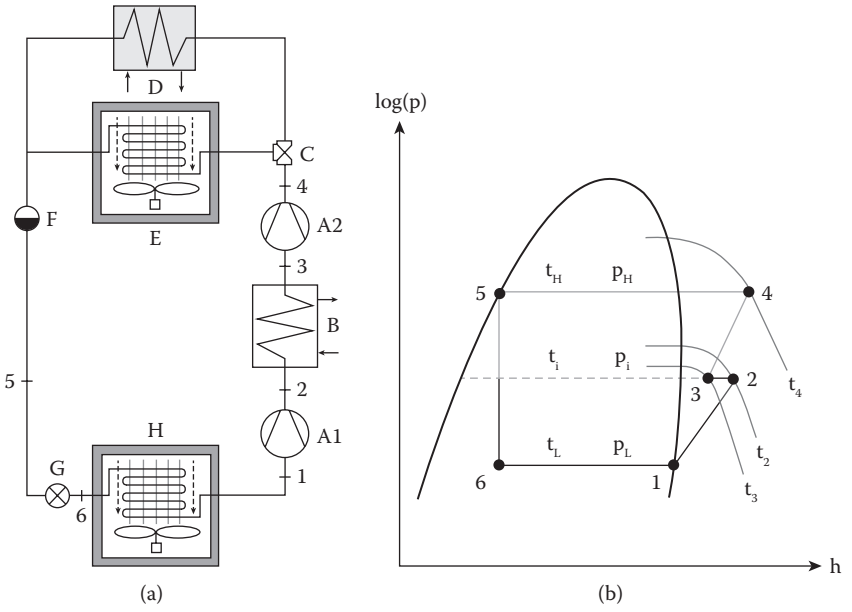

FIGURE 3.1
Two-stage vapour compression heat pump system with gas intercooler. (a) Main components: A1 – low-pressure compressor, A2 – high-pressure compressor, B – gas intercooler, C – three-way valve, D – external condenser, E – drying channel with air heater, F – liquid receiver, G – expansion valve, H – drying channel with air cooler. (b) Schematic of the cycle with intercooler in the pressure versus enthalpy diagram.

and it becomes saturated vapour at point 1 where it again enters the suction line of the first-stage compressor.

Then, the processes in this heat pump cycle are as follows:

1–2 is isentropic first-stage compression
2–3 is isobaric gas cooling
3–4 is isentropic second-stage compression
4–5 isobaric condensation
5–6 is adiabatic expansion
6–1 is isobaric–isothermal evaporation

The two-stage compression with gas cooler has the following advantages compared to single-stage compression:

- Smaller pressure ratios by splitting the large pressure range
- Higher compressor isentropic efficiency or lower compression energy loss
- Lower discharge temperature

The temperature lift or pressure range in a two-stage vapour compression heat pump system is related to the pressure ratio. It is the quotient of the high-to-low pressures as follows:

$$p_r = \frac{p_H}{p_L} \tag{3.1}$$

The splitting of the pressure range in a two-stage vapour compression system leads to an intermediate pressure defined by

$$p_i = \sqrt{p_L \cdot p_H} \tag{3.2}$$

The mass flow rate of working fluid is given by

$$\dot{m} = \frac{Q_L}{h_1 - h_6} = \frac{Q_L}{\Delta h_{16}} \tag{3.3}$$

The low- and high-pressure stage and total work equations are as follows:

$$W_L = \dot{m}(h_2 - h_1) = \dot{m} \cdot \Delta h_{21} \tag{3.4}$$

$$W_H = \dot{m}(h_4 - h_3) = \dot{m} \cdot \Delta h_{43} \tag{3.5}$$

$$W = \dot{m}(\Delta h_{21} + \Delta h_{43}) = W_L + W_H \tag{3.6}$$

The equations for the condensing capacity, the heat removed by the gas cooler and the total heat rejected equations are as follows:

$$Q_H = \dot{m}(h_4 - h_5) = \dot{m} \cdot \Delta h_{45} \tag{3.7}$$

$$Q_{gc} = \dot{m}(h_2 - h_3) = \dot{m} \cdot \Delta h_{23} \tag{3.8}$$

$$Q_{Ht} = \dot{m}(\Delta h_{23} + \Delta h_{45}) = Q_{gc} + Q_H \tag{3.9}$$

The coefficients of performance equations are as follows:

$$COP_L = \frac{Q_L}{W_L + W_H} = \frac{Q_L}{W} \tag{3.10}$$

$$COP_H = \frac{Q_H}{W_L + W_H} = \frac{Q_H}{W} = COP_L + 1 \tag{3.11}$$

3.2 Two-Stage Compression Heat Pump with Flash Intercooler and Compressors in Parallel

Figure 3.2 presents the layout, processes and cycle of the two-stage heat pump system with an open flash intercooler supplying saturated vapour to the intermediate-pressure compressors placed in parallel with each other. The flash intercooler purposes are to provide only saturated liquid to the throttling device for improving the cooling effect and to supply only saturated vapour to the second-stage compressor for enhanced efficiency. A beneficial consequence is reduction of the discharge temperature and compression losses by mixing the vapours discharged by the two compressors.

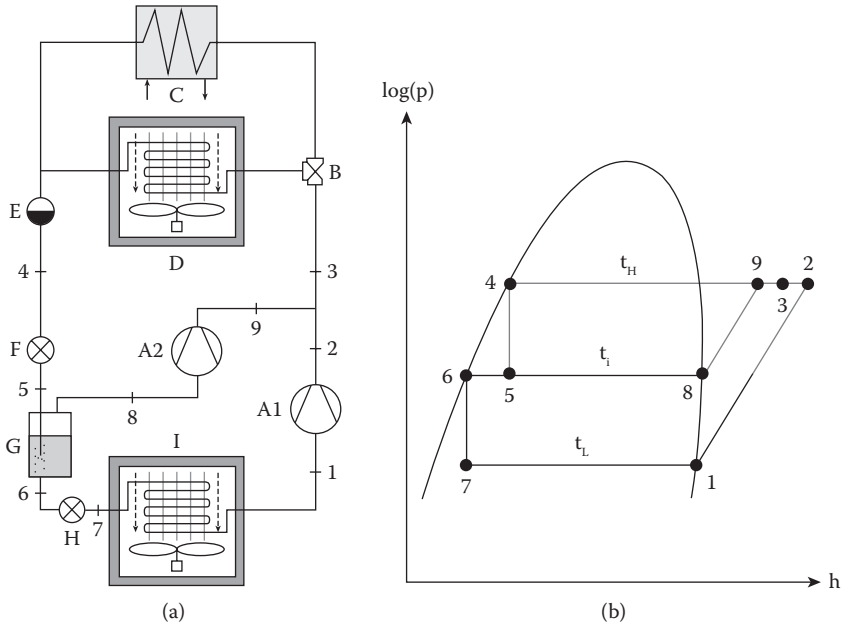

FIGURE 3.2
Two-stage heat pump system with open flash intercooler and compressors in parallel. (a) Main components: A1 – low-pressure compressor, A2 – intermediate-pressure compressor, B – three-way valve, C – external condenser, D – drying channel with air heater, E – liquid receiver, F – intermediate-pressure expansion valve, G – open flash intercooler, H – low-pressure expansion valve, I – drying channel with air cooler. (b) Cycle with open intercooler and parallel compressors in the pressure versus enthalpy diagram.

Figure 3.2a illustrates the layout of the components in the system with the drying channel. Figure 3.2b shows the heat pump cycle and processes in the pressure versus enthalpy diagram. The saturated vapour at point 1 enters the compressor A1, and it is discharged as superheated vapour at condensing pressure at point 2. Simultaneously, saturated vapour at point 8 enters the parallel compressor A2 and exits as superheated vapour at the condensing pressure at point 9. The discharged vapours from points 9 and 2 are mixed and reach point 3. Then, the mixed vapours flow into the three-way valve B, through the condensers C and D, changes phase to saturated liquid at point 4, and is collected into the liquid receiver E. The saturated liquid flows into the throttling device F, changes phase to a liquid–vapour mixture, and is released into the flash intercooler G at point 5. From the bottom of the flash intercooler, the saturated liquid at point 6 is throttled by the expansion valve H to become liquid–vapour mixture at evaporating pressure at point 7. Then, the mixture flows through the evaporator I changing to saturated vapour at point 1 where it re-enters the first-stage compressor A1 once again. Concurrently, saturated vapour at point 8 and at intermediate pressure is available to again enter the parallel compressor A2.

Thus, the processes in this heat pump cycle are as follows:

1–2 is isentropic compression from evaporating to condensing pressure

3–4 isobaric condensation

4–5 is adiabatic expansion to intermediate pressure

6–7 is adiabatic expansion to evaporating pressure

7–1 is isobaric–isothermal evaporation

8–3 is isentropic compression

Observe that the main purpose of the flash intercooler G is to separate the liquid and vapour phases and to ensure that saturated vapour enters the suction line at point 8 and that only saturated liquid is available to enter the expansion valve H at point 6. The effect is an increased cooling effect from $h_1 - h_5$ to $h_1 - h_7$. Besides separation of liquid and vapour, the other processes occurring in the intercooler and discharge of the two compressors are as follows: isobaric mixing of discharged superheated vapours from 2 and 9 to reach point 3, isobaric–isothermal cooling from 5 to 6 and heating from 5 to 8.

The advantages of the two-stage compression heat pump with flash intercooler and compressors placed in parallel are as follows:

- Reduction of the discharge temperature
- Reduction of the compression energy loss and certainty that only saturated vapour at intermediate pressure occurs at point 8
- Increasing of the cooling effect and the ensurance that only saturated liquid at intermediate pressure enters the expansion device at point 6

The equation for mass flow rate at evaporating pressure is as follows:

$$\dot{m}_L = \frac{Q_L}{h_1 - h_7} = \frac{Q_L}{\Delta h_{17}} \tag{3.12}$$

The energy balance in the open flash intercooler leads to the equation for the mass flow rate on the high-pressure side:

$$\dot{m}_H h_5 = \dot{m}_L h_6 + \dot{m}_i h_8 = \dot{m}_L h_6 + \left(\dot{m}_H - \dot{m}_L\right) h_8 \tag{3.13}$$

$$\dot{m}_H = \dot{m}_L \frac{\Delta h_{86}}{\Delta h_{85}} = \dot{m}_L \frac{\Delta h_{87}}{\Delta h_{84}} \tag{3.14}$$

The mass flow rate at intermediate pressure is found by the difference as follows:

$$\dot{m}_i = \dot{m}_H - \dot{m}_L \tag{3.15}$$

The specific enthalpy at point 3 is found by the equation obtained from an energy balance in the convergence of points 2, 3 and 9:

$$h_3 \dot{m}_H = h_2 \dot{m}_L + h_9 \dot{m}_i \tag{3.16}$$

$$h_3 = \frac{h_2 \dot{m}_L + h_9 \left(\dot{m}_H - \dot{m}_L\right)}{\dot{m}_H} \tag{3.17}$$

The equations for compressor work on the low- and intermediate-pressure sides are as follows:

$$W_L = \dot{m}_L \left(h_2 - h_1\right) = \dot{m}_L \Delta h_{21} \tag{3.18}$$

$$W_i = \dot{m}_i \cdot (h_9 - h_8) = \dot{m}_i \Delta h_{98} \tag{3.19}$$

The total compressor work is

$$W = W_L + W_i \tag{3.20}$$

The condensing capacity equation is as follows:

$$Q_H = \dot{m}_H \cdot (h_3 - h_4) = \dot{m}_H \Delta h_{34} \tag{3.21}$$

The equations for coefficients of performance on the low- and high-pressure sides are as follows:

$$COP_L = \frac{Q_L}{W} = \frac{\dot{m}_L \Delta h_{17}}{\dot{m}_L \Delta h_{21} + \dot{m}_i \Delta h_{98}} \tag{3.22}$$

$$COP_H = \frac{Q_H}{W} = \frac{\dot{m}_H \Delta h_{34}}{\dot{m}_L \Delta h_{21} + \dot{m}_i \Delta h_{98}} \tag{3.23}$$

3.3 Two-Stage Compression Heat Pump with Open Flash Intercooler and Compressors in Series

Figure 3.3 presents the layout and cycle to the two-stage heat pump system with an open flash intercooler supplying saturated vapour between the compressors placed in series to each other.

The main features of the open flash intercooler are improving the cooling effect by supplying only saturated liquid for throttling and reducing the second-stage compressor discharge temperature. This occurs as the flash intercooler supplies saturated vapour that mixes with the superheated vapour discharged by the first-stage compressor.

Figure 3.3a illustrates the heat pump layout, and the numbers in the components inlet and outlet are the same as the numbers in the cycle.

Figure 3.3b shows the heat pump cycle in the pressure versus enthalpy diagram. The saturated vapour at point 1 enters the compressor A1 and exits as superheated vapour at intermediate pressure at point 2. This vapour is desuperheated to point 3 by mixing it with saturated vapour supplied by the flash intercooler at point 7. From point 3, the vapour enters the second-stage compressor A2 and exits as superheated vapour at condensing pressure at point 4. This superheated vapour flows into the three-way valve B and through the condensers C and D, becomes saturated liquid and is collected in liquid receiver E. The saturated liquid at point 5 flows into the float-controlled valve F and becomes a liquid–vapour mixture at point 6 where it is released into the flash intercooler G at intermediate pressure. From the bottom of the flash intercooler, the saturated liquid at point 8 is throttled by the expansion valve H to become liquid–vapour mixture at evaporating pressure at point 9. Then, the mixture flows through the evaporator I, changing phase to saturated vapour at point 1 and re-enters the first-stage compressor again.

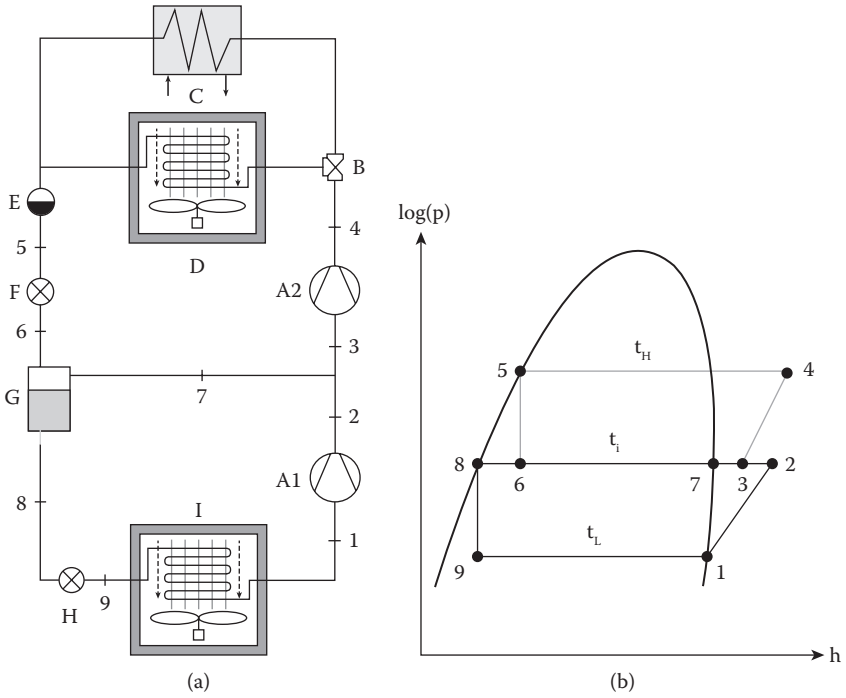

FIGURE 3.3
Two-stage heat pump system with flash chamber. (a) Main components: A1 – first-stage compressor, A2 – second-stage compressor, B – three-way valve, C – external condenser, D – condenser or air heater with the drying channel, E – liquid receiver, F – expansion valve, G – flash chamber, H – expansion valve, I – evaporator or air cooler with the drying channel. (b) Cycle in the pressure versus enthalpy diagram.

The processes in this heat pump cycle are as follows:

1–2 is isentropic first-stage compression to intermediate pressure
3–4 is isentropic second-stage compression to condensing pressure
4–5 is isobaric condensation
5–6 is adiabatic expansion to intermediate pressure
8–9 is adiabatic expansion to evaporating pressure
9–1 is isobaric and isothermal evaporation

Observe that two additional processes occur due to the flash intercooler G: 6 to 7 is separation of the saturated vapour fraction and 6 to 8 is separation of the sub-cooled liquid fraction. The liquid flows through the float-controlled valve F and flashes at intercooler G into vapour and liquid fractions. Thus, the purpose of the flash intercooler is the separation of saturated vapour and liquid. The saturated vapour fraction is formed by transfer of enthalpy from the liquid phase that becomes saturated at evaporating pressure. The major effect of supplying only saturated liquid to the expansion valve H is the increasing of the cooling effect from $h_1 - h_6$ to $h_1 - h_9$.

The advantages of heat pump system are as follows:

- Lower pressure ratio
- Increased cooling effect with the practical importance of a lower cost and smaller first-stage compressor
- Reduction of the discharge temperature and shaft work for the second compressor

The equation for the mass flow rate at the evaporator is as follows:

$$\dot{m}_L = \frac{Q_L}{h_1 - h_9} = \frac{Q_L}{\Delta h_{19}} \tag{3.24}$$

The energy balance in the flash intercooler leads to the mass flow rates

$$\dot{m}_H \cdot h_6 = \dot{m}_L \cdot h_8 + (\dot{m}_H - \dot{m}_L) \cdot h_7 \tag{3.25}$$

$$\dot{m}_H = \dot{m}_L \frac{\Delta h_{78}}{\Delta h_{76}} = \dot{m}_L \frac{\Delta h_{79}}{\Delta h_{75}} \tag{3.26}$$

The enthalpy at point 3 is unknown, and it results from mixing superheated and saturated vapours from points 2 and 7, respectively. It is determined by energy balance at the convergence of these three points as follows:

$$h_3 \dot{m}_H = h_2 \dot{m}_L + h_7 \dot{m}_i \tag{3.27}$$

$$h_3 = \frac{h_2 \dot{m}_L + h_7 (\dot{m}_H - \dot{m}_L)}{\dot{m}_H} \tag{3.28}$$

The equations for low, high and total work for the compressors are as follows:

$$W_L = \dot{m}_L (h_2 - h_1) = \dot{m}_L \Delta h_{21} \tag{3.29}$$

$$W_H = \dot{m}_H (h_4 - h_3) = \dot{m}_H \Delta h_{43} \tag{3.30}$$

$$W = \dot{m}_L \Delta h_{21} + \dot{m}_H \Delta h_{43} = W_L + W_H \tag{3.31}$$

The equation for the condensation capacity is as follows:

$$Q_H = \dot{m}_H (h_4 - h_5) = \dot{m}_H \Delta h_{45} \tag{3.32}$$

The equations for the coefficients of performance are as follows:

$$COP_L = \frac{\dot{m}_L \Delta h_{19}}{W_L + W_H} = \frac{Q_L}{W} \tag{3.33}$$

$$COP_H = \frac{\dot{m}_H \Delta h_{45}}{W_L + W_H} = \frac{Q_H}{W} \tag{3.34}$$

3.4 Two-Stage Heat Pump with Single Screw Compressor and Economiser

Figure 3.4 shows the system with a single screw compressor having the features of reciprocating and turbo compressors. The system also has double throttling valves connected to an intermediate-pressure economiser.

Figure 3.4a presents the layout of the system, and the numbers in the inlet and outlet of the components correspond to the numbers in the cycle.

Figure 3.4b shows the heat pump cycle in the pressure versus enthalpy diagram. The cycle starts at point 1 with saturated vapour that enters the screw compressor A and is discharged to intermediate pressure at point 2. This vapour is mixed with saturated vapour taken from the economiser at point 7. From point 3, the mixture is compressed and discharged as superheated vapour at condensing pressure at point 4. The vapour enters the three-way valve B and at the condensers C and D becomes saturated liquid that is collected by the receiver E. The saturated liquid at point 5 flows into the float-controlled valve F to become a liquid–vapour mixture at point 6 and enters the economiser G at intermediate pressure. From the bottom of the economiser the saturated liquid at point 8 is throttled by the expansion valve H to become liquid–vapour mixture at evaporating pressure at point 6. This mixture flows through the evaporator I and changes phase to saturated vapour at point 1 where it enters the screw compressor again.

The processes in this cycle are as follows:

1–2 is isentropic compression from evaporating to intermediate pressure

3–4 is isentropic compression from intermediate to condensing pressure

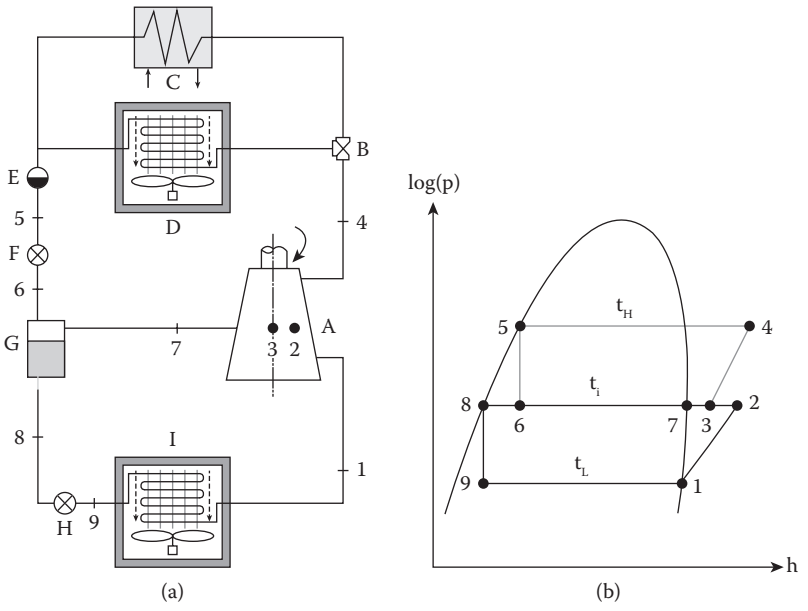

FIGURE 3.4
Two-stage heat pump with flash chamber and single screw compressor. (a) Main components: A – screw compressor, B – three-way valve, C – external condenser, D – condenser or air heater with the drying channel, E – liquid receiver, F – float-controlled expansion valve, G – economiser, H – expansion valve, I – evaporator or air cooler with the drying channel. (b) Cycle in the pressure versus enthalpy diagram.

4–5 isobaric condensation

5–6 is adiabatic expansion to intermediate pressure

8–9 is adiabatic expansion to evaporating pressure

9–1 is isobaric–isothermal evaporation

In addition to vapour and liquid separation, the additional processes occurring in the economiser are as follows: isobaric mixing of superheated and saturated vapours in the screw compressor from point 2 to 3 and 7 to 3 and isobaric–isothermal cooling and heating in the economiser from point 6 to 8 and 6 to 7.

The benefit of this heat pump system is low-pressure ratio and two-stage vapour compression performed by a single compressor. Similarly to the previous system, the other advantages are as follows:

- Increasing of the cooling effect
- Reduction in the discharge temperature
- Smaller compression ratio and lower energy loss

The calculations for this system are similar to those performed in Problem 3.3 for two-stage vapour compression heat pump with open flash intercooler.

The main problem of this system is the high discharged vapour temperature and consequent compression energy loss. This problem is solved by a two-stage compression heat pump with flash intercooler that is examined next.

3.5 Two-Stage Compression Heat Pump with Closed Intercooler for Combined Sub-Cooling and Desuperheating

Figure 3.5 illustrates the heat pump system. It has a closed intercooler with the following functions: sub-cooling of the liquid as it flows in a pipe connecting the liquid receiver and the expansion valve and desuperheating to saturation of the vapour discharged by the first-stage compressor.

Figure 3.5a shows the system layout and the numbers in the inlet and outlet of the components that are similar to the numbers in the cycle.

Figure 3.5b presents the heat pump cycle in the pressure versus enthalpy diagram. The saturated vapour at point 1 enters the first-stage compressor A1, and it is discharged as superheated vapour at point 2 where it flows into the pipe with terminal perforations G. This superheated vapour bubbles through the holes in the pipe segment immersed in the liquid held in the intercooler H. The mixture formed is separated into saturated vapour and sub-cooled liquid fractions. The saturated vapour enters the suction line at point 3 and then into the second-stage compressor A2 where is discharged as superheated vapour at point 4. Then, the vapour flows through the three-way valve B and into condensers C and D, changes phase to saturated liquid and is collected in the liquid receiver E.

From liquid receiver at point 5, the saturated liquid moves in two directions. First, the liquid flows through the float-controlled valve F and becomes a mixture at point 6. The mixture enters the closed intercooler H and is separated into saturated vapour and liquid fractions. Part of the liquid fraction remains in the intercooler at point 9 to maintain

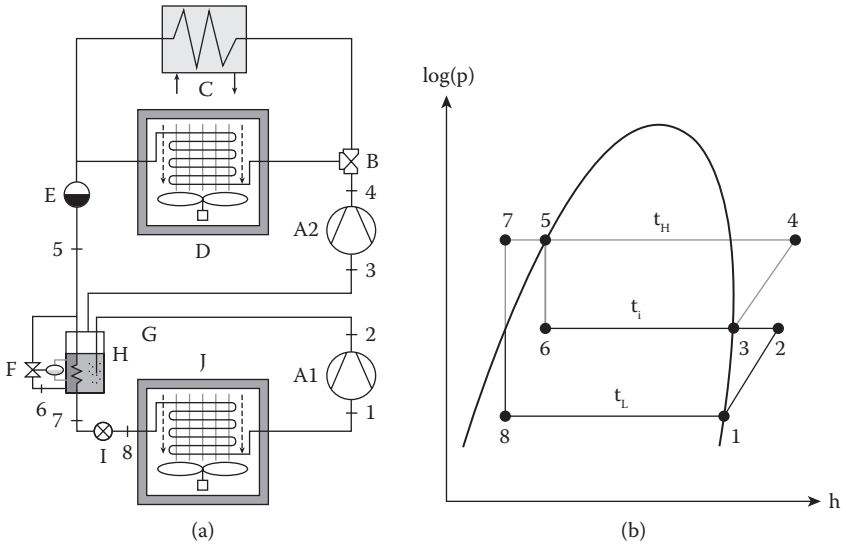

FIGURE 3.5
Two-stage heat pump with closed intercooler for combined sub-cooling and desuperheating. (a) Main components: A1 – first-stage compressor, A2 – second-stage compressor, B – three-way valve, C – external condenser, D – condenser or air heater with the drying channel, E – liquid receiver, F – float-controlled expansion valve, G – perforated pipe for bubbling vapour, H – closed intercooler, I – expansion valve, J – evaporator or air cooler with the drying channel. (b) Cycle in the pressure versus enthalpy diagram.

a constant liquid level while the saturated vapour enters the suction line of the second-stage compressor A2 again.

Second, the saturated liquid from point 5 flows through the coils immersed in the liquid in the intercooler H and becomes sub-cooled at point 7. From this point, it flows through the expansion valve I and becomes a vapour–liquid mixture at point 8. Then, it enters the evaporator J and changes phase to saturated vapour at point 1 to re-enter the cycle once more.

The processes in this heat pump cycle are as follows:

1–2 is isentropic first-stage compression
3–4 is isentropic second-stage compression
4–5 isobaric condensation
5–6 is adiabatic expansion from condensing to intermediate pressure
7–8 is adiabatic expansion from condensing to evaporating pressure
8–1 is isothermal and isobaric evaporation

The closed intercooler is involved in two additional processes: 5 to 7 is liquid sub-cooling in the coil immersed into the liquid in the closed intercooler, and 2 to 3 is desuperheating by vapour bubbling into liquid in the closed intercooler.

The equation for the mass flow rate at the evaporator is as follows:

$$\dot{m}_L = \frac{Q_L}{h_1 - h_8} = \frac{Q_L}{\Delta h_{18}} \tag{3.35}$$

The energy balance in the closed intercooler leads to the mass flow rates

$$\dot{m}_H \cdot h_5 + \dot{m}_L \cdot h_2 = \dot{m}_h \cdot h_3 + \dot{m}_L \cdot h_7 \tag{3.36}$$

$$\dot{m}_H = \dot{m}_L \frac{\Delta h_{27}}{\Delta h_{35}} \tag{3.37}$$

The equations for low, high and total work for the compressors are as follows:

$$W_L = \dot{m}_L (h_2 - h_1) = \dot{m}_L \Delta h_{21} \tag{3.38}$$

$$W_H = \dot{m}_H (h_4 - h_3) = \dot{m}_H \Delta h_{43} \tag{3.39}$$

$$W = W_L + W_H \tag{3.40}$$

The equation for condensation capacity is as follows:

$$Q_H = \dot{m}_H (h_4 - h_5) = \dot{m}_H \Delta h_{45} \tag{3.41}$$

The equations for the coefficients of performance are as follows:

$$COP_L = \frac{\dot{m}_L \Delta h_{18}}{W_L + W_H} = \frac{Q_L}{W} \tag{3.42}$$

$$COP_H = \frac{\dot{m}_H \Delta h_{45}}{W_L + W_H} = \frac{Q_H}{W} \tag{3.43}$$

3.6 Two-Stage Vapour Compression Heat Pump with Open Intercooler

Figure 3.6 shows the layout and cycle of the two-stage vapour compression heat pump system with open intercooler and two-step throttling. The purpose of the two compressors and two throttling valves is to reduce the pressure ratio in each stage and to improve the system efficiency. The open intercooler is modified and positioned in the system layout to receive superheated vapour from the first-stage compressor, mix it with liquid and supply only saturated vapour to the second-stage compressor.

The function of the open intercooler is to then ensure that only saturated vapour is supplied to the second-stage compressor, leading to lower discharge temperature and associated energy loss. The other purpose of the intercooler is to ensure only saturated liquid flows to the expansion valve for improving the cooling effect and reducing the throttling losses.

Figure 3.6a presents the system layout and the numbers in the components of the inlet and outlet corresponding to the numbers in the cycle.

Figure 3.6b shows the cycle with open intercooler in the pressure versus enthalpy diagram. The saturated vapour at point 1 enters the first-stage compressor A1 and becomes superheated vapour at point 2 where it is discharged to the intermediate pressure at open intercooler G. From the top of intercooler, the saturated vapour at point 3 is compressed

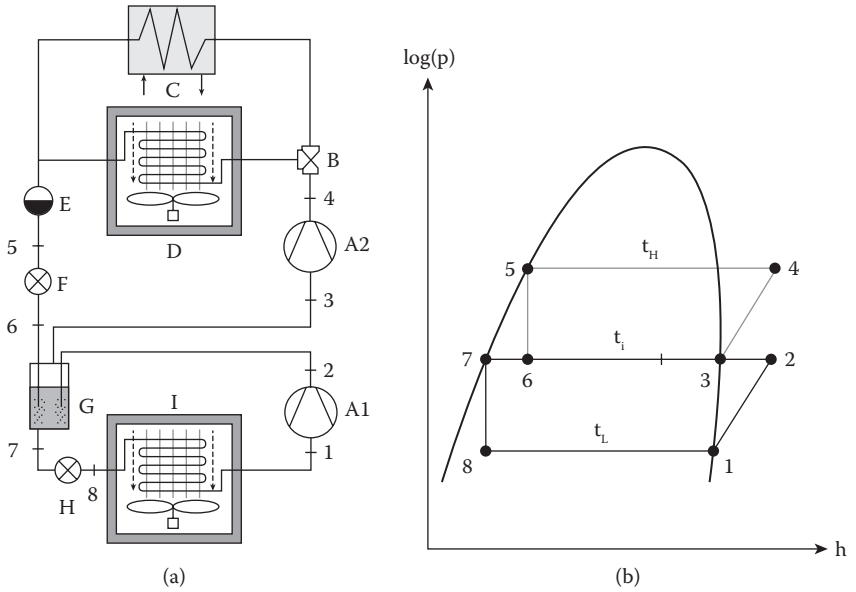

FIGURE 3.6
Two-stage vapour compression heat pump system with open intercooler. (a) Main components: A1 – low-pressure compressor, A2 – high-pressure compressor, B – three-way valve, C – external condenser, D – condenser or air heater with drying channel, E – liquid receiver, F – float-controlled expansion valve, G – open intercooler, H – expansion valve, I – evaporator or air cooler with drying channel. (b) Schematic of the cycle with open flash intercooler in the pressure versus enthalpy diagram.

A2 to superheated vapour at point 4. From the three-way valve B, the vapour flows through the condensers C or D, changes phase to liquid and is collected by the liquid receiver E. From point 5, the saturated liquid flows through and exits the float-controlled valve F at point 6, and then it flows as a liquid–vapour mixture into the intermediate-pressure open intercooler G. From the bottom of the intercooler, the saturated liquid at point 7 is throttled by the expansion valve H and becomes a liquid–vapour mixture at evaporating pressure at point 8. Then, the mixture flows through the evaporator I and turns to saturated vapour at point 1 and enters again the suction line of first-stage compressor.

Then, the processes in this heat pump cycle are as follows:

1–2 is isentropic first-stage compression
3–4 is isentropic second-stage compression
4–5 isobaric condensation
5–6 is adiabatic expansion to intermediate pressure
7–8 is adiabatic expansion to evaporating pressure
8–1 is isobaric–isothermal evaporation

The open intercooler is also responsible for the two additional processes: 2 to 3 is isobaric vapour desuperheating and 6 to 7 is isobaric–isothermal cooling.

The equation for the mass flow rate at the evaporator is as follows:

$$\dot{m}_L = \frac{Q_L}{h_1 - h_8} = \frac{Q_L}{\Delta h_{18}} \tag{3.44}$$

The energy balance in the closed intercooler leads the equation for mass flow rate in the condenser:

$$\dot{m}_H \cdot h_6 + \dot{m}_L \cdot h_2 = \dot{m}_h \cdot h_3 + \dot{m}_L \cdot h_7 \tag{3.45}$$

$$\dot{m}_H = \dot{m}_L \frac{\Delta h_{27}}{\Delta h_{36}} \tag{3.46}$$

The equations for low, high and total work for the compressors are as follows:

$$W_L = \dot{m}_L (h_2 - h_1) = \dot{m}_L \Delta h_{21} \tag{3.47}$$

$$W_H = \dot{m}_H (h_4 - h_3) = \dot{m}_H \Delta h_{43} \tag{3.48}$$

$$W = W_L + W_H \tag{3.49}$$

The equation for condensation capacity is as follows:

$$Q_H = \dot{m}_H (h_4 - h_5) = \dot{m}_H \Delta h_{45} \tag{3.50}$$

The equations for the coefficients of performance are as follows:

$$COP_L = \frac{\dot{m}_L \Delta h_{18}}{W_L + W_H} = \frac{Q_L}{W} \tag{3.51}$$

$$COP_H = \frac{\dot{m}_H \Delta h_{45}}{W_L + W_H} = \frac{Q_H}{W} \tag{3.52}$$

The next section presents solved problems on performance of different two-stage compression heat pump systems based on the previously developed equations and cycles.

3.7 Problems and Solutions

PROBLEM 3.1

Comparison of Performances of Two-Stage Compression Heat Pump with Gas Intercooler Operating with R717 and R134a

Consider the two-stage vapour compression heat pump system with gas cooler operating in a cycle as shown in Figure 3.1b. Make a summarised table and compare the heat pump systems operating with R717 and R134a based on mass flow rate, specific cooling effect, shaft work, condensing capacity and coefficients of performance.

Given:

Both systems operate at constant cooling capacity of 100 kW and the evaporating and condensing temperatures are −40°C and 40°C, respectively. Consider that the compressions are isentropic or constant entropy, throttling is adiabatic or constant enthalpy and the temperature at the vapour entering the second-stage compressor is the average between the intermediate saturation temperature and the temperature at state point 2.

Solution:

1. Calculation of the intermediate saturation pressure and temperature for refrigerants R717 and R134a

   Calculation of the saturation pressures, temperatures and properties of R717 and R134a obtained from the tables and graphs given in Chapter 7.

   1.1. Calculations for R717

   For evaporating temperature at −40°C, the saturation pressure is $p_L = 0.72$ bar

   For condensing temperature at 40°C, the saturation pressure is $p_H = 15.55$ bar

   The intermediate pressure is as follows:

$$p_i = \sqrt{p_L \cdot p_H} = \sqrt{0.72 \cdot 15.55} = 3.34 \text{ bar}$$

   From the saturation properties for R717 in Table 7.25, the intermediate saturation temperature is $t_i = -6.5$°C.

   1.2. Calculations for R134a

   For evaporating temperature at −40°C, the saturation pressure is $p_L = 0.52$ bar

   For condensing temperature at 40°C, the saturation pressure is $p_H = 10.16$ bar

   The intermediate pressure is as follows:

$$p_i = \sqrt{p_L \cdot p_H} = \sqrt{0.52 \cdot 10.16} = 2.29 \text{ bar}$$

   From the saturation properties for R134a in Table 7.9, the intermediate saturation temperature is $t_i = -6.6$°C.

2. Determination of the required properties for refrigerants 717 and 134a

   Table 3.1 shows the properties for R717 for a system with evaporating temperature at −40°C, intermediate temperature at −6.5°C and condensing temperature at 40°C. Table 3.2 gives the properties for R134a for evaporating temperature at −40°C, intermediate temperature at −6.6°C and condensing temperature at 40°C.

3. Calculation of temperature at state point 3

   The temperature at state point 3 is the average of the intermediate saturation temperature and superheated vapour temperature at point 2.

TABLE 3.1

Properties of R717 in the Cycle State Points for the Heat Pump with Gas Cooler

	Refrigerant and State Point					
	R717					
Property	**1**	**2**	**3**	**4**	**5**	**6**
t, °C	−40.0	60.1	26.8	150.3	40.0	−40.0
p, bar	0.72	3.34	3.34	15.55	15.55	0.72
h, kJ/kg	1568.6	1774.6	1697.8	1956.8	552.4	552.4
s, kJ/kg·K	6.8017	6.8017	6.5588	6.5588	—	—

TABLE 3.2

Properties of R134a in the Cycle State Points for the Heat Pump with Gas Cooler

	Refrigerant and State Point					
	R134a					
Property	**1**	**2**	**3**	**4**	**5**	**6**
t, °C	−40.0	3.5	−1.5	49.8	40.0	−40.0
p, bar	0.52	2.29	2.29	10.16	10.16	0.52
h, kJ/kg	372.9	402.3	397.8	429.5	256.2	256.2
s, kJ/kg·K	1.7591	1.7591	1.7427	1.7427	—	—

For R717, the temperature is as follows:

$$t_3 = 0.5(t_i + t_2) = 0.5(-6.5 + 60.1) = 26.8°C$$

For R134a, the temperature is a follows:

$$t_3 = 0.5(t_i + t_2) = 0.5(-6.6 + 3.5) = -1.5°C$$

4. Calculation of specific enthalpy differences between the state points in the cycle
   4.1. The specific enthalpy differences for R717 are as follows:

$$\Delta h_{21} = h_2 - h_1 = 1774.6 - 1568.6 = 206.0 \text{ kJ/kg}$$

$$\Delta h_{23} = h_2 - h_3 = 1774.6 - 1697.8 = 76.8 \text{ kJ/kg}$$

$$\Delta h_{43} = h_4 - h_3 = 1956.8 - 1697.8 = 259.0 \text{ kJ/kg}$$

$$\Delta h_{45} = h_4 - h_5 = 1956.8 - 552.4 = 1404.4 \text{ kJ/kg}$$

$$\Delta h_{16} = h_1 - h_6 = 1568.6 - 552.4 = 1016.2 \text{ kJ/kg}$$

   4.2. The specific enthalpy differences for R134a are as follows:

$$\Delta h_{21} = h_2 - h_1 = 402.3 - 372.9 = 29.4 \text{ kJ/kg}$$

$$\Delta h_{23} = h_2 - h_3 = 402.3 - 397.8 = 4.5 \text{ kJ/kg}$$

$$\Delta h_{43} = h_4 - h_3 = 429.5 - 397.8 = 31.7 \text{ kJ/kg}$$

$$\Delta h_{45} = h_4 - h_5 = 429.5 - 256.2 = 173.3 \text{ kJ/kg}$$

$$\Delta h_{16} = h_1 - h_6 = 372.9 - 256.2 = 116.7 \text{ kJ/kg}$$

5. Calculation of mass flow rates of circulating refrigerant
   Considering a cooling capacity of 100 kW, the mass flow rate for R717 is as follows:

$$\dot{m} = \frac{Q_L}{h_1 - h_6} = \frac{100}{1016.2} = 0.0984 \text{ kg/s}$$

   The R134a mass flow rate is as follows:

$$\dot{m} = \frac{Q_L}{h_1 - h_6} = \frac{100}{116.7} = 0.8570 \text{ kg/s}$$

6. Calculation of the total work
   6.1. Calculations for R717
   The compressors work for the low- and high-pressure sides are as follows:

$$W_L = \dot{m}(h_2 - h_1) = 0.0984 \cdot 206 = 20.3 \text{ kW}$$

$$W_H = \dot{m}(h_4 - h_3) = 0.0984 \cdot 259 = 25.5 \text{ kW}$$

   The total work is as follows:

$$W = W_L + W_H = 20.3 + 25.5 = 45.8 \text{ kW}$$

   6.2. Calculations for R134a
   The work for the low- and high-pressure stages and total work are as follows:

$$W_L = \dot{m}(h_2 - h_1) = 0.8570 \cdot 29.4 = 25.2 \text{ kW}$$

$$W_H = \dot{m}(h_4 - h_3) = 0.8570 \cdot 173.3 = 27.2 \text{ kW}$$

$$W = W_L + W_H = 25.2 + 27.2 = 52.4 \text{ kW}$$

7. Calculation of the condensing capacity
   7.1. Calculations for R717
   The condensing capacity Q_H, the heat removed by the gas cooler Q_{gc} and the total heat rejected Q_{Ht} are as follows:

$$Q_H = \dot{m}(h_4 - h_5) = 0.0984 \cdot 1404.4 = 138.2 \text{ kW}$$

$$Q_{gc} = \dot{m}(h_2 - h_3) = 0.0984 \cdot 76.8 = 7.6 \text{ kW}$$

$$Q_{Ht} = 138.2 + 7.6 = 145.8 \text{ kW}$$

This value balances correctly with sum of work and cooling capacity:

$$Q_{Ht} = Q_L + W_L + W_H = 100.0 + 45.8 = 145.8 \text{ kW}$$

7.2. Calculations for R134a

The condensing capacity and energy removed by the gas cooler are as follows:

$$Q_H = \dot{m}(h_4 - h_5) = 0.8570 \cdot 173.3 = 148.6 \text{ kW}$$

$$Q_{gc} = \dot{m}(h_2 - h_3) = 0.8570 \cdot 4.5 = 3.8 \text{ kW}$$

$$Q_{Ht} = 148.6 + 3.8 = 152.4 \text{ kW}$$

As required, this value balances correctly with sum of work and cooling capacity:

$$Q_{Ht} = Q_L + W_L + W_H = 100.0 + 52.4 = 152.4 \text{ kW}$$

8. Calculation of coefficients of performance

For the refrigerant 717, the coefficients are as follows:

$$COP_L = \frac{Q_L}{W} = \frac{100.0}{45.8} = 2.19$$

$$COP_H = \frac{Q_H}{W} = \frac{148.6}{45.8} = 3.02$$

For the refrigerant 134a, the coefficients are as follows:

$$COP_L = \frac{Q_L}{W} = \frac{100.0}{52.4} = 1.91$$

$$COP_H = \frac{Q_H}{W} = \frac{148.6}{52.4} = 2.83$$

9. Summarised table and comparison of performances

Table 3.3 gives the main parameters to compare characteristics and performances of the two-stage compression heat pump with gas cooler operating with R717 and R134a.

The coefficients of performance for the two-stage compression heat pump with gas cooler are calculated for the given evaporating and condensing temperatures. The R717 system has lower mass flow rate, lower work, higher cooling effect and higher coefficients of performance than the corresponding values for R134a.

Nevertheless, this system is unpractical and has limitations. A drawback is the uncertainty of the position of state point 3 that should be at or just slightly above the saturated temperature at the intermediate pressure. Another limit is the large

TABLE 3.3

Summary of Characteristics and Performances of the Two-Stage Compression Heat Pump with Gas Cooler

	Characteristics and COP					
Refrigerant	$\dot{m}$, **kg/s**	Δh_{16}, **kJ/kg**	**W, kW**	Q_H, **kW**	COP_L	COP_H
R717	0.0984	1016.2	45.8	138.2	2.19	3.02
R134a	0.8570	116.7	52.4	148.6	1.91	2.83

single-step throttling from point 5 to 6, leading to energy loss and a smaller cooling capacity. These problems are solved by the two-stage vapour compression system with a flash intercooler and two compressors in parallel, which is described next.

PROBLEM 3.2

Comparison of Performances of Two-Stage Compression Heat Pump with Flash Intercooler and Compressors in Parallel with R717 and R134a

Consider that the two-stage vapour compression heat pump with open flash intercooler and two compressors in parallel operates in a cycle as shown in Figure 3.2. Make a summarised table and compare the systems operating with R717 and R134a based on mass flow rate, specific cooling effect, shaft work, condensing capacity and coefficients of performance.

Given:

Both systems operate at constant cooling capacity of 100 kW and the evaporating and condensing temperatures are −40°C and 40°C, respectively. Consider that the compressions are isentropic and the throttling is adiabatic.

Solution:

1. Calculation of the intermediate saturation pressure and temperature for refrigerants R717 and R134a

   1.1. Calculations for R717

   Table 3.4 gives the saturated temperatures and pressures for R717, which were previously calculated in Problem 3.1.

   1.2. Calculations for R134a

   Table 3.5 gives the saturated temperatures and pressures for R134a as previously calculated.

2. Determination of the required properties for refrigerants 717 and 134a

   Table 3.6 shows the properties for R717 for the system with evaporating temperature at −40°C, intermediate temperature at −6.5°C and condensing temperature at 40°C. Table 3.7 lists the properties for R134a for the heat pump with evaporating temperature at −40°C, intermediate temperature at −6.6°C and condensing temperature at 40°C.

3. Calculation of specific enthalpy differences between state points in the cycle

   3.1. The specific enthalpy differences for R717 are as follows:

$$\Delta h_{21} = h_2 - h_1 = 2064.7 - 1568.7 = 496.0 \text{ kJ/kg}$$

$$\Delta h_{17} = h_1 - h_7 = 1568.7 - 331.8 = 1236.9 \text{ kJ/kg}$$

TABLE 3.4

Saturated Pressures and Temperatures for R717

Pressure Level	t, °C	p, bar
Low	−40.0	0.72
Intermediate	−6.5	3.34
High	40.0	15.55

TABLE 3.5

Saturated Pressures and Temperatures for R134a

Pressure Level	t, °C	p, bar
Low	−40.0	0.52
Intermediate	−6.6	2.29
High	40.0	10.16

TABLE 3.6

Properties of R717 in the Cycle State Points for the Heat Pump with Open Flash Intercooler and Two Compressors in Parallel

	Refrigerant and State Point						
	R717						
Property	1	2	3	4	7	8	9
t, °C	−40.0	192.8	177.7	40.0	−40.0	−6.5	105.2
p, bar	0.72	15.55	15.55	15.55	0.72	3.34	15.55
h, kJ/kg	1568.7	2064.7	2026.3	552.4	331.8	1616.1	1841.0
s, kJ/kg·K	6.8017	6.8017	—	—	—	6.2697	6.2697

TABLE 3.7

Properties of R134a in the Cycle State Points for the Heat Pump with Open Flash Intercooler and Two Compressors in Parallel

	Refrigerant and State Point						
	R134a						
Property	1	2	3	4	7	8	9
t, °C	−40.0	54.4	51.4	40.0	−40.0	−6.6	45.1
p, bar	0.52	10.16	10.16	10.16	0.52	2.29	10.16
h, kJ/kg	372.9	434.8	431.4	256.2	191.3	393.3	424.2
s, kJ/kg·K	1.7591	1.7591	—	—	—	1.7260	1.7260

$$\Delta h_{84} = h_8 - h_4 = 1616.1 - 552.4 = 1063.7 \text{ kJ/kg}$$

$$\Delta h_{87} = h_8 - h_7 = 1616.1 - 331.8 = 1284.3 \text{ kJ/kg}$$

$$\Delta h_{98} = h_9 - h_8 = 1841.0 - 1616.1 = 224.9 \text{ kJ/kg}$$

3.2. The specific enthalpy differences for R134a are as follows:

$$\Delta h_{21} = h_2 - h_1 = 434.8 - 372.9 = 61.9 \text{ kJ/kg}$$

$$\Delta h_{17} = h_1 - h_7 = 372.9 - 191.3 = 181.6 \text{ kJ/kg}$$

$$\Delta h_{84} = h_8 - h_4 = 393.3 - 256.2 = 137.1 \text{ kJ/kg}$$

$$\Delta h_{87} = h_8 - h_7 = 393.3 - 191.3 = 202.0 \text{ kJ/kg}$$

$$\Delta h_{98} = h_9 - h_8 = 424.2 - 393.3 = 30.9 \text{ kJ/kg}$$

4. Calculation of mass flow rates of circulating refrigerant

   For cooling capacity of 100 kW, the mass flow rate at the evaporator for R717 is as follows:

$$\dot{m}_L = \frac{Q_L}{\Delta h_{17}} = \frac{100}{1236.9} = 0.0808 \text{ kg/s}$$

   The mass flow rate at the evaporator for R134a is as follows:

$$\dot{m}_L = \frac{Q_L}{\Delta h_{17}} = \frac{100}{181.6} = 0.5509 \text{ kg/s}$$

   From energy balance in the open flash intercooler, the mass flow rates in the high and the intermediate pressures for R717 are as follows:

$$\dot{m}_H = \dot{m}_L \frac{\Delta h_{87}}{\Delta h_{84}} = 0.0808 \frac{1284.4}{1063.7} = 0.0976 \text{ kg/s}$$

$$\dot{m}_i = \dot{m}_H - \dot{m}_L = 0.0976 - 0.0808 = 0.0168 \text{ kg/s}$$

   The mass flow rates in the high and the intermediate pressures for R134a are as follows:

$$\dot{m}_H = \dot{m}_L \frac{\Delta h_{87}}{\Delta h_{84}} = 0.5509 \frac{202}{137.1} = 0.8112 \text{ kg/s}$$

$$\dot{m}_i = \dot{m}_H - \dot{m}_L = 0.8112 - 0.5509 = 0.2603 \text{ kg/s}$$

5. Calculation of the total work

   5.1. Calculations for R717

   The compression work for the low- and the intermediate-pressure sides are as follows:

$$W_L = \dot{m}_L \Delta h_{21} = 0.0808 \cdot 496 = 40.1 \text{ kW}$$

$$W_i = \dot{m}_i \Delta h_{98} = 0.0168 \cdot 224.9 = 3.8 \text{ kW}$$

   The total work is as follows:

$$W = W_L + W_i = 40.1 + 3.8 = 43.9 \text{ kW}$$

5.2. Calculations for R134a

The work input for the low and the intermediate compressors is as follows:

$$W_L = \dot{m}_L \Delta h_{21} = 0.5509 \cdot 61.9 = 34.1 \text{ kW}$$

$$W_i = \dot{m}_i \Delta h_{98} = 0.2603 \cdot 30.9 = 8.0 \text{ kW}$$

The total work is as follows:

$$W = W_L + W_i = 34.1 + 8.0 = 42.1 \text{ kW}$$

6. Calculation of the condensing capacity

6.1. Calculations for R717

The condensing capacity requires the specific enthalpy at point 3 and the enthalpy difference between points 3 and 4:

$$h_3 = \frac{h_2 \dot{m}_L + h_9 (\dot{m}_H - \dot{m}_L)}{\dot{m}_H} = 2026.3 \text{ kJ/kg}$$

$$\Delta h_{34} = h_3 - h_4 = 2026.3 - 552.4 = 1473.9 \text{ kJ/kg}$$

The condensing capacity is as follows:

$$Q_H = \dot{m}_H \Delta h_{34} = 0.0976 \cdot 1473.9 = 143.9 \text{ kW}$$

This value is correct because it is equal to the sum of the total work and the cooling capacity as follows:

$$Q_H = Q_L + W_L + W_i = 100.0 + 43.9 = 143.9 \text{ kW}$$

6.2. Calculations for R134a

The condensing capacity requires the specific enthalpy at point 3 and the enthalpy difference between points 3 and 4:

$$h_3 \dot{m}_H = h_2 \dot{m}_L + h_9 \dot{m}_i$$

$$h_3 = \frac{h_2 \dot{m}_L + h_9 (\dot{m}_H - \dot{m}_L)}{\dot{m}_H} = 431.4 \text{ kJ/kg}$$

$$\Delta h_{34} = h_3 - h_4 = 431.4 - 256.2 = 175.2 \text{ kJ/kg}$$

The condensing capacity is as follows:

$$Q_H = \dot{m}_H \Delta h_{34} = 0.8112 \cdot 175.2 = 142.1 \text{ kW}$$

This value is also correct since it is equal to the sum of the total work and the cooling capacity:

$$Q_H = Q_L + W_L + W_i = 100.0 + 42.1 = 142.1 \text{ kW}$$

7. Calculation of coefficients of performance

7.1. Calculation of coefficients of performance for R717:

$$COP_L = \frac{Q_L}{W} = \frac{100.0}{43.9} = 2.28$$

$$COP_H = \frac{Q_H}{W} = \frac{143.9}{43.9} = 3.28$$

7.2. Calculation of coefficients of performance for R134a:

$$COP_L = \frac{Q_L}{W} = \frac{100.0}{42.1} = 2.37$$

$$COP_H = \frac{Q_H}{W} = \frac{142.1}{42.1} = 3.37$$

8. Summarised table and comparison of performances

Table 3.8 gives the main parameters to compare characteristics and performances of the two-stage vapour compression heat pump with open flash intercooler and two compressors in parallel operating with R717 and R134a.

The coefficients of performance for the two-stage vapour compression heat pump with open flash intercooler and compressors in parallel are calculated for the given evaporating and condensing temperatures. The R717 system has a lower mass flow rate and higher cooling capacity but slightly higher shaft work and lower coefficient of performance (COP) than the system with R134a.

The main problems of this system are the high vapour discharge temperature and high pressure ratio in one of the compressors, leading to energy loss. These problems are solved either by a two-stage heat pump system with open flash intercooler and two compressors in series or a screw compressor system. These heat pump systems have similar cycles and they are described next.

TABLE 3.8

Summary of Characteristics and Performances of the Two-Stage Vapour Compression Heat Pump with Open Flash Intercooler and Compressors in Parallel

	Characteristics and COP					
Refrigerant	**$\dot{m}$, kg/s**	**Δh_{17}, kJ/kg**	**W, kW**	**Q_H, kW**	**COP_L**	**COP_H**
R717	0.0976	1236.9	43.9	143.9	2.28	3.28
R134a	0.5509	181.6	42.1	142.1	2.37	3.37

PROBLEM 3.3

Performances of Two-Stage Compression Heat Pump with Open Flash Intercooler with Compressors in Series and Single Screw Compressor with Economiser with R717 and 134a

Figure 3.3 illustrates the two-stage compression heat pump with flash intercooler operating in a cycle. Make a summarised table and compare the systems operating with R717 and R134a based on mass flow rate, specific cooling effect, shaft work, condensing capacity and coefficients of performance.

Given:

Both systems operate at constant cooling capacity of 100 kW, and the evaporating and condensing temperatures are −40°C and 40°C, respectively. Consider that the compressions are isentropic and the throttling is adiabatic.

Solution:

1. Calculation of the intermediate saturation pressure and temperature for refrigerants R717 and R134a

   Tables 3.4 and 3.5 gives the saturated temperatures and pressures for R717 and R134a that were previously calculated in Problem 3.2.

2. Determination of the required properties for refrigerants 717 and 134a

   Table 3.9 gives the properties for R717 for the system with evaporating temperature at −40°C, intermediate temperature at −6.5°C and condensing temperature at 40°C.

   Table 3.10 lists the properties for R134a for the heat pump with evaporating of −40°C, intermediate temperature at −6.6°C and condensing temperature at 40°C.

3. Calculation of the specific enthalpy at point 3

   The specific enthalpy at point 3 for R717 is as follows:

$$h_3 = \frac{h_2 \dot{m}_L + h_7 (\dot{m}_H - \dot{m}_L)}{\dot{m}_H} = 1747.6 \text{ kJ/kg}$$

TABLE 3.9

Properties of R717 in the Cycle State Points for the Two-Stage Compression Heat Pump with Flash Intercooler with Compressors in Series

	Refrigerant and State Point						
	R717						
Property	**1**	**2**	**3**	**4**	**5**	**7**	**9**
t, °C	−40.0	60.2	48.2	177.9	40.0	−6.5	−40.0
p, bar	0.72	3.34	3.34	15.55	15.55	3.34	0.72
h, kJ/kg	1568.7	1774.8	1747.6	2026.7	552.4	1616.1	331.8
s, kJ/kg·K	6.8017	6.8017	6.7187	6.7187	—	—	—

TABLE 3.10

Properties of R134a in the Cycle State Points for the Two-Stage Compression Heat Pump with Flash Intercooler and Compressors in Series

	Refrigerant and State Point						
	R134a						
Property	**1**	**2**	**3**	**4**	**5**	**7**	**9**
t, °C	−40.0	3.6	0.3	51.5	40.0	−6.6	−40.0
p, bar	0.52	2.29	2.29	10.16	10.16	2.29	0.52
h, kJ/kg	372.9	402.4	399.5	431.5	256.2	393.3	191.3
s, kJ/kg·K	1.7591	1.7591	1.7260	1.7260	—	—	—

For R134a,

$$h_3 = \frac{h_2\dot{m}_L + h_7\left(\dot{m}_H - \dot{m}_L\right)}{\dot{m}_H} = 399.5\ \text{kJ/kg}$$

4. Calculation of specific enthalpy differences between state points in the cycle

4.1. The specific enthalpy differences for R717 are as follows:

$$\Delta h_{21} = h_2 - h_1 = 1774.8 - 1568.7 = 206.1\ \text{kJ/kg}$$

$$\Delta h_{23} = h_2 - h_3 = 1774.8 - 1747.6 = 27.2\ \text{kJ/kg}$$

$$\Delta h_{43} = h_4 - h_3 = 2026.7 - 1747.6 = 279.1\ \text{kJ/kg}$$

$$\Delta h_{45} = h_4 - h_5 = 2026.7 - 552.4 = 1474.3\ \text{kJ/kg}$$

$$\Delta h_{19} = h_1 - h_9 = 1568.7 - 331.8 = 1236.9\ \text{kJ/kg}$$

$$\Delta h_{75} = h_7 - h_5 = 1616.1 - 552.4 = 1063.7\ \text{kJ/kg}$$

$$\Delta h_{79} = h_7 - h_9 = 1616.1 - 331.8 = 1284.3\ \text{kJ/kg}$$

4.2. The specific enthalpy differences for R134a are as follows:

$$\Delta h_{21} = h_2 - h_1 = 402.4 - 372.9 = 29.5\ \text{kJ/kg}$$

$$\Delta h_{23} = h_2 - h_3 = 402.4 - 399.5 = 2.9\ \text{kJ/kg}$$

$$\Delta h_{43} = h_4 - h_3 = 431.5 - 399.5 = 32.0\ \text{kJ/kg}$$

$$\Delta h_{45} = h_4 - h_5 = 2026.7 - 552.4 = 1474.3\ \text{kJ/kg}$$

$$\Delta h_{19} = h_1 - h_9 = 372.9 - 191.3 = 181.6\ \text{kJ/kg}$$

$$\Delta h_{75} = h_7 - h_5 = 393.3 - 256.2 = 137.1\ \text{kJ/kg}$$

$$\Delta h_{79} = h_7 - h_9 = 393.3 - 191.3 = 202.0\ \text{kJ/kg}$$

5. Calculation of mass flow rates of circulating refrigerant

   For cooling capacity of 100 kW, the mass flow rate at the evaporator for R717 is as follows:

$$\dot{m}_L = \frac{Q_L}{\Delta h_{19}} = \frac{100}{1236.9} = 0.0808 \text{ kg/s}$$

   The mass flow rate at the evaporator for R134a is as follows:

$$\dot{m}_L = \frac{Q_L}{\Delta h_{19}} = \frac{100}{181.6} = 0.5509 \text{ kg/s}$$

   From energy balance in the open flash intercooler, the high- and intermediate-pressure mass flow rates for R717 are as follows:

$$\dot{m}_H = \dot{m}_L \frac{\Delta h_{78}}{\Delta h_{76}} = \dot{m}_L \frac{\Delta h_{79}}{\Delta h_{75}} = 0.0808 \frac{1284.3}{1063.7} = 0.0976 \text{ kg/s}$$

$$\dot{m}_i = \dot{m}_H - \dot{m}_L = 0.0976 - 0.0808 = 0.0168 \text{ kg/s}$$

   The high- and intermediate-pressure mass flow rates for R134a are as follows:

$$\dot{m}_H = \dot{m}_L \frac{\Delta h_{78}}{\Delta h_{76}} = \dot{m}_L \frac{\Delta h_{79}}{\Delta h_{75}} = 0.5509 \frac{202}{137.1} = 0.8113 \text{ kg/s}$$

$$\dot{m}_i = \dot{m}_H - \dot{m}_L = 0.8113 - 0.5509 = 0.2604 \text{ kg/s}$$

6. Calculation of the total work

   6.1. Calculations for R717

   The compressor work for the low- and high-pressure sides are as follows:

$$W_L = \dot{m}_L \Delta h_{21} = 0.0808 \cdot 206.1 = 16.7 \text{ kW}$$

$$W_H = \dot{m}_H \Delta h_{43} = 0.0976 \cdot 279.1 = 27.2 \text{ kW}$$

   The total work is as follows:

$$W = W_L + W_H = 16.7 + 27.2 = 43.9 \text{ kW}$$

   6.2. Calculations for R134a

   The equations for compressor work for the low- and high-pressure sides are as follows:

$$W_L = \dot{m}_L \Delta h_{21} = 0.5509 \cdot 29.5 = 16.3 \text{ kW}$$

$$W_H = \dot{m}_H \Delta h_{43} = 0.8113 \cdot 32 = 26.0 \text{ kW}$$

The total work is as follows:

$$W = W_L + W_H = 16.3 + 26.0 = 42.3 \text{ kW}$$

7. Calculation of the condensing capacity
   For R717,

$$Q_H = \dot{m}_H \Delta h_{45} = 0.0976 \cdot 1474.3 = 143.9 \text{ kW}$$

   For R134a,

$$Q_H = \dot{m}_H \Delta h_{45} = 0.8113 \cdot 137.1 = 142.3 \text{ kW}$$

   This value agrees with the sum of the total work and the cooling capacity, and for R717 is as follows:

$$Q_H = Q_L + W_L + W_H = 100.0 + 43.9 = 143.9 \text{ kW}$$

   For R134a,

$$Q_H = Q_L + W_L + W_H = 100.0 + 42.3 = 142.3 \text{ kW}$$

8. Calculation of coefficients of performance
   8.1. Calculation of coefficients for R717:

$$COP_L = \frac{Q_L}{W} = \frac{100.0}{43.9} = 2.28$$

$$COP_H = \frac{Q_H}{W} = \frac{143.9}{43.9} = 3.28$$

   8.2. Calculation of coefficients for R134a:

$$COP_L = \frac{Q_L}{W} = \frac{100.0}{42.3} = 2.37$$

$$COP_H = \frac{Q_H}{W} = \frac{143.9}{42.3} = 3.37$$

9. Summarised table and comparison of performances
   Table 3.11 shows the main parameters to compare characteristics and performances of the two-stage compression heat pump with open flash intercooler with compressors in series and operating with R717 and R134a.
   The coefficients of performance for the two-stage vapour compression heat pump with open flash intercooler are calculated for evaporating and condensing

TABLE 3.11

Summary of Characteristics and Performances of the Two-Stage Compression Heat Pump with Open Flash Intercooler and Compressors in Series

	Characteristics and COP					
Refrigerant	$\dot{m}_L$, kg/s	Δh_{19}, kJ/kg	W, kW	Q_H, kW	COP_L	COP_H
R717	0.0808	1236.9	43.9	143.9	2.28	3.28
R134a	0.5509	181.6	42.3	142.3	2.37	3.37

temperatures of −40°C and 40°C, respectively. The R717 heat pump system has a lower mass flow rate, higher cooling effect and shaft work but lower coefficients of performance compared with the corresponding values for R134a.

The limitation of this system is that the expansion valve may underfeed the evaporator with consequent reduction in mass flow and capacity. This occurs if the flash intercooler is far from the evaporator, leading to a high pressure drop and heat gain from surroundings and liquid flashes into the expansion valve.

The additional limitation of this system is the high discharge temperature at the second-stage compressor and subsequent energy loss. These problems are solved by a system with a closed intercooler and two compressors that is covered in Section 3.5. Another solution is a two-stage heat pump with single screw compressor and an economiser that is described now.

PROBLEM 3.4

Performances of Two-Stage Compression Heat Pump with Closed Intercooler for Combined Sub-Cooling and Desuperheating with R717 and R134a

Consider the two-stage heat pump with closed intercooler for combined sub-cooling and desuperheating as illustrated in Figure 3.5. Make a summarised table and compare the systems operating with R717 and R134a based on mass flow rate, specific cooling effect, shaft work, condensing capacity and coefficients of performance.

Given:

Both systems operate at constant cooling capacity of 100 kW, and the evaporating and condensing temperatures are −40°C and 40°C, respectively. Consider that the compressions are isentropic and the throttling is adiabatic.

Solution:

1. Calculation of the intermediate saturation pressure and temperature for refrigerants R717 and R134a

   Tables 3.4 and 3.5 give the saturated temperatures and pressures for R717 and R134a that were previously calculated in Problem 3.2.

2. Determination of the required properties for refrigerants 717 and 134a

   Table 3.12 shows the properties for R717 for the heat pump system with evaporating temperature at −40°C, intermediate temperature at −6.5°C and condensing temperature at 40°C. Table 3.13 lists the properties for R134a for the heat pump with evaporating temperature at −40°C, intermediate temperature at −6.6°C and condensing temperature at 40°C.

TABLE 3.12

Properties of R717 in the Cycle State Points for the Two-Stage Heat Pump with Closed Intercooler for Combined Sub-Cooling and Desuperheating

	Refrigerant and State Point						
	R717						
Property	**1**	**2**	**3**	**4**	**5**	**7**	**8**
t, °C	−40.0	60.1	−6.5	105.2	40.0	36.0	−40.0
p, bar	0.72	3.34	3.34	15.55	15.55	15.55	0.72
h, kJ/kg	1568.7	1774.6	1616.1	1841.0	552.4	532.7	532.7
s, kJ/kg·K	6.8017	6.8017	6.2697	6.2697	—	—	—

TABLE 3.13

Properties of R134a in the Cycle State Points for the Two-Stage Heat Pump with Closed Intercooler for Combined Sub-Cooling and Desuperheating

	Refrigerant and State Point						
	R134a						
Property	**1**	**2**	**3**	**4**	**5**	**7**	**8**
t, °C	−40.0	3.5	−6.6	45.1	40.0	36.0	−40.0
p, bar	0.52	2.29	2.29	10.16	10.16	10.16	0.52
h, kJ/kg	372.9	402.3	393.3	424.2	256.2	250.2	250.2
s, kJ/kg·K	1.7591	1.7591	1.7260	1.7260	—	—	—

3. Calculation of specific enthalpy differences between state points in the cycle

3.1. The specific enthalpy differences for R717 are as follows:

$$\Delta h_{21} = h_2 - h_1 = 1774.6 - 1568.7 = 205.9 \text{ kJ/kg}$$

$$\Delta h_{23} = h_2 - h_3 = 1774.6 - 1616.1 = 158.5 \text{ kJ/kg}$$

$$\Delta h_{27} = h_2 - h_7 = 1774.6 - 532.7 = 1241.9 \text{ kJ/kg}$$

$$\Delta h_{43} = h_4 - h_3 = 1841.0 - 1616.1 = 224.9 \text{ kJ/kg}$$

$$\Delta h_{35} = h_3 - h_5 = 1616.1 - 552.4 = 1063.7 \text{ kJ/kg}$$

$$\Delta h_{45} = h_4 - h_5 = 1841.0 - 552.4 = 1288.6 \text{ kJ/kg}$$

$$\Delta h_{57} = h_5 - h_7 = 552.4 - 532.7 = 19.7 \text{ kJ/kg}$$

$$\Delta h_{18} = h_1 - h_8 = 1568.7 - 532.7 = 1036.0 \text{ kJ/kg}$$

3.2. The specific enthalpy differences for R134a are as follows:

$$\Delta h_{21} = h_2 - h_1 = 402.3 - 372.9 = 29.4 \text{ kJ/kg}$$

$$\Delta h_{23} = h_2 - h_3 = 402.3 - 393.3 = 9.0 \text{ kJ/kg}$$

$$\Delta h_{27} = h_2 - h_7 = 402.3 - 250.2 = 152.1 \text{ kJ/kg}$$

$$\Delta h_{43} = h_4 - h_3 = 424.2 - 393.3 = 30.9 \text{ kJ/kg}$$

$$\Delta h_{43} = h_4 - h_3 = 424.2 - 393.3 = 30.9 \text{ kJ/kg}$$

$$\Delta h_{35} = h_3 - h_5 = 393.3 - 256.2 = 137.1 \text{ kJ/kg}$$

$$\Delta h_{45} = h_4 - h_5 = 424.2 - 256.2 = 168.0 \text{ kJ/kg}$$

$$\Delta h_{57} = h_5 - h_7 = 256.2 - 250.2 = 6.0 \text{ kJ/kg}$$

$$\Delta h_{18} = h_1 - h_8 = 372.9 - 250.2 = 122.7 \text{ kJ/kg}$$

4. Calculation of mass flow rates of circulating refrigerant

   For cooling capacity of 100 kW, the mass flow rate at the evaporator for R717 is as follows:

$$\dot{m}_L = \frac{Q_L}{\Delta h_{18}} = \frac{100}{1036} = 0.0965 \text{ kg/s}$$

   The mass flow rate at the evaporator for R134a is as follows:

$$\dot{m}_L = \frac{Q_L}{\Delta h_{18}} = \frac{100}{122.7} = 0.8155 \text{ kg/s}$$

   From an energy balance in the closed intercooler, the high- and intermediate-pressure mass flow rates for R717 are as follows:

$$\dot{m}_H = \dot{m}_L \frac{\Delta h_{27}}{\Delta h_{35}} = 0.0965 \frac{1241.9}{1063.7} = 0.1127 \text{ kg/s}$$

$$\dot{m}_i = \dot{m}_H - \dot{m}_L = 0.0965 - 0.1127 = 0.0162 \text{ kg/s}$$

   The high- and intermediate-pressure mass flow rates for R134a are as follows:

$$\dot{m}_H = \dot{m}_L \frac{\Delta h_{27}}{\Delta h_{35}} = 0.8155 \frac{152.1}{137.1} = 0.9041 \text{ kg/s}$$

$$\dot{m}_i = \dot{m}_H - \dot{m}_L = 0.9041 - 0.8155 = 0.0886 \text{ kg/s}$$

5. Calculation of the total work

   5.1. Calculations for R717

   The equations for compressor work for the low- and the high-pressure sides are as follows:

$$W_L = \dot{m}_L \Delta h_{21} = 0.0965 \cdot 205.9 = 19.9 \text{ kW}$$

$$W_H = \dot{m}_H \Delta h_{43} = 0.1127 \cdot 224.9 = 25.3 \text{ kW}$$

The total work is as follows:

$$W = W_L + W_H = 19.9 + 25.3 = 45.2 \text{ kW}$$

5.2. Calculations for R134a

The equations for compressor work for the low- and the high-pressure sides are as follows:

$$W_L = \dot{m}_L \Delta h_{21} = 0.8155 \cdot 29.4 = 24.0 \text{ kW}$$

$$W_H = \dot{m}_H \Delta h_{43} = 0.9041 \cdot 30.9 = 27.9 \text{ kW}$$

The total work is as follows:

$$W = W_L + W_H = 24.0 + 27.9 = 51.9 \text{ kW}$$

6. Calculation of the condensing capacity

For R717,

$$Q_H = \dot{m}_H \Delta h_{45} = 0.1127 \cdot 1288.6 = 145.2 \text{ kW}$$

For R134a,

$$Q_H = \dot{m}_H \Delta h_{45} = 0.9041 \cdot 168.0 = 151.9 \text{ kW}$$

This value is correct since it is equal to the sum of the total work and the cooling capacity, and for R717 is as follows:

$$Q_H = Q_L + W_L + W_H = 100.0 + 45.2 = 145.2 \text{ kW}$$

For R134a,

$$Q_H = Q_L + W_L + W_H = 100.0 + 51.9 = 151.9 \text{ kW}$$

7. Calculation of coefficients of performance

7.1. Calculation of coefficients of performance for R717:

$$COP_L = \frac{Q_L}{W} = \frac{100.0}{45.2} = 2.21$$

$$COP_H = \frac{Q_H}{W} = \frac{145.2}{45.2} = 3.21$$

7.2. Calculation of coefficients of performance for R134a:

$$COP_L = \frac{Q_L}{W} = \frac{100.0}{51.9} = 1.93$$

TABLE 3.14

Summary of Characteristics and Performances of the Two-Stage Heat Pump with Closed Intercooler for Combined Sub-Cooling and Desuperheating

	Characteristics and COP					
Refrigerant	$\dot{m}_L$, **kg/s**	Δh_{18}, **kJ/kg**	**W, kW**	Q_H, **kW**	COP_L	COP_H
R717	0.0965	1036.0	45.2	145.2	2.21	3.21
R134a	0.8155	122.7	51.9	151.9	1.93	2.93

$$COP_H = \frac{Q_H}{W} = \frac{151.9}{51.9} = 2.93$$

8. Summarised table and comparison of performances

   Table 3.14 shows the main parameters to compare characteristics and performances of the two-stage heat pump with closed intercooler for combined sub-cooling and desuperheating operating with R717 and R134a.

   The coefficients of performance for the systems are calculated for an evaporating temperature at −40°C and condensing temperature at 40°C. The R717 system has lower mass flow rate and shaft work, higher cooling effect, and condensing capacity and higher coefficients of performance than the values for the system with R134a.

   It was seen that the closed intercooler combined with cooling and desuperheating has the advantages of higher cooling effect due to liquid sub-cooling before expansion, smaller discharge temperature by the second-stage compressor, higher compressor isentropic efficiency and lower compression losses.

   However, there are problems with this system. The first problem is the requirement of a safety valve that must be activated during shut down otherwise the intercooler liquid level overflows, causing damage to the compressors. The second problem is the large energy loss due to a single-step expansion from point 7 to 8.

   We proceed to solve these and previous problems with the alternative choice of a two-stage vapour compression system and a modified open intercooler.

PROBLEM 3.5

Comparison of Performances of a Two-Stage Vapour Compression Heat Pump with Open Intercooler Operating with R717 and R134a

Consider the two-stage vapour compression heat pump system with open intercooler and two-step throttling as shown in Figure 3.6. Make a summarised table and compare the systems operating with R717 and R134a based on mass flow rate, specific cooling effect, shaft work, condensing capacity and coefficients of performance.

Given:

Both systems operate at constant cooling capacity of 100 kW and the evaporating and condensing temperatures are −40°C and 40°C, respectively. Consider that the compressions are isentropic and the throttling is adiabatic.

Solution:

1. Calculation of the intermediate saturation pressure and temperature for refrigerants R717 and R134a

   Tables 3.4 and 3.5 give the saturated temperatures and pressures for R717 and R134a that were previously calculated in Problem 3.2.

2. Determination of the required properties for refrigerants 717 and 134a

   Table 3.15 lists the properties for R717 for the system with evaporating temperature at −40°C, intermediate temperature at −6.5°C and condensing temperature at 40°C. Table 3.16 shows the properties for R134a for the heat pump with evaporating temperature at −40°C, intermediate temperature at −6.6°C and condensing temperature at 40°C.

3. Calculation of specific enthalpy differences between state points in the cycle

   3.1. The specific enthalpy differences for R717 are as follows:

$$\Delta h_{21} = h_2 - h_1 = 1774.6 - 1568.7 = 205.9 \text{ kJ/kg}$$

$$\Delta h_{23} = h_2 - h_3 = 1774.6 - 1616.1 = 158.5 \text{ kJ/kg}$$

$$\Delta h_{27} = h_2 - h_7 = 1774.6 - 331.8 = 1442.9 \text{ kJ/kg}$$

$$\Delta h_{35} = h_3 - h_5 = 1616.1 - 552.4 = 1063.7 \text{ kJ/kg}$$

$$\Delta h_{43} = h_4 - h_3 = 1841.0 - 1616.1 = 224.9 \text{ kJ/kg}$$

TABLE 3.15

Properties of R717 in the Cycle State Points for the Two-Stage Heat Pump with Closed Intercooler for Combined Sub-Cooling and Desuperheating

	Refrigerant and State Point						
	R717						
Property	**1**	**2**	**3**	**4**	**5**	**7**	**8**
t, °C	−40.0	60.1	−6.5	105.2	40.0	−6.5	−40.0
p, bar	0.72	3.34	3.34	15.55	15.55	3.34	0.72
h, kJ/kg	1568.7	1774.6	1616.1	1841.0	552.4	331.8	331.8
s, kJ/kg·K	6.8017	6.8017	6.2697	6.2697	—	—	—

TABLE 3.16

Properties of R134a in the Cycle State Points for the Two-Stage Heat Pump with Open Intercooler

	Refrigerant and State Point						
	R134a						
Property	**1**	**2**	**3**	**4**	**5**	**7**	**8**
t, °C	−40.0	3.5	−6.6	45.1	40.0	−6.6	−40.0
p, bar	0.52	2.29	2.29	10.16	10.16	2.29	0.52
h, kJ/kg	372.9	402.3	393.3	424.2	256.2	191.3	191.3
s, kJ/kg·K	1.7591	1.7591	1.7260	1.7260	—	—	—

$$\Delta h_{45} = h_4 - h_5 = 1841.0 - 552.4 = 1288.6 \text{ kJ/kg}$$

$$\Delta h_{57} = h_5 - h_7 = 552.4 - 331.8 = 220.6 \text{ kJ/kg}$$

$$\Delta h_{18} = h_1 - h_8 = 1568.7 - 331.8 = 1236.9 \text{ kJ/kg}$$

3.2. The specific enthalpy differences for R134a are as follows:

$$\Delta h_{21} = h_2 - h_1 = 402.3 - 372.9 = 29.4 \text{ kJ/kg}$$

$$\Delta h_{23} = h_2 - h_3 = 402.3 - 393.3 = 9.0 \text{ kJ/kg}$$

$$\Delta h_{27} = h_2 - h_7 = 402.3 - 191.3 = 211.0 \text{ kJ/kg}$$

$$\Delta h_{35} = h_3 - h_5 = 393.3 - 256.2 = 137.1 \text{ kJ/kg}$$

$$\Delta h_{43} = h_4 - h_3 = 424.2 - 393.3 = 30.9 \text{ kJ/kg}$$

$$\Delta h_{45} = h_4 - h_5 = 424.2 - 256.2 = 168.0 \text{ kJ/kg}$$

$$\Delta h_{57} = h_5 - h_7 = 256.2 - 191.3 = 64.8 \text{ kJ/kg}$$

$$\Delta h_{18} = h_1 - h_8 = 372.9 - 191.3 = 181.6 \text{ kJ/kg}$$

4. Calculation of mass flow rates of circulating refrigerant

For cooling capacity of 100 kW, the mass flow rate at the evaporator for R717 is as follows:

$$\dot{m}_L = \frac{Q_L}{\Delta h_{18}} = \frac{100}{1236.9} = 0.0808 \text{ kg/s}$$

The mass flow rate at the evaporator for R134a is as follows:

$$\dot{m}_L = \frac{Q_L}{\Delta h_{18}} = \frac{100}{181.6} = 0.5509 \text{ kg/s}$$

From an energy balance in the open intercooler, the high- and intermediate-pressure mass flow rates for R717 are as follows:

$$\dot{m}_H = \dot{m}_L \frac{\Delta h_{27}}{\Delta h_{36}} = \dot{m}_L \frac{\Delta h_{27}}{\Delta h_{35}} = 0.0808 \frac{1242.9}{1063.7} = 0.1097 \text{ kg/s}$$

$$\dot{m}_i = \dot{m}_H - \dot{m}_L = 0.1097 - 0.0808 = 0.0288 \text{ kg/s}$$

The high- and intermediate-pressure mass flow rates for R134a are as follows:

$$\dot{m}_H = \dot{m}_L \frac{\Delta h_{27}}{\Delta h_{36}} = \dot{m}_L \frac{\Delta h_{27}}{\Delta h_{35}} = 0.5509 \frac{211.0}{137.1} = 0.8473 \text{ kg/s}$$

$$\dot{m}_i = \dot{m}_H - \dot{m}_L = 0.8473 - 0.5509 = 0.2964 \text{ kg/s}$$

5. Calculation of the total work

   5.1. Calculations for R717

   The equations for compressor work for the low- and the high-pressure sides are as follows:

$$W_L = \dot{m}_L \Delta h_{21} = 0.0808 \cdot 205.9 = 16.6 \text{ kW}$$

$$W_H = \dot{m}_H \Delta h_{43} = 0.1097 \cdot 224.9 = 24.7 \text{ kW}$$

   The total work is as follows:

$$W = W_L + W_H = 16.6 + 24.7 = 41.3 \text{ kW}$$

   5.2. Calculations for R134a.

   The equations for compressor work for the low- and the high-pressure sides are as follows:

$$W_L = \dot{m}_L \Delta h_{21} = 0.5509 \cdot 29.4 = 16.2 \text{ kW}$$

$$W_H = \dot{m}_H \Delta h_{43} = 0.8473 \cdot 30.9 = 26.1 \text{ kW}$$

   The total work is as follows:

$$W = W_L + W_H = 16.2 + 26.1 = 42.3 \text{ kW}$$

6. Calculation of the condensing capacity

   For R717,

$$Q_H = \dot{m}_H \Delta h_{45} = 0.1097 \cdot 1288.6 = 141.3 \text{ kW}$$

   For R134a,

$$Q_H = \dot{m}_H \Delta h_{45} = 0.5509 \cdot 168.0 = 142.3 \text{ kW}$$

   This value is verified with the sum of the total work and the cooling capacity, which for R717 is as follows:

$$Q_H = Q_L + W_L + W_H = 100.0 + 41.3 = 141.3 \text{ kW}$$

   For R134a,

$$Q_H = Q_L + W_L + W_H = 100.0 + 42.3 = 142.3 \text{ kW}$$

7. Calculation of coefficients of performance

7.1. Calculation of coefficients for R717:

$$COP_L = \frac{Q_L}{W} = \frac{100.0}{41.3} = 2.42$$

$$COP_H = \frac{Q_H}{W} = \frac{141.3}{41.3} = 3.42$$

7.2. Calculation of coefficients for R134a:

$$COP_L = \frac{Q_L}{W} = \frac{100.0}{42.3} = 2.36$$

$$COP_H = \frac{Q_H}{W} = \frac{142.3}{42.3} = 3.36$$

8. Summarised table and comparison of performances

Table 3.17 shows the main parameters to compare characteristics and performances of the two-stage heat pump with open intercooler and two-step throttling operating with R717 and R134a.

The coefficients of performance for the systems are calculated for evaporating and condensing temperatures at −40°C and 40°C, respectively. The R717 system has lower mass flow rate, lower shaft work and condensing capacity, higher cooling effect and higher coefficients of performance compared to the R134a system.

The enhancements of this two-stage heat pump with the open intercooler integrated to both compressors, heat exchangers and throttling devices are as follows:

- Reduction in the discharge temperature in the second-stage compressor A2
- Reduction of the energy loss and protection of the compressor A2 by certainty that only saturated vapour is available in the suction line at the intermediate pressure

TABLE 3.17

Summary of Characteristics and Performances of the Two-Stage Heat Pump with Open Intercooler and Two-Step Throttling

	Characteristics and COP					
Refrigerant	$\dot{m}_L$, **kg/s**	Δh_{18}, **kJ/kg**	**W, kW**	Q_H, **kW**	COP_L	COP_H
R717	0.0808	1236.9	41.3	141.3	2.42	3.42
R134a	0.5509	181.6	42.3	142.3	2.36	3.36

- Reduction of the expansion losses or increasing efficiency by operating with smaller pressure ratios
- Improved cooling effect by ensuring that only saturated liquid is supplied for throttling at intermediate pressure

This chapter closes with this system applied for the improved functions of ensuring that only saturated vapour enters the suction line protecting the second-stage compressor and ensuring that only saturated liquid is available for throttling into the evaporator, resulting in higher cooling capacity.

4

Design of Single-Stage Vapour Compression Heat Pump Drying

The major drawbacks of conventional medium- and high-temperature drying are energy expenditure and losses through the exhaust air. An approach in trying to reduce the energy loss is partially recycling the exhaust air to the drying chamber inlet. However, the energy recovery by this approach is insignificant due to limitations in heat gain and moisture removal by the recirculating mixture of air and vapour.

A modern alternative for substantial energy recovery with suitable drying rates is the heat pump drying technology operating with full recirculation of the exhaust air. The main features of the heat pump dryer are the ability to fully recycle exhaust air by using a closed loop design, condensation of water vapour in the air and energy transfer for boiling the refrigerant inside the evaporator, with subsequent release of this energy to the air inlet during condensation of refrigerant inside the condenser.

The single-stage vapour compression heat pump dryer applies with high coefficient of performance (COP) and specific moisture extraction ratio (SMER) for medium-temperature drying. The COP and SMER are particularly high for heat pump drying systems with medium or small temperature difference between evaporation and condensation.

The air–vapour and refrigerant loops of this heat pump dryer are interconnected mainly by the drying chamber, blower, compressor, evaporator, condensers, and three-way and throttling valves. The design of the single-stage vapour compression heat pump dryer and integration with the two loops requires the application of the laws, governing equations, cycles and processes scrutinised in Chapter 2.

The properties of the working fluid and the air and water vapour in the inlet and outlet of each component characterise the state points of heat pump and drying loop cycles. The properties of the working fluid and the properties of air and water vapour mixture are obtained from the tables, charts and psychrometric equations, or graphs given in Chapters 6 and 7 as well as by using a variety of computer software.

This chapter covers the design, dimensioning and principles of operation of single-stage vapour compression heat pump dryers operating with natural and conventional fluids.

The simplest classical drying process is the open loop that is a reference to compare more advanced heat pump drying systems. Then, Sections 4.1 to 4.3 provide an overview and comparison of classical dryers with and without recirculation of exhaust air. Sections 4.4 to 4.9 present the design and layout and discuss the performance of single-stage vapour compression heat pump dryers compared to fully or partially open loop in classical dryers.

4.1 Conventional Drying without Recirculation of the Exhaust Air

A conventional dryer in open loop or without recirculation of the exhaust air is shown in Figure 4.1. The dryer is located in a region where the ambient air temperature is 22°C and relative humidity is 50%. The air inlet temperature is 55°C and the relative humidity of the air at the chamber outlet is 65%. Consider that drying is adiabatic at atmospheric pressure and (a) sketch the state points of the heating and drying processes in the Mollier diagram, (b) determine and tabulate the psychrometric conditions for all state points, (c) estimate the dryer effectiveness ε_D (in kg/kWh) and (d) estimate the evaporation specific energy E_e (kJ/kg) and dryer thermal efficiency η_t.

Given:

$t_A = 55°C$	$\phi_C = 50\%$	$p = 101{,}325$ Pa
$t_C = 22°C$	$\phi_B = 65\%$	

Solution:

(a) Sketching the state points of the heating and drying processes in the Mollier diagram

The state points of the drying process are shown in Figure 4.2.

(b) Determining and tabulating the psychrometric conditions for all state points

Table 4.1 presents the known and unknown properties for each state point of the heating and drying process.

Since drying is adiabatic, the relations between *points A*, *B*, *C* and *S* are as follows:

$$x_A = x_C$$

$$h_A = h_B = h_S$$

At *point C*, from the given temperature and relative humidity, the other properties are as follows:

$$h_C = 42.99 \text{ kJ/kg}$$

$$x_C = 0.008223 \text{ kg/kg}$$

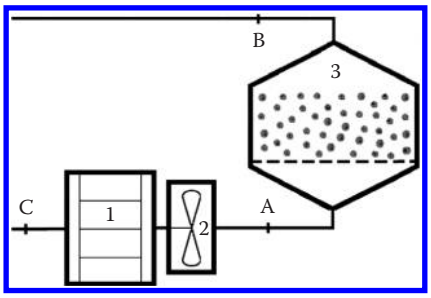

FIGURE 4.1
Conventional drying process in open loop or without recirculation of exhaust air: 1 – heater, 2 – blower, 3 – drying chamber.

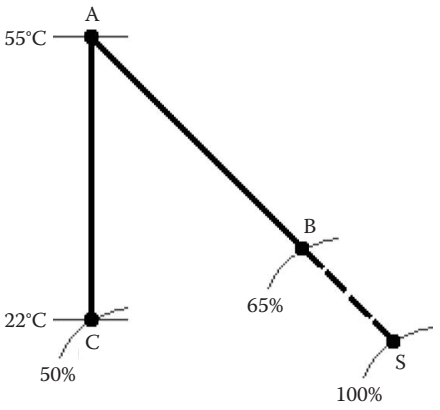

FIGURE 4.2
State points in the Mollier diagram: A – drying chamber inlet, B – drying chamber outlet, C – heater inlet or ambient condition, S – saturated air, CA – heating, AB – drying.

TABLE 4.1

Known and Unknown Properties for the State Points of the Processes

	Point			
Property	**A**	**B**	**C**	**S**
t, °C	55	Unknown	22	Unknown
ϕ, %	Unknown	65	50	100
h, kJ/kg	Unknown	Unknown	Unknown	Unknown
x, g/kg	Unknown	Unknown	Unknown	Unknown

At *point A*, using given temperature and since $x_C = x_A$, the other properties are as follows:

$$x_A = 0.008223 \text{ kg/kg}$$

$$\phi_A = 8.39\%$$

$$h_A = 76.68 \text{ kJ/kg}$$

At *point B*, from given relative humidity and since $h_A = h_B$, the other properties are as follows:

$$h_B = 76.68 \text{ kJ/kg}$$

$$t_B = 30.55°C$$

$$x_B = 0.017984 \text{ kg/kg}$$

At *point S*, from given relative humidity and since $h_A = h_S$, then

$$h_S = 76.68 \text{ kJ/kg}$$

$$t_S = 25.10°C$$

$$x_S = 0.020204 \text{ kg/kg}$$

TABLE 4.2
Psychrometric Conditions for the State Points

	Point			
Property	**A**	**B**	**C**	**S**
t, °C	55	30.55	22	25.1
ϕ, %	8.39	65	50	100
h, kJ/kg	76.68	76.68	42.99	76.68
x, g/kg	8.22	17.98	8.22	20.20

Therefore, the answer for (b) is shown in Table 4.2 obtained by using the previously determined values to fill the gaps in Table 4.1.

(c) Estimation of dryer effectiveness

The dryer effectiveness requires knowledge of specific enthalpy and absolute moisture differences, which are calculated from the data in Table 4.2:

$$\Delta h = h_A - h_C = 33.69 \text{ kJ/kg}$$

$$\Delta x = x_B - x_A = 0.009761 \text{ kg/kg}$$

Hence, the dryer effectiveness is

$$\varepsilon_D = \frac{\Delta x}{\Delta h} = 1.0430 \text{ kg/kWh}$$

(d) Estimation of the evaporation specific energy and the dryer thermal efficiency

These values are calculated using the data available in Table 4.2 as follows:

$$E_e = \frac{\Delta h}{\Delta x} = 3451.5 \text{ kJ/kg}$$

$$\eta_t = \frac{t_A - t_B}{t_A - t_S} = \frac{24.45}{29.90} = 0.8178$$

4.2 Conventional Drying with 50% Recirculation of the Exhaust Air and Constant Outlet Relative Humidity

The conventional dryer is modified to recirculate 50% of the exhaust air (or the mass ratio is 0.5) is illustrated in Figure 4.3. As in the previous case the ambient air temperature is 22°C and relative humidity is 50%. The drying chamber air inlet temperature is 55°C and exhaust relative humidity is 65%. Consider that drying is adiabatic and occurs at atmospheric pressure an (a) draw the state points of the conventional drying processes with and without 50% recirculation in the Mollier diagram; (b) determine and tabulate the psychrometric conditions for state points for drying process with recirculation; (c) estimate the dryer effectiveness ε_D (in kg/kWh); (d) estimate the evaporation specific energy E_e (kJ/kg) and dryer thermal efficiency η_t; and (e) tabulate the ε_D, E_e, and ηt values and compare the conventional drying processes with and without 50% recirculation at constant outlet relative humidity.

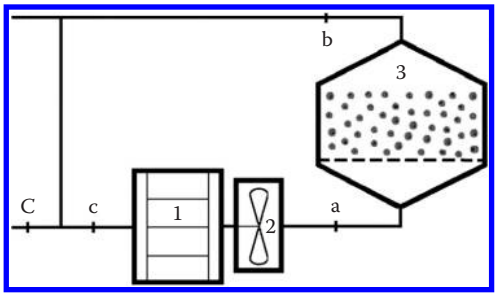

FIGURE 4.3
Conventional drying process with 50% recirculation of exhaust air: 1 – heater, 2 – blower, 3 – drying chamber.

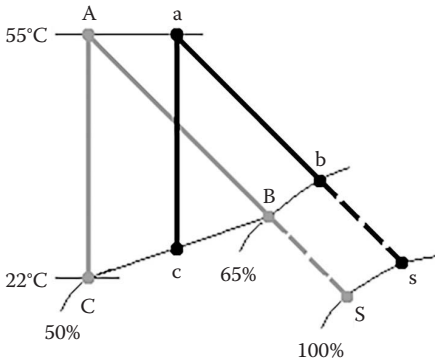

FIGURE 4.4
State points in the Mollier diagram: A, a – inlet of the drying chambers; B, b – outlet of the drying chambers; C, c – inlet of heaters; S, s – saturated air in both processes; CA, ca – heating; AB, ab – drying.

Given:

$t_a = 55°C$	$\phi_C = 50\%$	$p = 101{,}325$ Pa
$t_C = 22°C$	$\phi_b = 65\%$	$r = 0.5$

Solution:

(a) Drawing the state points of the conventional drying processes with and without 50% recirculation in the Mollier diagram

The state points of conventional drying processes with and without recirculation are represented in Figure 4.4 in uppercase and lowercase fonts, respectively.

(b) Determining and tabulating the psychrometric conditions for state points of drying process with recirculation

Table 4.3 lists the given and unknown properties for each state point the heat pump dryer.

Since drying is adiabatic, the relations between *points a, b, c* and *s* are as follows:

$$x_a = x_c$$

$$h_a = h_b = h_s$$

TABLE 4.3

Given and Unknown Properties for the State Points in the Heat Pump Drying Cycle

	Point			
Property	**a**	**b**	**c**	**s**
t, °C	55	Unknown	Unknown	Unknown
ϕ, %	Unknown	65	Unknown	100
h, kJ/kg	Unknown	Unknown	Unknown	Unknown
x, g/kg	Unknown	Unknown	Unknown	Unknown

The determination of the properties of *point c* requires knowledge of properties at *points C, A* and *B*.

At *point C*, from the given temperature and relative humidity, the other properties are found:

$$h_C = 42.99 \text{ kJ/kg}$$

$$x_C = 0.008223 \text{ kg/kg}$$

At *point A*, using given temperature and since $x_C = x_A$, the other properties are as follows:

$$x_A = 0.008223 \text{ kg/kg}$$

$$\phi_A = 8.39\%$$

$$h_A = 76.68 \text{ kJ/kg}$$

At *point B*, from given relative humidity and since $h_B = h_A$, the other properties are as follows:

$$h_B = 76.68 \text{ kJ/kg}$$

$$t_B = 30.55°C$$

$$x_B = 0.017984 \text{ kg/kg}$$

Point c results from a mixture of the air–vapour from *points B* and *C*. For a recirculation of 50% a mass and energy balance leads to the mass recirculation ratio r, x_c and h_c as follows:

$$r = \frac{\dot{m}a_B}{\dot{m}a_C} = 0.5 \quad \therefore r = \frac{x_c - x_C}{x_B - x_c} = \frac{h_c - h_C}{h_B - h_c} \quad \therefore x_c = \frac{x_B + x_C}{2} \quad \therefore h_c = \frac{h_B + h_C}{2}$$

The absolute humidity of the air–vapour mixture at *point c* is

$$x_c = \frac{x_B + x_C}{2} = \frac{0.017984 + 0.008223}{2} = 0.013104 \text{ kg/kg}$$

The specific enthalpy of the air–vapour mixture at *point c* is

$$h_c = \frac{h_B + h_C}{2} = \frac{76.68 + 42.99}{2} = 59.84 \text{ kJ/kg}$$

From psychrometry, the other temperature and relative humidity at *point c* are as follows:

$$t_c = 26.31°C$$

$$\phi_c = 61.04\%$$

At *point a*, using given temperature and since $x_c = x_a$, the other properties are as follows:

$$x_a = 0.013104 \text{ kg/kg}$$

$$\phi_a = 13.27\%$$

$$h_a = 89.39 \text{ kJ/kg}$$

At *point b*, from given relative humidity and since $h_b = h_a$, the other properties are as follows:

$$h_b = 89.39 \text{ kJ/kg}$$

$$t_b = 33.73°C$$

$$x_b = 0.021651 \text{ kg/kg}$$

At *point s*, from given relative humidity and since $h_s = h_a$, then

$$h_s = 89.39 \text{ kJ/kg}$$

$$t_s = 27.94°C$$

$$x_s = 0.024023 \text{ kg/kg}$$

Therefore, the answer for (b) is provided in Table 4.4 obtained from the previous calculations and Table 4.3.

(c) Estimation of the dryer effectiveness

The specific enthalpy and absolute moisture differences are calculated from the data in Table 4.4:

$$\Delta h = h_a - h_c = 29.55 \text{ kJ/kg}$$

$$\Delta x = x_b - x_a = 0.008547 \text{ kg/kg}$$

Hence, the dryer effectiveness is

$$\varepsilon_D = \frac{\Delta x}{\Delta h} = 1.0412 \text{ kg/kWh}$$

(d) Estimation of the evaporation specific energy and the dryer thermal efficiency

Based on the data from Table 4.4,

$$E_e = \frac{\Delta h}{\Delta x} = 3457.7 \text{ kJ/kg}$$

$$\eta_t = \frac{t_a - t_b}{t_a - t_s} = \frac{21.27}{27.06} = 0.7859$$

(e) Tabulation of the ε_D, E_e, and η_t values and comparison of the conventional drying processes with and without 50% recirculation at constant outlet relative humidity

Table 4.5 gives the performance values to compare the classical drying without recirculation (from Section 4.1) and with 50% recirculation at constant outlet relative humidity.

The comparison suggests that the conventional drying with 50% recirculation at constant absolute humidity and constant relative humidity removes about the same amount of water, uses more energy per unit mass of removed water and has lower thermal efficiency than drying without recirculation of the exhaust air. The reason for the worse performance for the recirculation case is the assumption of constant relative humidity in the outlet. The improvement in drying performance recirculation case occurs by keeping constant the absolute humidity difference causing an increase in the outlet relative humidity.

TABLE 4.4

Psychrometric Conditions for the State Points

	Point			
Property	**a**	**b**	**c**	**s**
t, °C	55	33.73	26.31	27.94
ϕ, %	13.27	65	61.04	100
h, kJ/kg	89.39	89.39	59.84	89.39
x, g/kg	13.10	21.65	13.10	24.02

TABLE 4.5

Performance Comparison for Drying Processes without and with 50% Recirculation of Exhaust Air

	Drying Process	
Performance	**Without Recirculation**	**50% Recirculation and Keeping $\phi_B = \phi_b$**
ε_D, kg/kWh	1.0430	1.0412
E_e, kJ/kg	3451.5	3457.7
η_t	0.8178	0.7859

4.3 Conventional Drying with 50% Recirculation of the Exhaust Air with Constant Absolute Humidity Difference

Compare the conventional dryer with a modified dryer to recirculate 50% of the exhaust air as shown in Figure 4.3. Consider that the absolute humidity difference between *points A* and *B* is equal the difference between *points a* and *b*. This difference is 0.009761 kg/kg. The ambient air temperature is 22°C, relative humidity is 50% and the drying chamber air inlet is 55°C. Considering that drying is adiabatic and occurs at atmospheric pressure, (a) draw the state points of the conventional drying processes with and without 50% recirculation in the Mollier diagram; (b) determine and tabulate the psychrometric conditions for the state points for drying process with recirculation; (c) estimate the dryer effectiveness ε_D (in kg/kWh); (d) estimate the evaporation specific energy E_e (kJ/kg) and dryer thermal efficiency η_t; and (e) tabulate the ε_D, E_e, and η_t values and compare the conventional drying processes with and without 50% recirculation at constant absolute humidity difference.

Given:

$t_a = 55°C$	$\Delta x = 0.009761$ kg/kg	$p = 101{,}325$ Pa	$\phi_C = 50\%$
$t_C = 22°C$	$x_B - x_A = x_b - x_a$	$r = 0.5$	

Solution:

(a) Drawing the state points of the conventional drying processes without and with 50% recirculation in the Mollier diagram

The state points of conventional drying processes without and with recirculation are represented in Figure 4.5 in capital and lower cases, respectively.

(b) Determining and tabulating the psychrometric conditions for state points of drying process with recirculation

Table 4.6 shows the known and unknown properties on each state point of process with 50% recirculation and constant absolute humidity difference.

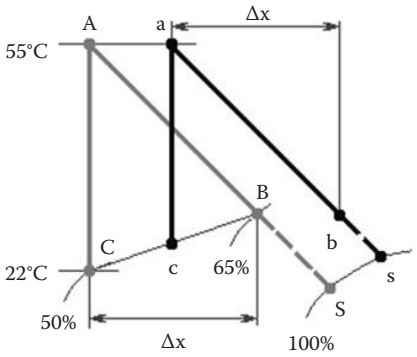

FIGURE 4.5
State points in the Mollier diagram: A, a – inlet of the drying chambers; B, b – outlet of the drying chambers; C, c – inlet of heaters; S, s – saturated air in both processes; CA, ca – heating; AB, ab – drying.

TABLE 4.6

Known and Unknown Properties for the State Points for Drying with Recirculation and Constant Absolute Humidity Difference

	Point			
Property	**a**	**b**	**c**	**s**
t, °C	55	Unknown	Unknown	Unknown
ϕ, %	Unknown	Unknown	Unknown	100
h, kJ/kg	Unknown	Unknown	Unknown	Unknown
x, g/kg	Unknown	Unknown	Unknown	Unknown

Since drying is adiabatic the relations between *points a, b, c* and *s* are:

$$x_a = x_c$$

$$h_a = h_b = h_s$$

The determination of the properties of *point c* requires knowledge of properties at *points C, A* and *B*.

At *point C* from the given temperature and relative humidity the other properties are:

$$h_C = 42.99 \text{ kJ/kg}$$

$$x_C = 0.008223 \text{ kg/kg}$$

At *point A* using given temperature and since $x_C = x_A$, the other properties are:

$$x_A = 0.008223 \text{ kg/kg}$$

$$\phi_A = 8.39\%$$

$$h_A = 76.68 \text{ kJ/kg}$$

At *point B* from given relative humidity and since $h_B = h_A$, the other properties are:

$$h_B = 76.68 \text{ kJ/kg}$$

$$t_B = 30.55°C$$

$$x_B = 0.017984 \text{ kg/kg}$$

Point c results from a mixture of the air–vapour from *points B* and *C*. For a recirculation of 50% a mass and energy balances lead to the mass flow ratio r, x_c and h_c as follows:

$$r = \frac{\dot{m}a_B}{\dot{m}a_C} = 0.5 \quad \therefore r = \frac{x_c - x_C}{x_B - x_c} = \frac{h_c - h_C}{h_B - h_c} \quad \therefore x_c = \frac{x_B + x_C}{2} \quad \therefore h_c = \frac{h_B + h_C}{2}$$

The absolute humidity of the air–vapour mixture at *point c* is as follows:

$$x_c = \frac{x_B + x_C}{2} = \frac{0.017984 + 0.008223}{2} = 0.013104 \text{ kg/kg}$$

The specific enthalpy of the air–vapour mixture at *point c* is as follows:

$$h_c = \frac{h_B + h_C}{2} = \frac{76.68 + 42.99}{2} = 59.84 \text{ kJ/kg}$$

From psychrometry, the other temperature and relative humidity at *point c* are:

$$t_c = 26.31°C$$

$$\phi_c = 61.04\%$$

At *point a* using given temperature and since $x_c = x_a$, the other properties are:

$$x_a = 0.013104 \text{ kg/kg}$$

$$\phi_a = 13.27\%$$

$$h_a = 89.39 \text{ kJ/kg}$$

At *point b* from given relative humidity and since $h_b = h_a$ the other properties are:

$$x_b = x_c + \Delta x = 0.013104 + 0.009761 = 0.022865 \text{ kg/kg}$$

$$h_b = 89.39 \text{ kJ/kg}$$

$$\phi_b = 81.02\%$$

$$t_b = 30.76°C$$

At *point s* from given relative humidity and since $h_s = h_a$, then:

$$h_s = 89.39 \text{ kJ/kg}$$

$$t_s = 27.94°C$$

$$x_s = 0.024023 \text{ kg/kg}$$

Therefore, the answer for (b) is provided in Table 4.7 based on the previous calculations and Table 4.6.

(c) Estimation of the dryer effectiveness

The specific enthalpy is calculated from the data in Table 4.7:

$$\Delta h = h_a - h_c = 29.55 \text{ kJ/kg}$$

$$\Delta x = x_b - x_a = 0.009761 \text{ kg/kg}$$

Hence, the dryer effectiveness is

$$\varepsilon_D = \frac{\Delta x}{\Delta h} = 1.1890 \text{ kg/kWh}$$

(d) Estimation of the evaporation specific energy and the dryer thermal efficiency

From the data in Table 4.7:

$$E_e = \frac{\Delta h}{\Delta x} = 3027.7 \text{ kJ/kg}$$

$$\eta_t = \frac{t_a - t_b}{t_a - t_s} = \frac{24.24}{27.06} = 0.8957$$

(e) Tabulation of the ε_D, E_e and η_t values and comparison of the conventional drying processes without and with 50% recirculation at constant absolute humidity difference

Table 4.8 shows the performances for both dryers. The values for the conventional dryer without recirculation were obtained in Section 4.1.

Comparison indicates that the conventional drying without recirculation removes less water per unit of energy, uses more energy per unit mass of removed water and has lower thermal efficiency than drying with 50% recirculation of the exhaust air while keeping a constant absolute humidity difference.

TABLE 4.7

Psychrometric Conditions for the State Points for Recirculation and Constant Absolute Humidity Difference

	Point			
Property	**a**	**b**	**c**	**s**
t, °C	55	30.76	26.31	27.94
ϕ, %	13.27	81.02	61.04	100
h, kJ/kg	89.39	89.39	59.84	89.39
x, g/kg	13.10	22.87	13.10	24.02

TABLE 4.8

Performance Data for Drying Processes without and with 50% Recirculation of Exhaust Air

	Drying Process	
Performance	**Without Recirculation**	**50% Recirculation and Keeping Constant Δx**
ε_D, kg/kWh	1.0430	1.1890
E_e, kJ/kg	3451.5	3027.7
η_t	0.8178	0.8957

This confirms that the performance of exhaust recirculation drying improves when the absolute humidity difference is kept constant due to an increasing in the outlet relative humidity.

The full energy recovery from the air–vapour exhaust and better performances are achieved by applying the heat pump dryer cases that will be examined in Sections 4.4 through 4.9.

4.4 Heat Pump Drying in a Closed Cycle

A heat pump dryer fully recirculates the exhaust air in a closed loop and it operates with the same inlet conditions as in the previous conventional dryer. Figure 4.6 shows the closed loop heat pump dryer in which the blower supplies the air that flows through the drying chamber, evaporator and condenser. The conventional drying process starts from the ambient air at temperature of 22°C and relative humidity of 50% and it is heated to 55°C at the inlet drying chamber. The water removal is 20 kg/h. The absolute humidity difference between *points A* and *B* or *a* and *b* is 0.009761 kg/kg. The heat pump fluid is ammonia or R717, the evaporating temperature is 10°C below the dew-point temperature at point a, the condensing temperature is 5°C above the inlet air temperature at *point a*, compression is isentropic ($\eta_i = 1.0$) and throttling is adiabatic (h = constant). Consider that drying is adiabatic and done at atmospheric pressure and: (a) draw the air state points for the heat pump drying cycle in the Mollier diagram, (b) determine and tabulate the psychrometric conditions for the state points of the cycle, (c) draw the heat pump cycle on the log(p)–h diagram

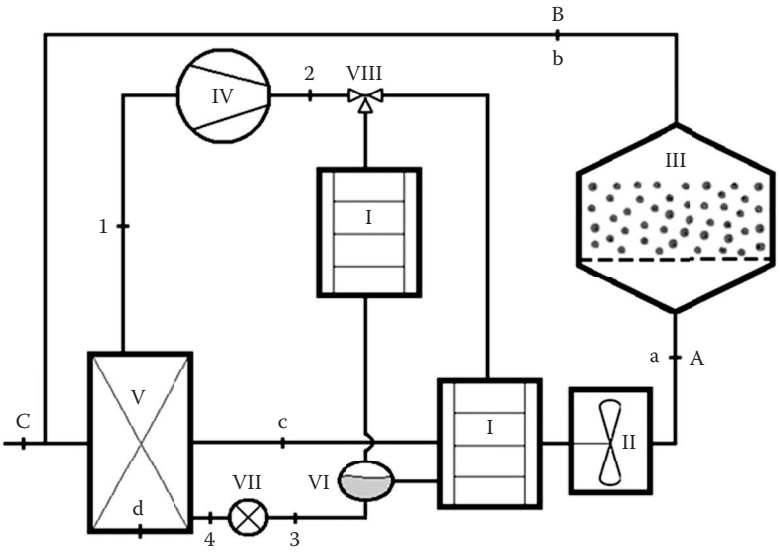

FIGURE 4.6
Heat pump drying in a closed cycle: I – condenser (heater), II – blower, III – drying chamber, IV – compressor, V – evaporator, VI – receiver, VII – throttling valve, VIII – three-way valve, 1 – saturated vapour, 2 – superheated vapour, 3 – saturated liquid, 4 – vapour and liquid mixture, A, a – inlet of the drying chambers; B, b – outlet of the drying chambers; C – inlet of air heater; c – inlet of condenser; d – evaporator surface.

and tabulate the heat pump fluid properties, (d) calculate the compressor shaft work, evaporating and condensing capacities, COP and SMER and (e) tabulate and compare the energy and water removal performances of the heat pump dryer and conventional dryer.

Given:

R717	$\phi_C = 50\%$
$t_a = 55°C$	$\phi_c = \phi_s = \phi_d = 100\%$
$t_C = 22°C$	$\Delta x = 0.009761$ kg/kg
$t_{ev} = t_d = t_{dpa} - 10°C$	p = 101,325 Pa
$t_{con} = t_a + 5°C = 60°C$	h = constant
$\dot{m}_w = 20$ kg/h	

Solution:

(a) Drawing the air state points for the heat pump drying cycle in the Mollier diagram

The state points of conventional drying without recirculation and heat pump drying processes are shown in Figure 4.7 in capital and lower case fonts, respectively.

(b) Determining and tabulating the psychrometric conditions for the state points of the cycle

Table 4.9 lists the known and unknown properties for each state point of the heat pump dryer.

The properties of *point a* are the same as at *point A*, then

$$\phi_a = 8.39\%$$

$$h_a = 76.68 \text{ kJ/kg}$$

$$x_a = 0.008223 \text{ kg/kg}$$

$$t_{dpa} = 11.11°C$$

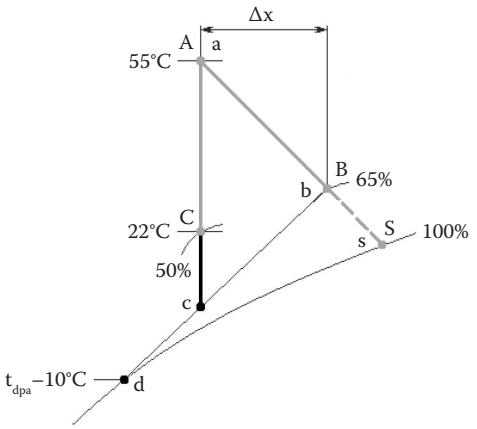

FIGURE 4.7
State points in the Mollier diagram: A, a – inlet of the drying chambers; B, b – outlet of the drying chambers; C – inlet of air heater; c – inlet of condenser; S, s – saturated air in both processes; d – evaporator surface; CA – heating; ca – heating and condensation; AB, ab – drying; bc – cooling and evaporation.

TABLE 4.9

Known and Unknown Properties for the State Points for the Heat Pump Drying Air

	Point				
Property	**a**	**b**	**C**	**d**	**s**
t, °C	55	Unknown	Unknown	Unknown	Unknown
ϕ, %	Unknown	Unknown	100	100	100
h, kJ/kg	Unknown	Unknown	Unknown	Unknown	Unknown
x, g/kg	Unknown	Unknown	Unknown	Unknown	Unknown

The properties of *point b* are:

$$x_b = x_a + \Delta x = x_a + (x_B - x_A) = 0.008223 + (0.17984 - 0.008223) = 0.017984 \text{ kg/kg}$$

$$h_b = h_a = 76.68 \text{ kJ/kg}$$

$$t_b = 30.55°C$$

$$\phi_b = 65\%$$

From the given relative humidity, the properties at *point c* are as follows:

$$x_c = x_a = 0.008223 \text{ kg/kg}$$

$$t_c = 11.11°C$$

$$h_c = 31.89 \text{ kJ/kg}$$

From the given relative humidity, the properties at *point d* are as follows:

$$t_d = t_{dpa} - 10°C = 1.11°C$$

$$h_d = 11.35 \text{ kJ/kg}$$

$$x_d = 0.004091 \text{ kg/kg}$$

From the given relative humidity, the properties at *point s* are as follows:

$$h_s = h_a = h_b = 76.68 \text{ kJ/kg (since the process is adiabatic)}$$

$$t_s = 25.10°C$$

$$x_s = 0.020204 \text{ kg/kg}$$

Therefore, the answer for (b) is presented in Table 4.10 based on Table 4.9 and the previous determined properties.

(c) Drawing the heat pump cycle on the log(p)–h diagram and tabulating the heat pump fluid properties

This requires the properties R717 in all state points of cycle in the heat pump dyer.

The known and unknown properties in the ammonia fluid cycle are listed in Table 4.11.

TABLE 4.10

Psychrometric Conditions for the State Points for the Air in Heat Pump Dryer

	Point				
Property	**a**	**b**	**c**	**d**	**s**
t, °C	55	30.55	11.11	1.11	25.10
ϕ, %	8.39	65	100	100	100
h, kJ/kg	76.68	76.68	31.89	11.35	76.68
x, g/kg	8.22	17.98	8.22	4.09	20.20

TABLE 4.11

Known and Unknown Properties for the State Points of the Heat Pump Fluid (R717)

	State Point			
Property	**1**	**2**	**3**	**4**
t, °C	1.11	Unknown	60	Unknown
p, kPa	Unknown	Unknown	Unknown	Unknown
h, kJ/kg	Unknown	Unknown	Unknown	Unknown
s, kJ/kg·K	Unknown	Unknown	Unknown	—
v, m^3/kg	Unknown	—	—	—

The other properties in the cycle are determined considering the following:

- Evaporating temperature is 1.11°C.
- Condensing temperature is 60°C.
- Compression is isentropically ($\eta_i = 1$) done on saturated vapour.
- Throttling is adiabatically ($h_3 = h_4$ = constant) done on saturated liquid.

Point 1 is saturated vapour at temperature at 1.11°C, and the other properties are as follows:

$$p_1 = 447.44 \text{ kPa}$$

$$h_1 = 1624.85 \text{ kJ/kg}$$

$$s_1 = 61.68 \text{ kJ/kg·K}$$

$$v_1 = 0.278273 \text{ m}^3/\text{kg}$$

Point 2 is superheated vapour. Since the process is isentropic, then

$$s_2 = s_1 = 61.68 \text{ kJ/kg·K}$$

The other properties are as follows:

$$p_2 = 2614.53 \text{ kPa}$$

$$t_2 = 135.95°\text{C}$$

$$h_2 = 1893.24 \text{ kJ/kg}$$

Point 3 is saturate liquid at temperature at 60°C, and the other properties are as follows:

$$p_3 = 2614.53 \text{ kPa}$$

$$h_3 = 653.72 \text{ kJ/kg}$$

$$s_3 = 25.15 \text{ kJ/kg·K}$$

Point 4 is vapour–liquid mixture after adiabatic throttling, then

$$h_4 = h_3 = 653.72 \text{ kJ/kg}$$

The other properties are as follows:

$$t_4 = t_1 = 1.11°C$$

$$p_4 = 447.44 \text{ kPa}$$

Table 4.12 presents the properties of R717 in each point of the cycle.

Now, with the data and properties in Table 4.12, the cycle for the heat pump with R717 is sketched on the log(p)–h diagram shown in Figure 4.8.

TABLE 4.12

Properties for the State Points of the Cycle for the Heat Pump with Ammonia

	State Point			
Property	**1**	**2**	**3**	**4**
t, °C	1.11	135.95	60	1.11
p, kPa	447.44	2614.53	2614.53	447.44
h, kJ/kg	1624.85	1893.24	653.72	653.72
s, kJ/kg·K	61.68	61.68	25.15	—
v, m^3/kg	0.278273	—	—	—

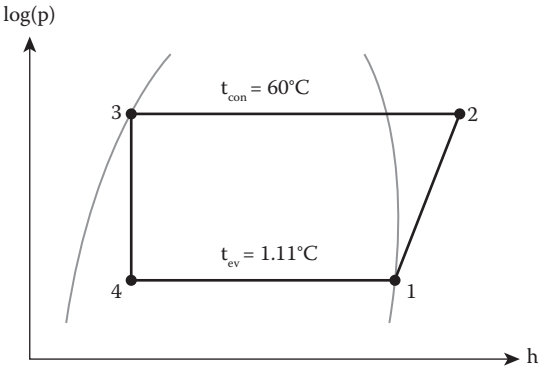

FIGURE 4.8
State points on the log(p)–h diagram. 1–2: isentropic compression, 2–3: isobaric condensation, 3–4: adiabatic throttling, 4–1: isothermal and isobaric evaporation, 1: saturated vapour, 2: superheated vapour, 3: saturated liquid, 4: vapour and liquid mixture.

(d) Calculation of compressor shaft work, evaporating and condensing capacities, and SMER

The evaporating capacity is calculated from the given water removal and the properties of the drying air–vapour in Table 4.12:

$$Q_{ev} = \dot{m}_a \Delta h = \frac{\dot{m}_w}{3600 \cdot \Delta x} \Delta h = \frac{20 \cdot 44.79}{3600 \cdot 0.009761} = 25.49 \text{ kW}$$

The refrigerant mass flow rate is determined by

$$\dot{m}_r = \frac{Q_{ev}}{h_1 - h_4} = 0.0263 \text{ kg/s}$$

Then, the compressor shaft work and the condensing capacity are as follows:

$$W = \dot{m}_r (h_2 - h_1) = 7.05 \text{ kW}$$

$$Q_{con} = \dot{m}_r (h_2 - h_3) = 32.54 \text{ kW}$$

The COP and SMER are calculated as follows:

$$COP = \frac{Q_{ev}}{W} = 3.618$$

$$SMER = COP \frac{\Delta x}{\Delta h} = 2.838 \text{ kg/kWh}$$

(e) Comparison of energy and water removal performances of the heat pump dryer and conventional dryer

The performances values for both dryers are summarised in Table 4.13.

Comparison of the data indicates that for an input of 1 kWh, the heat pump dryer removes 2.84 kg of water, whereas the conventional removes only 1.04 kg of water. In addition, the amount of paid energy for heating the drying air by the heat pump dryer is only 7.1 kW, whereas the conventional dryer uses 39.8 kW.

TABLE 4.13

Comparison of the Performances of the Conventional and Heat Pump Drying Processes

	Drying Process	
Performance	**Conventional Drying**	**Heat Pump Drying**
Heating capacity, kW	39.79 (81.8% efficient)	32.54
Cooling capacity, kW	0	25.49
Shaft work, kW	0	7.05
COP	—	3.618
SMER, kg/kWh	1.043	2.838

The reasons for the enhanced performance of the heat pump dryer are as follows: closed cycle, full recycling and condensing the vapour fraction of the exhaust air; recovery of the latent heat of condensation of the exhaust vapour; and transfer of this energy for reheating the drying air.

Sections 4.5 through 4.7 provide illustrative cases and examples on design of pilot scale heat pump drying applied to convert different wet materials into high-quality products.

4.5 Heat Pump Fluidised Bed Drying of Onion Flakes

Figure 4.9 illustrates a pilot heat pump fluidised bed dryer working with R22 refrigerant used to dry 5 × 5 × 8 mm onion flakes with a water removal rate of 30 kg/h. The drying chamber inlet air temperature and relative humidity are 40°C and 20%, respectively, and the outlet air relative humidity is 70%. The evaporating temperature is 7.78°C; the condensing temperature is 45°C; and the isentropic and volumetric efficiencies are 0.6 and 0.7, respectively. Saturated vapour is compressed and saturated liquid is throttled adiabatically. Consider that drying is adiabatic and at atmospheric pressure and (a) draw the air state points for drying air cycle in the Mollier diagram; (b) determine and tabulate the psychrometric conditions for the air state points in the cycle; (c) draw the heat pump cycle on the log(p)–h diagram and tabulate the heat pump fluid properties; (d) calculate the compressor shaft work and volumetric flow rate, evaporating and condensing capacities, COP, SMER and the total energy paid; and (e) tabulate and discuss the energy and water removal performances of the heat pump dryer.

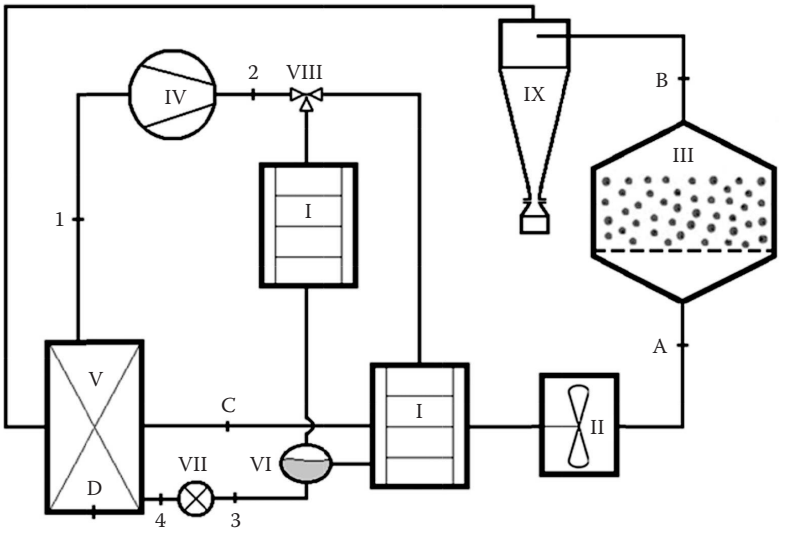

FIGURE 4.9
Heat pump fluidised bed drying: I – condensers (heaters), II – blower, III – fluidised bed drying chamber with onion flakes, IV – compressor, V – evaporator, VI – receiver, VII – throttling valve, VIII – three-way valve, IX – cyclone, 1 – saturated vapour, 2 – superheated vapour, 3 – saturated liquid, 4 – vapour and liquid mixture, A – inlet of the drying chamber, B – outlet of the drying chamber, C – inlet of condenser, D – evaporator surface.

Given:

R22	$t_A = 40°C$	$\phi_A = 20\%$	$\eta_i = 0.60$
$\dot{m}_w = 30$ kg/h	$t_{ev} = t_D = 7.78°C$	$\phi_B = 70\%$	$\lambda = 0.70$
$h_A = h_B$ = constant	$t_{con} = 45°C$	$\phi_D = 100\%$	p = 101,325 Pa

Solution:

(a) Drawing the air state points for the heat pump drying cycle in the Mollier diagram
The state points of the heat pump dryer are shown in Figure 4.10.

(b) Determining and tabulating the psychrometric conditions for the state points of the cycle
Table 4.14 gives the known and unknown properties for each state point for the heat pump dryer.
The properties of *point A* are as follows:

$$h_A = 63.86 \text{ kJ/kg}$$

$$x_A = 0.009196 \text{ kg/kg}$$

$$t_{dpA} = 12.78°C$$

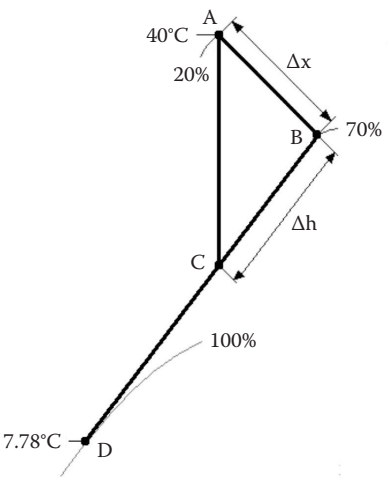

FIGURE 4.10
State points in the Mollier diagram: A – inlet of the drying chamber, B – inlet of the evaporator, C – inlet of the condenser, D – evaporator surface, CA – heating and condensation, AB – drying, BC – cooling and evaporation.

TABLE 4.14

Known and Unknown Properties for the State Points for the Heat Pump Dryer

	Point			
Property	**A**	**B**	**C**	**D**
t, °C	40	Unknown	Unknown	Unknown
ϕ, %	20	70	Unknown	100
h, kJ/kg	Unknown	Unknown	Unknown	Unknown
x, g/kg	Unknown	Unknown	Unknown	Unknown

The properties of *point B* are as follows:

$$h_B = h_A = 63.86 \text{ kJ/kg}$$

$$x_B = 0.014804 \text{ kg/kg}$$

$$t_B = 26.01°C$$

From the given relative humidity, the properties at *point D* are as follows:

$$h_D = 6.56 \text{ kJ/kg}$$

$$x_D = 0.006555 \text{ kg/kg}$$

$$t_D = 7.78°C$$

The properties at *point C* are as follows:

$$x_C = x_A = 0.009196 \text{ kg/kg}$$

$$h_C = \frac{x_C - x_D}{x_B - x_D}(h_B - h_D) + h_D = 36.96 \text{ kJ/kg}$$

$$t_C = 13.68°C$$

$$\phi_C = 94.30\%$$

The answer for (b) is given in Table 4.15 based the previous calculations and Table 4.14.

(c) Drawing the heat pump cycle on the log(p)–h diagram and tabulating the heat pump fluid properties

The drawing of the cycle in the heat pump dyer requires the properties of R22 for all state points of the heat pump drying.

The known and unknown properties in the cycle are listed in Table 4.16. The other properties in cycle are determined considering that the following:

- Evaporating temperature is 7.78°C.
- Condensing temperature is 45°C.
- Compression is done on saturated vapour and it is non-isentropic with $\eta_i = 0.60$.
- Throttling is done on saturated liquid and it is adiabatic ($h_3 = h_4$).

TABLE 4.15

Psychrometric Conditions for the State Points for the Heat Pump Drying with R22

	Point			
Property	**A**	**B**	**C**	**D**
t, °C	40.00	26.01	13.68	7.78
ϕ, %	20	70	94.30	100
h, kJ/kg	63.86	63.86	36.96	24.30
x, g/kg	9.20	14.80	9.20	6.56

TABLE 4.16

Known and Unknown Properties for the State Points of the Heat Pump with R22

	State Point				
Property	**1**	**2i**	**2**	**3**	**4**
t, °C	7.78	Unknown	Unknown	45.00	Unknown
p, kPa	Unknown	Unknown	Unknown	Unknown	Unknown
h, kJ/kg	Unknown	Unknown	Unknown	Unknown	Unknown
s, kJ/kg·K	Unknown	Unknown	Unknown	Unknown	—
v, m^3/kg	Unknown	—	—	—	—

Point 1 is saturated vapour at temperature at 7.78°C, and the other properties are as follows:

$$p_1 = 636.02 \text{ kPa}$$

$$h_1 = 408.17 \text{ kJ/kg}$$

$$s_1 = 1.74 \text{ kJ/kg·K}$$

$$v_1 = 0.037110 \text{ m}^3\text{/kg}$$

Point 2i is superheated vapour after isentropic compression, then

$$s_{2i} = s_1 = 1.74 \text{ kJ/kg·K}$$

$$p_{2i} = 1728.43 \text{ kPa}$$

The other properties are as follows:

$$t_{2i} = 61.28°\text{C}$$

$$h_{2i} = 432.95 \text{ kJ/kg}$$

Point 2 is superheated vapour. This point is non-isentropic, then

$$p_2 = 1728.43 \text{ kPa}$$

$$h_2 = h_1 + \frac{h_{2i} - h_1}{\eta_i} = 449.47 \text{ kJ/kg}$$

The other properties are as follows:

$$s_2 = 1.79 \text{ kJ/kg·K}$$

$$t_2 = 79.76°\text{C}$$

Point 3 is saturate liquid at temperature at 15°C, and the other properties are as follows:

$$p_3 = 1728.43 \text{ kPa}$$

$$h_3 = 256.46 \text{ kJ/kg}$$

$$s_3 = 1.19 \text{ kJ/kg·K}$$

Point 4 is vapour–liquid mixture following an adiabatic throttling, then

$$h_4 = h_3 = 256.46 \text{ kJ/kg}$$

The other properties are as follows:

$$t_4 = t_1 = 7.78°C$$

$$p_4 = 636.02 \text{ kPa}$$

The calculated values are inserted in Table 4.17, providing the properties in all state points of the heat pump with R22.

Table 4.17, with the properties defined in all state points of the R22 heat pump cycle, provides the data to draw the cycle on the log(p)–h diagram as sketched in Figure 4.11.

TABLE 4.17

Properties for the State Points of the Heat Pump with R22

	State Point				
Property	**1**	**2i**	**2**	**3**	**4**
t, °C	7.78	61.28	79.76	45.00	7.78
p, kPa	636.02	1728.43	1728.43	1728.43	636.02
h, kJ/kg	636.02	432.95	449.47	256.46	256.46
s, kJ/kg·K	1.74	1.74	1.79	1.19	—
v, m^3/kg	0.037110	—	—	—	—

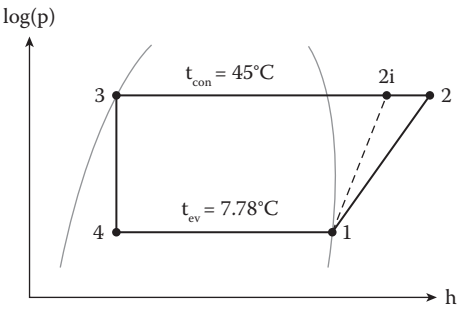

FIGURE 4.11

State points on the log(p)–h diagram. 1–2i and 1–2: isentropic and non-isentropic compression, 2–3: isobaric condensation, 3–4: adiabatic throttling, 4–1: isobaric and isothermal evaporation, 1: saturated vapour, 2: superheated vapour, 3: saturated liquid, 4: vapour and liquid mixture.

(d) Calculation of compressor shaft work and volumetric flow rate, evaporating and condensing capacities, SMER and the total energy paid

The calculation requires the data available in Tables 4.15 and 4.17:

$$\Delta x = x_B - x_A = 0.005608 \text{ kg/kg}$$

$$\Delta h = h_A - h_C = 26.90 \text{ kJ/kg}$$

$$Q_{ev} = \dot{m}_a \Delta h = \frac{\dot{m}_w}{3600 \cdot \Delta x} \Delta h = \frac{30 \cdot 26.90}{3600 \cdot 0.005608} = 39.97 \text{ kW}$$

The refrigerant mass flow rate is as follows:

$$\dot{m}_r = \frac{Q_{ev}}{h_1 - h_4} = 0.2635 \text{ kg/s}$$

The compressor shaft work is as follows:

$$W = \dot{m}_r (h_2 - h_1) = 10.88 \text{ kW}$$

The volumetric flow rate of the compressor is as follows:

$$\dot{V}_r = \frac{3600 \cdot \dot{m}_r v_1}{\lambda} = 50.28 \text{ m}^3/\text{h}$$

The condensing capacity is as follows:

$$Q_{con} = \dot{m}_r (h_2 - h_3) = 50.85 \text{ kW}$$

The COP and SMER are calculated by

$$COP = \frac{Q_{ev}}{W} = 3.674$$

$$SMER = COP \frac{\Delta x}{\Delta h} = 2.757 \text{ kg/kWh}$$

The total energy paid for heating and drying is the inverse of the shaft work,

$$E_{use} = \frac{1}{COP} 100\% = 27.2\%$$

(e) Tabulation and discussion of the energy and water removal performances of the heat pump dryer

The calculated performances of heat pump dryer are presented in Table 4.18.

The data in Table 4.18 show that the heat pump dryer uses 1 kWh to remove 2.76 kg of water.

TABLE 4.18

Energy and Water Removal Performances of the Heat Pump Drying Process

Drying Process	
Performance	**Heat Pump Drying**
Heating capacity, kW	50.85
Cooling capacity, kW	39.97
Shaft work, kW	10.88
COP	3.674
SMER, kg/kWh	2.757
Total energy paid, %	27.2

The COP indicates that the heat pump dryer uses only 27.2% of the total energy required for heating and drying. The reason for the improved performance of the heat pump dryer is a full energy recovery from exhaust vapour and using it to reheat the drying air.

4.6 Heat Pump Belt Drying of Leek Cubes

Figure 4.12 shows a pilot heat pump belt dryer working with R134a refrigerant used to dry 6-mm leek cubes at a water removal rate of 20 kg/h.

The drying chamber air temperature and relative humidity are 30°C and 25%, respectively, and the exhaust air is at 65% relative humidity. The evaporating temperature is 5°C lower than the dew-point temperature at *point A*, and the condensing temperature is 10°C above the temperature at *point A*. The isentropic and volumetric efficiencies are 0.6 and 0.7, respectively. Consider that saturated vapour is compressed, saturated liquid is adiabatically throttled, drying is adiabatic and at atmospheric pressure and (a) draw the air state points for drying air cycle in the Mollier diagram; (b) determine and tabulate the psychrometric conditions for the air–vapour state points in the cycle; (c) draw the heat pump cycle on the log(p)–h diagram and tabulate the heat pump fluid properties; (d) calculate the compressor shaft work and volumetric flow rate, evaporating and condensing capacities, COP, SMER and the total energy paid; and (e) tabulate and discuss the energy and water removal performances of the heat pump dryer with R134a.

Given:

R134a	$t_A = 30°C$	$\phi_A = 25\%$	$\eta_i = 0.60$
$\dot{m}_w = 20$ kg/h	$t_{ev} = t_D = t_{dpA} - 5°C$	$\phi_B = 65\%$	$\lambda = 0.70$
$h_A = h_B$ = constant	$t_{con} = t_A + 10°C = 40°C$	$\phi_D = 100\%$	p = 101,325 Pa

Solution:

(a) Drawing the air state points for the heat pump drying cycle in the Mollier diagram
The state points of the heat pump drying processes are represented in Figure 4.13.

(b) Determining and tabulating the psychrometric conditions for the state points of the cycle

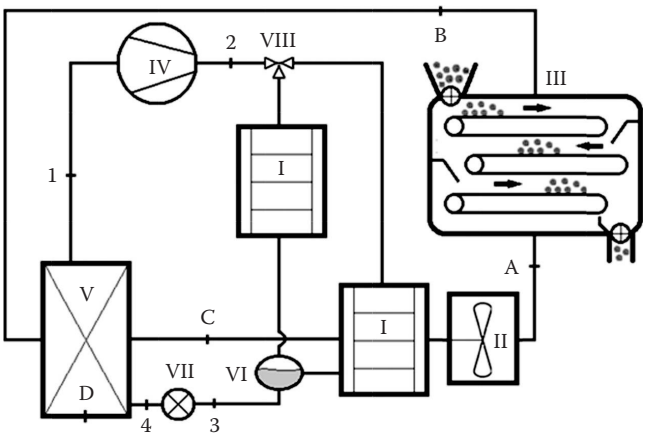

FIGURE 4.12
Heat pump belt dryer with R134a: I – condensers (heaters), II – blower, III – belt dryer with leek cubes, IV – compressor, V – evaporator, VI – receiver, VII – throttling valve, VIII – three-way valve, 1 – saturated vapour, 2 – superheated vapour, 3 – saturated liquid, 4 – vapour and liquid mixture, A – inlet of the drying chamber, B – inlet of the evaporator, C – inlet of condenser, D – evaporator surface.

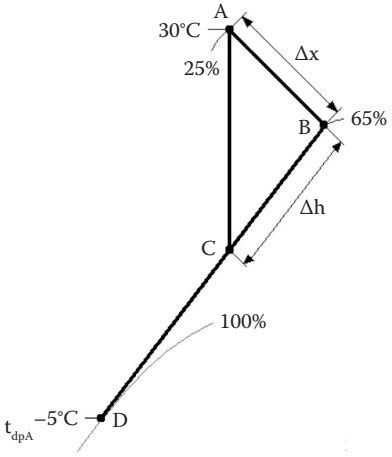

FIGURE 4.13
State points in the Mollier diagram: A – inlet of the drying chamber, B – inlet of the evaporator, C – inlet of the condenser, D – evaporator surface, CA – heating and condensation, AB – drying, BC – cooling and evaporation.

Table 4.19 provides the known and unknown properties for each state point for the heat pump dryer with R134a.

The properties of *point A* are as follows:

$$h_A = 46.96 \text{ kJ/kg}$$

$$x_A = 0.006583 \text{ kg/kg}$$

$$t_{dpA} = 7.84°C$$

TABLE 4.19

Known and Unknown Properties for the State Points for the Heat Pump Dryer with R134a

	Point			
Property	**A**	**B**	**C**	**D**
t, °C	30	Unknown	Unknown	Unknown
ϕ, %	25	65	Unknown	100
h, kJ/kg	Unknown	Unknown	Unknown	Unknown
x, g/kg	Unknown	Unknown	Unknown	Unknown

TABLE 4.20

Psychrometric Conditions for the State Points for the Heat Pump Dryer with R134a

	Point			
Property	**A**	**B**	**C**	**D**
t, °C	30.00	21.10	9.34	2.84
ϕ, %	25	65	90.35	100
h, kJ/kg	46.96	46.96	25.95	14.47
x, g/kg	6.58	10.15	6.58	4.64

The properties of *point B* are as follows:

$$h_B = h_A = 46.96 \text{ kJ/kg}$$

$$t_B = 21.10°C$$

$$x_B = 0.010147 \text{ kg/kg}$$

From the given relative humidity the properties at *point D* are as follows:

$$t_D = 2.84°C$$

$$h_D = 14.47 \text{ kJ/kg}$$

$$x_D = 0.004635 \text{ kg/kg}$$

The properties at *point C* are as follows:

$$x_C = x_A = 0.006583 \text{ kg/kg}$$

$$h_C = \frac{x_C - x_D}{x_B - x_D}\left(h_B - h_D\right) + h_D = 25.95 \text{ kJ/kg}$$

$$t_C = 9.34°C$$

$$\phi_C = 90.35\%$$

The answer for (b) is provided in Table 4.20 obtained from the previous calculations and Table 4.19.

(c) Drawing the heat pump cycle on the log(p)–h diagram and tabulating the heat pump fluid properties

The drawing requires the properties of R134a for all state points of the heat pump drying cycle.

The known and unknown properties at the state points are listed in Table 4.21. The other properties in the cycle are determined considering the following:

- Evaporating temperature is 2.84°C.
- Condensing temperature is 40°C.
- Compression is done on saturated vapour and it is non-isentropic with $\eta_i = 0.60$.
- Throttling is done on saturated liquid and it is adiabatic ($h_3 = h_4$).

Point 1 is saturated vapour at temperature at 2.84°C, and the other properties are as follows:

$$p_1 = 324.16 \text{ kPa}$$

$$h_1 = 398.84 \text{ kJ/kg}$$

$$s_1 = 1.72 \text{ kJ/kg·K}$$

$$v_1 = 0.062438 \text{ m}^3/\text{kg}$$

Point 2i is superheated vapour after isentropic compression, then

$$s_{2i} = s_1 = 1.72 \text{ kJ/kg·K}$$

$$p_{2i} = 1016.38 \text{ kPa}$$

The other properties are as follows:

$$t_{2i} = 43.59°\text{C}$$

$$h_{2i} = 422.42 \text{ kJ/kg}$$

Point 2 is superheated vapour after non-isentropic compression, then

$$p_2 = 1016.38 \text{ kPa}$$

$$h_2 = h_1 + \frac{h_{2i} - h_1}{\eta_i} = 438.14 \text{ kJ/kg}$$

TABLE 4.21

Known and Unknown Properties for the State Points of the Heat Pump with R134a

	State Point				
Property	**1**	**2i**	**2**	**3**	**4**
t, °C	2.84	Unknown	Unknown	40.00	Unknown
p, kPa	Unknown	Unknown	Unknown	Unknown	Unknown
h, kJ/kg	Unknown	Unknown	Unknown	Unknown	Unknown
s, kJ/kg·K	Unknown	Unknown	Unknown	Unknown	—
v, m^3/kg	Unknown	—	—	—	—

The other properties are as follows:

$$s_2 = 1.77 \text{ kJ/kg·K}$$

$$t_2 = 57.41°\text{C}$$

Point 3 is saturated liquid at temperature at 40°C, and the other properties are as follows:

$$p_3 = 1016.38 \text{ kPa}$$

$$h_3 = 256.17 \text{ kJ/kg}$$

$$s_3 = 1.19 \text{ kJ/kg·K}$$

Point 4 is vapour–liquid mixture after an adiabatic process, then

$$h_4 = h_3 = 256.17 \text{ kJ/kg}$$

The other properties are as follows:

$$t_4 = t_1 = 2.84°\text{C}$$

$$p_4 = p_1 = 324.16 \text{ kPa}$$

The calculated values are now inserted in Table 4.12 providing the properties of R134a in all state points of the heat pump cycle.

Table 4.22 with the properties R134a in all state points provides the data to draw the cycle on the log(p)–h diagram as illustrated in Figure 4.14.

(d) Calculation of compressor shaft work and volumetric flow rate, evaporating and condensing capacities, SMER and the total energy paid

The calculation requires the properties available in Tables 4.20 and 4.22:

$$\Delta x = x_B - x_A = 0.003564 \text{ kg/kg}$$

$$\Delta h = h_A - h_C = 21.01 \text{ kJ/kg}$$

$$Q_{ev} = \dot{m}_a \Delta h = \frac{\dot{m}_w}{3600 \cdot \Delta x} \Delta h = \frac{20 \cdot 21.01}{3600 \cdot 0.003564} = 32.74 \text{ kW}$$

TABLE 4.22

Properties for the State Points of the Heat Pump with R134a

	State Point				
Property	**1**	**2i**	**2**	**3**	**4**
t, °C	2.84	43.59	57.41	40.00	2.84
p, kPa	324.16	1016.38	1016.38	1016.38	324.16
h, kJ/kg	398.84	422.42	438.14	256.17	256.17
s, kJ/kg·K	1.72	1.72	1.77	1.19	—
v, m^3/kg	0.062438	—	—	—	—

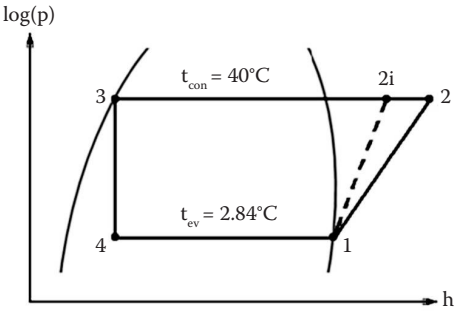

FIGURE 4.14
State points on the log(p)–h diagram. 1–2i and 1–2: isentropic and non-isentropic compression, 2–3: isobaric condensation, 3–4: adiabatic throttling, 4–1: isobaric and isothermal evaporation, 1: saturated vapour, 2: superheated vapour, 3: saturated liquid, 4: vapour and liquid mixture.

The refrigerant mass flow rate is determined by

$$\dot{m}_r = \frac{Q_{ev}}{h_1 - h_4} = 0.2295 \text{ kg/s}$$

The compressor shaft work is as follows:

$$W = \dot{m}_r (h_2 - h_1) = 9.02 \text{ kW}$$

The volumetric flow rate of the compressor is as follows:

$$\dot{V}_r = \frac{3600 \cdot \dot{m}_r v_1}{\lambda} = 73.69 \text{ m}^3/\text{h}$$

The condensing capacity is as follows:

$$Q_{con} = \dot{m}_r (h_2 - h_3) = 41.76 \text{ kW}$$

The COP and SMER are calculated by

$$COP = \frac{Q_{ev}}{W} = 3.63$$

$$SMER = COP \frac{\Delta x}{\Delta h} = 2.22 \text{ kg/kWh}$$

The total energy paid for heating and drying is the inverse of the shaft work

$$E_{use} = \frac{1}{COP} 100\% = 27.5\%$$

(e) Tabulation and discussion of the energy and water removal performances of the heat pump dryer

The calculated performances of heat pump dryer are summarised in Table 4.23.

TABLE 4.23

Energy and Water Removal Performances of the Heat Pump Dryer with R134a

	Drying Process
Performance	**Heat Pump Drying**
Heating capacity, kW	41.76
Cooling capacity, kW	32.74
Shaft work, kW	9.02
COP	3.63
SMER, kg/kWh	2.22
Total energy paid, %	27.5

The data in Table 4.23 show that the heat pump belt dryer uses 1 kWh to remove 2.22 kg of water. The COP indicates that the heat pump belt dryer uses only 27.5% of the total energy required for heating or drying. The enhanced performance of the heat pump dryer results from energy recovery from exhaust vapour and using it to reheat the drying air.

4.7 Heat Pump Stationary Bed Drying of Mushroom Slices

Mushroom slices are dried in stationary bed in the R404A heat pump dryer illustrated in Figure 4.15. The drying chamber air temperature and relative humidity are 25°C and 30%, respectively, and the exhaust air is at 60% relative humidity. The water removal rate is 10 kg/h, the evaporating temperature is 3.5°C below the dew-point temperature at *point A* and the condensing temperature is 5°C above the drying air inlet temperature. The isentropic and volumetric efficiencies are 0.65 and 0.75, respectively.

Consider that saturated vapour is compressed, saturated liquid is adiabatically throttled, drying is adiabatic and at atmospheric pressure and then (a) draw the air state points drying air cycle in the Mollier diagram; (b) determine and tabulate the psychrometric conditions for the state points of the cycle; (c) draw the heat pump cycle on the log(p)–h diagram and tabulate the heat pump fluid properties; (d) calculate the compressor shaft work and volumetric flow rate, evaporating and condensing capacities, COP, SMER and the total energy paid; and (e) tabulate and discuss the energy and water removal performances of the heat pump dryer R404A.

Given:

R404A	$t_A = 25°C$	$\phi_A = 30\%$	$\eta_i = 0.65$
$\dot{m}_w = 10$ kg/h	$t_{ev} = t_D = t_{dpA} - 3.5°C$	$\phi_B = 60\%$	$\lambda = 0.75$
$h_A = h_B$ = constant	$t_{con} = t_A + 5°C = 30°C$	$\phi_D = 100\%$	p = 101,325 Pa

Solution:

(a) Drawing the air state points for the heat pump drying cycle in the Mollier diagram. The state points of the heat pump dryer with R404A are shown in Figure 4.16.

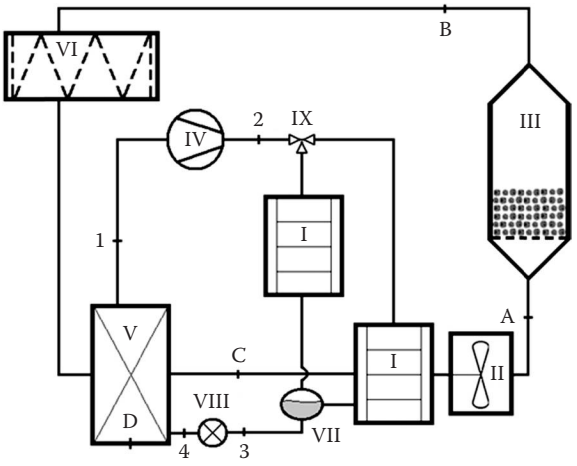

FIGURE 4.15
Heat pump stationary bed dryer with R404A: I – condensers (heaters), II – blower, III – drying chamber and stationary bed of mushrooms, IV – compressor, V – evaporator, VI – filter, VII – receiver, VIII – throttling valve, IX – three-way valve, 1 – saturated vapour, 2 – superheated vapour, 3 – saturated liquid, 4 – vapour and liquid mixture, A – inlet of the drying chamber, B – inlet of the evaporator, C – inlet of the condenser, D – evaporator surface.

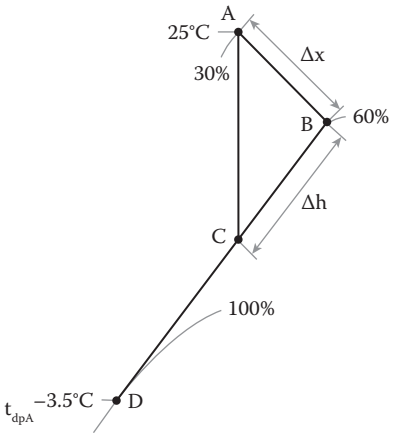

FIGURE 4.16
State points in the Mollier diagram: A – inlet of the drying chamber, B – inlet of the evaporator, C – inlet of the condenser, D – evaporator surface, CA – heating and condensation, AB – drying, BC – cooling and evaporation.

(b) Determining and tabulating the psychrometric conditions for the state points of the cycle

Table 4.24 presents the known and unknown properties for each state point for the heat pump drying cycle.

The properties of *point A* are as follows:

$$h_A = 40.11 \text{ kJ/kg}$$

$$x_A = 0.005890 \text{ kg/kg}$$

$$t_{dpA} = 6.24°C$$

TABLE 4.24

Known and Unknown Properties for the State Points for the Heat Pump Dryer with R404A

	Point			
Property	**A**	**B**	**C**	**D**
t, °C	25	Unknown	Unknown	Unknown
ϕ, %	30	60	Unknown	100
h, kJ/kg	Unknown	Unknown	Unknown	Unknown
x, g/kg	Unknown	Unknown	Unknown	Unknown

TABLE 4.25

Psychrometric Conditions for the State Points for the Heat Pump Dryer with R404A

	Point			
Property	**A**	**B**	**C**	**D**
t, °C	25.00	19.10	8.54	2.74
ϕ, %	30	60	85.40	100
h, kJ/kg	40.11	40.11	23.40	14.28
x, g/kg	5.89	8.25	5.89	4.60

The properties of *point B* are as follows:

$$h_B = h_A = 40.11 \text{ kJ/kg}$$

$$t_B = 19.10°C$$

$$x_B = 0.008252 \text{ kg/kg}$$

From the given relative humidity, the properties at *point D* are as follows:

$$t_D = 2.74°C$$

$$h_D = 14.28 \text{ kJ/kg}$$

$$x_D = 0.004600 \text{ kg/kg}$$

The properties at *point C* are as follows:

$$x_C = x_A = 0.005890 \text{ kg/kg}$$

$$h_C = \frac{x_C - x_D}{x_B - x_D}\left(h_B - h_D\right) + h_D = 23.40 \text{ kJ/kg}$$

$$t_C = 8.54°C$$

$$\phi_C = 85.40\%$$

The answer for (b) is provided in Table 4.25 obtained from the previous calculations and Table 4.24.

TABLE 4.26

Known and Unknown Properties for the State Points of the Heat Pump Fluid R404A

	State Point				
Property	**1**	**2i**	**2**	**3**	**4**
t, °C	2.74	Unknown	Unknown	30.00	Unknown
p, kPa	Unknown	Unknown	Unknown	Unknown	Unknown
h, kJ/kg	Unknown	Unknown	Unknown	Unknown	Unknown
s, kJ/kg·K	Unknown	Unknown	Unknown	Unknown	—
v, m^3/kg	Unknown	—	—	—	—

(c) Drawing the heat pump cycle on the log(p)–h diagram and tabulating the heat pump fluid properties

The properties of R134a for all state points are required to draw heat pump drying cycle.

The known and unknown properties at the state points are listed in Table 4.26. The other properties of the R404A in the cycle are determined considering that the following:

- Evaporating temperature is 2.74°C.
- Condensing temperature is 30°C.
- Compression is done on saturated vapour and it is non-isentropic with $\eta_i = 0.65$.
- Throttling is done on saturated liquid and it is adiabatic ($h_3 = h_4$).

Point 1 is saturated vapour at temperature at 2.74°C, and the other properties are as follows:

$$p_1 = 656.87 \text{ kPa}$$

$$h_1 = 369.63 \text{ kJ/kg}$$

$$s_1 = 1.62 \text{ kJ/kg·K}$$

$$v_1 = 0.030524 \text{ m}^3\text{/kg}$$

Point 2i is superheated vapour. Since this point is isentropic, then

$$s_{2i} = s_1 = 1.62 \text{ kJ/kg·K}$$

$$p_{2i} = 1429.78 \text{ kPa}$$

And the other properties are as follows:

$$t_{2i} = 33.06°\text{C}$$

$$h_{2i} = 385.09 \text{ kJ/kg}$$

Point 2 is superheated vapour. This point is non-isentropic, then

$$p_2 = 1429.78 \text{ kPa}$$

$$h_2 = h_1 + \frac{h_{2i} - h_1}{\eta_i} = 393.42 \text{ kJ/kg}$$

The other properties are as follows:

$$s_2 = 1.64 \text{ kJ/kg·K}$$

$$t_2 = 40.86°C$$

Point 3 is saturate liquid at temperature at 30°C, and the other properties are as follows:

$$p_3 = 1429.78 \text{ kPa}$$

$$h_3 = 246.03 \text{ kJ/kg}$$

$$s_3 = 1.16 \text{ kJ/kg·K}$$

Point 4 is vapour–liquid mixture. Since the process is isenthalpic, then

$$h_4 = h_3 = 246.03 \text{ kJ/kg}$$

$$p_4 = p_1 = 656.87 \text{ kPa}$$

$$t_4 = 2.38°C$$

The calculated values are inserted in Table 4.27 providing the properties of R404 for all state points of the heat pump cycle.

Table 4.27, with the properties R404A in all state points provides, the data to draw the cycle on the log(p)–h diagram as sketched in Figure 4.17.

TABLE 4.27

Properties for the State Points of the Heat Pump Fluid R404A

	State Point				
Property	**1**	**2i**	**2**	**3**	**4**
t, °C	2.74	33.06	40.86	30	2.38
p, kPa	656.87	1429.78	1429.78	1429.78	656.87
h, kJ/kg	369.63	385.09	393.42	246.03	246.03
s, kJ/kg·K	1.62	1.62	1.64	1.16	—
v, m^3/kg	0.030524	—	—	—	—

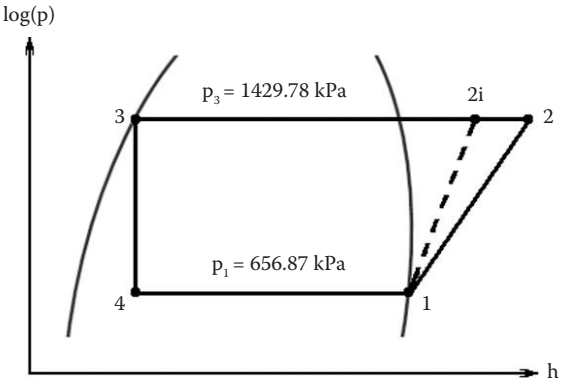

FIGURE 4.17
State points on the log(p)–h diagram. 1–2i and 1–2: isentropic and non-isentropic compression, 2–3: isobaric condensation, 3–4: adiabatic throttling, 4–1: isobaric and isothermal evaporation, 1: saturated vapour, 2: superheated vapour, 3: saturated liquid, 4: vapour and liquid mixture.

(d) Calculation of compressor shaft work and volumetric flow rate, evaporating and condensing capacities, SMER and the total energy paid

The calculations require data from Tables 4.25 and 4.27:

$$\Delta x = x_B - x_A = 0.002362 \text{ kg/kg}$$

$$\Delta h = h_A - h_C = 16.71 \text{ kJ/kg}$$

$$Q_{ev} = \dot{m}_a \Delta h = \frac{\dot{m}_w}{3600 \cdot \Delta x} \Delta h = \frac{10 \cdot 16.71}{3600 \cdot 0.002362} = 19.65 \text{ kW}$$

The refrigerant mass flow rate is determined by

$$\dot{m}_r = \frac{Q_{ev}}{h_1 - h_4} = 0.1590 \text{ kg/s}$$

The compressor shaft work is as follows:

$$W = \dot{m}_r (h_2 - h_1) = 3.78 \text{ kW}$$

The volumetric flow rate of the compressor is as follows:

$$\dot{V}_r = \frac{3600 \cdot \dot{m}_r v_1}{\lambda} = 23.30 \text{ m}^3/\text{h}$$

The condensing capacity is as follows:

$$Q_{con} = \dot{m}_r (h_2 - h_3) = 23.44 \text{ kW}$$

The COP and SMER are calculated by

$$COP = \frac{Q_{ev}}{W} = 5.197$$

$$SMER = COP \frac{\Delta x}{\Delta h} = 2.65 \text{ kg/kWh}$$

The total energy paid for heating and drying is the inverse of the shaft work

$$E_{use} = \frac{1}{COP} 100\% = 19.2\%$$

(e) Tabulation and discussion of the energy and water removal performances of the heat pump dryer

The calculated performances of heat pump dryer with R404A are shown in Table 4.28.

The data in Table 4.28 indicate that the stationary heat pump dryer uses 1 kWh to remove 2.65 kg of water. The COP indicates that this heat pump uses only 19.2% of the total energy required for heating and drying. This enhanced performance results from energy recovery from exhaust vapour that is used to reheat the drying air.

Sections 4.8 and 4.9 cover the design of commercial scale heat pump dryers operating with natural fluids.

TABLE 4.28

Energy and Water Removal Performances of the Heat Pump Dryer with R404A

Drying Process	
Performance	**Heat Pump Drying**
Heating capacity, kW	23.44
Cooling capacity, kW	19.65
Shaft work, kW	3.78
COP	5.197
SMER, kg/kWh	2.65
Total energy paid, %	19.2

4.8 Heat Pump Fluidised Bed Drying of Cauliflower

Figure 4.18 shows a heat pump fluidised bed dryer operating with natural carbon dioxide fluid or R744 that is applied to dry cauliflower florets. The drying chamber air temperature and relative humidity are 5°C and 35%, respectively, and the exhaust air is at 75% relative humidity. The water removal rate is 5 kg/h, the evaporating temperature is 5°C below the dew-point temperature at *point A* and the condensing temperature is 5°C above the drying air inlet temperature. The isentropic and volumetric efficiencies are 0.7 and 0.75, respectively.

Consider that saturated vapour is compressed, saturated liquid is adiabatically throttled, drying is adiabatic and at atmospheric pressure and (a) draw the air state points drying air cycle in the Mollier diagram; (b) determine and tabulate the psychrometric conditions for the state points of the cycle; (c) draw the heat pump cycle on the log(p)–h diagram and tabulate the heat pump fluid properties; (d) calculate the compressor shaft work and volumetric flow rate, evaporating and condensing capacities, COP, SMER; and the total energy paid; and (e) tabulate and discuss the energy and water removal performances of the heat pump dryer.

Given:

R744	$t_A = 5°C$	$\phi_A = 35\%$	$\eta_i = 0.7$
$\dot{m}_w = 5$ kg/h	$t_{ev} = t_D = t_{dpA} - 5°C$	$\phi_B = 75\%$	$\lambda = 0.75$
$h_A = h_B$ = constant	$t_{con} = t_A + 5°C = 10°C$	$\phi_D = 100\%$	p = 101,325 Pa

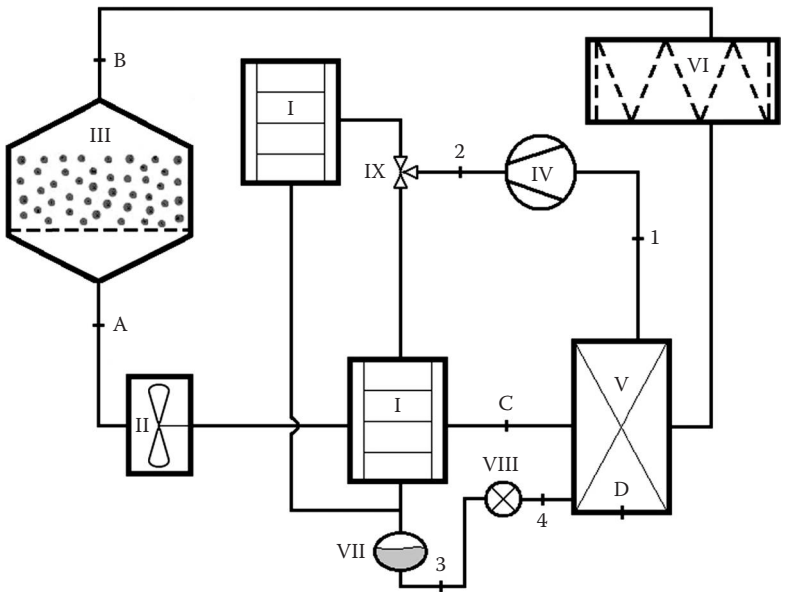

FIGURE 4.18
Heat pump fluidised bed dryer with natural fluid R744: I – condensers (heaters), II – blower, III – fluidised bed dryer with cauliflower florets, IV – compressor, V – evaporator, VI – filter, VII – receiver, VIII – throttling valve, IX – three-way valve, 1 – saturated vapour, 2 – superheated vapour, 3 – saturated liquid, 4 – vapour and liquid mixture, A – inlet of the drying chamber, B – inlet of the evaporator, C – inlet of the condenser, D – evaporator surface.

Solution:

(a) Drawing the air state points for the heat pump drying cycle in the Mollier diagram

The state points of the heat pump dryer with R744 are shown in Figure 4.19.

(b) Determining and tabulating the psychrometric conditions for the state points of the cycle

Table 4.29 lists the known and unknown properties for each state point for the heat pump dryer with carbon dioxide fluid.

The properties of *point A* are as follows:

$$h_A = 9.74 \text{ kJ/kg}$$
$$x_A = 0.001880 \text{ kg/kg}$$
$$t_{dpA} = -8.17°C$$

The properties of *point B* are as follows:

$$h_B = h_A = 9.74 \text{ kJ/kg}$$
$$t_B = 1.72°C$$
$$x_B = 0.003201 \text{ kg/kg}$$

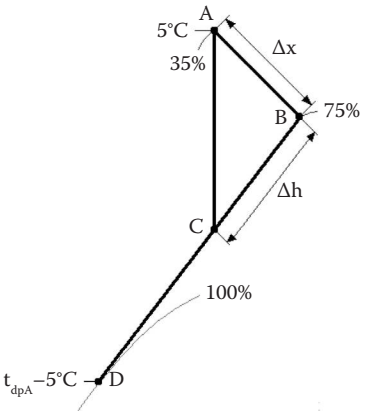

FIGURE 4.19
State points in the Mollier diagram: A – inlet of the drying chamber, B – inlet of the evaporator, C – inlet of condenser, D – evaporator surface, CA – heating and condensation, AB – drying, BC – cooling and evaporation.

TABLE 4.29

Known and Unknown Properties for the State Points for the Heat Pump Dryer with R744

	Point			
Property	**A**	**B**	**C**	**D**
t, °C	5	Unknown	Unknown	Unknown
ϕ, %	35	75	Unknown	100
h, kJ/kg	Unknown	Unknown	Unknown	Unknown
x, g/kg	Unknown	Unknown	Unknown	Unknown

From the given relative humidity, the properties at *point D* are as follows:

$$t_D = -13.17°C$$

$$h_D = -10.24\ kJ/kg$$

$$x_D = 0.001202\ kg/kg$$

The properties at *point C* are as follows:

$$x_C = x_A = 0.001880\ kg/kg$$

$$h_C = \frac{x_C - x_D}{x_B - x_D}(h_B - h_D) + h_D = -3.46\ kJ/kg$$

$$t_C = -8.11°C$$

$$\phi_C = 99.45\%$$

The answer for (b) is provided by Table 4.30 obtained from the previous calculations and Table 4.29.

(c) Drawing the heat pump cycle on the log(p)–h diagram and tabulating the heat pump fluid properties

The drawing of the heat pump drying cycle requires the properties of R744 for all state points.

The known and unknown properties of fluid at the state points of the cycle are listed in Table 4.31. The other properties of the R744 cycle are determined considering that the following:

- Evaporating temperature is –13.17°C.
- Condensing temperature is 10°C.
- Compression is done on saturated vapour and it is non-isentropic with $\eta_i = 0.7$.
- Throttling on saturated liquid is done adiabatically ($h_3 = h_4$).

Point 1 is saturated vapour at temperature at –13.17°C, and the other properties are as follows:

$$p_1 = 2418.45\ kPa$$

$$h_1 = 436.89\ kJ/kg$$

TABLE 4.30

Psychrometric Conditions for the State Points for the Heat Pump Drying Air

	Point			
Property	**A**	**B**	**C**	**D**
t, °C	5.00	1.72	–8.11	–13.17
ϕ, %	35	75	99.45	100
h, kJ/kg	9.74	9.74	–3.46	–10.24
x, g/kg	1.88	3.20	1.88	1.20

TABLE 4.31

Known and Unknown Properties for the State Points of the Heat Pump with Natural R744

	State Point				
Property	**1**	**2i**	**2**	**3**	**4**
t, °C	–13.17	Unknown	Unknown	10.00	Unknown
p, kPa	Unknown	Unknown	Unknown	Unknown	Unknown
h, kJ/kg	Unknown	Unknown	Unknown	Unknown	Unknown
s, kJ/kg·K	Unknown	Unknown	Unknown	Unknown	—
v, m^3/kg	Unknown	—	—	—	—

$$s_1 = 1.92 \text{ kJ/kg·K}$$

$$v_1 = 0.015456 \text{ m}^3\text{/kg}$$

Point 2i is superheated vapour after isentropic compression, then

$$s_{2i} = s_1 = 1.92 \text{ kJ/kg·K}$$

$$p_{2i} = 4501.55 \text{ kPa}$$

The other properties are as follows:

$$t_{2i} = 30.27°\text{C}$$

$$h_{2i} = 461.08 \text{ kJ/kg}$$

Point 2 is superheated vapour after non-isentropic compression, then

$$p_2 = 4501.55 \text{ kPa}$$

$$h_2 = h_1 + \frac{h_{2i} - h_1}{\eta_i} = 471.44 \text{ kJ/kg}$$

The other properties are as follows:

$$s_2 = 1.95 \text{ kJ/kg·K}$$

$$t_2 = 37.54°\text{C}$$

Point 3 is saturated liquid at temperature at 10°C, and the other properties are as follows:

$$p_3 = 4501.55 \text{ kPa}$$

$$h_3 = 225.56 \text{ kJ/kg}$$

$$s_3 = 1.09 \text{ kJ/kg·K}$$

Point 4 is vapour–liquid mixture after an adiabatic process, then

$$h_4 = h_3 = 225.56 \text{ kJ/kg}$$

The other properties are as follows:

$$t_4 = t_1 = -13.17°C$$

$$p_4 = p_1 = 2418.45 \text{ kPa}$$

Table 4.32 is obtained from the calculations and Table 4.31 and provides the properties in all points of the heat pump cycle.

Table 4.32, with the properties of R744 in all state points, allows drawing the cycle on the log(p)–h diagram as sketched in Figure 4.20.

(d) Calculation of compressor shaft work and volumetric flow rate, evaporating and condensing capacities, SMER and the total energy paid

The calculations are made based on the data shown in Tables 4.30 and 4.32:

$$\Delta x = x_B - x_A = 0.001321 \text{ kg/kg}$$

$$\Delta h = h_A - h_C = 13.20 \text{ kJ/kg}$$

$$Q_{ev} = \dot{m}_a \Delta h = \frac{\dot{m}_w}{3600 \cdot \Delta x} \Delta h = \frac{5 \cdot 13.20}{3600 \cdot 0.001321} = 13.88 \text{ kW}$$

TABLE 4.32

Properties for the State Points of the Heat Pump with Natural Fluid R744

	State Point				
Property	**1**	**2i**	**2**	**3**	**4**
t, °C	–13.17	30.27	37.54	10.00	–13.17
p, kPa	2418.45	4501.55	4501.55	4501.55	2418.45
h, kJ/kg	436.89	461.08	471.44	225.56	225.56
s, kJ/kg·K	1.92	1.92	1.95	1.09	—
v, m³/kg	0.015456	—	—	—	—

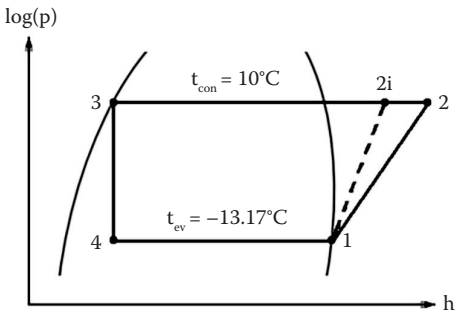

FIGURE 4.20
State points on the log(p)–h diagram. 1–2i and 1–2: isentropic and non-isentropic compression, 2–3: isobaric condensation, 3–4: adiabatic throttling, 4–1: isobaric and isothermal evaporation, 1: saturated vapour, 2: superheated vapour, 3: saturated liquid, 4: vapour and liquid mixture.

The refrigerant mass flow rate is as follows:

$$\dot{m}_r = \frac{Q_{ev}}{h_1 - h_4} = 0.0657 \text{ kg/s}$$

The compressor shaft work is as follows:

$$W = \dot{m}_r (h_2 - h_1) = 2.27 \text{ kW}$$

The volumetric flow rate of the compressor is as follows:

$$\dot{V}_r = \frac{3600 \cdot \dot{m}_r v_1}{\lambda} = 4.87 \text{ m}^3/\text{h}$$

The condensing capacity is as follows:

$$Q_{con} = \dot{m}_r (h_2 - h_3) = 16.16 \text{ kW}$$

The COP and SMER are calculated by

$$COP = \frac{Q_{ev}}{W} = 6.116$$

$$SMER = COP \frac{\Delta x}{\Delta h} = 2.20 \text{ kg/kWh}$$

The total energy paid for heating and drying is the inverse of the shaft work

$$E_{use} = \frac{1}{COP} 100\% = 19.2\%$$

(e) Tabulation and discussion of the energy and water removal performances of the heat pump dryer

The calculated performances of heat pump dryer with R744 are shown in Table 4.33.

The data in Table 4.33 indicate that the heat pump fluidised bed dryer with R744 uses 1 kWh to remove 2.2 kg of water. Based on the COP, this heat pump fluidised

TABLE 4.33

Energy and Water Removal Performances of the Heat Pump Dryer with Natural R744

Drying Process	
Performance	**Heat Pump Drying**
Heating capacity, kW	16.16
Cooling capacity, kW	13.88
Shaft work, kW	2.27
COP	6.116
SMER, kg/kWh	2.20
Total energy paid, %	16.4

bed dryer uses only 16.4% of the total energy required for heating and drying. The reasons for the improved performances are energy recovery from exhaust vapour by the evaporator and its transfer from the condenser to reheat the drying air.

4.9 Heat Pump Tunnel Drying of Salted Cod Fish

The heat pump tunnel dryer shown in Figure 4.21 operates with natural ammonia refrigerant or R717, and it is used to dry salted and split cod fish. The drying chamber air temperature and relative humidity are 20°C and 35%, respectively, and the exhaust air is at 85% relative humidity. The tunnel holds six trolleys, each containing 400 kg of wet cod fish. The initial and final moisture contents are 80%wb and 20%wb, respectively. The dryer operates 20 h/day and produces two trolleys of dried cod daily (simultaneously, two trolleys with wet fish are loaded in the dryer per day). The evaporating temperature is 2.5°C and the condensing temperature is 35°C. The isentropic and volumetric efficiencies are 0.65 and 0.75, respectively. Consider that saturated vapour is superheated 6°C before its compression, saturated liquid is sub-cooled to 4°C before adiabatic throttling and drying is adiabatic and at atmospheric pressure, then (a) draw the air state points drying air cycle in the Mollier diagram; (b) determine and tabulate the psychrometric conditions for the state points of the cycle; (c) draw the heat pump cycle on the log(p)–h diagram and tabulate the heat pump fluid properties; and (d) calculate the compressor shaft work and volumetric flow rate, evaporating and condensing capacities, COP and SMER.

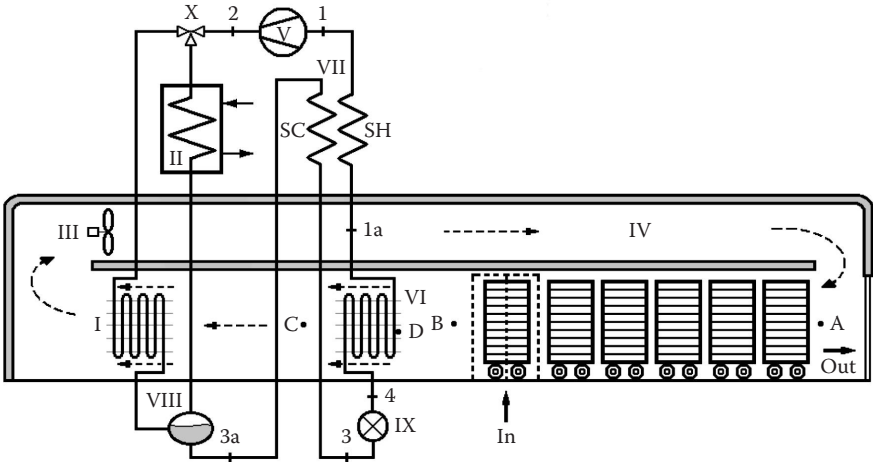

FIGURE 4.21
Heat pump tunnel dryer with natural fluid R717: I – internal condenser, II – external condenser, III – blower, IV – tunnel drying chamber with salted split cod, V –compressor, VI – evaporator, VII – internal heat exchanger, VIII – liquid receiver, IX – throttling valve, X – three-way valve, 1a: saturated vapour, 1: superheated vapour at low pressure, 2: superheated vapour at high pressure, 3a: saturated liquid, 3: sub-cooled liquid, 4: vapour and liquid mixture, A – inlet of the drying chamber, B – inlet of the evaporator, C – inlet of condenser, D – evaporator surface SC – sub-cooled liquid, SH – superheated vapour, in – trolley with wet material inlet, out – trolley with dry product outlet.

Given:

R717	$t_A = 20°C$	$\phi_A = 35\%$
$\dot{m}_{tr} = 400$ kg/day	$t_{ev} = t_D = 2.5°C$	$\phi_B = 85\%$
$X_0 = 80\%$wb	$t_{con} = 35°C$	$\phi_D = 100\%$
$X_f = 20\%$wb	$t_{sh} = 6°C$	$\eta_i = 0.65$
$n_h = 20$ h/day	$t_{sc} = 4°C$	$\lambda = 0.75$
$n_{tr} = 2$	$p = 101{,}325$ Pa	$h_A = h_B =$ constant

Solution:

(a) Drawing the air state points for the heat pump drying cycle in the Mollier diagram

The state points of the heat pump dryer with R717 are shown in Figure 4.22.

(b) Determining and tabulating the psychrometric conditions for the state points of the cycle

Table 4.34 shows the known and unknown properties for each state point for the heat pump dryer with R717.

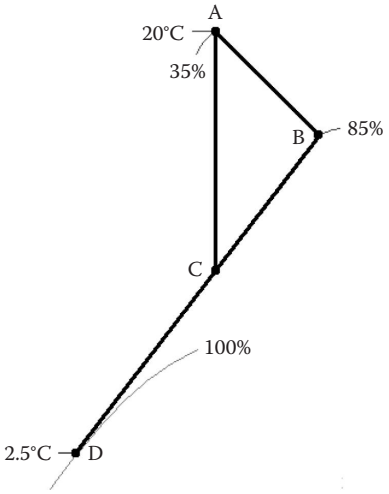

FIGURE 4.22
State points in the Mollier diagram: A – inlet of the drying chamber, B – inlet of the evaporator, C – inlet of the condenser, D – evaporator surface, CA – heating and condensation, AB – drying, BC – cooling and evaporation.

TABLE 4.34

Known and Unknown Properties for the State Points in the Cycle of the Heat Pump Dryer

	Point			
Property	**A**	**B**	**C**	**D**
t, °C	20.0	Unknown	Unknown	2.5
ϕ, %	35	65	Unknown	100
h, kJ/kg	Unknown	Unknown	Unknown	Unknown
x, g/kg	Unknown	Unknown	Unknown	Unknown

The properties of *point A* are as follows:

$$h_A = 32.93 \text{ kJ/kg}$$

$$x_A = 0.005065 \text{ kg/kg}$$

The properties of *point B* are as follows:

$$h_B = h_A = 32.93 \text{ kJ/kg}$$

$$t_B = 12.96°C$$

$$x_B = 0.007892 \text{ kg/kg}$$

From the given temperature and relative humidity, the properties at *point D* are as follows:

$$h_D = 13.84 \text{ kJ/kg}$$

$$x_D = 0.004522 \text{ kg/kg}$$

The properties at *point C* are as follows:

$$x_C = x_A = 0.005065 \text{ kg/kg}$$

$$h_C = \frac{x_C - x_D}{x_B - x_D}\left(h_B - h_D\right) + h_D = 16.91 \text{ kJ/kg}$$

$$t_C = 4.19°C$$

$$\phi_C = 99.28\%$$

The answer for (b) is given in Table 4.35, which was obtained from the previous calculations and Table 4.34.

(c) Drawing the heat pump cycle on the log(p)–h diagram and tabulating the heat pump fluid properties

The properties of R717 are required in all state points to draw heat pump drying cycle.

TABLE 4.35

Psychrometric Conditions for the State Points for the Heat Pump Drying Air

	Point			
Property	**A**	**B**	**C**	**D**
t, °C	20.00	12.96	4.19	2.50
ϕ, %	35	85	99.28	100
h, kJ/kg	32.93	32.93	16.91	13.84
x, g/kg	5.06	7.89	5.06	4.52

TABLE 4.36

Known and Unknown Properties for the State Points of the Heat Pump with Natural Fluid R717

	Point						
Property	**1a**	**1**	**2i**	**2**	**3a**	**3**	**4**
t, °C	2.5	Unknown	Unknown	Unknown	35	Unknown	Unknown
p, kPa	Unknown	Unknown	Unknown	Unknown	Unknown	Unknown	Unknown
h, kJ/kg	Unknown	Unknown	Unknown	Unknown	Unknown	Unknown	Unknown
s, kJ/kg·K	Unknown	Unknown	Unknown	Unknown	Unknown	Unknown	—
v, m^3/kg	Unknown	Unknown	—	—	—	—	—

The known and unknown properties at the state points are listed in Table 4.36. The other properties of R717 in cycle are determined considering that the following:

- Evaporating temperature is 2.5°C.
- Condensing temperature is 35°C.
- Compression is done on superheated vapour and it is non-isentropic with $\eta_i = 0.65$.
- Throttling is done on sub-cooled liquid and it is adiabatic ($h_3 = h_4$).

The evaporating and condensing pressures are now determined for the corresponding temperatures.

$$\text{For } t_{ev} = 2.5°C \qquad p_{ev} = 470.94 \text{ kPa}$$

$$\text{For } t_{con} = 35°C \qquad p_{con} = 1350.02 \text{ kPa}$$

Point 1a is saturated vapour at temperature at 2.5°C and the other properties are as follows:

$$p_{1a} = p_{ev} = 470.94 \text{ kPa}$$

$$h_{1a} = 1626.33 \text{ kJ/kg}$$

$$s_{1a} = 6.15 \text{ kJ/kg·K}$$

$$v_{1a} = 0.2650 \text{ m}^3\text{/kg}$$

Point 1 is superheated vapour at low pressure with the following properties:

$$p_1 = p_{ev} = 470.94 \text{ kPa}$$

$$t_1 = t_{1a} + t_{sh} = 2.5 + 6 = 8.5°C$$

$$h_1 = 1642.50 \text{ kJ/kg}$$

$$s_1 = 6.21 \text{ kJ/kg·K}$$

$$v_1 = 0.2729 \text{ m}^3\text{/kg}$$

Point 2i is superheated vapour at high pressure and it is an isentropic point, then

$$s_{2i} = s_1 = 6.21 \text{ kJ/kg·K}$$

$$p_{2i} = p_{con} = 1350.02 \text{ kPa}$$

$$t_{2i} = 84.92°\text{C}$$

$$h_{2i} = 1794.93 \text{ kJ/kg}$$

Point 2 is superheated vapour at high pressure and it is a non-isentropic point, then

$$p_2 = p_{con} = 1350.02 \text{ kPa}$$

$$h_2 = h_1 + \frac{h_{2i} - h_1}{\eta_i} = 1877.01 \text{ kJ/kg}$$

$$s_2 = 6.37 \text{ kJ/kg·K}$$

$$t_2 = 77.18°\text{C}$$

Point 3a is saturate liquid at temperature at 35°C and the other properties are as follows:

$$p_{3a} = p_{con} = 1350.02 \text{ kPa}$$

$$h_{3a} = 527.86 \text{ kJ/kg}$$

$$s_{3a} = 2.13 \text{ kJ/kg·K}$$

Point 3 is sub-cooled liquid with the following properties:

$$p_3 = p_{con} = 1350.02 \text{ kPa}$$

$$t_3 = t_{3a} - t_{sc} = 35 - 4 = 31°\text{C}$$

$$h_3 = 508.41 \text{ kJ/kg}$$

$$s_3 = 2.07 \text{ kJ/kg·K}$$

Point 4 is vapour–liquid mixture. Since the process is isenthalpic, then

$$h_4 = h_3 = 508.41 \text{ kJ/kg}$$

$$p_4 = p_{ev} = 470.94 \text{ kPa}$$

$$t_4 = t_{ev} = 2.5°\text{C}$$

TABLE 4.37

Properties for the State Points of the Heat Pump Tunnel Dryer

	Point						
Property	**1a**	**1**	**2i**	**2**	**3a**	**3**	**4**
t, °C	2.50	8.50	84.92	77.18	35.00	31.00	2.50
p, kPa	470.94	470.94	1350.02	1350.02	1350.02	1350.02	470.94
h, kJ/kg	1626.33	1642.50	1794.93	1877.01	527.86	508.41	508.41
s, kJ/kg·K	6.15	6.21	6.21	6.37	2.13	2.07	—
v, m^3/kg	0.2650	0.2729	—	—	—	—	—

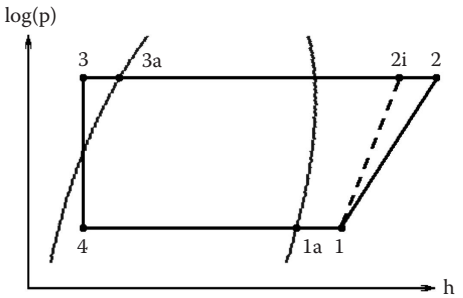

FIGURE 4.23
State points on the log(p)–h diagram. 1–2: non-isentropic compression, 2–3a: isobaric desuperheating and condensation, 3a–3: isobaric sub-cooling, 3–4: adiabatic throttling, 4–1a: isobaric and isothermal evaporation, 1a–1: isobaric superheating, 1a: saturated vapour, 1: superheated vapour at low pressure, 2: superheated vapour at high pressure, 2i: superheated vapour and isentropic point, 3a: saturated liquid, 3: sub-cooled liquid, 4: vapour and liquid mixture.

Table 4.37 presents the properties in all state points of cycle of the heat pump dryer with R717.

Table 4.37, with the properties natural ammonia fluid in all state points, allows to draw the cycle on the log(p)–h diagram as shown in Figure 4.23.

(d) Calculation of compressor shaft work and volumetric flow rate, evaporating and condensing capacities, COP and SMER

The calculations are based on the data available in Tables 4.35 and 4.37:

$$\Delta x = x_B - x_A = 0.002827 \text{ kg/kg}$$

$$\Delta h = h_A - h_C = 16.02 \text{ kJ/kg}$$

$$Q_{ev} = \dot{m}_a \Delta h = \frac{\dot{m}_w}{3600 \cdot \Delta x} \Delta h$$

The water removal mass flow rate is as follows:

$$\dot{m}_w = \dot{m}_0 - \dot{m}_p$$

$$\dot{m}_0 = \frac{n_{tr} \cdot \dot{m}_{tr}}{n_h} = \frac{800}{20} = 40 \text{ kg/h}$$

$$\dot{m}_p = \frac{\dot{m}_{dm}}{1 - 0.01X_f}$$

$$\dot{m}_{dm} = \dot{m}_0\left(1 - 0.01X_0\right) = 40 \cdot 0.2 = 8 \text{ kg/h}$$

$$\dot{m}_p = \frac{8}{0.8} = 10 \text{ kg/h}$$

$$\dot{m}_w = 40 - 10 = 30 \text{ kg/h}$$

$$Q_{ev} = \frac{30 \cdot 16.02}{0.002827 \cdot 3600} = 47.23 \text{ kW}$$

The compressor shaft work is as follows:

$$W = \dot{m}_r\left(h_2 - h_1\right)$$

The refrigerant mass flow rate is as follows:

$$\dot{m}_r = \frac{Q_{ev}}{h_{1a} - h_4} = 0.0422 \text{ kg/s}$$

Hence, W = 9.91 kW

The volumetric flow rate of the compressor is as follows:

$$\dot{V}_r = \frac{3600 \cdot \dot{m}_r v_1}{\lambda} = 55.33 \text{ m}^3/\text{h}$$

The condensing capacity is as follows:

$$Q_{con} = W + Q_{ev} = 57.14 \text{ kW}$$

The COP and SMER are calculated by

$$COP = \frac{Q_{ev}}{W} = 4.767$$

$$SMER = COP\frac{\Delta x}{\Delta h} = 3.03 \text{ kg/kWh}$$

The single vapour compression heat pump systems perform especially well for relatively low temperature differences between the heat source and sink. Consequently, they are not recommended for large pressure or temperature differences between the evaporator and condenser as occurring in low temperature air drying where a single-stage vapour compression has low COP and SMER. Chapter 5 considers the alternative solution to this challenge by the application of two-stage vapour compression heat pump drying with high performance even for large temperature or pressure differences.

5

Design of Two-Stage Vapour Compression Heat Pump Drying

A properly designed two-stage vapour compression heat pump dryer has better performance than single-stage vapour compression for large temperature and pressure differences between evaporation and condensation. The reason is that the extra components in the dryer allow operation in smaller pressure intervals, resulting in enhanced coefficients of performance (COPs), energy utilisation and water removal rate. A major advantage of this dryer is its ability to process heat-sensitive wet-solids, liquids and pastes since the evaporator and air inlet temperatures can be set slightly below the material freezing point, resulting in high-quality product while operating with high performance and enhanced water removal rates.

The additional benefits of this heat pump dryer are a lower pressure ratio, higher cooling capacity, higher isentropic efficiency, lower discharge temperature or compressor overheating protection, lower compression and expansion energy losses.

This chapter covers the design and dimensioning of the two-stage vapour compression heat pump. Understanding information in this chapter requires knowledge and applications of the laws, governing equations, heat pump cycles and processes examined in detail in Chapter 3. The favoured dryer uses natural fluid, such as ammonia, and has two compressors, an open flash intercooler and two throttling devices.

This chapter covers the design and dimensioning of two-stage heat pump drying and provides illustrative cases applied in the manufacturing of different dried products.

5.1 Two-Stage Vapour Compression Heat Pump Drying of Green Peas

Figure 5.1 shows a two-stage vapour compression heat pump fluidised bed dryer with ammonia refrigerant (R717) that produces 96 tons of dried green peas per year. The peas are dried to 66.7%db from an initial moisture content of 566.7%db, and the dryer operates 7200 h/year. The drying chamber air inlet temperature and relative humidity are –5°C and 50%, respectively, and the exhaust air is at 86% relative humidity. The evaporating and condensing temperatures are –15.87°C and 20°C, respectively. Saturated vapour is compressed isentropically ($\eta_i = 1$), and saturated liquid is adiabatically throttled (h = constant).

Consider that the blower requires 25% of total compression work and drying is atmospheric and adiabatic, then (a) draw the air state points for drying air cycle in the Mollier diagram; (b) determine and tabulate the psychrometric conditions for the cycle state points; (c) draw the heat pump cycle on the log(p)–h diagram and tabulate the heat pump fluid properties; (d) calculate and specify the evaporator, compressor, and condenser; (e) calculate the COP and specific moisture extraction ratio (SMER) with and without

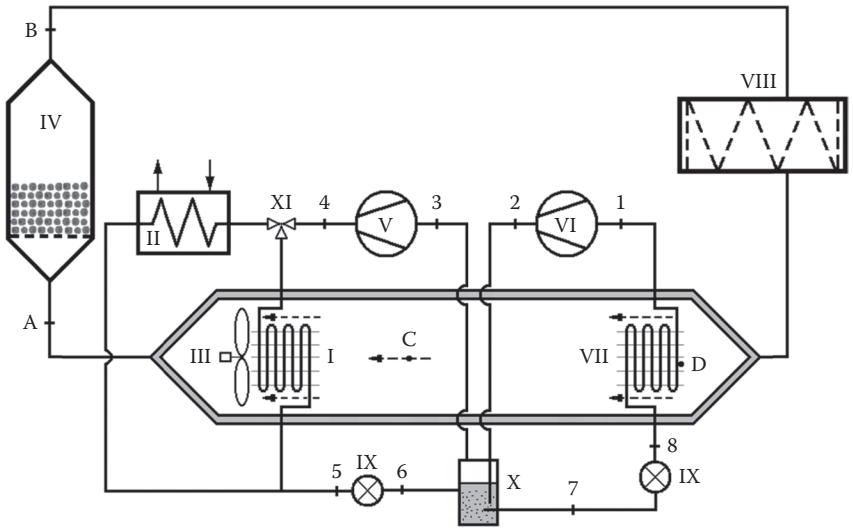

FIGURE 5.1
Two-stage vapour compression heat pump dryer with natural R717 or ammonia: I – internal condenser; II – external condenser; III – blower; IV – fluidised bed drying chamber with green peas; V – high-stage compressor; VI – low-stage compressor; VII – evaporator; VIII – filter; IX – throttling valve; X – open flash intercooler at intermediate pressure; XI – three-way valve; 1, 3: saturated vapour; 2, 4: superheated vapour; 5, 7: saturated liquid; 6, 8: vapour and liquid mixture; A – inlet of the drying chamber; B – inlet of the evaporator; C – inlet of condenser; D – evaporator surface.

accounting for blower work; and (f) calculate the percent change in COP and SMER based on the estimation without blower work and discuss the results.

Given:

R717	$t_A = -5°C$	$\phi_A = 50\%$
$\dot{m}_p = 96$ t/yr	$t_{ev} = t_D = -15.87°C$	$\phi_B = 86\%$
$X_0 = 566.7\%$db	$t_{con} = 20°C$	$\phi_D = 100\%$
$X_f = 66.7\%$db	$W_b = 0.25\ W_c$	p = 101,325 Pa
$n_h = 7200$ h/yr		

Solution:

(a) Drawing the air state points for drying air cycle in the Mollier diagram

The state points of two-stage vapour compression heat pump dryer are illustrated in Figure 5.2.

(b) Determining and tabulating the psychrometric conditions for the state points of the cycle

Table 5.1 shows the known and unknown properties for R717 on each state point for the two-stage vapour compression heat pump dryer.

The properties of *point A* are as follows:

$$h_A = -1.94 \text{ kJ/kg}$$

$$x_A = 0.001235 \text{ kg/kg}$$

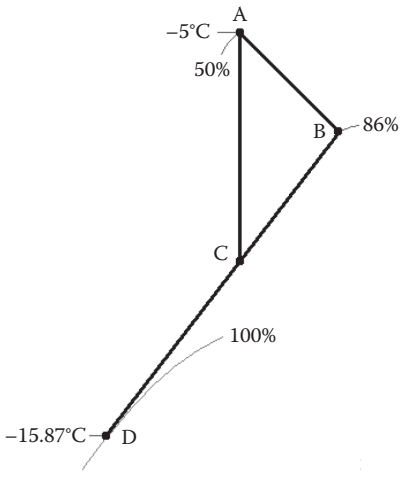

FIGURE 5.2
State points in the Mollier diagram: A – inlet of the drying chamber; B – inlet of the evaporator; C – inlet of condenser; D – evaporator surface; CA – blower and condenser heating; AB – drying; BC – cooling and evaporation.

TABLE 5.1

Known and Unknown Properties for the State Points for the Ammonia Heat Pump Dryer

	Point			
Property	**A**	**B**	**C**	**D**
t, °C	−5.00	Unknown	Unknown	−15.87
ϕ, %	50	86	Unknown	100
h, kJ/kg	Unknown	Unknown	Unknown	Unknown
x, g/kg	Unknown	Unknown	Unknown	Unknown

The properties of *point B* are as follows:

$$h_B = h_A = -1.94 \text{ kJ/kg}$$

$$t_B = -6.55°C$$

$$x_B = 0.001862 \text{ kg/kg}$$

From the given temperature and relative humidity, the properties at *point D* are as follows:

$$h_D = -13.60 \text{ kJ/kg}$$

$$x_D = 0.000938 \text{ kg/kg}$$

The properties at *point C* are as follows:

$$x_C = x_A = 0.001235 \text{ kg/kg}$$

$$t_C = t_B - \frac{x_B - x_C}{x_B - x_D}\left(t_B - t_D\right) = -12.87°C$$

$$h_C = -9.85\ kJ/kg$$

$$\phi_C = 99.96\%$$

The answer for (b) is provided by Table 5.2 that is obtained substituting the previous calculated properties into Table 5.1.

(c) Drawing the heat pump cycle on the log(p)–h diagram and tabulating the heat pump fluid properties

The known properties of R717 are summarised in Table 5.3, and the unknown values are calculated considering that the following:

- Evaporating temperature is –15.87°C.
- Condensing temperature is 20°C.
- Both compressions are isentropic ($\eta_i = 1$).
- Both expansions are adiabatic ($h_5 = h_6$ and $h_7 = h_8$).

The intermediate temperature requires the intermediate pressure, which is determined based on the evaporating and condensing pressures as follows:

$$p_{int} = \sqrt{p_{ev} \cdot p_{con}}$$

$$p_{ev} = 227.65\ kPa$$

TABLE 5.2

Psychrometric Conditions for the State Points for the R717 Heat Pump Dryer

	Point			
Property	**A**	**B**	**C**	**D**
t, °C	–5.00	–6.55	–12.87	–15.87
ϕ, %	50	86	99.96	100
h, kJ/kg	–1.94	–1.94	–9.85	–13.60
x, g/kg	1.24	1.86	1.24	0.94

TABLE 5.3

Known and Unknown Properties at the State Points of the Heat Pump with R717

	State Point							
Property	**1**	**2**	**3**	**4**	**5**	**6**	**7**	**8**
t, °C	–15.87	Unknown	Unknown	Unknown	20	Unknown	Unknown	Unknown
p, kPa	Unknown	Unknown	Unknown	Unknown	Unknown	Unknown	Unknown	Unknown
h, kJ/kg	Unknown	Unknown	Unknown	Unknown	Unknown	Unknown	Unknown	Unknown
s, kJ/kg·K	Unknown	Unknown	Unknown	Unknown	Unknown	—	Unknown	—
v, m^3/kg	Unknown	—	Unknown	—	—	—	—	—

$$p_{con} = 857.08 \text{ kPa}$$

$$p_{int} = 441.72 \text{ kPa}$$

Then, the intermediate temperature is

$$t_{int} = 0.8°C$$

Point 1 is saturated vapour at temperature at –15.87°C, and the other properties are as follows:

$$p_1 = 227.65 \text{ kPa}$$

$$h_1 = 1604.3 \text{ kJ/kg}$$

$$s_1 = 6.40 \text{ kJ/kg·K}$$

$$v_1 = 0.5265 \text{ m}^3/\text{kg}$$

Point 2 is superheated vapour that is reached after isentropic throttling, then

$$s_2 = s_1 = 6.40 \text{ kJ/kg·K}$$

$$p_2 = p_{int} = 441.72 \text{ kPa}$$

The other properties are as follows:

$$t_2 = 26.40°C$$

$$h_2 = 1690.1 \text{ kJ/kg}$$

Point 3 is saturated vapour, then

$$p_3 = p_{int} = 441.72 \text{ kPa}$$

$$t_3 = t_{int} = 0.8°C$$

$$h_3 = 1624.47 \text{ kJ/kg}$$

$$s_3 = 6.17 \text{ kJ/kg·K}$$

$$v_3 = 0.2817 \text{ m}^3/\text{kg}$$

Point 4 is superheated vapour after isentropic compression, then

$$s_4 = s_3 = 6.17 \text{ kJ/kg·K}$$

$$p_4 = 857.08 \text{ kPa}$$

$$t_4 = 45.40°C$$

$$h_4 = 1713.36 \text{ kJ/kg}$$

Point 5 is saturated liquid at temperature at 20°C, and the other properties are as follows:

$$p_5 = 857.08 \text{ kPa}$$

$$h_5 = 455.67 \text{ kJ/kg}$$

$$s_5 = 1.89 \text{ kJ/kg·K}$$

Point 6 is vapour–liquid mixture that is reached after adiabatic throttling, then

$$h_6 = h_5 = 455.67 \text{ kJ/kg}$$

$$t_6 = t_{int} = 0.8°C$$

$$p_6 = p_{int} = 441.72 \text{ kPa}$$

Point 7 is saturated liquid at intermediate temperature at 0.8°C, and the other properties are as follows:

$$p_7 = p_{int} = 441.72 \text{ kPa}$$

$$h_7 = 365.49 \text{ kJ/kg}$$

$$s_7 = 1.58 \text{ kJ/kg·K}$$

Point 8 is vapour–liquid mixture after an adiabatic process, then

$$h_8 = h_7 = 365.49 \text{ kJ/kg}$$

$$t_8 = t_{ev} = -15.87°C$$

$$p_8 = p_{ev} = 227.65 \text{ kPa}$$

Now, the two-stage vapour compression heat pump dyer is sketched in Figure 5.3 based on the heat pump fluid properties provided by the previous calculation and Table 5.4.

(d) Calculation and specification of the evaporator, compressor and condenser

The calculations and specifications are made based on the properties of the air and vapour mixture and R717 provided in Tables 5.2 and 5.4:

$$Q_{ev} = \dot{m}_a \Delta h = \frac{\dot{m}_w}{3600 \cdot \Delta x} \Delta h$$

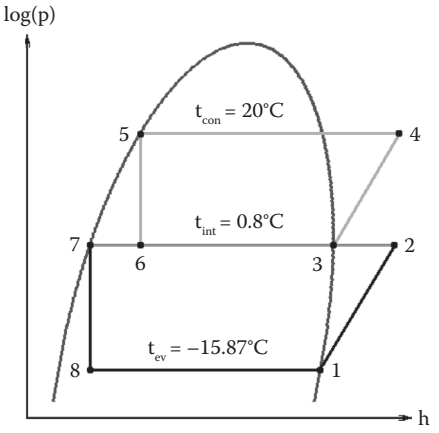

FIGURE 5.3
State points on the log(p)–h diagram. 1–2: low-stage compression, 2–3: vapour desuperheating, 3–4: high-stage compression, 4–5: condensation, 5–6: high-stage throttling, 6–7: cooling to saturated liquid, 7–8: low-stage throttling, 8–1: evaporation, 1, 3: saturated vapour; 2, 4: superheated vapour; 5, 7: saturated liquid; 6, 8: vapour and liquid mixture.

TABLE 5.4
Properties for the State Points of the Heat Pump Fluid with R717

	State Point							
Property	**1**	**2**	**3**	**4**	**5**	**6**	**7**	**8**
t, °C	−15.87	26.40	0.8	45.40	20.0	0.8	0.8	−15.87
p, kPa	227.65	441.72	441.72	857.08	857.08	441.72	441.72	227.65
h, kJ/kg	1604.3	1690.1	1624.47	1713.36	455.67	455.67	365.49	365.49
s, kJ/kg·K	6.40	6.40	6.17	6.17	1.89	—	1.58	—
v, m^3/kg	0.5265	—	0.2817	—	—	—	—	—

$$\Delta x = x_B - x_A = 0.000626 \text{ kg/kg}$$

$$\Delta h = h_A - h_C = 7.91 \text{ kJ/kg}$$

The water mass flow rate is calculated as follows:

$$\dot{m}_w = \dot{m}_0 - \dot{m}_p$$

$$\dot{m}_p = 96 \text{ t/yr} = \frac{96,000}{n_h} = \frac{96,000}{7200} = 13.33 \text{ kg/h}$$

$$\dot{m}_0 = \frac{\dot{m}_{dm}}{1 - \dfrac{0.01X_0}{1 + 0.01X_0}}$$

$$\dot{m}_{dm} = \dot{m}_p \cdot \left(1 - \frac{0.01X_f}{1 + 0.01X_f}\right) = 13.33 \cdot \left(1 - \frac{0.667}{1 + 0.667}\right) = 13.33 \cdot 0.60 = 8.00 \text{ kg/h}$$

$$\dot{m}_0 = \frac{8.00}{1 - \frac{5.667}{1 + 5.667}} = \frac{8}{0.15} = 53.33 \text{ kg/s}$$

$$\dot{m}_w = 53.33 - 13.33 = 40 \text{ kg/h}$$

$$Q_{ev} = \frac{\dot{m}_w}{\Delta x}\Delta h = \frac{40 \cdot 7.91}{3600 \cdot 0.000625} = 140.31 \text{ kW}$$

The refrigerant mass and volumetric flow rates on the low-pressure side are determined by

$$\dot{m}_L = \frac{Q_{ev}}{h_1 - h_8} = 0.1133 \text{ kg/s}$$

$$\dot{V}_L = 3600 \cdot \dot{m}_L \cdot v_1 = 3600 \cdot 0.1133 \cdot 0.5265 = 214.69 \text{ m}^3/\text{h}$$

The equations for shaft work for the low- and high-stage compressors are as follows:

$$W_L = \dot{m}_L (h_2 - h_1) = 9.72 \text{ kW}$$

$$W_H = \dot{m}_H (h_4 - h_3)$$

The refrigerant mass flow rate on the high-stage side is determined by an energy balance on the open flash intercooler as follows:

$$\dot{m}_H = \dot{m}_L \frac{h_2 - h_7}{h_3 - h_6} = 0.1133 \frac{1324.6}{1168.8} = 0.1284 \text{ kg/s}$$

$$W_H = 0.1284 \ (1713.36 - 1624.47) = 11.41 \text{ kW}$$

The refrigerant volumetric flow rate on the high-pressure side is as follows:

$$\dot{V}_H = 3600 \cdot \dot{m}_H \cdot v_3 = 3600 \cdot 0.1284 \cdot 0.2817 = 130.18 \text{ m}^3/\text{h}$$

The total shaft work is the sum of the work on the low- and high-pressure sides, then

$$W_c = W_L + W_H = 21.13 \text{ kW}$$

The condensing capacity is as follows:

$$Q_{cond} = \dot{m}_H (h_4 - h_5) = W_c + Q_{ev} = 161.45 \text{ kW}$$

The air volumetric flow rate is as follows:

$$\dot{V}_a = \dot{m}_a \cdot v_A$$

The specific volume of the air at the *point A* is as follows:

$$v_A = 0.7603 \text{ m}^3/\text{kg}$$

The mass flow rate of air is as follows:

$$\dot{m}_a = \frac{\dot{m}_w}{\Delta x} = \frac{40}{0.000625} = 63871.60 \text{ kg/h}$$

$$\dot{V}_a = \dot{m}_a \cdot v_A = 63,871.60 \cdot 0.7603 = 48,559.07 \text{ m}^3/\text{h}$$

Based on the previous calculations, the specification for each component of the two-stage vapour compression heat pump dryer with R717 is summarised in Table 5.5.

(e) Calculation of the COP and SMER with and without accounting for blower work

These performance parameters are calculated as follows:

$$COP_c = \frac{Q_{ev}}{W_c} = 6.64$$

$$COP_{cb} = \frac{Q_{ev}}{W_c + W_b} = \frac{Q_{ev}}{W_c(1 + 0.25)} = 5.53$$

TABLE 5.5

Specification for Each Component of the Heat Pump Dryer Operating with Natural Ammonia

	Component				
		Compressor		Condenser	
Performance	**Evaporator**	**Low Stage**	**High Stage**	**Internal**	**External**
Q, kW	140.31	—	—	≥140.31	21.13
W, kW	—	9.72	11.41	—	—
$\dot{V}_r$, m³/h	214.69	214.69	130.18	—	—
$\dot{V}_a$, m³/h	48,559.07	—	—	48,559.07	—
p, kPa	227.7	—	—	857.08	857.08
ϕ_{in}, %	—	—	—	99.96	—
t_{ev}, °C	−15.87	−15.87	—	—	—
t_{con}, °C	—	—	20.0	20.0	20.0
$t_{a_{in}}$, °C	−6.55	—	—	−12.87	—
$t_{a_{out}}$, °C	−12.87	—	—	−15.87	—
t_{int}, °C	—	0.8	0.8	0.8	—

$$SMER_c = COP_c \frac{\Delta x}{\Delta h} = 1.893 \text{ kg/kWh}$$

$$SMER_{cb} = COP_{cb} \frac{\Delta x}{\Delta h} = 1.577 \text{ kg/kWh}$$

(f) Calculation of the percent change in COP and SMER based on the estimation without blower work and discussion of the results

$$r_{COP} = \frac{COP_c - COP_{cb}}{COP_c} 100\% = 20.072\%$$

$$r_{SMER} = \frac{SMER_c - SMER_{cb}}{SMER_c} 100\% = 20.038\%$$

A central discussion about the results is that COP and SMER would be 20.1% overestimated if the blower work is unaccounted in the calculations.

5.2 Two-Stage Compression Heat Pump Drying of Aromatic Leaves

Figure 5.4 illustrates a two-stage compression heat pump belt dryer with refrigerant R134a that produces aromatic leaves dried to 8%wb. The wet material input to the dryer is 331.2 t/year and the initial moisture content is 88%wb. The drying chamber air inlet temperature and relative humidity are –2°C and 60%, respectively, and the exhaust air is at 90% relative humidity. The evaporating and condensing temperatures are –11°C and 23°C, respectively. Saturated vapour is isentropically compressed, saturated liquid is adiabatically expanded and the blower requires 20% of total compression work. Consider that the dryer operates 7200 h/year and the drying process is atmospheric and adiabatic, then (a) draw the air state points for drying air cycle in the Mollier diagram; (b) determine and tabulate the psychrometric state points of the drying loop cycle; (c) tabulate the heat pump fluid properties and draw the heat pump cycle on the log(p)–h diagram; (d) calculate and specify the evaporator, compressor, and condenser; (e) calculate the COP and SMER with and without accounting the blower work; and (f) calculate the percent change in COP and SMER based on the estimation without blower work and comment the results.

Given:

R134a	$t_A = -2°C$	$\phi_A = 60\%$
$\dot{m}_0 = 331.2$ t/yr	$t_{ev} = t_D = -11°C$	$\phi_B = 90\%$
$X_0 = 88\%$db	$t_{con} = 23°C$	$\phi_D = 100\%$
$X_f = 8\%$db	$W_b = 0.2W_c$	$p = 101{,}325$ Pa
$n_h = 7200$ h/yr		

Solution:

(a) Drawing the air state points for drying air cycle in the Mollier diagram

The state points of two-stage vapour compression heat pump dryer are illustrated in Figure 5.5.

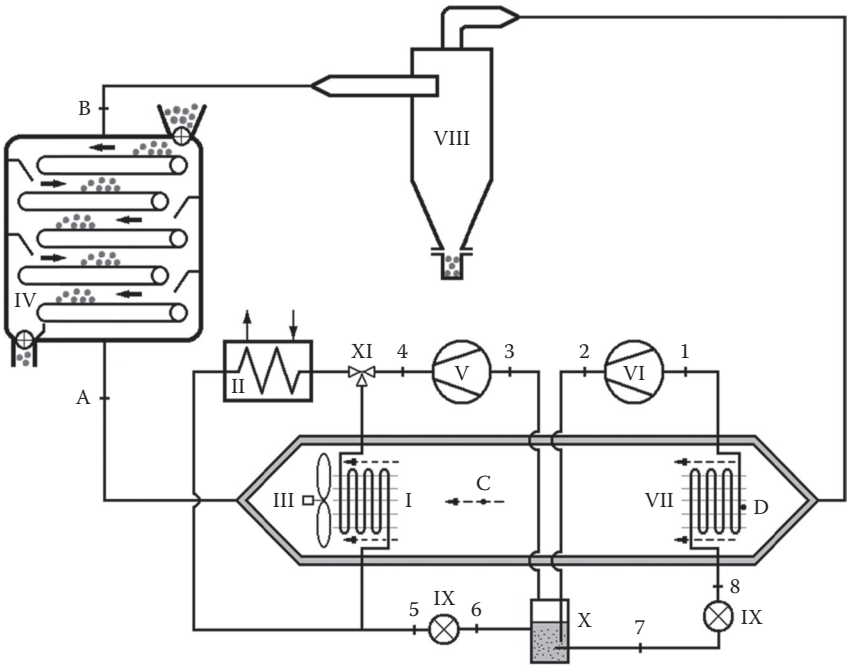

FIGURE 5.4
Two-stage vapour compression heat pump dryer with R134a: I – internal condenser; II – external condenser; III – blower; IV – conveyor belt drying chamber with the aromatic leaves; V – high-stage compressor; VI – low-stage compressor; VII – evaporator; VIII – cyclone; IX – throttling valves; X – open flash intercooler at intermediate pressure; XI – three-way valve; 1, 3: saturated vapour; 2, 4: superheated vapour; 5, 7: saturated liquid; 6, 8: vapour and liquid mixture; A – inlet of the drying chamber; B – inlet of the evaporator; C – inlet of condenser; D – evaporator surface.

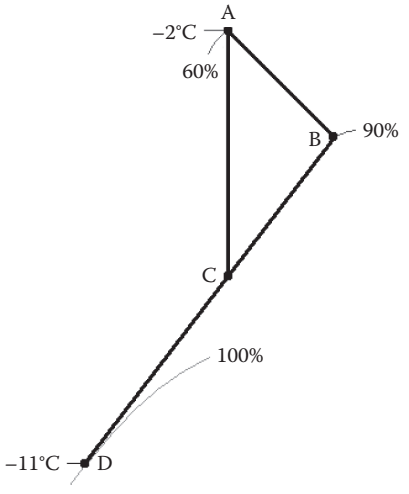

FIGURE 5.5
State points in the Mollier diagram: A – inlet of the drying chamber; B – inlet of the evaporator; C – inlet of condenser; D – evaporator surface; CA – blower and condenser heating; AB – drying; BC – cooling and evaporation.

TABLE 5.6

Known and Unknown Properties at the State Points for the R134a Heat Pump Dryer

	Point			
Property	**A**	**B**	**C**	**D**
t, °C	–2.0	Unknown	Unknown	–11.0
ϕ, %	60	90	Unknown	100
h, kJ/kg	Unknown	Unknown	Unknown	Unknown
x, g/kg	Unknown	Unknown	Unknown	Unknown

(b) Determining and tabulating the psychrometric conditions for the state points of the cycle

Table 5.6 shows the known and unknown properties on each state point for the R134a heat pump dryer.

The properties at *point A* are as follows:

$$h_A = 2.77 \text{ kJ/kg}$$

$$x_A = 0.001912 \text{ kg/kg}$$

The properties at *point B* are as follows:

$$h_B = h_A = 2.77 \text{ kJ/kg}$$

$$t_B = -3.52°C$$

$$x_B = 0.002527 \text{ kg/kg}$$

From the given temperature and relative humidity, the properties at *point D* are as follows:

$$h_D = -7.40 \text{ kJ/kg}$$

$$x_D = 0.001463 \text{ kg/kg}$$

The properties at *point C* are as follows:

$$x_C = x_A = 0.001912 \text{ kg/kg}$$

$$t_C = t_B - \frac{x_B - x_C}{x_B - x_D}\left(t_B - t_D\right) = -7.84°C$$

$$h_C = -3.11 \text{ kJ/kg}$$

$$\phi_C = 98.81\%$$

From the previous calculations and Table 5.6, the answer for (b) is provided in Table 5.7.

TABLE 5.7

Psychrometric Conditions at the State Points of the R134a Heat Pump Dryer

	Point			
Property	**A**	**B**	**C**	**D**
t, °C	–2.00	–3.52	–7.84	–11.00
ϕ, %	60	90	98.81	100
h, kJ/kg	2.77	2.77	–3.11	–7.40
x, g/kg	1.91	2.53	1.91	1.46

(c) Drawing the heat pump cycle on the log(p)–h diagram and tabulating the heat pump fluid properties

The known properties of R134a are shown in Table 5.8, and the unknown values are determined considering that the following:

- Evaporating temperature is –11°C.
- Condensing temperature is 23°C.
- Both compressions are isentropic.
- Both expansions are adiabatic.

The intermediate pressure and temperature are determined based on the evaporating and condensing pressures as follows:

$$p_{int} = \sqrt{p_{ev} \cdot p_{con}}$$

$$p_{ev} = 192.97 \text{ kPa}$$

$$p_{con} = 626.49 \text{ kPa}$$

$$p_{int} = 347.70 \text{ kPa}$$

The intermediate temperature is as follows:

$$t_{int} = 4.8°C$$

Point 1 is saturated vapour at temperature at –11°C, and the other properties are as follows:

$$p_1 = 192.97 \text{ kPa}$$

$$h_1 = 390.73 \text{ kJ/kg}$$

$$s_1 = 1.73 \text{ kJ/kg·K}$$

$$v_1 = 0.1028 \text{ m}^3/\text{kg}$$

TABLE 5.8

Known and Unknown Properties for the State Points of the Heat Pump with R134a

	State Point							
Property	**1**	**2**	**3**	**4**	**5**	**6**	**7**	**8**
t, °C	−11.0	Unknown	Unknown	Unknown	23	Unknown	Unknown	Unknown
p, kPa	Unknown	Unknown	Unknown	Unknown	Unknown	Unknown	Unknown	Unknown
h, kJ/kg	Unknown	Unknown	Unknown	Unknown	Unknown	Unknown	Unknown	Unknown
s, kJ/kg·K	Unknown	Unknown	Unknown	Unknown	Unknown	—	Unknown	—
v, m^3/kg	Unknown	—	Unknown	—	—	—	—	—

Point 2 is superheated vapour that is reached after isentropic compression, then

$$s_2 = s_1 = 1.73 \text{ kJ/kg·K}$$

$$p_2 = p_{int} = 347.70 \text{ kPa}$$

The other properties are as follows:

$$t_2 = 7.7°C$$

$$h_2 = 402.64 \text{ kJ/kg}$$

Point 3 is saturated vapour and

$$p_3 = p_{int} = 347.70 \text{ kPa}$$

$$t_3 = t_{int} = 4.8°C$$

$$h_3 = 399.98 \text{ kJ/kg}$$

$$s_3 = 1.72 \text{ kJ/kg·K}$$

$$v_3 = 0.0583 \text{ m}^3/\text{kg}$$

Point 4 is superheated vapour. Since this point is isentropic, then

$$s_4 = s_3 = 1.72 \text{ kJ/kg·K}$$

$$p_4 = 626.49 \text{ kPa}$$

$$t_4 = 25.1°C$$

$$h_4 = 412.07 \text{ kJ/kg}$$

Point 5 is saturated liquid at temperature at 23°C and the other properties are as follows:

$$p_5 = 626.49 \text{ kPa}$$

$$h_5 = 231.46 \text{ kJ/kg}$$

$$s_5 = 1.11 \text{ kJ/kg·K}$$

Point 6 is vapour–liquid mixture after adiabatic throttling, then

$$h_6 = h_5 = 231.46 \text{ kJ/kg}$$

$$t_6 = t_{int} = 4.8°C$$

$$p_6 = p_{int} = 347.70 \text{ kPa}$$

Point 7 is saturated liquid at intermediate temperature at 4.8°C, and the other properties are as follows:

$$p_7 = p_{int} = 347.70 \text{ kPa}$$

$$h_7 = 206.44 \text{ kJ/kg}$$

$$s_7 = 1.02 \text{ kJ/kg·K}$$

Point 8 is vapour–liquid mixture after an adiabatic process, then

$$h_8 = h_7 = 206.44 \text{ kJ/kg}$$

$$t_8 = t_{ev} = -11°C$$

$$p_8 = p_{ev} = 192.97 \text{ kPa}$$

Table 5.9 gives the properties at each state point of the cycle for the heat pump with R134a fluid based on the previous calculations.

From the calculations and the data in Table 5.9, the R134a heat pump cycle is sketched on the log(p)–h diagram in Figure 5.6.

(d) Calculation and specification of the evaporator, compressor and condenser

The calculation and specification are based on the properties of the air–vapour mixture and R134a available in Tables 5.7 and 5.9:

$$Q_{ev} = \dot{m}_a \Delta h = \frac{\dot{m}_w}{3600 \cdot \Delta x} \Delta h$$

$$\Delta x = x_B - x_A = 0.000614 \text{ kg/kg}$$

$$\Delta h = h_A - h_C = 5.88 \text{ kJ/kg}$$

TABLE 5.9

Properties for the State Points of the Heat Pump Cycle with R134a

	State Point							
Property	**1**	**2**	**3**	**4**	**5**	**6**	**7**	**8**
t, °C	–11.0	7.7	4.8	25.1	23.0	4.8	4.8	–11.0
p, kPa	192.97	347.70	347.70	626.49	626.49	347.70	347.70	192.97
h, kJ/kg	390.73	402.64	399.98	412.07	231.46	231.46	206.44	206.44
s, kJ/kg·K	1.73	1.73	1.72	1.72	1.11	—	1.02	—
v, m^3/kg	0.1028	—	0.0583	—	—	—	—	—

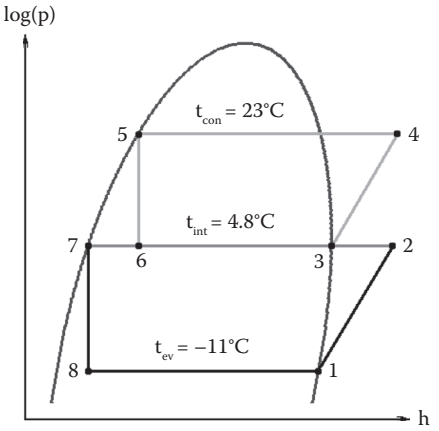

FIGURE 5.6
State points on the log(p)–h diagram. 1–2: low-stage compression, 2–3: vapour desuperheating, 3–4: high-stage compression, 4–5: condensation, 5–6: high-stage throttling, 6–7: cooling to saturated liquid, 7–8: low-stage throttling, 8–1: evaporation, 1, 3: saturated vapour; 2, 4: superheated vapour; 5, 7: saturated liquid; 6, 8: vapour and liquid mixture.

The water mass flow rate is calculated as follows:

$$\dot{m}_w = \dot{m}_0 - \dot{m}_p$$

$$\dot{m}_0 = 331.2 \text{ t/yr} = \frac{331,200}{n_h} = \frac{331,200}{7200} = 46 \text{ kg/h}$$

$$\dot{m}_p = \frac{\dot{m}_{dm}}{1 - X_f}$$

$$\dot{m}_{dm} = \dot{m}_0 \cdot (1 - 0.01X_0) = 46 \cdot (1 - 0.88) = 5.52 \text{ kg/h}$$

$$\dot{m}_p = \frac{5.52}{1 - 0.08} = 6.0 \text{ kg/s}$$

$$\dot{m}_w = 46 - 6 = 40 \text{ kg/h}$$

$$Q_{ev} = \frac{\dot{m}_w}{3600 \cdot \Delta x} \Delta h = \frac{40 \cdot 5.88}{3600 \cdot 0.000614} = 106.33 \text{ kW}$$

The refrigerant mass and volumetric flow rates on the low-pressure side are determined by

$$\dot{m}_L = \frac{Q_{ev}}{h_1 - h_8} = 0.5770 \text{ kg/s}$$

$$\dot{V}_L = 3600 \cdot \dot{m}_L \cdot v_1 = 3600 \cdot 0.5770 \cdot 0.1028 = 213.50 \text{ m}^3/\text{h}$$

The equations for shaft work for the low- and high-stage compressors are as follows:

$$W_L = \dot{m}_L (h_2 - h_1) = 6.87 \text{ kW}$$

$$W_H = \dot{m}_H (h_4 - h_3)$$

The refrigerant mass flow rate on the high-pressure side is determined by energy balance in the open flash intercooler as follows:

$$\dot{m}_H = \dot{m}_L \frac{h_2 - h_7}{h_3 - h_6} = 0.5770 \frac{196.2}{168.5} = 0.6718 \text{ kg/s}$$

$$W_H = 0.6718(412.07 - 399.98) = 8.12 \text{ kW}$$

The refrigerant volumetric flow rate on the high-pressure side is as follows:

$$\dot{V}_H = 3600 \cdot \dot{m}_H \cdot v_3 = 3600 \cdot 0.6718 \cdot 0.0583 = 141.09 \text{ m}^3/\text{h}$$

The total shaft work is the sum of the values on low- and high-pressure sides, then

$$W_c = W_L + W_H = 15.0 \text{ kW}$$

The condensing capacity is as follows:

$$Q_{cond} = \dot{m}_H (h_4 - h_5) = W_c + Q_{ev} = 121.33 \text{ kW}$$

The air volumetric flow rate is as follows:

$$\dot{V}_a = \dot{m}_a \cdot v_A \text{ m}^3/\text{h}$$

The specific volume of the air at the *point A* is as follows:

$$v_A = 0.7691 \text{ m}^3/\text{kg}$$

The mass flow rate of air is as follows:

$$\dot{m}_a = \frac{\dot{m}_w}{\Delta x} = \frac{40}{0.000614} = 65,146.57 \text{ kg/h}$$

$$\dot{V}_a = \dot{m}_a \cdot v_A = 65,146.57 \cdot 0.7691 = 50,104.23 \text{ m}^3/\text{h}$$

Based on the previous calculations, the specification for each component of the two-stage vapour compression heat pump dryer with R134a is summarised in Table 5.10.

TABLE 5.10

Specification for Each Component of the Heat Pump Dryer with R134a

	Component				
		Compressor		Condenser	
Performance	**Evaporator**	**Low Stage**	**High Stage**	**Internal**	**External**
Q, kW	106.33	—	—	≥106.33	15.00
W, kW	—	6.87	8.12	—	—
$\dot{V}_r$, m³/h	213.50	213.50	141.09	—	—
$\dot{V}_a$, m³/h	50,080.08	—	—	50,080.08	—
p, kPa	192.97	—	—	626.49	626.49
ϕ_{in}, %	—	—	—	98.81	—
t_{ev}, °C	−11	−11	—	—	—
t_{con}, °C	—	—	23	23	23
$t_{a_{in}}$, °C	−3.52	—	—	−7.84	—
$t_{a_{out}}$, °C	−7.84	—	—	−11	—
t_{int}, °C	—	4.8	4.8	4.8	—

(e) Calculation of SMER with and without accounting the blower work
These values are calculated as follows:

$$COP_c = \frac{Q_{ev}}{W_c} = 7.09$$

$$COP_{cb} = \frac{Q_{ev}}{W_c + W_b} = \frac{Q_{ev}}{W_c(1 + 0.2)} = 5.91$$

$$SMER_c = COP_c \frac{\Delta x}{\Delta h} = 2.667 \text{ kg/kWh}$$

$$SMER_{cb} = COP_{cb} \frac{\Delta x}{\Delta h} = 2.223 \text{ kg/kWh}$$

(f) Calculation of the percent change in COP and SMER based on the estimation without blower work and work and comment of the results

$$r_{COP} = \frac{COP_c - COP_{cb}}{COP_c} 100\% = 16.643\%$$

$$r_{SMER} = \frac{SMER_c - SMER_{cb}}{SMER_c} 100\% = 16.648\%$$

The results suggest that both the actual COP and SMER are 16.6% lower when the blower work is taken into account in the calculations.

6

Psychrometry of Moist Air Applied to Water Removal and Energy Consumption

Convective drying involves simultaneous exchange of moisture and heat between the material undergoing drying and the flowing moist air. The magnitude of the exchange depends on the driving forces provided by the temperature and vapour pressure gradients that are established inside the material and at the air boundary layer over the surface. Moist air is the most suitable drying agent because it has acceptable properties and is nearly cost free and readily available worldwide. Thus, knowledge of the moist air properties at each state point of drying is essential in the calculations of water removal, energy utilisation and dryer capacity. Psychrometric charts, equations and software libraries are applied to determine the moist air properties that are fundamental in design, analysis and evaluation of energy, moisture removal and capacity of heat pump dryers. The continuous phase in the majority of convective drying processes is a mixture of air and water vapour. The state points and properties of the mixture change as it flows through the components of the heat pump drying processes. The changes must be determined at the inlet and outlet of the heat exchangers and the drying chamber to establish the state points in each process and for calculations of energy use and water removal during drying.

This chapter describes the major equations and graphical methods to determine the properties of the moist air. Illustrative cases are discussed and problems are solved considering the changes of properties at different state points of the moist air as it flows through the components of the heat pump dryer.

6.1 Main Moist Air Psychrometric Properties

6.1.1 Definition and Identification of the Main Moist Air Properties in Psychrometry

The design and analysis of a heat pump drying process requires knowledge of the moist air main properties: temperature (t), specific enthalpy (h), vapour pressure (p_v), specific volume (v), absolute humidity (x) and relative humidity (ϕ). These essential properties are determined by equations and graphically by the psychrometric charts and diagrams. Figure 6.1 illustrates how to identify the moist air properties through the constant lines and curves that are always shown in the Mollier diagram (Dossat 1981; Mujumdar 2008).

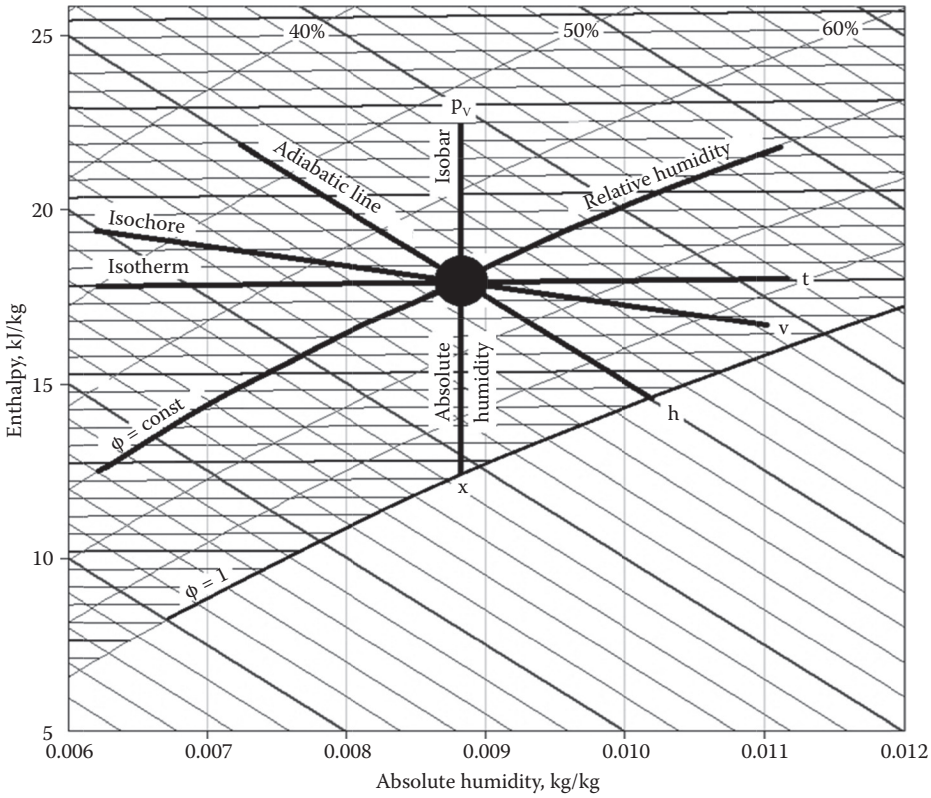

FIGURE 6.1
Illustration with identification of the moist air main properties in the psychrometric chart.

6.1.2 Absolute Humidity

The absolute humidity is the actual mass of water vapour in the mixture per unit mass of dry air. The equations for the actual absolute humidity for air and water vapour mixture behaving as an ideal gas are

$$x = \frac{m_v}{m_a} = \frac{M_v p_v}{M_a\left(p - p_v\right)} = \frac{M_v p_v V}{RT}\frac{RT}{M_a p_a V} \tag{6.1}$$

$$x = \frac{M_v}{M_a}\frac{p_v}{p_a} = \frac{18.015}{28.9645}\frac{p_v}{p_a} = 0.62198\frac{p_v}{p - p_v} \tag{6.2}$$

where x is actual absolute humidity, m_v is mass of vapour, m_a is mass of air, M_v is molecular mass of water vapour, M_a is molecular mass of air, p is total pressure, p_v is water vapour pressure, p_a is air pressure, R is universal gas constant, T is absolute temperature and V is total volume of mixture.

Similarly, the saturated absolute humidity of the mixture is

$$x_s = \frac{m_{vs}}{m_a} = \frac{M_{vs}}{M_a}\frac{p_{vs}}{p_a} = 0.62198\frac{p_{vs}}{p_a} \tag{6.3}$$

where x_s is saturated absolute humidity, p_{vs} is saturated water vapour pressure and M_{vs} is molecular mass of saturated water vapour.

The absolute humidity at thermodynamic wet-bulb temperature is as follows:

$$x_s^* = 0.62198 \frac{p_{vs}^*}{p - p_{vs}^*} \tag{6.4}$$

$$x = \frac{\left[\Delta h_{lv}^0 - \left(c_{pw}^0 - c_{pv}^0\right)t_{wb}\right]x_s^* - c_{pa}^0\left(t - t_{wb}\right)}{\Delta h_{lv}^0 + c_{pv}^0 t - c_{pw}^0 t_{wb}} \tag{6.5}$$

$$x = \frac{\left(2501 - 2.326t_{wb}\right)x_s^* - 1.006\left(t - t_{wb}\right)}{2501 + 1.86t - 4.186t_{wb}} \tag{6.6}$$

$$x = \frac{h - 1.006t}{2501 + 1.86t} \tag{6.7}$$

where * designates the properties at wet-bulb temperature or at equilibrium state *point*, t is mixture's temperature, t_{wb} is wet-bulb temperature, h is enthalpy, Δh_{lv}^0 is latent heat of vaporisation at the reference point, c_{pa}^0 is the specific heat of air and c_{pw}^0 and c_{pv}^0 are water specific heat of the liquid and vapour phases, respectively.

6.1.3 Degree of Saturation

The degree of saturation is the absolute humidity ratio given by

$$\mu = \frac{x}{x_s} = \frac{0.62195\phi}{0.62195 + \left(1 - \phi\right)x_s} \tag{6.8}$$

$$\mu = \frac{x}{x_s} = \frac{p - p_{vs}}{p - p_v}\frac{p_v}{p_{vs}} \tag{6.9}$$

where μ is degree of saturation, and ϕ is relative humidity.

6.1.4 Relative Humidity

The relative humidity is the ratio of the actual partial pressure of water vapour in the mixture and the saturation pressure of vapour at the same temperature. For moist of air behaving as an ideal gas, the relative humidity is also the ratio of the actual mass of water vapour and the mass of saturated vapour as follows:

$$\phi = \frac{m_v}{m_w} = \frac{p_v V}{R_v T}\frac{R_v T}{p_w V} = \frac{p_v}{p_{vs}} \tag{6.10}$$

Replacing the partial vapour pressure leads to

$$\phi = \frac{p_v}{p_{vs}} = \frac{x}{0.62198}\frac{p_a}{p_{vs}} \tag{6.11}$$

$$\phi = \frac{\mu p}{p - (1 - \mu) p_{vs}} \tag{6.12}$$

$$\phi = \frac{x}{0.62198 + x} \frac{p}{p_{vs}} \tag{6.13}$$

6.1.5 Actual and Saturated Vapour Pressure of Air–Vapour Mixture

Generally, it is difficult to distinguish the actual, saturated and equilibrium vapour pressures and the corresponding absolute humidities and temperatures. This distinction is important to apply the equations and correlations for the properties that are described herein. Figure 6.2 provides a better visualisation of these properties position and relative values on psychrometric charts.

The equations for vapour pressure of the air–vapour mixture and dry air are as follows:

$$p_v = \phi \cdot p_{vs} \tag{6.14}$$

$$p_v = \frac{p \cdot x}{0.62197 + x} \tag{6.15}$$

$$p_v = p - p_a \tag{6.16}$$

The saturation pressure for water vapour in the temperature range of 0°C < t ≤ 40°C is determined (Holman 1988) by

$$p_{vs} = \exp\left[30.9154 - \frac{6789}{T} - 5.031 \ln\left(\frac{T}{293.15}\right)\right] \tag{6.17}$$

$$p_{vs} = \frac{x}{0.62198 + x} \frac{p}{\phi} \tag{6.18}$$

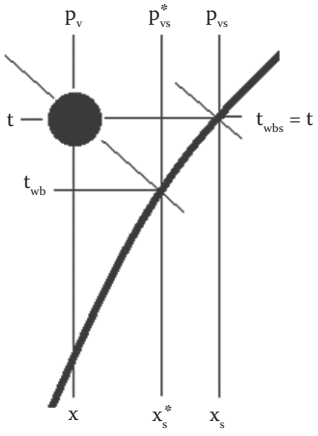

FIGURE 6.2
Psychrometric charts for distinction of the actual, saturated, and equilibrium vapour pressures and the corresponding absolute humidities and temperatures.

The recommended (ASHRAE Handbook of Fundamentals 2009) expression for vapour pressure in the temperature range of 0°C < t ≤ 200°C is

$$p_{vs} = \exp\left[\begin{array}{l} -5800.2206T^{-1} + 1.3914993 + -4.8640239\cdot 10^{-2}T + \\ +4.1764768\cdot 10^{-5}T^{2} + -1.4452093\cdot 10^{-8}T^{3} + 6.5459673\cdot \ln(T) \end{array}\right] \tag{6.19}$$

From these equations, the saturated vapour pressure at the state point wet-bulb temperature is

$$p_{vs}^{*} = \exp\left[30.9154 - \frac{6789}{T_{wb}} - 5.031\ln\left(T_{wb}\right)\right] \tag{6.20}$$

$$p_{vs}^{*} = \exp\left[\begin{array}{l} -5800.2206T_{wb}^{-1} + 1.3914993 - 4.8640239\cdot 10^{-2}T_{wb} + \\ +4.1764768\cdot 10^{-5}T_{wb}^{2} - 1.4452093\cdot 10^{-8}T_{wb}^{3} + 6.5459673\cdot \ln(T_{wb}) \end{array}\right] \tag{6.21}$$

6.1.6 Specific Enthalpy of Dry Air and Mixture Components

The specific enthalpy of an air–water vapour mixture is the sum of the specific enthalpies of the components. For a reference point at 0°C and temperatures between 0 and 100°C, the expressions (ASHRAE Handbook of Fundamentals 2009) for the dry air and saturated vapour and saturated liquid water are

$$h_a = c_{pa}^{0}(t - t^{0}) = 1.006t \tag{6.22}$$

$$h_v = \Delta h_{lv}^{0} + cp_v^{0}\left(t - t^{0}\right) = h_l^{0} - h_v^{0} + cp_v^{0}\left(t - t^{0}\right) \tag{6.23}$$

$$h_v = (2500.89 + 0.04) + 1.86t \cong 2501 + 1.86t \tag{6.24}$$

$$h_w = c_{pw}^{0}\cdot t_{wb} = 4.186t_{wb} \tag{6.25}$$

where t^0 is reference temperature, h_l^0 and h_v^0 are water specific enthalpies of saturated liquid and vapour at reference temperature; and h_a, h_v and h_w are specific enthalpies of air, vapour and liquid water, respectively.

Substitution of the variables above leads to the equation for specific enthalpy of the mixture:

$$h = h_a + xh_v = 1.006t + (2501 + 1.86t)x \tag{6.26}$$

6.1.7 Specific Volume

The specific volume of the dry air is a relevant quantity for solving convective air drying problems since it is constant as the air–vapour mixture flows through the closed

drying loop. This is the reason the specific volume of dry air appears on the psychrometric charts. It is expressed in terms of mass of dry-air mass as follows:

$$v_a = \frac{V}{m_a} = \frac{V}{M_a \cdot n_a} \quad \therefore m_a = M_a \cdot n_a \quad \therefore p_a = p - p_v \tag{6.27}$$

$$v_a = \frac{R}{M_a}\frac{T}{p_a} = \frac{R_a T}{p - p_v} = 287\frac{T}{p_a} = 461.539x\frac{T}{p_v} \quad \therefore x = 0.62198\frac{p_v}{p_a} \tag{6.28}$$

$$v_a = \frac{R_a T}{p}(1 + 1.6078x) = (287 + 461.539x)\frac{T}{p} \tag{6.29}$$

where n_a is number of moles of air, v_a is air specific volume and R_a is gas constant for air.

For constant total pressure of 101325 Pa, this equation simplifies to

$$v_a = \left(\frac{1}{353.05} + \frac{x}{219.54}\right)T \tag{6.30}$$

The total true specific volume of the vapour in the mixture is found by

$$v = \frac{V}{m} = \frac{m_a v_a}{m_a + m_v} = \frac{m_a v_a}{m_a(1+x)} = \frac{v_a}{1+x} \tag{6.31}$$

where v is total true specific volume.

6.1.8 Specific Heat

The specific heat of a substance is highly dependent on pressure, temperature and volume. In a system with constant pressure or volume, it is defined as follows:

$$c_p \equiv \left(\frac{\partial h}{\partial t}\right)_p \qquad c_p \equiv \left(\frac{\partial u}{\partial t}\right)_V \tag{6.32}$$

where u is internal energy.

Considering the main fractions of the moist air, the specific heat of dry air and water vapour depends on the temperature and initial specific heat. The equations in terms of temperatures are as follows:

$$c_{pa} = c_{pa}^0 + K_a t = c_{pa}^0 + 1.05 \cdot 10^{-4} t \tag{6.33}$$

$$c_{pv} = c_{pv}^0 + K_v t = c_{pv}^0 + 2.15 \cdot 10^{-4} t \tag{6.34}$$

where K_a and K_v are the slopes of the line from correlation of specific heat versus temperature for the air and water vapour, respectively.

Thus, for the moist air the equation becomes

$$c_p = c_{pa} + x \cdot c_{pv} = 1.006 + 1.05 \cdot 10^{-4} t + \left(1.858 + 2.15 \cdot 10^{-4} t\right)x \tag{6.35}$$

In a temperature range from 0°C to 100°C, the specific heats of dry air varies only from 1.006 to 1.011 kJ/kg·K (Holman 1988) and water vapour from 1.858 to 1.890 kJ/kg·K. Then, for this condition the expression for moist air simplifies to

$$c_p = c_{pa} + x \cdot c_{pv} = 1.01 + 1.88 \cdot x \tag{6.36}$$

6.1.9 Dry-Bulb, Dew-Point and Wet-Bulb Temperatures

Psychrometric calculations involve three types of temperatures: dry bulb, dew point and wet bulb. One of the main properties known or given in the calculations is the dry-bulb temperature, simply identified by temperature and denoted by t. The dry-bulb temperature is indicated by the ordinary thermometer's sensor inserted in a representative position in the volume of the moist air. The dew-point temperature is the temperature in which the mixture's vapour starts condensing. It occurs by cooling at constant pressure or absolute humidity until the mixture reaches the saturation curve ($\phi = 1$). The wet-bulb temperature is indicated by a thermometer's sensor covered by a wick or similar material saturated with a liquid.

Figure 6.3 illustrates these temperatures in Mollier diagram. From point 1 cooling at constant absolute humidity, the dew-point temperature (t_{dp}) will be reached at point 2, which is the intersection of the cooling line with the saturation curve ($\phi = 1$). The adiabatic drying and dehumidification processes start at point 1 and finish at point 3, which is the wet-bulb temperature (t_{wb}). Either from the wet-bulb or dew-point temperature, continuing cooling leads to condensation from point 3 to 4 along the saturated curve ($\phi = 1$). At constant absolute humidity, continuous heating from point 4 leads to point 5 that is another dry-bulb temperature.

The expression (ASHRAE Handbook of Fundamentals 2009) for dew-point temperature between 0° and 93°C is

$$t_{dp} = \sum_{i=1}^{3} a_i \cdot \alpha^i + a_4 + a_5 \cdot p_v^{0.1984} \tag{6.37}$$

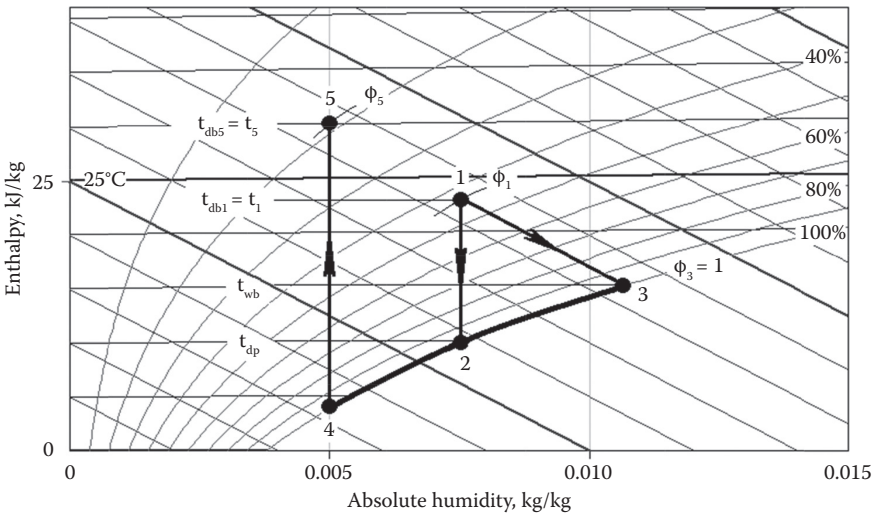

FIGURE 6.3
State points to distinguish the three different types of temperatures used in psychrometric calculations.

Another expression is

$$t_{dp} = b_1 \cdot pv^{b_2} + b_3 \cdot \alpha + a_4 \tag{6.38}$$

where $a_1 = 14.526$, $a_2 = 0.7389$, $a_3 = 0.09486$, $a_4 = 6.54$, $a_5 = 0.4569$, $b_1 = 33.38269$, $b_2 = 0.22262$, $b_3 = 7.15602$, $b_4 = -26.39589$ and $\alpha = \ln(p_v)$ (t_{dp} is in °C and p_v is in kPa).

For dry-bulb temperature from 0°C to 100°C or vapour pressure from 0.610 to 101.325 kPa, the dew-point temperature expression is

$$t_{dp} = 33.38269 \cdot p_v^{0.222616} + 7.156019 \cdot \ln\left(p_v\right) - 26.39589 \tag{6.39}$$

The wet-bulb temperature and the corresponding saturation vapour pressure are unknown and are found by any root finding method and by trial and error through the Carrier's equation

$$p_v - p_{vsx} + \frac{\left(p - p_{vsx}\right)\left(t - t_{wbx}\right)}{1537.8 - t_{wbx}} = z(t_{wbx}) = 0 \tag{6.40}$$

Hence, if the function z is 0, then $p_{vsx} = p_{vs}$ and $t_{wbx} = t_{wb}$.

The wet-bulb temperature based on temperature and actual and equilibrium saturation absolute humidities is

$$t_{wb} = \frac{\left(\Delta h_{lv}^0 - c_{pv}^0 t\right)x - c_{pa}^0 t - \Delta h_{lv}^0 x_s^*}{c_{pa}^0 + c_{pw}^0 x - \left(c_{pw}^0 - c_{pv}^0\right)x} \tag{6.41}$$

$$t_{wb} = \frac{\left(2501 + 1.86t\right)x + 1.006t - 2501x_s^*}{1.006 + 4.186x - 2.326x_s^*} \tag{6.42}$$

where t_{dp} is in °C and p_v is in kPa.

6.1.10 Air–Vapour Properties at Freezing Conditions

For temperature below freezing, the expression (ASHRAE Handbook of Fundamentals 2009) for absolute humidity-frost is as follows:

$$x = \frac{\left(2830 - 0.24t_{wb}\right)x_s^* - 1.006\left(t - t_{wb}\right)}{2830 + 1.86t - 2.1t_{wb}} \tag{6.43}$$

$$x = \frac{h - 1.006\left(t + 17.78\right)}{2501 + 1.86t} \tag{6.44}$$

The recommended (ASHRAE Handbook of Fundamentals 2009) expression for saturation pressure over ice for temperatures between $-100°C < t \le 0°C$ is

$$p_{vs}^* = \exp\begin{bmatrix} -5.6745359T^{-1} + 6.3925247 - 9.677843 \cdot 10^{-3}T + \\ + 6.2215701 \cdot 10^{-7}T^2 + 2.0747825 \cdot 10^{-9}T^3 - \\ - 9.484024 \cdot 10^{-13}T^4 + 4.1635019 \cdot \ln(T) \end{bmatrix} \tag{6.45}$$

At the thermodynamic wet-bulb temperature the saturation pressure over ice is

$$p_{vs}^{*} = \exp\left[\begin{array}{l} -5.6745359T_{wb}^{-1} + 6.3925247 - 9.677843\cdot 10^{-3}T_{wb} + \\ + 6.2215701\cdot 10^{-7}T_{wb}^{2} + 2.0747825\cdot 10^{-9}T_{wb}^{3} - \\ - 9.484024\cdot 10^{-13}T_{wb}^{4} + 4.1635019\cdot \ln(T_{wb}) \end{array}\right] \tag{6.46}$$

where T_{wb} is in K and p_{vs}^{*} is in Pa.

The expression for dew-point temperature below freezing point is as follows:

$$t_{dp} = 6.09 + 12.608\cdot\alpha + 0.4959\cdot\alpha^{2} \tag{6.47}$$

where $\alpha = \ln(p_v)$ and p_v is in kPa.

6.1.11 Application of Psychrometric Equations

The previously developed equations can be applied to calculate the main psychrometric properties of the moist air flowing through the heat pump drying cycle. However, the basic question is what equations to select to calculate the main properties in a state point of the cycle. The algorithm in Tables 6.1 through 6.4 provide the sequence of calculations and the equations to be applied when two properties are given and the total pressure is known.

The next four algorithms illustrate the equations, steps and the properties of moist air based on commonly known or given data.

1. Given: total pressure p, dry-bulb temperature t and relative humidity ϕ (Table 6.1)
2. Given: total pressure p, dry-bulb temperature t and wet-bulb temperature t_{wb} (Table 6.2)
3. Given: total pressure p, dry-bulb temperature t and enthalpy h (Table 6.3)
4. Given: total pressure p, dry-bulb temperature t and absolute humidity x (Table 6.4)

TABLE 6.1

Properties and Calculation Steps for the Given Pressure, Dry-Bulb Temperature and Relative Humidity

Sequence	1	2	3	4	5	6	7	8	9	10
Property	p_{vs}	x_s	p_v	x	h	t_{dp}	t_{wb}	μ	v	c_p
Equation	6.14	6.3	6.14	6.2	6.24	6.37	6.40	6.8	6.27	6.33
	6.17	—	—	—	—	6.38	—	6.9	6.28	6.34
	6.19	—	—	—	—	6.39	—	—	6.29	6.35

TABLE 6.2

Properties and Calculation Steps for the Given Pressure, Dry-Bulb and Wet-Bulb Temperatures

Sequence	1	2	3	4	5	6	7	8	9	10	11	12	13
Property	p_{vs}	x_s	p_{vs}^{*}	x_s^{*}	x_s	x	p_v	ϕ	μ	h	t_{dp}	v	c_p
Equation	6.17	6.3	6.20	6.4	6.3	6.2	6.14	6.10	6.8	6.24	6.39	6.27	6.33
	6.19	—	6.21	—	—	—	—	—	6.9	—	—	6.28	6.34
	—	—	—	—	—	—	—	—	—	—	—	6.29	6.35

TABLE 6.3

Properties and Calculation Steps for the Given Dry-Bulb Temperature, Enthalpy and Total Pressure

Sequence	**1**	**2**	**3**	**4**	**5**	**6**	**7**	**8**	**9**	**10**	**11**
Property	p_{vs}	x_s	x	p_v	ϕ	t_{dp}	t_{wb}	h	μ	v	c_p
Equation	6.17	6.3	6.7	6.14	6.10	6.39	6.40	6.24	6.8	6.27	6.33
	6.19	—	—	—	—	—	—	—	6.9	6.28	6.34
	—	—	—	—	—	—	—	—	—	6.29	6.35

TABLE 6.4

Properties and Calculation Steps for the Given Dry-Bulb Temperature, Absolute Humidity and Total Pressure

Sequence	**1**	**2**	**3**	**4**	**5**	**6**	**7**	**8**	**9**	**10**
Property	p_v	h	p_{vs}	ϕ	t_{dp}	t_{wb}	x_s	μ	v	c_p
Equation	6.14	6.24	6.17	6.10	6.39	6.40	6.3	6.8	6.27	6.33
	—	—	6.19	—	—	—	—	6.9	6.28	6.34
	—	—	—	—	—	—	—	—	6.29	6.35

6.2 Types of Psychrometric Processes

The type of drying and psychrometric process can be distinguished according to changes in the moist air properties at the initial and final state points. For instance, three processes occur at constant temperature, enthalpy and absolute humidity as illustrated in Figure 6.4.

These processes are as follows:

$$\text{Isothermal: } t_2 = t_1 = 40°C$$

$$\text{Isenthalpic: } h_2 = h_1 = 63.7 \text{ kJ/kg}$$

$$\text{Isohumid: } x_2 = x_1 = 0.15 \text{ kg/kg}$$

The three major types of drying processes based on the enthalpy change are shown in Figure 6.5.

These drying processes are as follows:

1–2: Adiabatic process, $h_2 = h_1 = 60$ kJ/kg
1–3: Low polytropic process, $h_3 < h_1$, $h_3 = 50$ kJ/kg
1–4: High polytropic process, $h_4 > h_1$, $h_3 = 40$ kJ/kg

The energy use and water removal capacity in the drying process changes as the moist air flows in a closed loop through the heat pump dryer components.

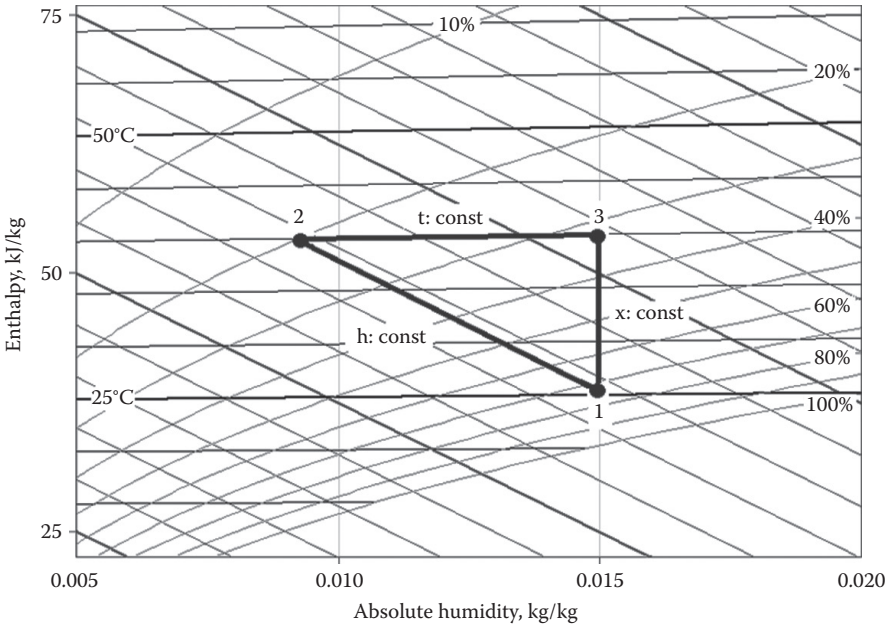

FIGURE 6.4
Isothermal, isenthalpic and isohumid processes on the h–x chart.

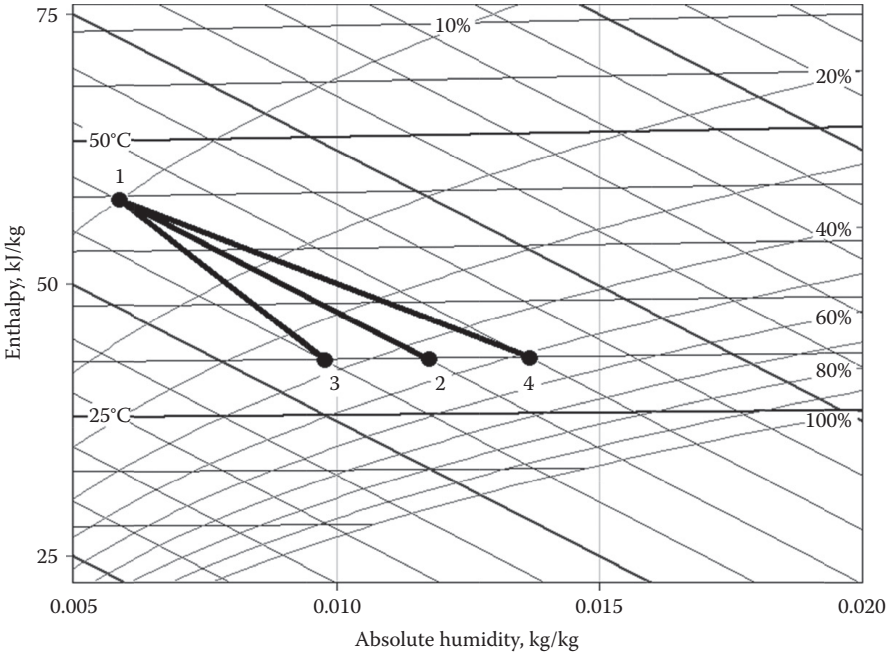

FIGURE 6.5
Adiabatic and low and high polytropic drying processes in the h–x diagram.

Figure 6.6 shows the heat pump drying cycle in the Mollier diagram with the following processes:

1–2: Isohumid air heating in the condenser (and blower) x = 10 g/kg
2–3: Adiabatic drying at $h_2 = h_3 = 65$ kJ/kg
2–4: Low polytropic drying at $h_4 < h_2$, $h_4 = 60$ kJ/kg
2–5: High polytropic drying at $h_4 < h_2$, $h_4 = 70$ kJ/kg
2–6: Isothermal drying at $t_2 = t_6 = 39.3$°C
3–1 (4–1, 5–1, 6–1): Moist air cooling and water vapour condensation in the evaporator
L: Moist air at evaporator surface conditions such as $t_L = 5$°C and $\phi = 1.0$

The energy use and water removal capacity in the pump drying process can be improved by design based on a number of layout configurations and procedures. Figure 6.7 (Alves-Filho 1996) shows a possible layout configuration of a continuous heat pump dryer with double drying chambers, condensers and compressors. The main objective of this heat pump dryer is to reheat the air exhausted from the first drying chamber and reuse it in chamber 2. This procedure leads to increased water removal by additional progressive drying. In this way, the exhaust air from the first chamber is heated by the condenser and supplied to the second drying chamber. The drying chambers are placed in series in the air drying loop, whereas the condensers are placed in parallel on the refrigerant path.

The components and symbols are as follows: DC1 and DC2 – drying chambers 1 and 2, FIL – filter, EVA – evaporator, CON1 – condenser for heating the air for DC1, CON2 – condenser for heating the air exhaust from DC1, COM1 and COM2 – low- and high-stage compressors, EX CON – external condenser, THR – throttling, FLA – intermediate

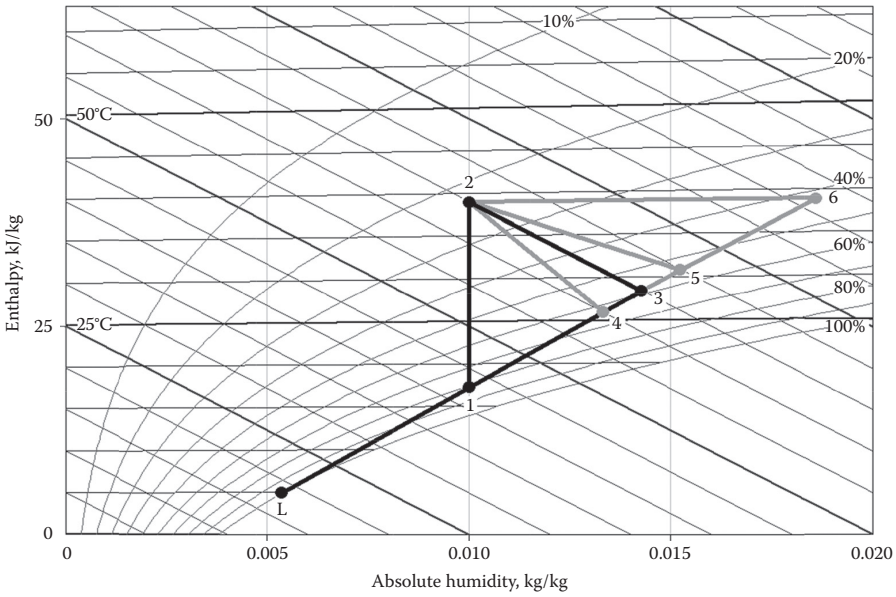

FIGURE 6.6
Heat pump drying cycle in the Mollier diagram.

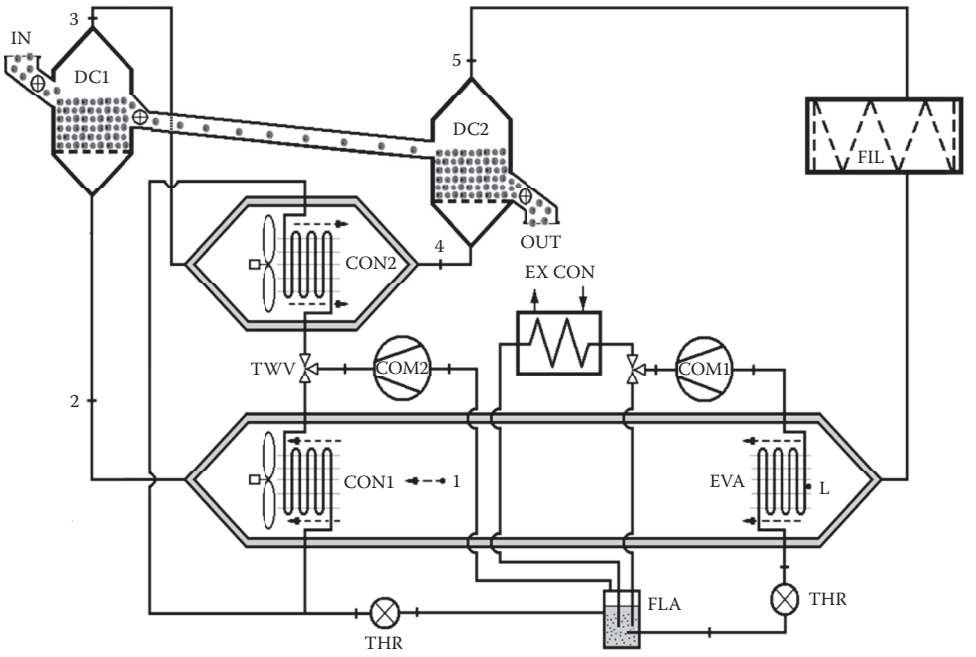

FIGURE 6.7
Layout configuration for a progressive and continuous two-stage heat pump dryer with double drying chambers and condensers: DC1, DC2 – drying chambers; FIL – filter; EVA – evaporator; CON1, CON2 – condensers; COM1, COM2 – low- and high-stage compressor, respectively; EX CON – external condenser; THR – throttling; FLA – intermediate open-flash tank; TWV – three-way valve; IN – wet material inlet; OUT – dry product outlet; L – evaporator's surface; 1 to 5 – state points of the drying air.

open-flash tank, TWV – three-way valve, IN – wet material inlet, OUT – dry product outlet, L – evaporator's surface.

The drying air state points for the heat pump dryer in Figure 6.7 are represented as cycles in the Mollier diagram in Figure 6.8. As the first drying chamber's exhaust air is heated and a second drying chamber is added, the polytropic cycle approaches the ideal isothermal cycle with x_6 = 18.6 g/kg. This progressive dryer has improved water removal since the final state point 5 (x_5 = 16.5 g/kg) is reached instead of point 3 (x_3 = 10.7 g/kg) for a single-stage dryer. In addition, the progressive dryer requires an enthalpy increase from 65 to 76.2 kJ/kg.

The processes and state points on the heat pump drying cycles are as follows:

1–2: Isohumid air heating in the first condenser and blower by condenser 1 at x_1 = 10.0 g/kg

2–3: Adiabatic first stage drying by DC1 at $h_2 = h_3$ = 65.0 kJ/kg

3–4: Isohumid air heating in the second condenser and blower at x_3 = 14.3 g/kg

4–5: Adiabatic second stage drying by DC2 at $h_4 = h_5$ = 76.2 kJ/kg and x_5 = 16.5 g/kg

2–6: Isothermal drying at $t_2 = t_6$ = 39.3°C and x_6 = 18.6 g/kg

3–1 (5–1, 6–1): Moist air cooling and water vapour condensation in the evaporator

L: Moist air at evaporator surface conditions such as t_L = 5°C and ϕ = 1.0

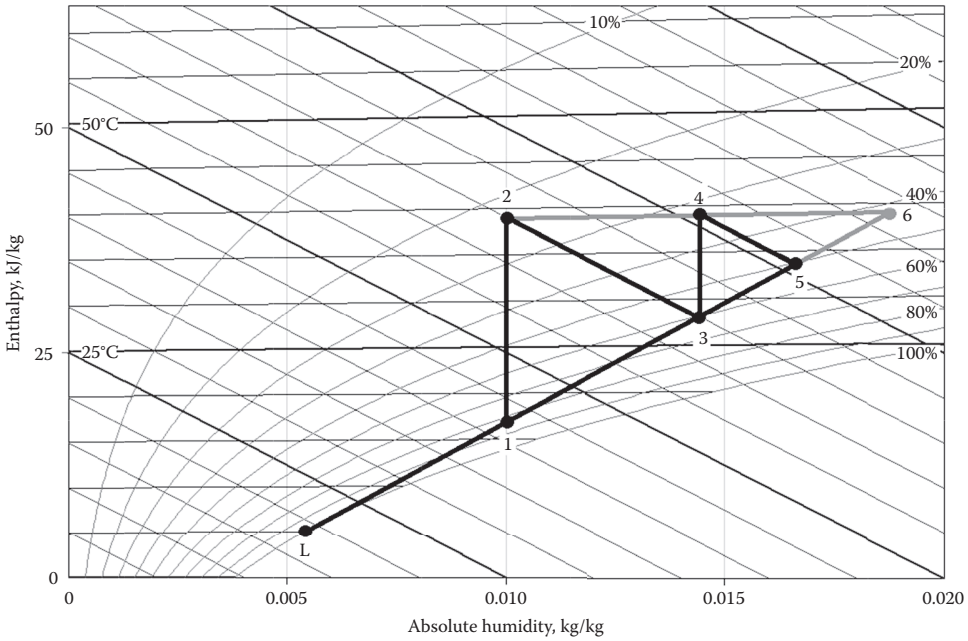

FIGURE 6.8
Cycles of the progressive heat pump dryer with double drying chambers and condensers in the h–x diagram.

6.3 Ratio of Moisture Removal and Specific Energy Consumption

The ratio of moisture removal to energy (R_{me}) is the quotient of the absolute humidity difference in the drying process to the enthalpy difference for heating the moist air in the condenser and blower. The specific energy consumption (S_{ec}) is the inverse of R_{me} or the ratio the enthalpy and absolute humidity differences. The R_{me} and S_{ec} are calculated by defining the processes and cycle based on the relevant properties on each state point.

Figure 6.9 shows the enthalpy–absolute humidity (h–x) diagram of the heat pump drying cycles I, II and III, which are defined by the state points 1351, 2462 and 2482, respectively.

The ratios of moisture removal to energy and specific energy consumption for cycle I are as follows:

$$R_{meI} = \frac{x_5 - x_1}{h_5 - h_1} \tag{6.48}$$

$$S_{ecI} = \frac{h_5 - h_1}{x_5 - x_1} \tag{6.49}$$

The moist air properties in the heat pump cycles are identified at each state point and determined graphically and by interpolation from Figure 6.9.

Table 6.5 presents the relevant properties calculated for each state in the cycles.

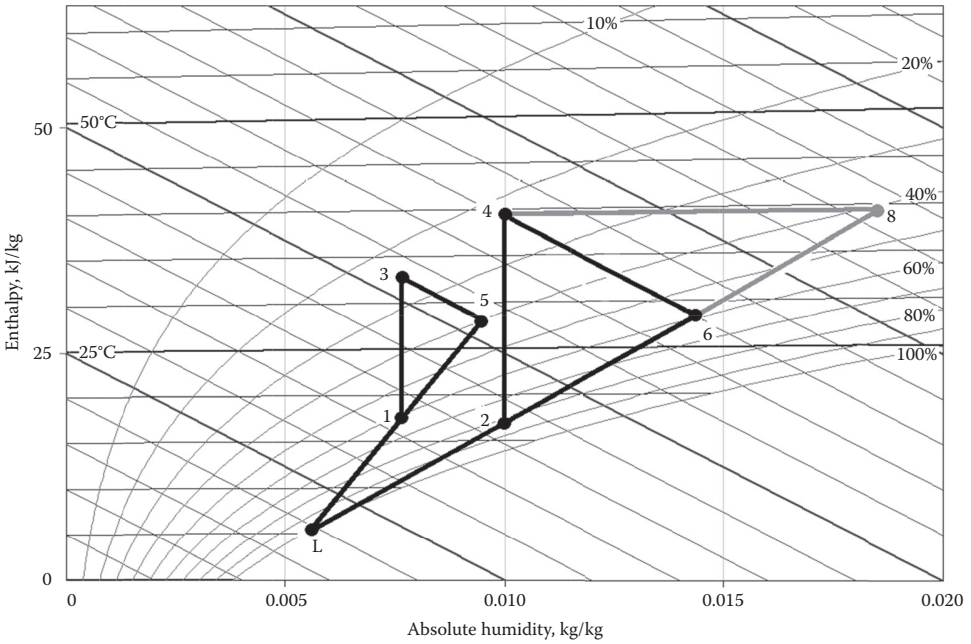

FIGURE 6.9
Cycles for three drying processes and the state points on the h–x diagram.

TABLE 6.5
Moist Air Properties at the State Points of the Cycles

	State Point						
Property	**1**	**3**	**5**	**2**	**4**	**6**	**8**
h, kJ/kg	37.2	52.5	52.5	42.2	65.0	65.0	87.22
x, g/kg	7.6	7.6	9.5	10.0	10.0	14.3	18.6

With the data in Table 6.5, we can calculate the ratio of moisture removal to energy for cycles I, II and III as follows:

$$R_{meI} = \frac{x_5 - x_1}{h_5 - h_1} = \frac{9.5 - 7.6}{52.5 - 37.2} = 0.12 \text{ g/kJ} \tag{6.50}$$

$$R_{meII} = \frac{x_6 - x_2}{h_6 - h_2} = \frac{14.3 - 10.0}{65.0 - 42.2} = 0.19 \text{ g/kJ} \tag{6.51}$$

$$R_{meIII} = \frac{x_8 - x_2}{h_8 - h_2} = \frac{18.6 - 10.0}{87.2 - 42.2} = 0.19 \text{ g/kJ} \tag{6.52}$$

The specific energy consumption for cycles I, II and III is as follows:

$$S_{ecI} = \frac{h_5 - h_1}{x_5 - x_1} = \frac{52.5 - 37.2}{9.5 - 7.6} = 8.05 \text{ kJ/g} \tag{6.53}$$

$$S_{ecII} = \frac{h_6 - h_2}{x_6 - x_2} = \frac{65.0 - 42.2}{14.3 - 10.0} = 5.30 \text{ kJ/g} \tag{6.54}$$

$$S_{ecIII} = \frac{h_8 - h_2}{x_8 - x_2} = \frac{87.2 - 42.2}{18.6 - 10.0} = 5.23 \text{ kJ/g} \tag{6.55}$$

This indicates that the water removal is lowest and specific energy consumption is highest for cycle I. The water removal is highest and specific energy consumption is lowest for cycles II and III, which means that these cycles remove more water per unit of energy input. Predictably, the R_{me} and S_{ec} values are equal for cycles II and III, implying that they are independent if drying is adiabatic or isothermal. Notice that the slight difference in S_{ec} I and II results from graphical interpolation discrepancy.

The reason that the R_{me} and S_{ec} values are equal is because in both cases, the final exhaust temperature is the same while keeping the conditions constant at the inlet and outlet of the condenser.

The R_{me} and S_{ec} can be thought of as a slope of h(x) or x(h) in the diagram, and the cycle with higher slopes has higher water removal per unit heating or lowest energy expenditure per mass of removed water.

6.4 Heat Pump Specific Moisture Extraction Ratio

The specific moisture extraction ratio (SMER) is the quotient of the coefficient of performance on the low-pressure side (COP_L) of the heat pump to the specific energy consumption in the drying process. It is expressed by

$$SMER = \frac{COP_L}{S_{ec}} = COP_L \cdot R_{me} = \frac{COP_L}{\Delta h/\Delta x} = COP_L \frac{\Delta x}{\Delta h} \tag{6.56}$$

Observe that it is desirable to design a heat pump dryer with the highest possible SMER in compliance with Equation 6.56. Then, how to maximise the SMER?

This equation indicates that SMER increases to maximum when R_{me} increases or S_{ec} drops. In addition, Equation 6.48 shows that R_{me} increases directly with absolute humidity difference and inversely with enthalpy difference. Therefore, the SMER is first maximised by increasing R_{me} through the increase of Δx or the drop of Δh.

This is confirmed by Equation 6.49 showing that S_{ec} increases directly with enthalpy difference and inversely with absolute humidity difference.

The next term to maximise in Equation 6.56 is the COP. In a single-stage vapour compression heat pump, the COP depends on the cycle as sketched in Figure 6.10. The COPs on the low- and high-pressure sides of the heat pump are as follows:

$$COP_L = \frac{h_1 - h_4}{h_2 - h_1} = \frac{\Delta h_{14}}{\Delta h_{21}} = \frac{q_L}{w} \tag{6.57}$$

$$COP_H = \frac{h_2 - h_3}{h_2 - h_1} = \frac{\Delta h_{23}}{\Delta h_{21}} = \frac{q_H}{w} \tag{6.58}$$

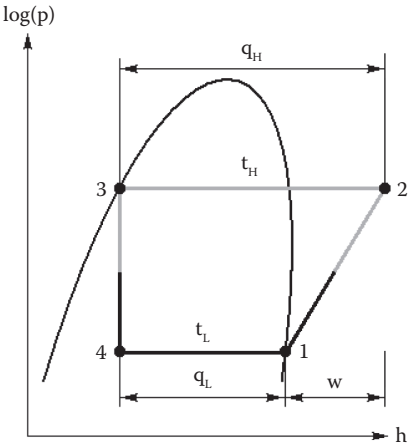

FIGURE 6.10
State points in the heat pump cycle in the log(p)–h diagram.

Then, the COP_L and COP_H increase by reducing the work of compression and by increasing the cooling effect or the specific heating capacity.

Therefore, second, the SMER is maximised COP_L that is achieved by increasing the cooling effect q_L that is achieved by increasing Δh_{14} or decreasing Δh_{21}.

Now, return and replace the terms of the SMER's equation as follows:

$$\text{SMER} = \frac{\text{COP}_L}{S_{ec}} = \text{COP}_L \cdot R_{me} = \left(\frac{h_1 - h_4}{h_2 - h_1}\right)_{hp} \left(\frac{\Delta x}{\Delta h}\right)_{dryer} = \frac{q_L}{w}\frac{\Delta x}{\Delta h},\ \text{kg/kJ} \tag{6.59}$$

where h is the refrigerant specific enthalpy in kJ/kg, and Δh and Δx are the drying air–specific enthalpy and absolute humidity differences in kJ/kg and kg/kg, respectively. The long-established unit of SMER is kg/kWh, whereas the unit from Equation 6.59 is kg/J, which is easily converted by

$$\text{SMER} = 3600 \cdot \text{COP}_L \cdot \frac{\Delta x}{\Delta h}, \text{kg/kWh} \tag{6.60}$$

What are the best position of the heat pump drying cycle to attain high R_{me} and SMER? In what type of dryer is this enhanced SMER achieved?

There are several cycle positions for this purpose, as exemplified next.

6.4.1 Case 1 – Effect on SMER by Increasing Relative Humidity

Figure 6.11 illustrates two heat pump drying cycles I (L135) and II (L246). The relative humidity increases from state point 3 to 4 while keeping other points at the same position. The increase of the relative humidity causes a decrease in the S_{ec}. It is clear that S_{ecI} is higher than S_{ecII} as indicated by comparison of the slopes of the lines connecting points L to 3 and L to 4. Hence, cycle II has higher SMER than cycle I.

This is achieved by designing the heat pump dryer to operate with a deeper bed, a longer bed length or in concurrent drying mode. This is opposed to cycle I (L135) where a shallow bed, a shorter bed length or crossflow drying mode is used.

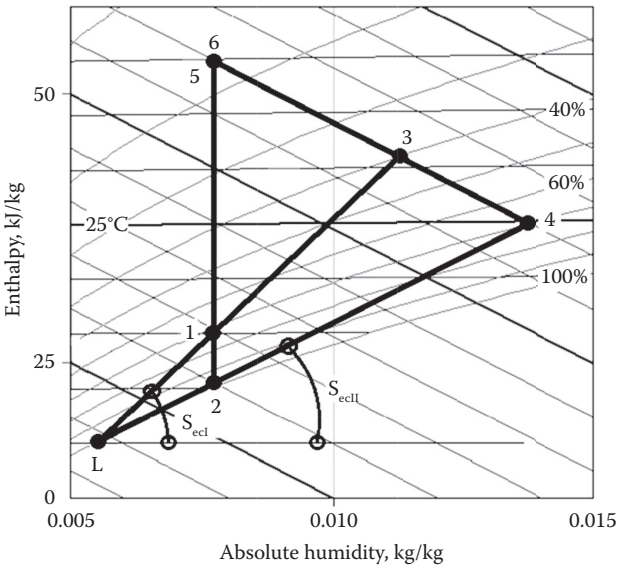

FIGURE 6.11
Cycles indicating the effect of drying chamber exhaust relative humidity on SMER.

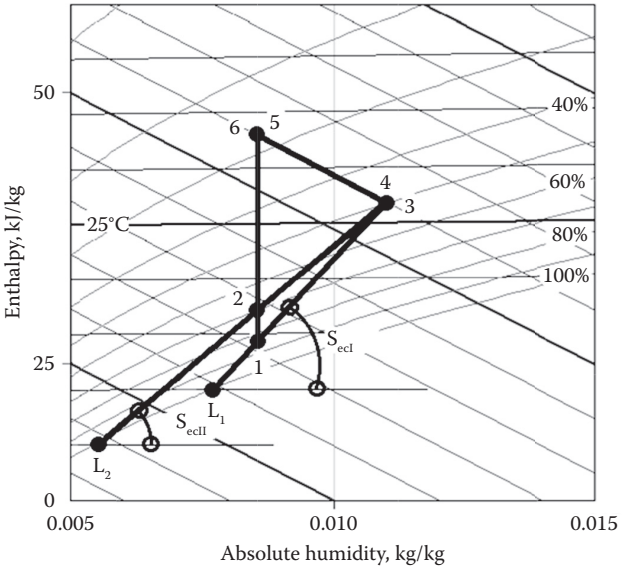

FIGURE 6.12
Cycles showing the effect of evaporating temperature on SMER.

6.4.2 Case 2 – Effect on SMER by Reducing Evaporating Temperature

Figure 6.12 presents the cycle I (L_1135) and cycle II (L_2246) with change in the evaporating temperature while keeping the other state points at the same position. The evaporating temperature decrease causes a reduction in the S_{ec} or the slope of the line. Thus, the S_{ecII} is smaller and SMER is higher for cycle II. This condition is achieved by

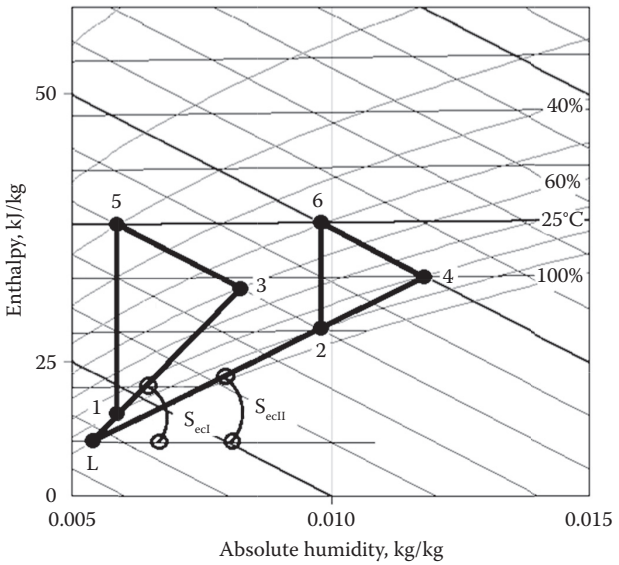

FIGURE 6.13
Cycles showing the effect of condenser inlet relative humidity on SMER at constant drying air inlet temperature.

designing the heat pump dryer to operate with an evaporating temperature lower than the temperature at *point* L_1.

6.4.3 Case 3 – Effect of Condenser Inlet Relative Humidity on SMER

Two cycles I (L135) and II (L246) are shown in Figure 6.13. The condenser inlet relative humidities in cycles I and II are at points 1 and 2, respectively.

Keep the same drying air inlet temperature and the same relative humidity difference in the drying chamber (lines 5 to 3 and 6 to 4). It is clear that cycle II (L246) has higher SMER due to lower S_{ecII}. This is indicated by comparison of the slopes of the lines L to 3 and L to 4.

6.4.4 Case 4 – Effect of Drying Chamber Air Inlet Temperature and Evaporating Temperature on SMER

Figure 6.14 illustrates the cycle I ($L_1$135) and cycle II ($L_2$246). It shows that the drying chamber inlet temperature changes from point 5 to 6 and the evaporating temperature changes from *point* L_1 to L_2. The relative humidities are constant in both cycles: $\phi_5 = \phi_6$ and $\phi_3 = \phi_4$. Figure 6.14 shows that as the evaporating temperature increases the S_{ec} drops. Consequently, cycle II has lower S_{ecII} and higher SMER due to the changes from *point* L_1 to L_2 for constant relative humidity difference in the drying process.

This is achieved by designing the heat pump dryer with higher evaporating temperature and by loading sufficient wet material to the drying chamber for attaining the same relative humidity at the inlet and outlet of the drying processes.

6.4.5 Case 5 – Effect of Evaporating Temperature on SMER

Figure 6.15 shows the three heat pump drying cycles I ($L_1$135), II (L_2abc) and III ($L_3$246) with the effect of evaporating temperatures that are located at *points* L_1, L_2 and L_3. It is considered that the other state points are at the same positions. Figure 6.15 shows that

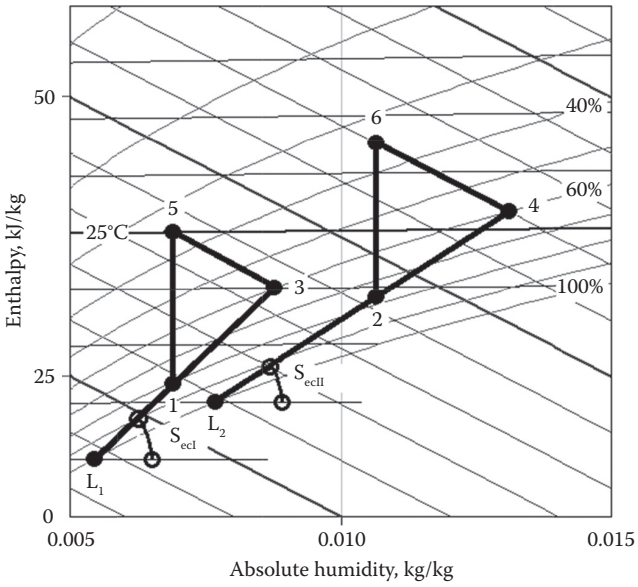

FIGURE 6.14
Cycles indicating the effect of the air inlet temperature in the drying chamber on SMER while keeping the same relative humidity at the inlet and outlet of the drying chamber.

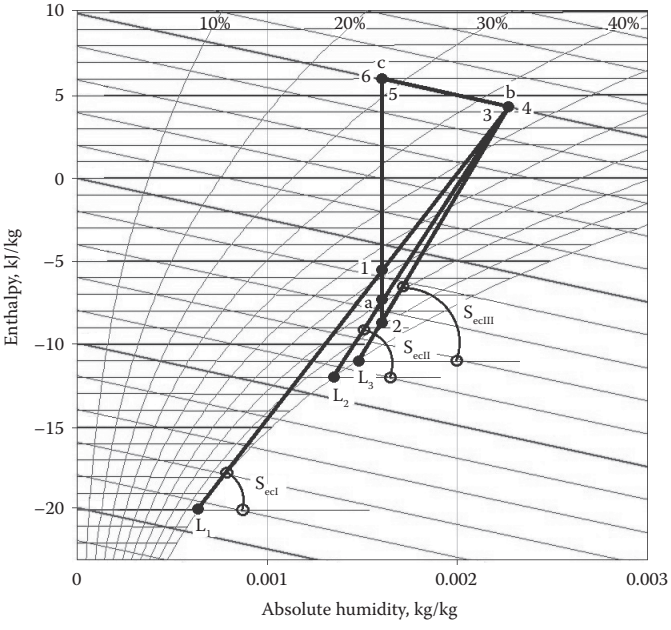

FIGURE 6.15
Cycles showing the effect of evaporating temperature on SMER.

the smallest is S_{ecI} and that the largest is S_{ecIII}. However, cycle II is the best choice because it has the optimum S_{eII} and SMER by complying with the requirement of having at least a 5°C temperature difference between the evaporator surface and the dew point. The cycle with evaporating temperature at *point* L_3 is unpractical since it is too close to the dew-point temperature at point 6. Moreover, the cycle I has the lowest evaporating temperature L_1, leading to the lowest COP compared to cycle II.

This is achieved by design of the heat pump dryer to operate with an evaporating temperature about 5°C below the dew-point temperature based on the state *point c*.

6.4.6 Case 6 – Effect of Exhaust Relative Humidity at Constant Drying Exhaust Temperature

Figure 6.16 illustrates the three cycles – I (L135), II (Labc) and III (L246) – with changes in the exhaust relative humidity at points 3, b and 4, while keeping a constant drying exhaust temperature at 30°C.

It shows that the S_{ec} drops sequentially for cycles I, II and III as the exhaust relative humidity increases in the same order. Cycle III has the highest SMER due to the lowest S_{ecIII} caused by the higher exhaust air relative humidity (point 4) at constant exhaust temperature. However, the best choice is cycle II because it is an adiabatic process with intermediate SMER and S_{ecII} in accordance with the exhaust air relative humidity at *point b*. This is confirmed by the differences in the slope of the lines L to 4, L to b and L to 3.

The condition in cycle II is achieved by designing the heat pump dryer with a standard adiabatic drying chamber as indicated by the line c to b.

FIGURE 6.16
Cycles indicating the effect of exhaust relative humidity at constant drying exhaust temperature.

Cycle III is achieved by designing the heat pump drying chamber with immersed heat exchanger with energy supplied by the condenser. This results in changing from adiabatic (line c to b) to a high polytropic drying process (line 6 to 4), but this requires an additional heat exchanger.

6.4.7 Case 7 – Effect of the Location of the Exhaust Temperature on SMER for the Same Inlet Drying Temperature

Figure 6.17 shows the cycles I (L123), II (L12345) and III (L126). The three exhaust temperatures are located on the line connecting L to 6, and all cycles have the same drying inlet temperature.

This is a particular case where the R_{me}, S_{ec}, and SMER are equal for the three cycles. This is indicated by the S_{ec} and a single slope of the line connecting the exhaust of the processes. In addition, these cycles have the same COP since they have the same evaporating (t_L) and condensing temperatures. The condensing temperature is a function of the drying inlet temperature that is the same for the three cycles ($t_2 = t_4 = t_6$).

The cycles are achieved in several ways. Cycle I is made with a single adiabatic drying chamber, and cycle II is designed with two adiabatic drying chambers and two condensers. Cycle III is more complex and can be designed to approach the isothermal process by placing a heat exchanger immersed in the bed of material, or by applying microwave or infrared radiation over the bed.

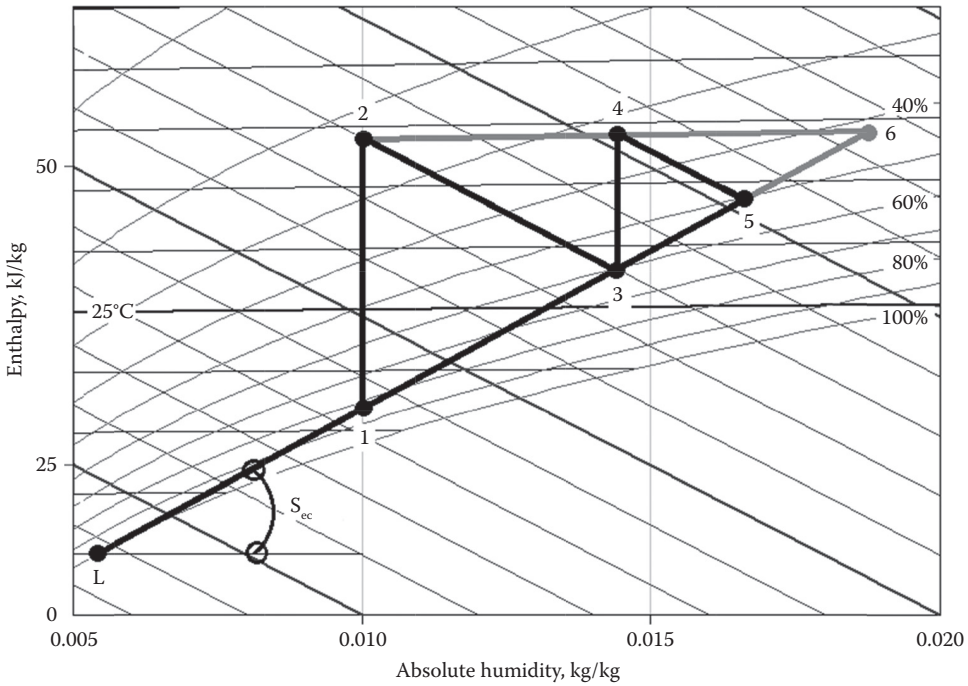

FIGURE 6.17
Three cycles with same inlet drying temperatures and the exhaust temperatures on the same line connecting L to 6.

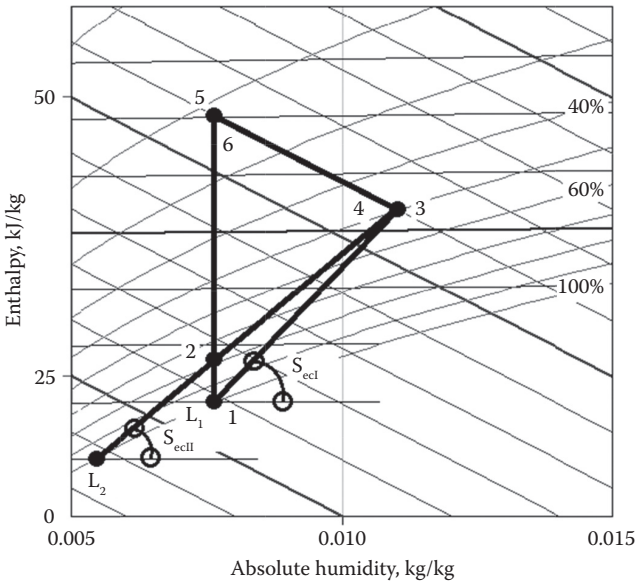

FIGURE 6.18
Cycles for the case of changing the evaporation temperature with the other state points at the same position.

6.4.8 Case 8 – Effect of Evaporation Temperature with the Other State Points at the Same Positions

Figure 6.18 illustrates the cycles I ($L_1$135) and II ($L_2$246) and the effect of changing the evaporating temperature while keeping the other state points in the same place.

It indicates that cycle II has the proper S_{ecII} and SMER because it fulfil the requirement of having the evaporating temperature at least 5°C below the dew-point temperature based on the condenser inlet (point 2). Cycle I has lower SMER, and it is also an impractical cycle since its evaporating temperature is equal to the heater inlet temperature (points L_1 and 1 overlap).

Cycle II is achieved by controlling the evaporating temperature to be 5°C below the dew-point temperature based on the state point 6.

6.4.9 Case 9 – Effect of Exhaust Air Recirculation for Drying at Constant Inlet Temperature and Constant Outlet Relative Humidity

Figure 6.19 presents the cycles I (135) and II (246) (the evaporating temperature is not shown for this case) with the effect of recirculation of exhaust air while drying occurs at constant inlet temperature and constant outlet relative humidity.

In cycle I, the drying chamber exhaust air at point 3 is rejected to the surroundings. In cycle II, the chamber exhaust air at point 4 and the ambient air at point 1 are mixed to reach point 2. Then, the air enters the heater and leaves at point 6 where it flows through the drying chamber and exhaust at point 4.

Figure 6.19 shows that cycle II has lower S_{ecII} and higher SMER due to the recirculation of exhaust air. The inlet air drying temperature and exhaust relative humidities are the same for both cycles.

However, the line position and the moist air properties at point 2 are unknown but can be determined by equations from mass and energy balance at the state

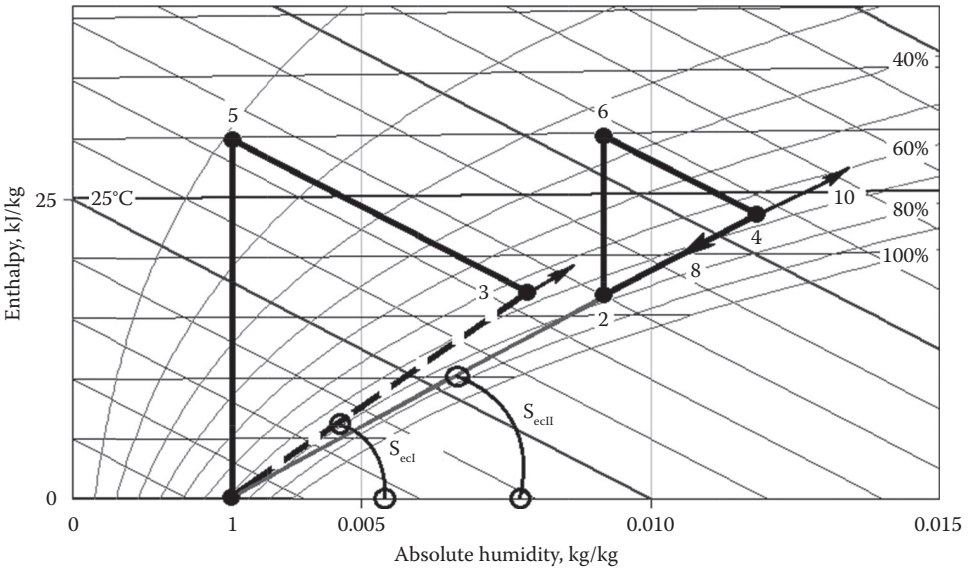

FIGURE 6.19
Cycles showing the effect of exhaust air recirculation for drying at constant inlet temperature and constant outlet relative humidity.

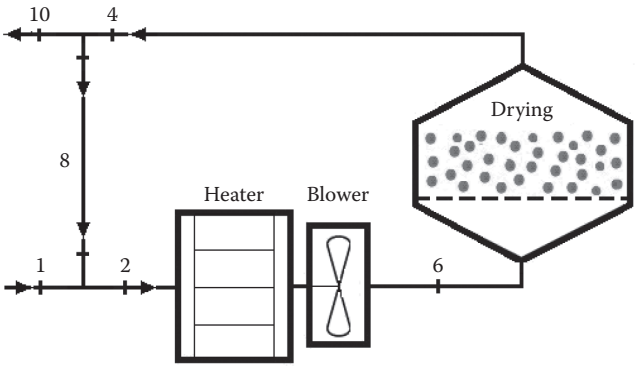

FIGURE 6.20
Layout of the dryer with exhaust air recirculation for cycle II.

points 1, 2 and 4. The equations are now developed considering Figure 6.20 that shows the layout of the dryer with exhaust air recirculation and the same state points as in Figure 6.19.

Even though point 2 is always on the line connecting 1 to 4 (see Figure 6.19), its position along the line is unknown. For instance, the moist air properties and absolute humidity at point 2 depends on the exhaust-ambient air mixing ratio defined by

$$r_m = \frac{\dot{m}_8}{\dot{m}_4} \quad \therefore r_{ma} = \frac{\dot{m}_{a8}}{\dot{m}_{a4}} \tag{6.61}$$

where r_m is moist air mixing ratio, r_{ma} is mixing ratio of exhaust and ambient air, and $\dot{m}$ and $\dot{m}_a$ is mass flow rate of mixture and dry air, respectively.

Of course, the proposed heat pump drying systems operate in closed loops and mixing of air occurs only between the exhaust and the evaporator surface. Thus, m_8 approaches m_4 and the mixing ratio is nearly 1.

However, open drying systems require determination of the properties at the mixing point 2. The equations for absolute humidity at point 2 are developed by starting with mass balance of dry air and vapour as follows

$$\dot{m}_{a8} = \dot{m}_{a4} - \dot{m}_{a10} = \dot{m}_{a2} - \dot{m}_{a1} \quad \therefore \dot{m}_{2a} = \dot{m}_{6a} = \dot{m}_{4a} \tag{6.62}$$

$$\dot{m}_{v8} = \dot{m}_{v4} - \dot{m}_{v10} = \dot{m}_{v2} - \dot{m}_{v1} \quad \therefore \dot{m}_{2v} = \dot{m}_{6v} = \dot{m}_{4v} \tag{6.63}$$

$$x_8\dot{m}_{a8} = x_4\dot{m}_{a4} - x_{10}\dot{m}_{a10} = x_2\dot{m}_{a2} - x_1\dot{m}_{a1} \quad \therefore x_2\dot{m}_{2a} = x_6\dot{m}_{6a} = x_4\dot{m}_{4a} \tag{6.64}$$

Then, the energy balance in adiabatic mixing in terms of individual enthalpy is as follows:

$$\dot{m}_{a8}\left(h_{a8} + x_8h_{v8}\right) + \dot{m}_{a1}\left(h_{a1} + x_1h_{v1}\right) = \dot{m}_{a2}\left(h_{a2} + x_2h_{v2}\right) \tag{6.65}$$

This leads to the mixing ratio of exhaust and ambient air:

$$r_{ma} = \frac{\dot{m}_{a8}}{\dot{m}_{a1}} = \frac{\left(h_{a2} + x_2h_{v2}\right) - \left(h_{a1} + x_1h_{v1}\right)}{\left(h_{a8} + x_8h_{v8}\right) - \left(h_{a2} + x_2h_{v2}\right)} \tag{6.66}$$

The energy balance in terms of mixture enthalpy gives

$$\dot{m}_{a8}h_{m8} + \dot{m}_{a1}h_{m1} = \dot{m}_{a2}h_{m2} \tag{6.67}$$

The mixing ratio of exhaust and ambient air in terms of absolute humidity is

$$r_{ma} = \frac{\dot{m}_{a8}}{\dot{m}_{a1}} = \frac{x_2 - x_1}{x_8 - x_2} = \frac{h_{m2} - h_{m1}}{h_{m8} - h_{m2}} \tag{6.68}$$

Hence, the determination of absolute humidity x_2 at the inlet of the heater can be determined using the known data and previous mixing ratio equations.

6.5 Problems and Solutions

PROBLEM 6.1

The Main Psychrometric Properties of the Air and Vapour Mixture

A mixture of air and water vapour is at atmospheric pressure, 25°C, and 50% relative humidity. The state point is shown on the psychrometric chart in Figure 6.21.

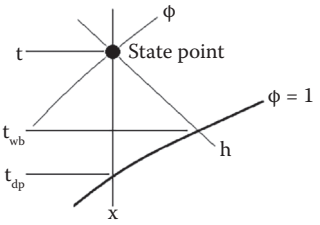

FIGURE 6.21
State point and main properties on the psychrometric chart.

TABLE 6.6

Sequence, Equations and Calculated Properties for Given Temperature and Relative Humidity

Property	**p_{vs}, Pa**	**x_s, g/kg**	**x, g/kg**	**p_v, kPa**	**h, kJ/kg**
Value	3.161	20.08	9.882	1.585	50.32
Equation	6.14	6.3	6.2	6.14	6.24
	t_{dp}, °C	**t_{wb}, °C**	**μ**	**v, m^3/kg**	**c_p, kJ/kg·K**
Value	13.88	17.89	0.492	0.8583	1.027
Equation	6.39	6.40	6.8	6.29	6.35

Calculate the main psychrometric properties of the mixture.

Given:

$$t = 25°C$$

$$\phi = 50\% = 0.5$$

$$p = 101{,}325 \text{ Pa}$$

Solution:

The calculations sequence is the determination of saturated and actual vapour pressures (p_{vs} and p_v), saturated and actual absolute humidities (x_s and x), specific enthalpy (h), dew-point and wet-bulb temperatures (t_{dp} and t_{wb}), degree of saturation (μ), specific volume (v) and specific heat (c_p). These properties are determined in the values, sequences and equations presented in Table 6.6.

PROBLEM 6.2

Moist Air Properties at the Inlet and Outlet of the Condenser

Moist air at atmospheric pressure and 40% relative humidity is heated from 15°C to 40°C. The blower supplies the air to the condenser that heats the air from state point 1 to 2. The heating process and state points on the psychrometric chart are shown in Figures 6.22 and 6.23, respectively. (a) Calculate the properties of the heated moist air and (b) estimate the energy in kW transferred to heat the air from point 1 to 2 if the airflow rate is 1.0 m^3/s.

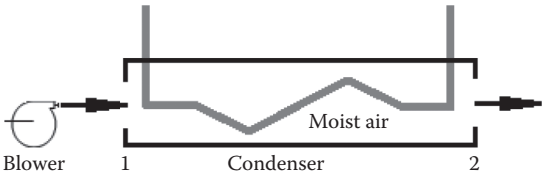

FIGURE 6.22
Sketch of the airflow in the condenser with the initial and final state points.

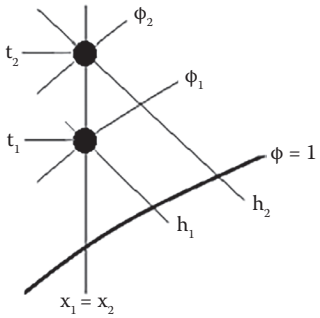

FIGURE 6.23
Heating of the moist air and main properties at the state point on the psychrometric chart.

Given:

$$p = 101{,}325 \text{ Pa}$$

$$t_1 = 15°C$$

$$x_2 = x_1 = 4.216 \text{ g/kg}$$

$$\phi_1 = 40\% = 0.4$$

$$t_2 = 40°C$$

Solution:

(a) Calculation of the properties of the heated moist air

Determination of the absolute humidity (x) requires actual and saturation vapour pressures (p_{vs} and p_v), whereas the determination of specific enthalpy (h) requires temperature (t) and absolute humidity (x).

$$x_2 = x_1$$

Given for state point 1:

$$p = 101{,}325 \text{ Pa}$$

$$t_1 = 15°C$$

$$\phi_1 = 40\% = 0.4$$

TABLE 6.7

Properties for State Point 1 at the Given Temperature, Relative Humidity and Total Pressure

Property	p_{vs}, Pa	x_s, g/kg	p_v, Pa	x, g/kg	h, kJ/kg
Value	1705.45	10.65	682.18	4.216	25.75
Equation	6.14	6.3	6.14	6.2	6.24

TABLE 6.8

Properties for State Point 2 at the Given Pressure, Temperature and Absolute Humidity

Property	p_v, Pa	h, kJ/kg	p_{vs}, Pa	ϕ, %	t_{dp}, °C
Value	682.19	51.13	7387.40	9.27	1.53
Equation	6.14	6.24	6.17	6.10	6.39
	t_{wb}, °C	x_s, kg/kg	μ	v, m³/kg	c_p, kJ/kg·K
Value	18.31	0.0487	0.087	0.8932	1.0181
Equation	6.40	6.3	6.8	6.29	6.35

The properties and equations with the sequence of calculations are shown in Table 6.7.

Given for state point 2:

$$p = 101{,}325 \text{ Pa}$$

$$t_2 = 40°C$$

$$x_2 = x_1 = 4.216 \text{ g/kg} = 0.004216 \text{ kg/kg}$$

Use t_2 to find p_{vs} by Equation 6.17, use x_2 to calculate p_v by Equation 6.14. With these values, determine the relative humidity by Equation 6.10. Then, similarly to Problem 6.1, calculate the other properties at point 2 substituting the relative humidity, t_2, and the found values into the appropriate equations as indicated in Table 6.8.

(b) Estimation of the energy in kW transferred to heat the air from point 1 to 2 if the airflow rate is 1.0 m³/s

$$\Delta h = h_2 - h_1 = 51.13 - 25.75 = 25.38 \text{ kJ/kg}$$

$$\dot{m}_a = \frac{\dot{V}}{v} = \frac{1}{0.8932} = 1.12 \text{ kg/s}$$

$$q_a = \dot{m}\Delta h = 1.12 \cdot 25.19 = 28.21 \text{ kW}$$

PROBLEM 6.3

Moist Air Properties at the Inlet and Outlet of the Drying Chamber

The heating and drying processes with the state points on the psychrometric chart are sketched in Figures 6.24 and 6.25. The heated air with properties calculated in Problem 6.2 enters the drying chamber at point 2. Then, it removes moisture from the wet material

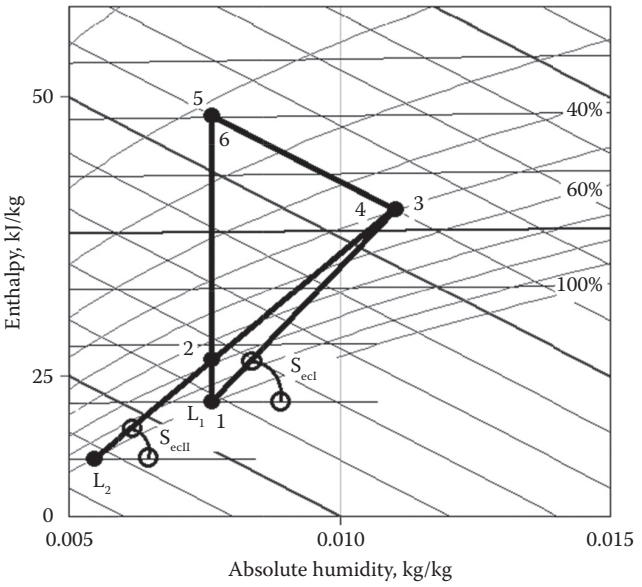

FIGURE 6.24
Drying and heating processes with the state points of the moist air.

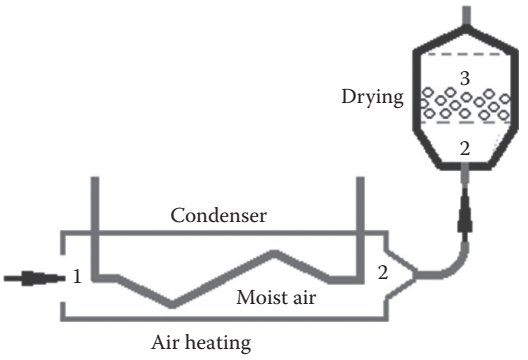

FIGURE 6.25
Drying process and state points on the psychrometric chart.

and exits the drying chamber at 24°C at point 3. Assume adiabatic drying process at atmospheric pressure and (a) calculate the psychrometric properties of the moist air at the exit of the drying chamber and (b) estimate the moisture removal rate in g/s and kg/h as the moist air changes state from point 2 to 3, keeping the air volumetric flow rate of 1.0 m^3/s.

Given:

$$p = 101{,}325 \text{ Pa}$$

$$t_3 = 24°C$$

$$h_3 = h_2 = 51.13 \text{ kJ/kg}$$

TABLE 6.9

Properties for State Point 3 at the Given Pressure, Temperature and Enthalpy

Property	**p_{vs}, kPa**	**x_s, g/kg**	**x, g/kg**	**p_v, kPa**	**ϕ, %**
Value	2.9851	1.888	10.602	1.6982	56.889
Equation	6.17	6.3	6.7	6.14	6.10
	t_{dp}, °C	**t_{wb}, °C**	**μ**	**v, m³/kg**	**c_p, kJ/kg·K**
Value	14.95	18.15	0.562	0.8560	1.0283
Equation	6.39	6.40	6.8	6.29	6.35

Solution:

(a) Calculation of the psychrometric properties of the moist air at the exit of the drying chamber

Use t_3 to find p_{vs} by Equation 6.17 and based on h_3 calculate x_3 by Equation 6.7. Then, find p_{v3} by Equation 6.14 and determine the relative humidity by Equation 6.10. Calculate the other properties at point 3 substituting the relative humidity, temperature and the newly determined values into the equations shown in Table 6.9.

(b) Estimation of the moisture removal rate in g/s and kg/h as the moist air changes from state point 2 to 3 keeping the air volumetric flow rate of 1.0 m³/s

$$\Delta x = x_3 - x_2 = 10.602 - 4.216 = 6.386 \text{ kg/kg}$$

$$\dot{m}_a = \frac{\dot{V}}{v} = \frac{1}{0.856} = 1.17 \text{ kg/s}$$

$$\dot{m}_w = \dot{m}_a \Delta x = 1.17 \cdot 6.386 = 7.472 \text{ g/s } (26.90 \text{ kg/h})$$

Therefore, this chapter examined the properties of moist air and related problems that were solved by the proposed equations and graphical methods. Properties are required to carry out calculations related to performance, water removal and capacity of conventional and heat pump drying. The dryer performance, moisture removal and energy utilisation change considerably depending on psychrometry and process position on the chart. This was illustrated with cases including the isothermal, adiabatic, and low and high polytropic drying processes.

7

Thermophysical Properties and Selection of Heat Pump Fluids

There is an abundance of heat pump fluids, or refrigerants, in the international market today because there is no ideal refrigerant satisfying all required conditions in different applications. Also, the availability of fluids is continuously changing and evolving according to the current energy policies and regulations protecting the environment and climate. The outcome is the generation of incentives for adopting or replacing refrigerants, which influences their cost and utilisation. Thus, how you would select a fluid from this wide variety? What are the criteria for selection? The answers to these questions are covered gradually in this chapter. The selection procedure involves comparison of fluids based on the properties at the state points of the heat pump cycle at specific operating conditions. The current selection favours fluids that are harmless and nontoxic, with near-zero ozone depletion potential (OZP) and global warming potential (GWP), and that are compatible with materials and lubricating oils and have favourable properties and low cost. As mentioned previously, there is no single fluid that satisfies all these requirements, and the most suitably selected fluid is the one with the best combined characteristics, taking into account performance, system operation, safety, health, sustainability and cost.

This chapter covers the selection, properties and characteristics of the common conventional refrigerants and the currently favoured natural fluids. Designs and equations are proposed and problems are solved in terms of performance or capacities and illustrated by the system's layout and heat pump cycles. The properties of commonly used refrigerants are given in tables and illustrated in pressure–enthalpy and temperature–entropy diagrams.

7.1 Types and Designation of Refrigerants

Based on chemical composition, Standard 34 (ASHRAE Handbook of Fundamentals 2009) divides the refrigerants into 10 series, blends and compounds:

1. Methane series
2. Ethane series
3. Propane series
4. Cyclic organic compounds
5. Zeotropic blends (ZEBs)
6. Azeotropic blends (AZBs)

7. Miscellaneous organic compounds
8. Nitrogen compounds
9. Inorganic compounds
10. Unsaturated organic compounds

Presently, the most common heat pump fluids belong to methane, ethane and propane series; miscellaneous organic and inorganic compounds; and ZEBs and AZBs.

The methane series includes the halogenated compounds such as fluorinated and chlorinated methane derivatives. They are designated by 'R' and two numbers with or without a letter 'B'. An example is R22 or chlorodifluoromethane; R22 was commonly used in the past because it was considered safe. However, it is not allowed in new systems built in some Scandinavian countries because it contains chloride atoms that cause harm to the ozone layer. Also, it has also a relatively high GWP. Since R22 is a well-known refrigerant that was widely used in the past, it is referred in this chapter only for comparison with better fluids. Another example is R50 or methane that is further described herein.

The ethane and propane series include hydrocarbon refrigerants that have zero ODP, small GWP and are flammable. These refrigerants are designated by R and three numbers with or without letters a, b, or B. Moreover, the ethane and propane refrigerants belong to the R100s and 200s series, respectively. Their applications are increasing for small household refrigerators and freezers entailing small fluid charges. The most common refrigerants in this series are tetrafluoroethane (R134a), ethane (R170) and propane (R290).

ZEBs are mixtures of two to four pure components designated as R4 plus two numbers followed or not by a letter A, B, C, or D, indicating the ratio of pure refrigerants in the mixture. The examples are as follows:

- R404A, which is a mixture of R125, 143a and 134a in mass fractions of 0.44, 0.52 and 0.4, respectively
- R407C, a blend of R32, R125 and 134a in mass fractions of 0.23, 0.25 and 0.52, respectively
- R410A, a mixture of R32 and 125 in mass fractions of 0.5 and 0.5, respectively

The main peculiarity of the ZEB is a variable temperature at constant pressure in the two-phase region. This is called temperature glide and depends on the fractions of pure compounds in the mixture. The glide may vary from 1 (near zeotropic) to 5 or more degrees Celsius and may be an advantage if matched with the temperature glide in the heat sink or source.

The intersection of a constant pressure with the saturation curves, or vapour quality from $x = 0$ to $x = 1$, defines the blend bubble-point and dew-point temperatures. An example of ZEB is R407C, with the cycle illustrated in the pressure–enthalpy diagram in Figure 7.1. It shows that R407C has a bubble-point temperature of 40.1°C ($x = 1$) and a dew-point temperature of 45.0°C ($x = 0$) at constant condensing pressure of 17.5 bar in the two-phase region. At a constant evaporating pressure of 1 bar, the bubble-point and dew-point temperatures are −44.1°C ($x = 0$) and −37.0°C ($x = 1$), respectively. Notice that in the plot the actual temperature of the fluid at the inlet evaporator is −40.1°C ($x = 0.47$).

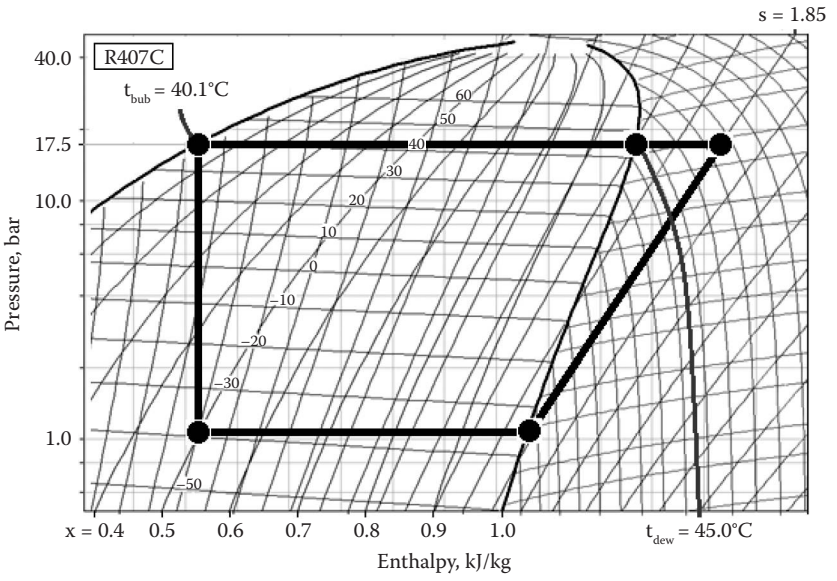

FIGURE 7.1
ZEB typical thermal behaviour and cycle in the pressure–enthalpy diagram.

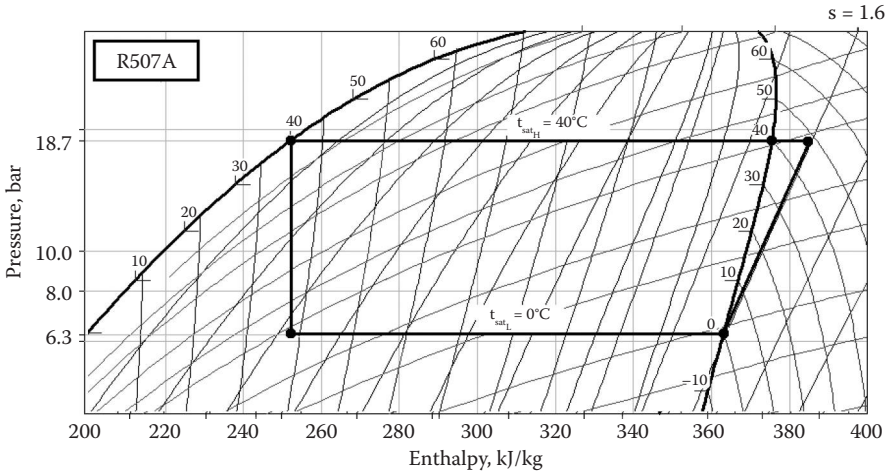

FIGURE 7.2
AZB typical behaviour in the pressure–enthalpy diagram.

AZBs are designated by R5 plus two numbers and a letter A or B, indicating the fractions of pure fluids in the mixture. An AZB is a mixture of two refrigerants and changes phase at constant temperature and constant pressure. An example is R507A, a mixture of R125 and 143a, each with a mass fraction of 0.5. The R507A cycle in the pressure–enthalpy diagram in Figure 7.2 shows a constant condensing temperature of 40°C (at $0 \leq x \leq 1$) and a constant condensing pressure of 18.7 bar. In addition, it has a constant saturation temperature of 0°C (at $0 \leq x \leq 1$) at a constant evaporating pressure of 6.3 bar.

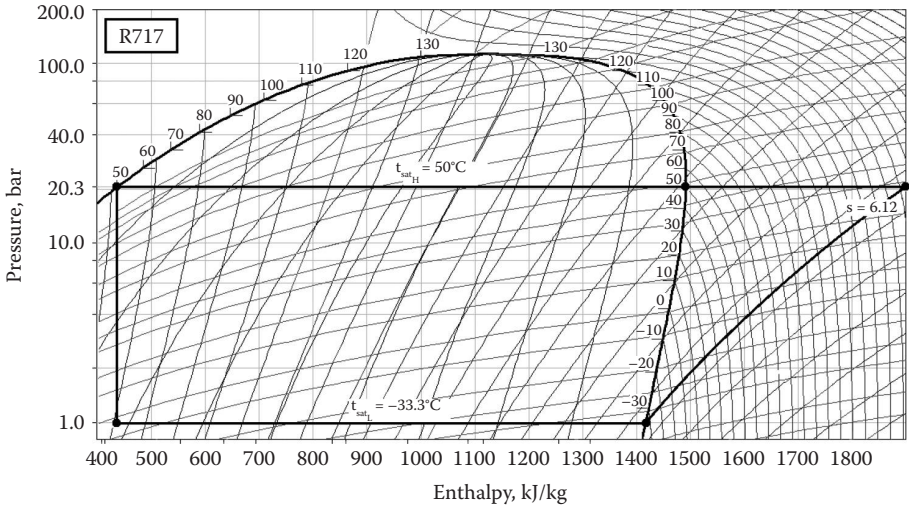

FIGURE 7.3
Natural fluid R717 thermal behaviour and cycle in the pressure–enthalpy diagram.

Miscellaneous organic compounds are designated by R6 plus two numbers without a letter, except isobutane represented by R600a. Isobutane has zero ODP, low GWP and a satisfactory coefficient of performance (COP), but it is flammable. This is tackled by using small charges and, presently, R600a is a replacement fluid and safely applied in domestic refrigerators and freezers.

Inorganic refrigerants include the natural fluids that have azeotropic behaviour with regard to pressure and temperature.

They are designated by R7 plus two numbers representing the molecular weight without letters, except for nitrous oxide represented by R744A. The main natural fluids are ammonia (R717), water (R718), air (R729) and carbon dioxide (R744). These fluids have no ozone depletion and near-zero GWP with excellent properties, allowing design of compact evaporators or condensers and highly efficient indirect systems. One of the most promising natural fluids is ammonia, with the cycle sketched in the pressure–enthalpy diagram in Figure 7.3. It indicates that R717 has a constant condensing temperature of 50°C (at $0 \le x \le 1$) at constant condensing pressure of 20.3 bar as well as a constant saturation temperature of –33.3°C (at $0 \le x \le 1$) at constant evaporating pressure of 1.0 bar.

7.2 Selection of Heat Pump Fluids

The refrigerant or heat pump fluid selection depends on a large number of parameters, including performance, energy, cost, stability, required charge, safety, compatibility with lubricants and environmental effects. All these parameters are related to the fluid properties at the state points of the fluid in the heat pump cycle and system layout.

Some of the relevant properties and characteristics of a favourable fluid are as follows:

- Zero ODP, near-zero GWP and safe operation
- Low cost
- Low temperature difference between evaporation and condensation for high COP
- Low condensing pressure to reduce amount of materials in the system
- Evaporating pressure above 1 bar to avoid leak and access of air or moisture
- Low compression ratio for high volumetric efficiency and low work input
- Low discharge temperature to avoid compressor damage or oil and material reaction
- Small vapour specific volume and large cooling effect for smaller charge and compressor size
- High latent heat of phase-change per unit mass for higher capacities
- High vapour specific heat to reduce superheat at suction
- Low liquid specific heat for lower sub-cooling and less flash gas
- High liquid and vapour thermal conductivity for better heat transfer
- Low liquid and vapour viscosity to reduce pressure drop in the system

Regrettably, there is no single fluid satisfying all of the above-mentioned requirements. Consequently, a compromise is made, and the fluid that best fulfils these requirements is selected from among a diverse range of available fluids.

7.2.1 Selection Based on Performance from Cycles at Similar Operating Conditions

A heat pump and refrigerator operates with a fluid or refrigerant that flows through the evaporator, absorbing energy from the heat source (medium to be cooled), and through the condenser, transferring energy to the heat sink (medium to be heated). The processes in a mechanical vapour compression heat pump system cycle are evaporation, condensation, compression and throttling. These processes and energy transport occur as the fluid changes phase and flows through the components.

The working fluid is selected among two or more refrigerants based on the properties at each state point of the cycle and on the most suitable overall performance. Figure 7.4 shows the cycles in the log pressure–enthalpy diagram of two fluids in a heat pump operating at the same evaporating and condensing temperatures and pressures. The different properties of the refrigerant leads to the different cycles 1 and 2 represented by the state points 12341 and 12561, respectively.

The heat pump COPs for the refrigerants in cycles 1 and 2 are as follows:

$$\mathrm{COP_{H1}} = \frac{h_2 - h_3}{h_2 - h_1} = \frac{q_{H1}}{w} \tag{7.1}$$

$$\mathrm{COP_{H2}} = \frac{h_2 - h_5}{h_2 - h_1} = \frac{q_{H2}}{w} \tag{7.2}$$

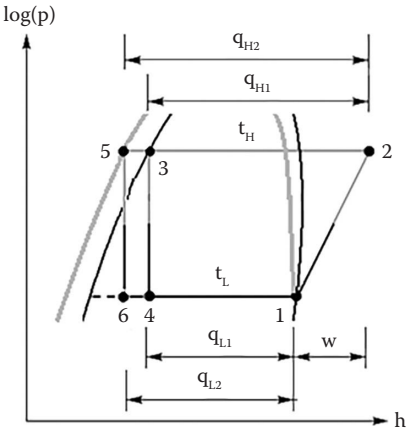

FIGURE 7.4
Cycles for two refrigerants at the same operating temperatures and pressures.

Since the work input is the same in both cycles and $q_{H2} > q_{H1}$, then the COP for refrigerant 2 is greater than for refrigerant 1, or

$$COP_{H2} > COP_{H1} \tag{7.3}$$

Also, the COPs based on the evaporation and cooling for the two refrigerants are as follows:

$$COP_{L1} = \frac{h_1 - h_4}{h_2 - h_1} = \frac{q_{L1}}{w} \tag{7.4}$$

$$COP_{L2} = \frac{h_1 - h_6}{h_2 - h_1} = \frac{q_{L2}}{w} \tag{7.5}$$

The COP at cooling for refrigerant 2 is greater than refrigerant 1 since $q_{L2} > q_{L1}$, or

$$COP_{L2} > COP_{L1} \tag{7.6}$$

Thus, refrigerant 2 is the better choice than refrigerant 1 if based purely on the COPs.

7.2.2 Selection Based on Performance at Transcritical Cycle

An important factor in selecting a fluid is the ability to operate in a transcritical cycle. This cycle has improved performance compared to a subcritical cycle for operation close to the critical point. In a conventional subcritical cycle, the condensation occurs in the two-phase region and the COP drops sharply as the pressure approaches the critical point.

The obvious questions are how to reverse this situation and what is the fluid to select. The situation is inverted by considering that condensation in a transcritical cycle (above critical point) happens without phase change and, as the condensation pressure approaches the critical point, the COP greatly increases by means of gas cooling.

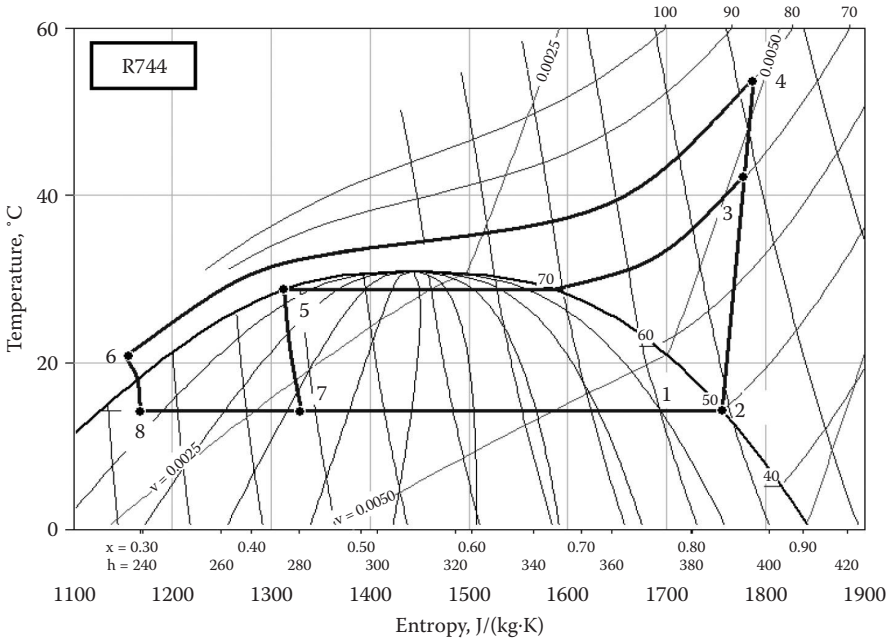

FIGURE 7.5
Transcritical and subcritical R744 heat pump cycles and versatility of performances.

An exceptional fluid choice for the heat pump transcritical cycle is the carbon dioxide (R744) since it has critical temperature and pressure of 31.03°C and 7380 kPa, respectively. Figure 7.5 illustrates and compares the performances of two heat pumps operating with R744 in subcritical and transcritical cycles at the same evaporating pressure.

The R744 heat pump performances are now compared considering a transcritical (even numbered as 24682) and a subcritical (odd numbered as 13571) cycle. The heat pump COPs are as follows:

$$COP_{Hod} = \frac{h_3 - h_5}{h_3 - h_1} = \frac{q_{Hod}}{w_{od}} \tag{7.7}$$

$$COP_{Hev} = \frac{h_4 - h_6}{h_4 - h_2} = \frac{q_{Hev}}{w_{ev}} \tag{7.8}$$

Since $q_{Hev} >> q_{Hod}$ and $w_{ev} \approx w_{od}$, the COP of the transcritical cycle is higher than that for the subcritical cycle, or

$$COP_{Hev} > COP_{Hod} \tag{7.9}$$

In addition, the COPs based on cooling effect for the two cycles are as follows:

$$COP_{Lev} = \frac{h_2 - h_8}{h_4 - h_2} = \frac{q_{Lev}}{w_{ev}} \tag{7.10}$$

$$COP_{Lod} = \frac{h_1 - h_7}{h_3 - h_1} = \frac{q_{Lod}}{w_{od}} \tag{7.11}$$

Since the work input is similar and $q_{Lev} >> q_{Lod}$, then the COP at cooling for the transcritical cycle is greater than that for the subcritical cycle, or

$$COP_{Lev} > COP_{Lod} \tag{7.12}$$

Accordingly, the heat pump with carbon dioxide in a transcritical cycle displays better performance characteristics compared to those of the subcritical cycle.

The reason for the better performance in a transcritical cycle is that after compression, the R744 vapour flows through the gas cooler and releases intense heat. Then, it enters the throttling device at lower enthalpy, resulting in higher enthalpy difference in condensation and evaporation processes and very high COPs. This improvement is a beneficial characteristic of the R744 cycle, and it is associated with a large enthalpy shift to the left of the critical point.

7.2.3 Selection Based on Operating Pressure and Temperature

The refrigerant can be selected based on the evaporating and condensing temperatures for pressures of 1 and 25 bar that are typical in commercial compressors as presented in Table 7.1.

The temperature and pressure are constant in the two-phase region for AZBs and natural fluids, implying a constant saturation temperature at a given pressure.

TABLE 7.1

Saturation, Bubble-Point and Dew-Point Temperatures for Selected Fluids at Compression Pressures of 1 and 25 bar

	R					
t	**R134a**	**R507A**	**R600a**	**R717**	**R718**	**R744**
1 bar						
t_{sat}	–26.43	–46.99	–12.20	–33.30	99.63	–94.55
25 bar						
t_{sat}	77.59	52.10	111.97	58.18	223.99	–12.04
	R404A	**R407A**	**R407C**	**R410A**	**R729**	
1 bar						
t_{bub}	–46.72	–45.72	–44.17	–52.53	–194.50	
t_{dew}	–46.00	–38.81	–36.81	–52.61	–191.44	
25 bar						
t_{bub}	53.57	53.52	55.57	41.56	–150.22	
t_{dew}	53.82	57.34	59.85	41.74	–149.11	

However, as previously mentioned for the two-phase region, the temperature varies with the pressure for ZEBs and air. This implies for these blends that the temperatures at each pressure are defined by bubble-point temperature (tbub) and dew-point temperature (tdew) rather than saturation temperature (tsat).

Table 7.1 shows that R718 has high saturation temperatures at the typical pressures and is seldom used in vapour compression heat pump systems. In contrast, R729 is a cryogenic fluid with very low saturation temperatures at the given pressures. The natural fluids have considerable variation in saturation temperatures, allowing a wide range of applications. The closeness of the bubble-point temperatures of the ZEBs indicates their similar purposes and performances.

7.2.4 Selection Based on Effect on Safety and Environmental Issues

The selection of the heat pump fluid depends strongly on the environmental effects of the fluid and potential health risks the fluid presents.

In terms of safety, the refrigerant selection depends on the classes and groups established according to the Standard 34 (ASHRAE Handbook of Fundamentals 2009).

The safety classes of refrigerants are expressed by letters:

A: Nontoxic for concentrations below 400 ppm by volume

B: Toxic at concentrations above 400 ppm

The safety groups are represented by numbers as follows:

1. No spread of flame in air at 18°C and 101 kPa
2. Flammable with low flammability limit greater than 0.1 kg/m^3 at 21°C and 101 kPa or heat of combustion less than 19 MJ/kg
3. Highly flammable with lower flammability limit less than or equal 0.1 kg/m^3 at 21°C and 101 kPa or heat of combustion greater than or equal 19 MJ/kg

Therefore, the safety ranges from A1 that is nontoxic without flame propagation to B3 that is toxic and highly flammable.

Table 7.2 gives the composition type, ODP, GWP, and safety class-group for selected conventional and natural heat pump fluids. The refrigerant type is either a pure compound or a blend of substances. Then, the type appears in Table 7.2 as a single substance, AZB and ZEB.

The GWP is equivalent to the amount of heat trapped as greenhouse gases (GHGs) relative to carbon dioxide, which is used as a reference value, with a GWP of 1.

The data show that ODP is 0 and GWP is below or equal unit only for ammonia, water, air and carbon dioxide. The ODP and GWP are higher for the hydrofluorocarbons (HFCs) and ZEBs, and from these blends R407C and R410A have the lower GWP and ODP, accordingly. It also indicates that the ODP contribution by the natural fluid carbon dioxide is 1300 and 1730 times smaller than that for R134a and R410A, respectively.

Conventional and natural fluids can be selected to replace non-zero ODP or non-unit GWP, phase-out schedule and applications as presented in Table 7.3.

TABLE 7.2

Composition Type, Ozone Depletion Potential, Global Warming Potentials and Safety Class for Selected Conventional and Natural Heat Pump Fluids

Fluid	Type	ODP	GWP	SAG
R22	SIN	0.055	1500	A1
R134a	SIN	<0.00050	1300	A1
R404A	ZEB	<0.00030	3260	A1
R407C	ZEB	<0.00027	1530	A1
R410A	ZEB	<0.00002	1730	A1
R507A	AZB	0	4000	A1
R600a	SIN	0	<20	A3
R717	SIN	0	0	B2
R718	SIN	0	0	—
R729	SIN	0	0	—
R744	SIN	0	1	A1

TABLE 7.3

Selected *HFCs* and Natural Fluids to Replace Non-Zero *ODP* or Non-Unit *GWP* Refrigerants, Phase-Out Schedule and Applications

Fluid	R134a	R404A	R407A	R407C	R410A	R507A
To replace	R12	R502	R22	R22	R22	R22
	—	—	—	—	—	R502
Phase-out	CRR	CRR	CRR	CRR	CRR	CRR
Apply	LTE	LTE	LTE	MTE	RCAC	—
	HTE	RCAC	MTE	RCAC	RCHP	CRE
	CRE	RCHP	DER	RCHP	—	—
	R600a	**R717**	**R718**	**R729**	**R744**	
To replace	R22	CFCs	—	—	CFCs	
	R134a	HCFCs	—	—	HCFCs	
	—	HFCs	—	—	HFCs	
Phase-out	—	Permanent	—	—	—	
Apply	—	LTE	—	—	LTE	
	—	MTE	RPGC	—	MTE	
	—	RCAC	EHSM	AACR	RCAC	
	—	RCHP	RABS	RQFF	RCHP	
	—	TSS	ADS	—	CHI	
	—	CHI	—	—	—	

The symbols in Table 7.3 are according to ASHRAE Handbook of Refrigeration (2010):

AACR: aircraft air conditioning and refrigeration

ADS: adsorption systems

CFCs: chlorofluorocarbons

CHI: process chilling
CRE: commercial refrigeration
CRR: phase-out regulated or scheduled by specific country or region
DER: direct expansion refrigeration
EHSM: energy-heat storage medium
HCFCs: hydrochlorofluorocarbons
HFCs: hydrofluorocarbons
HTE: high temperature
LTE: low temperature
MTE: medium temperature
PFL: process fluid
RABS: refrigeration absorption systems
RCAC: residential and commercial air conditioning
RCHP: residential and commercial heat pump
RMAD: refrigeration-mineral adsorber
RPGC: Rankine power generation cycle
RQFF: refrigeration for quick freezing of foods
TSS: thermal storage systems.

The preceding accounts confirm the potential for future adoption of natural fluids, for instance, the HFCs and ZEBs will eventually be phased out because they are refrigerants with non-zero ODP or non-unit GWP.

Table 7.4 lists the major safety parameters to select and compare conventional, ZEBs and natural fluids. The fluid safety is based on detectable odour (DOD), fire and explosion risks (FER), suffocation risk (SUR) in enclosures and density of gas higher

TABLE 7.4

Safety Comparison of Selected Conventional, Zeotropic and Natural Heat Pump Fluids

Fluid	DOD	FER	SUR	TXR
R134a	No	No	Yes	No
R404A	No	No	Yes	No
R407A	No	No	Yes	No
R407C	No	No	Yes	No
R410A	No	No	Yes	No
R507C	No	No	Yes	No
R600a	No	Yes	Yes	Yes
R717	Yes	Yes	No	Yes
R718	No	No	No	No
R729	No	No	No	No
R744	No	No	Yes	No

than air, toxicity risk (TXR) by threshold limit value and formation of hydrofluoric acid in exposure to open fire.

The data indicate that ammonia is the only fluid that has detectable odour but, as with R600a, it has the drawback of FER. Also, Table 7.4 shows that water, air and ammonia are the fluids without SUR and that R600a and R717 are the only fluids with TXR.

7.2.5 Selection of the Natural Fluids

Natural fluids have been used in refrigeration and heat pumps in the past, but they have lagged behind the CFCs and HCFCs since they were considered safer but are now phased out.

The current trend favours zero ODP and zero GWP fluids, and the future vision is intensified application of natural fluids in heat pumps and refrigeration systems. Research and demonstration (R&D) is increasing and encouraging the return to natural fluids in combination with today's advanced components, processes, controls and materials. The reasons are that natural fluids have excellent properties and are permanent solutions to the concerns about safety and impact to the environment and climate. Natural fluids are further subdivided into the safest fluids, such as water and air, and practical fluids, such as hydrocarbons, ammonia and carbon dioxide.

Water (R718) and air (R729) are safer because they are neither flammable nor toxic, but they are unusual in vapour compression systems due to high saturation temperatures at typical practical pressures, as given in Table 7.1. R718 has higher COP than HFC and latent heat of evaporation is about four times higher than that of R744 and about twice as high as that of than R717. Therefore, it is an excellent energy absorber by changing phase from liquid to vapour or vice versa at constant temperature and pressure. The R718 limitation is a very low vapour density, requiring an extremely high volumetric flow rate that is provided by an expensive and rare titanium turbine. In addition, operation of the R718 at relatively high pressure causes a fluid flow at a near perfect vacuum allowing penetration of undesirable contaminants and air. Table 7.1 shows that air has an extremely low temperature at the typical compression pressures. R729 is a cryogenic fluid with special applications in aircraft air conditioning, quick-freezing and refrigeration systems, but the low density results in low COP.

Hydrocarbons are highly flammable, explosive and heavier than air. They have a lower explosion limit, varying from 1.5 to 2.7 by volume; an upper explosion limit in air from 8.5 to 14.7% by volume; and an auto-ignition temperature ranging from 365°C to 515°C. Methane (R50) and isobutane (R600a) are among the most common hydrocarbon fluids. Their advantages are excellent thermal properties and variable boiling points, permitting a widespread application in areas such as air conditioning, chilling, refrigeration and cryogenics. Commercial examples are cold transport, chilling, portable air conditioning, refrigeration-freezing, cooling of soft-drink bottles, freezing of ice cream, and supermarket indirect refrigeration (ASHRAE Handbook of HVAC Applications 2011).

Carbon dioxide (R744) is non-flammable, odourless, denser than air and non-toxic, except in enclosed spaces at extreme concentrations of 5000 ppm. R744 is a primary refrigerant choice, and its importance is increasing because of its practical benefits and low impact on the environment and climate. The excellent properties of R744 allow the design of a compact system for a wide range of applications with very high

COPs, as previously compared with transcritical and subcritical cycles (Alves-Filho et al. 2000).

Ammonia (R717) has advantages compared to conventional refrigerants, including a strong odour, facilitating detection and adjustment to avoid accidents. The R717 drawback is toxicity at a threshold limit value of 25 ppm, and a lower explosion limit in air at 15% by volume, with auto-ignition at 651°C. Also, R717 has a lower density than air, it is corrosive to copper or zinc materials, and it may cause corrosion cracking to mild steel in the presence of air or carbon dioxide.

Now, we return to fluid selection with questions in connection with the preceding discussion. What is the proposal for heat pump fluid selection and what is the contribution to reduce the GHGs such as carbon dioxide and ODP?

The proposal is to select zero or near-zero GWP and ODP fluids and to design of heat pump dryers to replace systems currently heated using electricity from thermal power plants. Hence, let us select a medium-temperature heat pump drying with R717 and R744 natural fluids (Alves-Filho and Mujumdar 2005).

A properly designed heat pump dryer with R717 has a COP of 4. The contributions are the reduction of actual carbon dioxide emission to 33.3% (as well as energy use). Another benefit is the design of a sustainable drying process with zero ODP and GWP.

A correctly designed heat pump dryer with R744 operating in transcritical cycle has a COP of 5 (or higher). The contributions are reduction in the actual GHG emissions to 20% (with the same reduction in energy), capture of carbon dioxide from the emitting sources and containment in the closed loop of the R744 heat pump dryer. The additional benefit is a green technology drying process with zero ODP and near-zero GWP.

The next question is when these heat pump dryers can be implemented. The answer is right now, and this is a fundamental, economical and practical advantage of this proposal compared to long-term research and still-to-be-developed solutions to this problem.

7.3 New Heat Pump Dryers with Natural Fluids Designed at NTNU

Attracted by the collective advantages of natural fluids, several institutions and industries are currently engaged and developing heat pump systems with these fluids. In choosing the natural fluid alternatives, ammonia and carbon dioxide were considered as the best selections due to the benefits of zero ODP, unit GWP, safety, proper temperature and pressure levels, and excellent performance and energy utilisation. Process performance and impact on environment, climate and health have been the focus of R&D at the Norwegian University of Science and Technology (NTNU), and, as a consequence, several heat pump dryers with R717 and R744 have been designed and built. In addition to fluid, another choice was a full recirculation of exhaust air and maximum energy recovery by the heat pump dryer components. These parameters are considered in the design of the R717 and R744 heat pump dryers and, in particular, to the blower, drying chamber, evaporator, compressor, condenser and throttling device. The main objectives are to develop a sustainable and green heat pump technology to achieve and enhance COP and optimum specific moisture extraction ratio.

7.3.1 Carbon Dioxide Heat Pump Dryer

The only pilot-scale heat pump dryer working with carbon dioxide in a transcritical cycle for particulate materials in a fluidised or stationary bed was designed and built at NTNU. Figure 7.6 shows the picture of the R744 heat pump dryer in the laboratory.

The R744 heat pump dryer is designed to operate at variable conditions with a cleaning in place (CIP) system. The CIP system includes spray nozzles that are mounted in the drying loop, allowing proper cleaning of the blower, cyclone, heat exchangers, drying chamber and connecting ducts before and after drying. Air and gases such as nitrogen, helium and steam can be applied for drying or sterilisation since the drying loop is designed to stand a maximum absolute pressure of 220 kPa.

Potential applications for this dryer are biochemical, chemical, medical, pharmaceutical and food products technology. The wet material is loaded into the chamber; the gas velocity is adjusted for fluidisation or stationary modes; and the temperature is set according to the nature, stickiness and thermal sensitivity of the drying material.

The dryer's transcritical cycle is sketched in the temperature–entropy diagram for R744 in Figure 7.7. The main processes are as follows: AB – compression process, BC – heat rejection in the external heat exchanger, CD – gliding temperature during drying air heating, DE – heat rejection in auxiliary heat exchanger, EF – throttling and FA – evaporation or moist air cooling and dehumidification process.

Major benefits of this heat pump dryer as a green technology are zero ODP, near-zero GWP, and very high COP for high energy efficiency and lower cost.

7.3.2 Ammonia Heat Pump Dryers

Ammonia was selected as the natural fluid and used in the fluidised bed and tunnel drying technologies designed and built at NTNU.

FIGURE 7.6
Pilot-scale heat pump dryer operating with R744 in transcritical cycle: 1 – cyclone, 2 – drying chamber, 3 – condenser (R744 gas cooler), 4 – evaporator, 5 – adjustable external condenser (R744 gas sub-cooler), 6 – control panel, 7 – compressor, 8 – cleaning in place system.

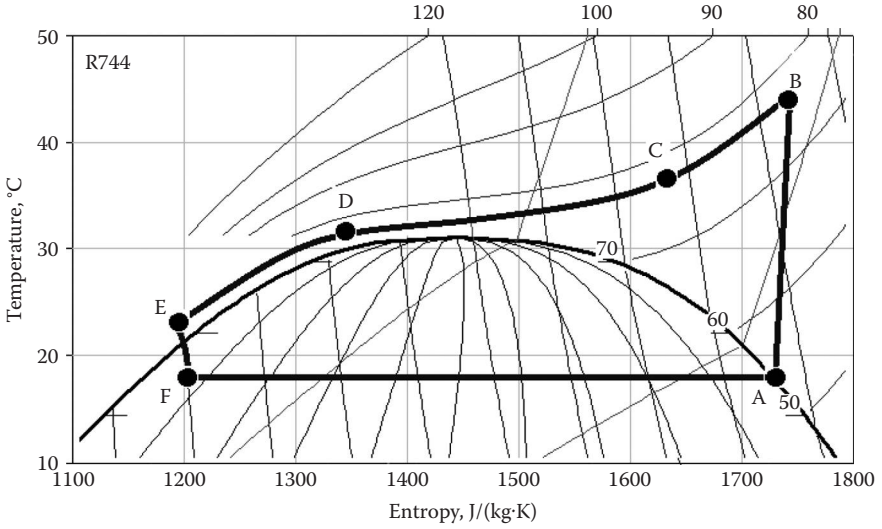

FIGURE 7.7
R744 transcritical cycle for the heat pump dryer in the temperature–entropy diagram.

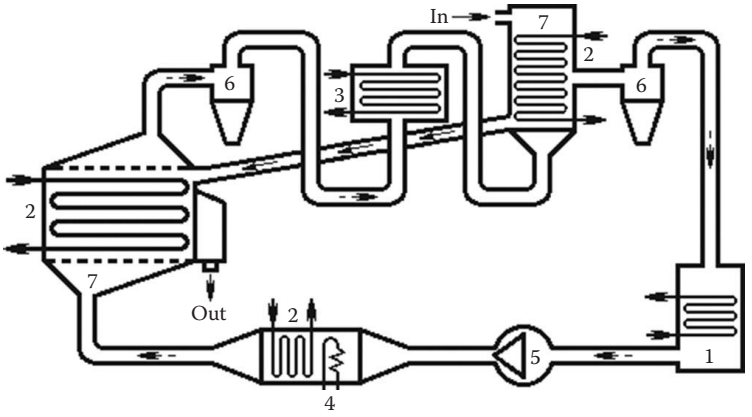

FIGURE 7.8
Nearly isothermal or non-adiabatic fluidised bed heat pump dryer with R717: 1 – evaporator, 2 – condenser, 3 – superheater, 4 – electric heater, 5 – blower, 6 – cyclone, 7 – fluidised bed drying chamber, *In* – wet material inlet, *Out* – dry product outlet, ⇢ airflow, → refrigerant flow and product movement.

The fluidised bed heat pump dryer working with R717 and main components is illustrated in Figure 7.8 (Strømmen et al. 2003).

This new dryer differs from the conventional adiabatic dryers because it is designed to operate close to isothermal or non-adiabatic processes. To achieve this operation, the air drying loop side has two drying chambers with immersed heat exchangers connected to the heat pump condensers. The wet material is continuously loaded into the first drying chamber operating in back-mixing fluidised bed, after which the semidried product flows

through a connecting duct and enters the second drying chamber operating in plug-flow where it is fully dried and discharged.

The R717 tunnel dryer is designed to operate in semicontinuous and countercurrent-flow modes with two closed loops, as illustrated in Figure 7.9. A typical tunnel dryer has a rectangular drying chamber with cross-section area of 8 m^2 (2 × 4 m) and the airflow is adjusted up to 16 m^3/s. The wet product is loaded on trays-in-trolleys that move through the chamber and is continuously dried as the trolleys reach the exit of the chamber. The dryer is sufficiently long, allowing the outlet air to reach the set exhaust relative humidity. The important design parameters are the COP, cooling and condensing capacity, and specific moisture extraction ratio.

A relevant aspect in the choice of R717 is that its properties change favourably in the inlet and outlet of each component in the heat pump closed loop. In addition, it is a sustainable dryer with a zero ODP, zero GWP and an improved COP with low energy use or cost.

Main characteristics, advantages and drawbacks of heat pump fluids were described in Section 7.1 through 7.3. Examples are provided as the basis to compare performances of heat pumps operating with different fluids.

The calculation and design of heat pump dryers require knowledge of the properties of the refrigerant in each state point of the cycle. Considering the relevant fluids, the next section provides the thermophysical properties in tables and graphs that were generated based on CoolPack (Skovrup 2001) that is a collection of simulation models for refrigeration systems (with permission from IPU Technology Development).

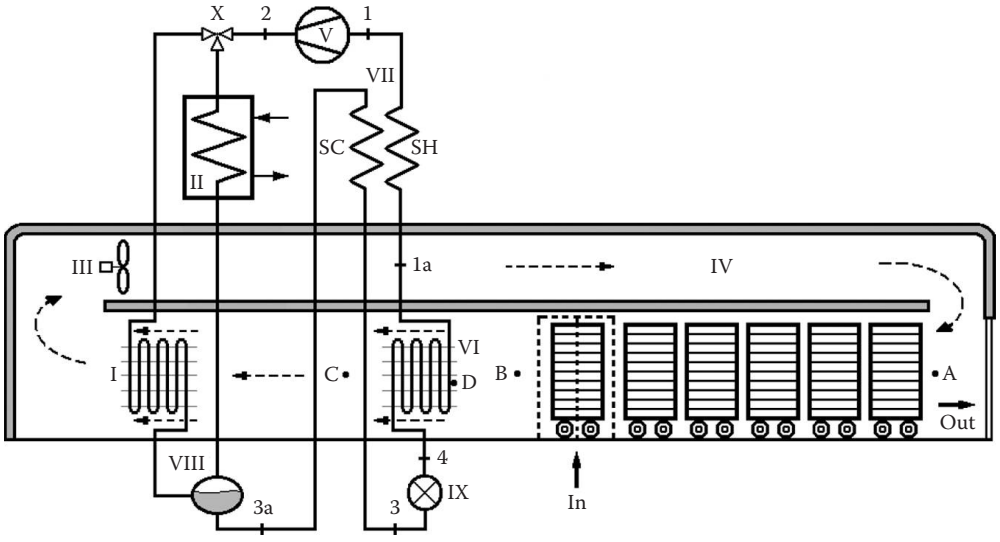

FIGURE 7.9
Semicontinuous tunnel heat pump dryer with R717 as working natural fluid: I – internal condenser, II – external condenser, III – blower, IV – tunnel drying chamber with salted split cod, V –compressor, VI – evaporator, VII – internal heat exchanger, VIII – liquid receiver, IX – throttling valve, X – three-way valve, 1a: saturated vapour, 1: superheated vapour at low pressure, 2: superheated vapour at high pressure, 3a: saturated liquid, 3: subcooled liquid, 4: vapour and liquid mixture, A – inlet of the drying chamber, B – inlet of the evaporator, C – inlet of condenser, D – evaporator surface, SC – subcooled liquid, SH – superheated vapour, in – trolley with wet material inlet, out – trolley with dry product outlet, ⇢ airflow, → product movement.

7.4 Main Properties of Selected Refrigerants

7.4.1 Refrigerant R22

This fluid is from methane series with chemical name chlorodifluoromethane and formula $CHClF_2$ (see Table 7.5, Figure 7.10, Figure 7.11, and Table 7.6).

Critical point: $t_c = 96.0°C$ and $p_c = 49.77$ bar

TABLE 7.5

Saturated Liquid and Saturated Vapour Properties for R22

t, °C	p, bar	v_{vap}, m³/kg	h_{liq}, kJ/kg	h_{vap}, kJ/kg	s_{liq}, kJ/kgK	s_{vap}, kJ/kgK
–56	0.469	0.43643	138.80	381.06	0.7512	1.8669
–54	0.522	0.39462	140.84	382.02	0.7606	1.8611
–52	0.580	0.35755	142.88	382.98	0.7699	1.8555
–50	0.644	0.32461	144.94	383.93	0.7791	1.8501
–48	0.713	0.29526	147.01	384.88	0.7883	1.8448
–46	0.787	0.26907	149.09	385.82	0.7975	1.8397
–44	0.868	0.24564	151.19	386.76	0.8066	1.8347
–42	0.955	0.22464	153.29	387.69	0.8157	1.8298
–40	1.049	0.20578	155.40	388.62	0.8248	1.8251
–38	1.151	0.18881	157.52	389.54	0.8339	1.8205
–36	1.259	0.17351	159.66	390.45	0.8429	1.8161
–34	1.376	0.15969	161.80	391.36	0.8518	1.8117
–32	1.501	0.14719	163.96	392.26	0.8608	1.8075
–30	1.635	0.13586	166.13	393.15	0.8697	1.8034
–28	1.778	0.12558	168.31	394.03	0.8786	1.7993
–26	1.930	0.11623	170.50	394.91	0.8874	1.7954
–24	2.092	0.10772	172.70	395.77	0.8963	1.7916
–22	2.265	0.09995	174.91	396.63	0.9050	1.7879
–20	2.448	0.09286	177.13	397.48	0.9138	1.7842
–18	2.643	0.08637	179.37	398.31	0.9226	1.7807
–16	2.849	0.08042	181.61	399.14	0.9313	1.7772
–14	3.068	0.07497	183.87	399.96	0.9399	1.7738
–12	3.299	0.06996	186.14	400.77	0.9486	1.7705
–10	3.543	0.06535	188.42	401.56	0.9572	1.7672
–8	3.801	0.06110	190.71	402.35	0.9658	1.7640
–6	4.072	0.05719	193.02	403.12	0.9744	1.7609
–4	4.358	0.05357	195.33	403.88	0.9830	1.7578
–2	4.659	0.05023	197.66	404.63	0.9915	1.7548
0	4.976	0.04714	200.00	405.37	1.0000	1.7519
2	5.308	0.04427	202.35	406.09	1.0085	1.7490
4	5.657	0.04162	204.72	406.80	1.0169	1.7461
6	6.023	0.03915	207.09	407.50	1.0254	1.7433
8	6.406	0.03685	209.48	408.18	1.0338	1.7405
10	6.807	0.03472	211.88	408.84	1.0422	1.7378
12	7.226	0.03273	214.30	409.49	1.0506	1.7351

(Continued)

TABLE 7.5 ***(Continued)***

Saturated Liquid and Saturated Vapour Properties for R22

t, °C	p, bar	v_{vap}, m³/kg	h_{liq}, kJ/kg	h_{vap}, kJ/kg	s_{liq}, kJ/kgK	s_{vap}, kJ/kgK
14	7.665	0.03087	216.70	410.13	1.0589	1.7325
16	8.123	0.02914	219.15	410.75	1.0672	1.7299
18	8.601	0.02752	221.60	411.35	1.0756	1.7273
20	9.099	0.02601	224.07	411.93	1.0839	1.7247
22	9.619	0.02459	226.56	412.49	1.0922	1.7221
24	10.160	0.02326	229.05	413.03	1.1005	1.7196
26	10.723	0.02201	231.57	413.56	1.1087	1.7171
28	11.309	0.02084	234.10	414.06	1.1170	1.7146
30	11.919	0.01974	236.65	414.54	1.1253	1.7121
32	12.552	0.01871	239.22	415.00	1.1335	1.7096
34	13.210	0.01774	241.80	415.43	1.1418	1.7071
36	13.892	0.01682	244.41	415.84	1.1500	1.7046
38	14.601	0.01595	247.03	416.22	1.1583	1.7021
40	15.335	0.01514	249.67	416.57	1.1666	1.6995
42	16.097	0.01437	252.34	416.89	1.1748	1.6970
44	16.885	0.01364	255.03	417.18	1.1831	1.6944
46	17.702	0.01295	257.74	417.44	1.1914	1.6918
48	18.548	0.01229	260.49	417.66	1.1998	1.6892
50	19.423	0.01167	263.25	417.85	1.2081	1.6865
52	20.328	0.01108	266.05	417.99	1.2165	1.6838
54	21.265	0.01052	268.88	418.09	1.2249	1.6810
56	22.232	0.00999	271.74	418.15	1.2333	1.6781
58	23.232	0.00948	274.64	418.15	1.2418	1.6752
60	24.266	0.00900	277.58	418.10	1.2504	1.6722
62	25.333	0.00854	280.57	417.99	1.2590	1.6690
64	26.435	0.00810	283.60	417.81	1.2677	1.6658
66	27.573	0.00768	286.68	417.56	1.2765	1.6624
68	28.747	0.00728	289.82	417.24	1.2854	1.6588
70	29.959	0.00689	293.03	416.82	1.2944	1.6551
72	31.210	0.00652	296.31	416.30	1.3035	1.6512
74	32.500	0.00616	299.69	415.67	1.3129	1.6470
76	33.832	0.00581	303.13	414.91	1.3224	1.6425
78	35.205	0.00548	306.71	414.00	1.3322	1.6377
80	36.623	0.00515	310.42	412.91	1.3422	1.6325
82	38.086	0.00483	314.29	411.60	1.3527	1.6267
84	39.595	0.00452	318.36	410.02	1.3637	1.6203
86	41.154	0.00420	322.70	408.10	1.3753	1.6130
88	42.763	0.00389	327.40	405.72	1.3878	1.6046
90	44.425	0.00357	332.60	402.67	1.4015	1.5945
92	46.144	0.00322	338.65	398.52	1.4175	1.5815

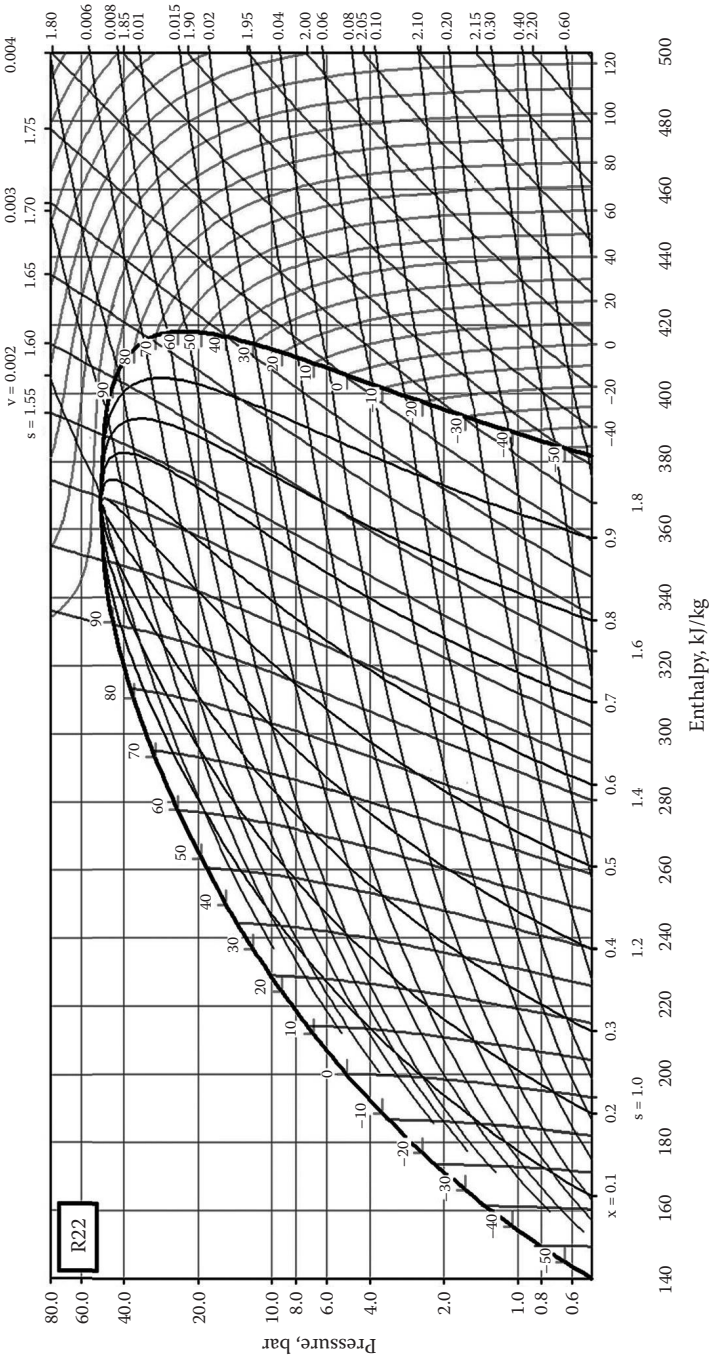

FIGURE 7.10
Pressure–enthalpy diagram for refrigerant R22.

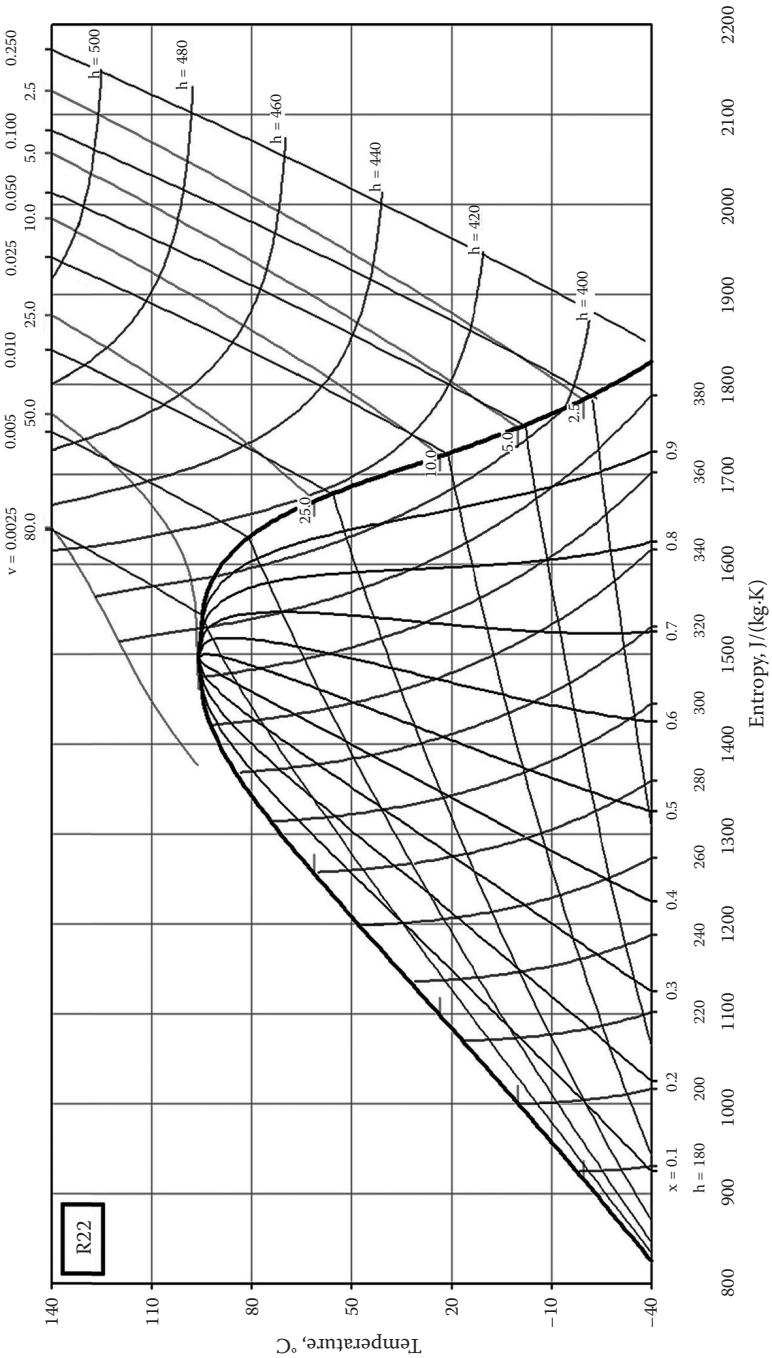

FIGURE 7.11
Temperature–entropy diagram for refrigerant R22.

TABLE 7.6

Properties of Superheated Vapour for R22

t, °C	s, kJ/kgK	h, kJ/kg	v, m³/kg	ρ, kg/m³
State Points at P = 1.01 bar				
Saturated Liquid at Bubble Point				
−40.82	0.8211	154.53	0.0007	1408.45
Saturated Vapour at Dew Point				
−40.82	1.8270	388.24	0.2133	4.69
Superheated Vapour				
−40	1.8291	388.73	0.2141	4.67
−30	1.8544	394.75	0.2245	4.45
−20	1.8791	400.87	0.2347	4.26
−10	1.9031	407.07	0.2448	4.08
0	1.9266	413.36	0.2549	3.92
10	1.9495	419.75	0.2648	3.78
20	1.9721	426.24	0.2748	3.64
30	1.9941	432.82	0.2846	3.51
40	2.0158	439.51	0.2945	3.40
50	2.0372	446.30	0.3043	3.29
60	2.0582	453.18	0.3140	3.18
70	2.0788	460.17	0.3238	3.09
80	2.0992	467.25	0.3335	3.00
90	2.1192	474.44	0.3432	2.91
100	2.1390	481.72	0.3529	2.83
State Points at P = 5 bar				
Saturated Liquid at Bubble Point				
0.15	1.0006	200.17	0.0008	1282.05
Saturated Vapour at Dew Point				
0.15	1.7516	405.42	0.0469	21.31
Superheated Vapour				
10	1.7772	412.53	0.0494	20.26
20	1.8021	419.72	0.0518	19.32
30	1.8262	426.90	0.0541	18.49
40	1.8496	434.11	0.0564	17.74
50	1.8724	441.35	0.0586	17.07
60	1.8946	448.64	0.0608	16.45
70	1.9163	455.97	0.0630	15.88
80	1.9375	463.37	0.0651	15.36
90	1.9584	470.83	0.0672	14.88
100	1.9788	478.36	0.0693	14.43
110	1.9989	485.96	0.0714	14.01
120	2.0187	493.63	0.0735	13.61
130	2.0381	501.38	0.0755	13.24

(Continued)

TABLE 7.6 ***(Continued)***

Properties of Superheated Vapour for R22

t, °C	s, kJ/kgK	h, kJ/kg	v, m³/kg	ρ, kg/m³
140	2.0573	509.21	0.0776	12.89
150	2.0762	517.11	0.0796	12.56
160	2.0949	525.09	0.0816	12.25
State Points at P = 10 bar				
Saturated Liquid at Bubble Point				
23.42	1.0980	228.32	0.0008	1204.82
Saturated Vapour at Dew Point				
23.42	1.7203	412.88	0.0236	42.37
Superheated Vapour				
30	1.7385	418.33	0.0246	40.64
40	1.7649	426.46	0.0260	38.47
50	1.7901	434.47	0.0273	36.60
60	1.8142	442.39	0.0286	34.96
70	1.8376	450.28	0.0298	33.51
80	1.8602	458.15	0.0310	32.21
90	1.8821	466.02	0.0322	31.04
100	1.9036	473.91	0.0334	29.97
110	1.9245	481.83	0.0345	28.99
120	1.9450	489.78	0.0356	28.08
130	1.9651	497.78	0.0367	27.24
140	1.9848	505.83	0.0378	26.45
150	2.0042	513.94	0.0389	25.72
160	2.0233	522.10	0.0399	25.03
170	2.0420	530.32	0.0410	24.39
180	2.0605	538.61	0.0421	23.78
State Points at P = 15 bar				
Saturated Liquid at Bubble Point				
39.10	1.1628	248.48	0.0009	1136.36
Saturated Vapour at Dew Point				
39.10	1.7007	416.41	0.0155	64.52
Superheated Vapour				
40	1.7034	417.27	0.0156	64.08
50	1.7323	426.47	0.0167	59.84
60	1.7593	435.33	0.0177	56.39
70	1.7848	443.95	0.0187	53.49
80	1.8092	452.43	0.0196	51.00
90	1.8326	460.82	0.0205	48.81
100	1.8552	469.14	0.0213	46.87
110	1.8772	477.44	0.0222	45.12
120	1.8985	485.72	0.0230	43.54

(Continued)

TABLE 7.6 ***(Continued)***

Properties of Superheated Vapour for R22

t, °C	s, kJ/kgK	h, kJ/kg	v, m³/kg	ρ, kg/m³
130	1.9193	494.00	0.0238	42.09
140	1.9396	502.31	0.0245	40.76
150	1.9596	510.64	0.0253	39.53
160	1.9791	519.00	0.0260	38.39
170	1.9983	527.40	0.0268	37.33
180	2.0171	535.85	0.0275	36.33
190	2.0357	544.35	0.0283	35.40
State Points at P = 20 bar				
Saturated Liquid at Bubble Point				
51.28	1.2135	265.04	0.0009	1075.27
Saturated Vapour at Dew Point				
51.28	1.6848	417.95	0.0113	88.57
Superheated Vapour				
60	1.7122	426.98	0.0121	82.40
70	1.7411	436.73	0.0130	76.86
80	1.7679	446.06	0.0138	72.39
90	1.7932	455.12	0.0146	68.66
100	1.8173	463.99	0.0153	65.45
110	1.8404	472.74	0.0160	62.65
120	1.8627	481.41	0.0166	60.17
130	1.8844	490.03	0.0173	57.94
140	1.9054	498.62	0.0179	55.92
150	1.9260	507.20	0.0185	54.08
160	1.9460	515.79	0.0191	52.39
170	1.9657	524.39	0.0197	50.82
180	1.9849	533.02	0.0203	49.37
190	2.0038	541.67	0.0208	48.02
200	2.0224	550.36	0.0214	46.76
210	2.0406	559.10	0.0219	45.57
220	2.0586	567.88	0.0225	44.45
State Points at P = 25 bar				
Saturated Liquid at Bubble Point				
61.38	1.2563	279.64	0.0010	1020.41
Saturated Vapour at Dew Point				
61.38	1.6700	418.03	0.0087	115.21
Superheated Vapour				
70	1.6997	428.10	0.0095	105.70
80	1.7303	438.75	0.0102	97.61
90	1.7583	448.76	0.0109	91.33
100	1.7843	458.36	0.0116	86.21

(Continued)

TABLE 7.6 ***(Continued)***

Properties of Superheated Vapour for R22

t, °C	s, kJ/kgK	h, kJ/kg	v, m³/kg	ρ, kg/m³
110	1.8090	467.68	0.0122	81.90
120	1.8326	476.82	0.0128	78.19
130	1.8552	485.83	0.0133	74.93
140	1.8770	494.76	0.0139	72.04
150	1.8983	503.62	0.0144	69.44
160	1.9189	512.46	0.0149	67.08
170	1.9390	521.28	0.0154	64.92
180	1.9587	530.10	0.0159	62.94
190	1.9780	538.93	0.0164	61.10
200	1.9969	547.78	0.0168	59.40
210	2.0154	556.65	0.0173	57.80
State Points at P = 30 bar				
Saturated Liquid at Bubble Point				
70.07	1.2947	293.14	0.0010	970.87
Saturated Vapour at Dew Point				
70.07	1.6550	416.80	0.0069	145.35
Superheated Vapour				
70	1.6547	416.71	0.0069	145.54
80	1.6928	429.95	0.0077	129.07
90	1.7249	441.46	0.0085	118.11
100	1.7538	452.08	0.0091	109.90
110	1.7804	462.17	0.0097	103.35
120	1.8055	471.89	0.0102	97.92
130	1.8293	481.38	0.0107	93.29
140	1.8521	490.69	0.0112	89.27
150	1.8741	499.89	0.0117	85.71
160	1.8954	509.00	0.0121	82.54
170	1.9161	518.07	0.0126	79.67
180	1.9363	527.10	0.0130	77.06
190	1.9559	536.12	0.0134	74.66
200	1.9752	545.13	0.0138	72.45
210	1.9941	554.15	0.0142	70.40
220	2.0126	563.19	0.0146	68.50
230	2.0308	572.25	0.0150	66.71
240	2.0487	581.34	0.0154	65.04
250	2.0663	590.46	0.0158	63.47
State Points at P = 35 bar				
Saturated Liquid at Bubble Point				
77.70	1.3307	306.17	0.0011	917.43
Saturated Vapour at Dew Point				
77.70	1.6384	414.14	0.0055	180.83

(Continued)

TABLE 7.6 ***(Continued)***

Properties of Superheated Vapour for R22

t, °C	s, kJ/kgK	h, kJ/kg	v, m³/kg	ρ, kg/m³
Superheated Vapour				
80	1.6498	418.15	0.0058	173.47
90	1.6904	432.69	0.0066	151.57
100	1.7237	444.93	0.0073	137.78
110	1.7531	456.06	0.0078	127.71
120	1.7802	466.55	0.0083	119.79
130	1.8054	476.62	0.0088	113.29
140	1.8294	486.40	0.0093	107.79
150	1.8523	495.98	0.0097	103.04
160	1.8744	505.41	0.0101	98.85
170	1.8957	514.75	0.0105	95.13
180	1.9163	524.01	0.0109	91.78
190	1.9365	533.23	0.0113	88.74
200	1.9561	542.42	0.0116	85.95
210	1.9753	551.61	0.0120	83.38
220	1.9941	560.79	0.0123	81.01
230	2.0126	569.98	0.0127	78.80
240	2.0307	579.18	0.0130	76.74
250	2.0485	588.41	0.0134	74.81
State Points at P = 40 bar				
Saturated Liquid at Bubble Point				
84.53	1.3667	319.48	0.0012	847.46
Saturated Vapour at Dew Point				
84.53	1.6185	409.56	0.0044	225.73
Superheated Vapour				
90	1.6504	421.04	0.0050	198.53
100	1.6922	436.42	0.0058	172.27
110	1.7259	449.17	0.0064	156.10
120	1.7556	460.69	0.0069	144.41
130	1.7827	471.50	0.0074	135.29
140	1.8081	481.84	0.0078	127.83
150	1.8321	491.87	0.0082	121.54
160	1.8549	501.67	0.0086	116.12
170	1.8769	511.31	0.0090	111.37
180	1.8982	520.83	0.0093	107.14
190	1.9188	530.27	0.0097	103.35
200	1.9389	539.66	0.0100	99.90
210	1.9584	549.01	0.0103	96.75
220	1.9775	558.35	0.0107	93.86
230	1.9963	567.67	0.0110	91.18
240	2.0146	577.00	0.0113	88.69
250	2.0326	586.33	0.0116	86.37

(Continued)

TABLE 7.6 *(Continued)*

Properties of Superheated Vapour for R22

t, °C	s, kJ/kgK	h, kJ/kg	v, m³/kg	ρ, kg/m³
260	2.0503	595.69	0.0119	84.19
270	2.0678	605.07	0.0122	82.15
State Points at P = 45 bar				
Saturated Liquid at Bubble Point				
90.68	1.4067	334.53	0.0013	769.23
Saturated Vapour at Dew Point				
90.68	1.5905	401.42	0.0035	289.86
Superheated Vapour				
100	1.6560	425.51	0.0046	219.07
110	1.6974	441.15	0.0052	190.52
120	1.7310	454.18	0.0058	172.70
130	1.7606	465.96	0.0063	159.77
140	1.7876	476.99	0.0067	149.67
150	1.8128	487.54	0.0071	141.41
160	1.8367	497.76	0.0074	134.46
170	1.8595	507.74	0.0078	128.46
180	1.8814	517.56	0.0081	123.20
190	1.9025	527.24	0.0084	118.53
200	1.9230	536.84	0.0087	114.33
210	1.9430	546.37	0.0090	110.53
220	1.9624	555.87	0.0093	107.05
230	1.9814	565.33	0.0096	103.85
240	2.0000	574.79	0.0099	100.89
250	2.0183	584.24	0.0102	98.15
260	2.0362	593.70	0.0105	95.58
270	2.0538	603.17	0.0107	93.19
280	2.0711	612.66	0.0110	90.93

7.4.2 Refrigerant R50

This fluid is from methane series with chemical name methane and formula CH_4 (see Table 7.7, Figure 7.12, Figure 7.13, and Table 7.8).

Critical point: $t_c = -82.59°C$ and $p_c = 45.99$ bar

TABLE 7.7

Saturated Liquid and Saturated Vapour Properties for R50

t, °C	p, bar	v_{vap}, m³/kg	h_{liq}, kJ/kg	h_{vap}, kJ/kg	s_{liq}, kJ/kgK	s_{vap}, kJ/kgK
−182	0.125	3.75827	90.09	632.48	−0.0262	5.9243
−180	0.160	2.99173	96.64	636.38	0.0447	5.8390
−178	0.203	2.40669	103.24	640.23	0.1148	5.7584
−176	0.254	1.95510	109.89	644.04	0.1838	5.6820
−174	0.316	1.60281	116.59	647.81	0.2519	5.6096
−172	0.388	1.32524	123.33	651.53	0.3191	5.5410

(Continued)

TABLE 7.7 ***(Continued)***

Saturated Liquid and Saturated Vapour Properties for R50

t, °C	p, bar	v_{vap}, m³/kg	h_{liq}, kJ/kg	h_{vap}, kJ/kg	s_{liq}, kJ/kgK	s_{vap}, kJ/kgK
−170	0.474	1.10448	130.11	655.19	0.3852	5.4757
−168	0.574	0.92736	136.93	658.79	0.4505	5.4135
−166	0.689	0.78405	143.78	662.34	0.5148	5.3543
−164	0.822	0.66721	150.67	665.82	0.5782	5.2978
−162	0.974	0.57123	157.59	669.23	0.6407	5.2438
−160	1.146	0.49184	164.56	672.57	0.7024	5.1922
−158	1.341	0.42574	171.56	675.83	0.7634	5.1426
−156	1.561	0.37036	178.60	679.01	0.8236	5.0950
−154	1.806	0.32368	185.69	682.10	0.8831	5.0493
−152	2.080	0.28413	192.82	685.10	0.9418	5.0052
−150	2.384	0.25042	200.00	688.00	1.0000	4.9627
−148	2.720	0.22157	207.23	690.81	1.0575	4.9215
−146	3.090	0.19674	214.51	693.50	1.1145	4.8817
−144	3.496	0.17528	221.84	696.09	1.1709	4.8430
−142	3.941	0.15665	229.23	698.56	1.2268	4.8054
−140	4.426	0.14041	236.68	700.91	1.2823	4.7688
−138	4.953	0.12619	244.19	703.12	1.3372	4.7330
−136	5.526	0.11371	251.77	705.20	1.3918	4.6979
−134	6.145	0.10270	259.42	707.14	1.4460	4.6635
−132	6.813	0.09297	267.15	708.93	1.4999	4.6297
−130	7.532	0.08434	274.90	710.56	1.5531	4.5965
−128	8.304	0.07664	282.79	712.02	1.6064	4.5635
−126	9.133	0.06977	290.76	713.31	1.6594	4.5309
−124	10.019	0.06361	298.84	714.41	1.7122	4.4985
−122	10.966	0.05808	307.01	715.31	1.7649	4.4661
−120	11.975	0.05309	315.30	715.99	1.8175	4.4338
−118	13.049	0.04859	323.71	716.45	1.8700	4.4014
−116	14.191	0.04451	332.25	716.67	1.9226	4.3688
−114	15.403	0.04080	340.93	716.62	1.9752	4.3359
−112	16.687	0.03742	349.77	716.29	2.0281	4.3025
−110	18.046	0.03434	358.78	715.66	2.0811	4.2685
−108	19.483	0.03152	367.99	714.68	2.1345	4.2338
−106	21.001	0.02892	377.41	713.33	2.1884	4.1981
−104	22.602	0.02653	387.08	711.57	2.2429	4.1612
−102	24.289	0.02433	397.02	709.34	2.2981	4.1229
−100	26.067	0.02228	407.30	706.57	2.3544	4.0828
−98	27.937	0.02037	417.96	703.17	2.4120	4.0404
−96	29.904	0.01859	429.09	699.04	2.4714	3.9952
−94	31.972	0.01690	440.82	694.00	2.5331	3.9463
−92	34.146	0.01531	453.31	687.80	2.5981	3.8925
−90	36.430	0.01376	466.86	680.06	2.6677	3.8318
−88	38.831	0.01225	481.99	670.06	2.7448	3.7606
−86	41.357	0.01068	499.88	656.20	2.8354	3.6706
−84	44.020	0.00886	524.21	633.35	2.9583	3.5354

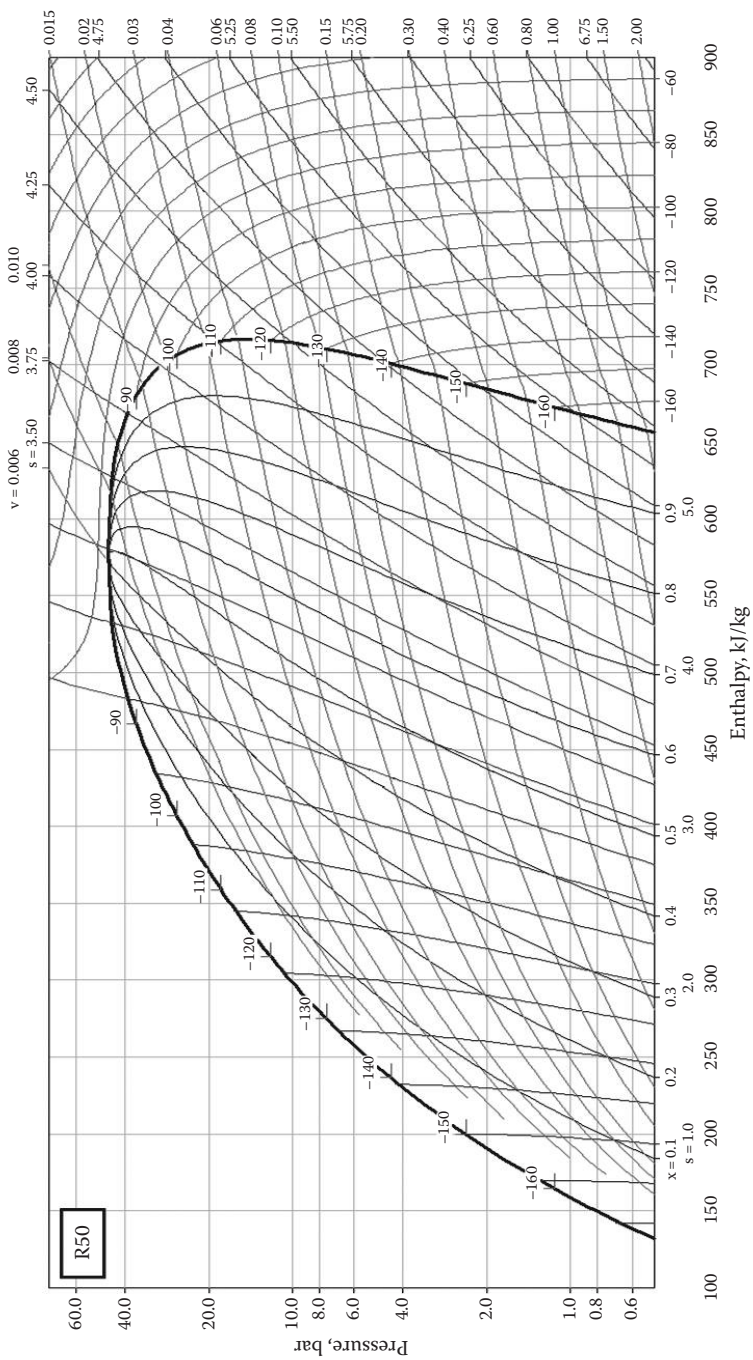

FIGURE 7.12
Pressure–enthalpy diagram for refrigerant R50.

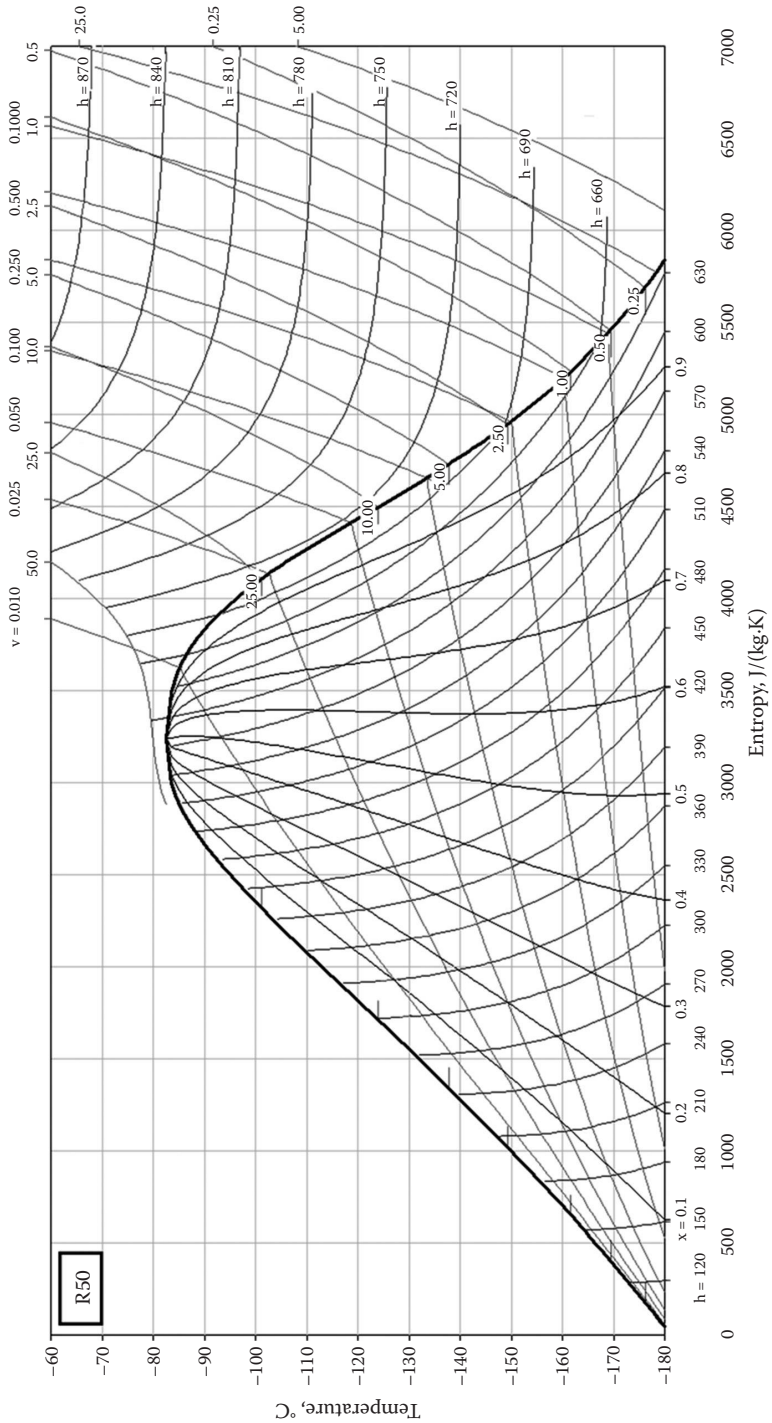

FIGURE 7.13
Temperature–entropy diagram for refrigerant R50.

TABLE 7.8

Properties of Superheated Vapour for R50

t, °C	s, kJ/kgK	h, kJ/kg	v, m^3/kg	ρ, kg/m^3
State Points at P = 1.01 bar				
Saturated Liquid at Bubble Point				
−161.56	0.6545	159.13	0.0024	421.94
Saturated Vapour at Dew Point				
−161.56	5.2322	669.98	0.5524	1.81
Superheated Vapour				
−160	5.2628	673.41	0.5609	1.78
−150	5.4475	695.22	0.6154	1.62
−140	5.6154	716.72	0.6691	1.49
−130	5.7697	738.02	0.7222	1.38
−120	5.9127	759.21	0.7750	1.29
−110	6.0462	780.31	0.8275	1.21
−100	6.1715	801.37	0.8799	1.14
−90	6.2896	822.41	0.9320	1.07
−80	6.4014	843.44	0.9841	1.02
−70	6.5076	864.49	1.0361	0.97
−60	6.6090	885.58	1.0880	0.92
−50	6.7059	906.72	1.1398	0.88
−40	6.7989	927.94	1.1916	0.84
−30	6.8884	949.25	1.2433	0.80
−20	6.9748	970.68	1.2950	0.77
−10	7.0584	992.25	1.3467	0.74
0	7.1394	1013.97	1.3983	0.72
State Points at P = 5 bar				
Saturated Liquid at Bubble Point				
−137.83	1.3419	244.83	0.0026	386.10
Saturated Vapour at Dew Point				
−137.83	4.7300	703.30	0.1251	7.99
Superheated Vapour				
−130	4.8672	722.40	0.1351	7.40
−120	5.0256	745.86	0.1472	6.79
−110	5.1698	768.65	0.1590	6.29
−100	5.3029	791.02	0.1706	5.86
−90	5.4269	813.11	0.1819	5.50
−80	5.5434	835.01	0.1931	5.18
−70	5.6533	856.79	0.2041	4.90
−60	5.7576	878.50	0.2151	4.65
−50	5.8571	900.19	0.2260	4.42
−40	5.9522	921.89	0.2369	4.22
−30	6.0435	943.64	0.2477	4.04

(Continued)

TABLE 7.8 ***(Continued)***

Properties of Superheated Vapour for R50

t, °C	s, kJ/kgK	h, kJ/kg	v, m³/kg	ρ, kg/m³
–20	6.1315	965.45	0.2584	3.87
–10	6.2164	987.37	0.2691	3.72
0	6.2986	1009.42	0.2798	3.57
10	6.3784	1031.61	0.2904	3.44
State Points at P = 10 bar				
Saturated Liquid at Bubble Point				
–124.04	1.7111	298.67	0.0028	359.71
Saturated Vapour at Dew Point				
–124.04	4.4991	714.39	0.0637	15.69
Superheated Vapour				
–120	4.5737	725.65	0.0668	14.98
–110	4.7396	751.88	0.0738	13.55
–100	4.8869	776.64	0.0804	12.44
–90	5.0209	800.49	0.0867	11.54
–80	5.1446	823.76	0.0928	10.78
–70	5.2601	846.64	0.0987	10.13
–60	5.3689	869.27	0.1045	9.57
–50	5.4719	891.74	0.1103	9.07
–40	5.5700	914.11	0.1160	8.62
–30	5.6637	936.44	0.1216	8.22
–20	5.7538	958.78	0.1272	7.86
–10	5.8405	981.17	0.1327	7.53
0	5.9243	1003.63	0.1382	7.23
10	6.0055	1026.21	0.1437	6.96
20	6.0844	1048.94	0.1491	6.70
State Points at P = 15 bar				
Saturated Liquid at Bubble Point				
–114.65	1.9581	338.08	0.0029	359.71
Saturated Vapour at Dew Point				
–114.65	4.3467	716.67	0.0420	23.83
Superheated Vapour				
–110	4.4381	731.37	0.0447	22.38
–100	4.6090	760.08	0.0499	20.03
–90	4.7573	786.49	0.0547	18.29
–80	4.8908	811.60	0.0592	16.90
–70	5.0133	835.87	0.0635	15.76
–60	5.1273	859.60	0.0676	14.79
–50	5.2345	882.96	0.0717	13.95
–40	5.3359	906.09	0.0757	13.22
–30	5.4324	929.07	0.0796	12.57

(Continued)

TABLE 7.8 ***(Continued)***

Properties of Superheated Vapour for R50

t, °C	s, kJ/kgK	h, kJ/kg	v, m³/kg	ρ, kg/m³
−20	5.5247	951.97	0.0834	11.99
−10	5.6133	974.85	0.0872	11.46
0	5.6988	997.77	0.0910	10.99
10	5.7814	1020.75	0.0948	10.55
20	5.8616	1043.84	0.0985	10.15
30	5.9395	1067.07	0.1022	9.78
40	6.0154	1090.46	0.1059	9.45
State Points at P = 20 bar				
Saturated Liquid at Bubble Point				
−107.31	2.1531	371.23	0.0031	322.58
Saturated Vapour at Dew Point				
−107.31	4.2216	714.26	0.0306	32.69
Superheated Vapour				
−100	4.3743	740.13	0.0342	29.23
−90	4.5457	770.64	0.0384	26.02
−80	4.6928	798.30	0.0422	23.68
−70	4.8243	824.35	0.0457	21.86
−60	4.9447	849.41	0.0491	20.37
−50	5.0567	873.83	0.0523	19.11
−40	5.1618	897.81	0.0555	18.03
−30	5.2613	921.50	0.0585	17.09
−20	5.3561	945.02	0.0615	16.25
−10	5.4469	968.44	0.0645	15.50
0	5.5341	991.82	0.0674	14.83
10	5.6182	1015.23	0.0703	14.22
20	5.6997	1038.70	0.0732	13.66
30	5.7788	1062.27	0.0760	13.15
40	5.8557	1085.98	0.0788	12.68
50	5.9307	1109.85	0.0816	12.25
State Points at P = 25 bar				
Saturated Liquid at Bubble Point				
−101.19	2.3209	401.15	0.0033	304.88
Saturated Vapour at Dew Point				
−101.19	4.1069	708.28	0.0235	42.59
Superheated Vapour				
−100	4.1387	713.77	0.0241	41.50
−90	4.3538	752.03	0.0284	35.21
−80	4.5212	783.51	0.0319	31.34
−70	4.6648	811.94	0.0350	28.55
−60	4.7932	838.66	0.0379	26.36

(Continued)

TABLE 7.8 ***(Continued)***

Properties of Superheated Vapour for R50

t, °C	s, kJ/kgK	h, kJ/kg	v, m³/kg	ρ, kg/m³
–50	4.9107	864.30	0.0407	24.58
–40	5.0202	889.26	0.0433	23.08
–30	5.1230	913.75	0.0459	21.79
–20	5.2205	937.93	0.0484	20.66
–10	5.3135	961.92	0.0509	19.66
0	5.4025	985.81	0.0533	18.77
10	5.4883	1009.65	0.0556	17.97
20	5.5711	1033.51	0.0580	17.24
30	5.6514	1057.44	0.0603	16.58
40	5.7294	1081.47	0.0626	15.97
50	5.8053	1105.64	0.0649	15.41
State Points at P = 30 bar				
Saturated Liquid at Bubble Point				
–95.91	2.4743	429.63	0.0035	287.36
Saturated Vapour at Dew Point				
–95.91	3.9930	698.82	0.0185	54.02
Superheated Vapour				
–90	4.1595	728.79	0.0213	46.91
–80	4.3612	766.69	0.0249	40.22
–70	4.5214	798.42	0.0278	35.97
–60	4.6599	827.23	0.0304	32.85
–50	4.7843	854.36	0.0329	30.40
–40	4.8985	880.42	0.0352	28.39
–30	5.0051	905.79	0.0375	26.69
–20	5.1055	930.70	0.0396	25.23
–10	5.2008	955.30	0.0418	23.95
0	5.2919	979.71	0.0438	22.82
10	5.3793	1004.02	0.0459	21.80
20	5.4635	1028.29	0.0479	20.89
30	5.5450	1052.59	0.0498	20.06
40	5.6241	1076.95	0.0518	19.30
50	5.7010	1101.42	0.0537	18.61
60	5.7760	1126.04	0.0557	17.97
State Points at P = 35 bar				
Saturated Liquid at Bubble Point				
–91.24	2.6239	458.31	0.0037	268.10
Saturated Vapour at Dew Point				
–91.24	3.8705	685.07	0.0147	67.98
Superheated Vapour				
–90	3.9249	695.00	0.0155	64.54
–80	4.2012	746.85	0.0196	50.96

(Continued)

TABLE 7.8 ***(Continued)***

Properties of Superheated Vapour for R50

t, °C	s, kJ/kgK	h, kJ/kg	v, m³/kg	ρ, kg/m³
–70	4.3863	783.50	0.0226	44.34
–60	4.5379	815.03	0.0250	39.92
–50	4.6704	843.93	0.0273	36.61
–40	4.7904	871.28	0.0294	33.98
–30	4.9010	897.64	0.0314	31.81
–20	5.0046	923.33	0.0334	29.96
–10	5.1025	948.59	0.0353	28.36
0	5.1956	973.56	0.0371	26.96
10	5.2847	998.34	0.0389	25.72
20	5.3704	1023.04	0.0406	24.60
30	5.4532	1047.71	0.0424	23.60
40	5.5334	1072.41	0.0441	22.68
50	5.6113	1097.19	0.0458	21.85
60	5.6871	1122.09	0.0474	21.08
70	5.7612	1147.14	0.0491	20.37
State Points at P = 40 bar				
Saturated Liquid at Bubble Point				
–87.06	2.7850	489.92	0.0041	243.90
Saturated Vapour at Dew Point				
–87.06	3.7216	664.21	0.0115	86.81
Superheated Vapour				
–80	4.0268	721.90	0.0154	64.94
–70	4.2534	766.72	0.0185	54.01
–60	4.4225	801.90	0.0210	47.71
–50	4.5651	832.98	0.0231	43.28
–40	4.6915	861.82	0.0251	39.89
–30	4.8069	889.28	0.0269	37.15
–20	4.9138	915.83	0.0287	34.86
–10	5.0144	941.78	0.0304	32.91
0	5.1097	967.33	0.0320	31.21
10	5.2007	992.62	0.0337	29.72
20	5.2879	1017.76	0.0352	28.38
30	5.3720	1042.82	0.0368	27.19
40	5.4533	1067.87	0.0383	26.11
50	5.5321	1092.96	0.0398	25.12
60	5.6089	1118.14	0.0413	24.22
70	5.6837	1143.45	0.0428	23.38
80	5.7569	1168.92	0.0442	22.62
90	5.8285	1194.57	0.0457	21.90
State Points at P = 44 bar				
Saturated Liquid at Bubble Point				
–84.01	2.9572	523.98	0.0047	215.05

(Continued)

TABLE 7.8 ***(Continued)***

Properties of Superheated Vapour for R50

t, °C	s, kJ/kgK	h, kJ/kg	v, m³/kg	ρ, kg/m³
Saturated Vapour at Dew Point				
–84.01	3.5367	633.59	0.0089	112.61
Superheated Vapour				
–80	3.8557	694.39	0.0123	81.15
–70	4.1446	751.48	0.0159	63.06
–60	4.3327	790.60	0.0183	54.57
–50	4.4850	823.80	0.0204	48.99
–40	4.6174	854.00	0.0223	44.86
–30	4.7369	882.43	0.0240	41.60
–20	4.8469	909.73	0.0257	38.91
–10	4.9497	936.27	0.0273	36.65
0	5.0468	962.31	0.0288	34.69
10	5.1393	988.02	0.0303	32.98
20	5.2278	1013.51	0.0318	31.46
30	5.3129	1038.89	0.0332	30.10
40	5.3951	1064.22	0.0346	28.88
50	5.4748	1089.57	0.0360	27.77
60	5.5523	1114.98	0.0374	26.75
70	5.6277	1140.51	0.0387	25.82
80	5.7014	1166.17	0.0401	24.96
90	5.7736	1192.00	0.0414	24.16
100	5.8443	1218.03	0.0427	23.42
110	5.9137	1244.27	0.0440	22.72
120	5.9819	1270.75	0.0453	22.08
130	6.0490	1297.48	0.0466	21.47
140	6.1152	1324.48	0.0479	20.90
150	6.1804	1351.75	0.0491	20.36

7.4.3 Refrigerant R134a

This fluid is from ethane series with chemical name 1,1,1,2-tetrafluoroethane and formula CH_2FCF_3 (see Table 7.9, Figure 7.14, Figure 7.15, and Table 7.10).

Critical point: t_c = 101.1°C and p_c = 40.67 bar

TABLE 7.9

Saturated Liquid and Saturated Vapour Properties for R134a

t, °C	p, bar	v_{vap}, m³/kg	h_{liq}, kJ/kg	h_{vap}, kJ/kg	s_{liq}, kJ/kgK	s_{vap}, kJ/kgK
–50	0.299	0.59570	138.42	366.54	0.7524	1.7747
–48	0.335	0.53549	140.70	367.81	0.7626	1.7713
–46	0.375	0.48239	142.99	369.07	0.7727	1.7680
–44	0.418	0.43545	145.30	370.33	0.7828	1.7648

(Continued)

TABLE 7.9 ***(Continued)***

Saturated Liquid and Saturated Vapour Properties for R134a

t, °C	p, bar	v_{vap}, m^3/kg	h_{liq}, kJ/kg	h_{vap}, kJ/kg	s_{liq}, kJ/kgK	s_{vap}, kJ/kgK
–42	0.465	0.39385	147.63	371.59	0.7929	1.7618
–40	0.516	0.35692	149.97	372.85	0.8030	1.7589
–38	0.572	0.32405	152.33	374.11	0.8130	1.7562
–36	0.633	0.29474	154.70	375.37	0.8231	1.7535
–34	0.699	0.26855	157.09	376.62	0.8331	1.7510
–32	0.770	0.24511	159.49	377.87	0.8431	1.7486
–30	0.847	0.22408	161.91	379.11	0.8530	1.7463
–28	0.930	0.20518	164.35	380.35	0.8630	1.7441
–26	1.020	0.18817	166.80	381.59	0.8729	1.7420
–24	1.116	0.17282	169.26	382.82	0.8828	1.7400
–22	1.219	0.15896	171.74	384.05	0.8927	1.7380
–20	1.330	0.14641	174.24	385.28	0.9025	1.7362
–18	1.448	0.13504	176.75	386.50	0.9124	1.7345
–16	1.575	0.12471	179.27	387.71	0.9222	1.7328
–14	1.710	0.11533	181.81	388.92	0.9320	1.7312
–12	1.854	0.10678	184.36	390.12	0.9418	1.7297
–10	2.007	0.09898	186.93	391.32	0.9515	1.7282
–8	2.170	0.09186	189.52	392.51	0.9613	1.7269
–6	2.344	0.08535	192.12	393.70	0.9710	1.7255
–4	2.527	0.07938	194.73	394.87	0.9807	1.7243
–2	2.722	0.07391	197.36	396.04	0.9903	1.7231
0	2.928	0.06889	200.00	397.20	1.0000	1.7220
2	3.146	0.06427	202.66	398.36	1.0096	1.7209
4	3.376	0.06001	205.33	399.50	1.0192	1.7199
6	3.619	0.05609	208.02	400.64	1.0288	1.7189
8	3.876	0.05248	210.72	401.77	1.0384	1.7179
10	4.145	0.04913	213.44	402.89	1.0480	1.7170
12	4.429	0.04604	216.17	404.00	1.0575	1.7162
14	4.728	0.04318	218.92	405.10	1.0670	1.7154
16	5.042	0.04052	221.68	406.18	1.0765	1.7146
18	5.371	0.03806	224.44	407.26	1.0859	1.7139
20	5.716	0.03577	227.23	408.33	1.0954	1.7132
22	6.078	0.03365	230.05	409.38	1.1049	1.7125
24	6.457	0.03166	232.87	410.42	1.1143	1.7118
26	6.853	0.02982	235.72	411.45	1.1237	1.7112
28	7.267	0.02809	238.58	412.47	1.1332	1.7106
30	7.701	0.02648	241.46	413.47	1.1426	1.7100
32	8.153	0.02498	244.36	414.45	1.1520	1.7094

(Continued)

TABLE 7.9 ***(Continued)***

Saturated Liquid and Saturated Vapour Properties for R134a

t, °C	p, bar	v_{vap}, m^3/kg	h_{liq}, kJ/kg	h_{vap}, kJ/kg	s_{liq}, kJ/kgK	s_{vap}, kJ/kgK
34	8.625	0.02357	247.28	415.42	1.1614	1.7088
36	9.117	0.02225	250.22	416.37	1.1708	1.7082
38	9.630	0.02102	253.18	417.30	1.1802	1.7077
40	10.164	0.01986	256.16	418.21	1.1896	1.7071
42	10.720	0.01877	259.16	419.11	1.1990	1.7065
44	11.299	0.01774	262.19	419.98	1.2084	1.7059
46	11.901	0.01678	265.24	420.83	1.2178	1.7053
48	12.526	0.01588	268.32	421.65	1.2273	1.7047
50	13.176	0.01502	271.42	422.44	1.2367	1.7041
52	13.851	0.01421	274.55	423.21	1.2462	1.7034
54	14.552	0.01345	277.71	423.95	1.2557	1.7027
56	15.278	0.01273	280.90	424.66	1.2652	1.7019
58	16.032	0.01205	284.13	425.32	1.2747	1.7011
60	16.813	0.01141	287.39	425.96	1.2843	1.7003
62	17.623	0.01079	290.68	426.54	1.2940	1.6994
64	18.462	0.01021	294.02	427.09	1.3037	1.6983
66	19.331	0.00966	297.40	427.58	1.3134	1.6973
68	20.231	0.00914	300.83	428.02	1.3232	1.6961
70	21.162	0.00864	304.31	428.40	1.3331	1.6947
72	22.126	0.00816	307.85	428.71	1.3431	1.6933
74	23.123	0.00770	311.45	428.94	1.3532	1.6917
76	24.154	0.00727	315.11	429.09	1.3635	1.6899
78	25.221	0.00685	318.86	429.15	1.3738	1.6879
80	26.324	0.00645	322.69	429.09	1.3844	1.6857
82	27.465	0.00606	326.60	428.91	1.3951	1.6831
84	28.645	0.00569	330.64	428.56	1.4061	1.6802
86	29.866	0.00532	334.81	428.05	1.4173	1.6769
88	31.128	0.00497	339.14	427.31	1.4289	1.6731
90	32.435	0.00462	343.66	426.29	1.4410	1.6685
92	33.788	0.00427	348.44	424.91	1.4537	1.6631
94	35.190	0.00392	353.56	423.03	1.4672	1.6564
96	36.644	0.00356	359.21	420.38	1.4820	1.6477
98	38.158	0.00317	365.77	416.41	1.4992	1.6356
100	39.742	0.00268	374.70	409.10	1.5225	1.6147

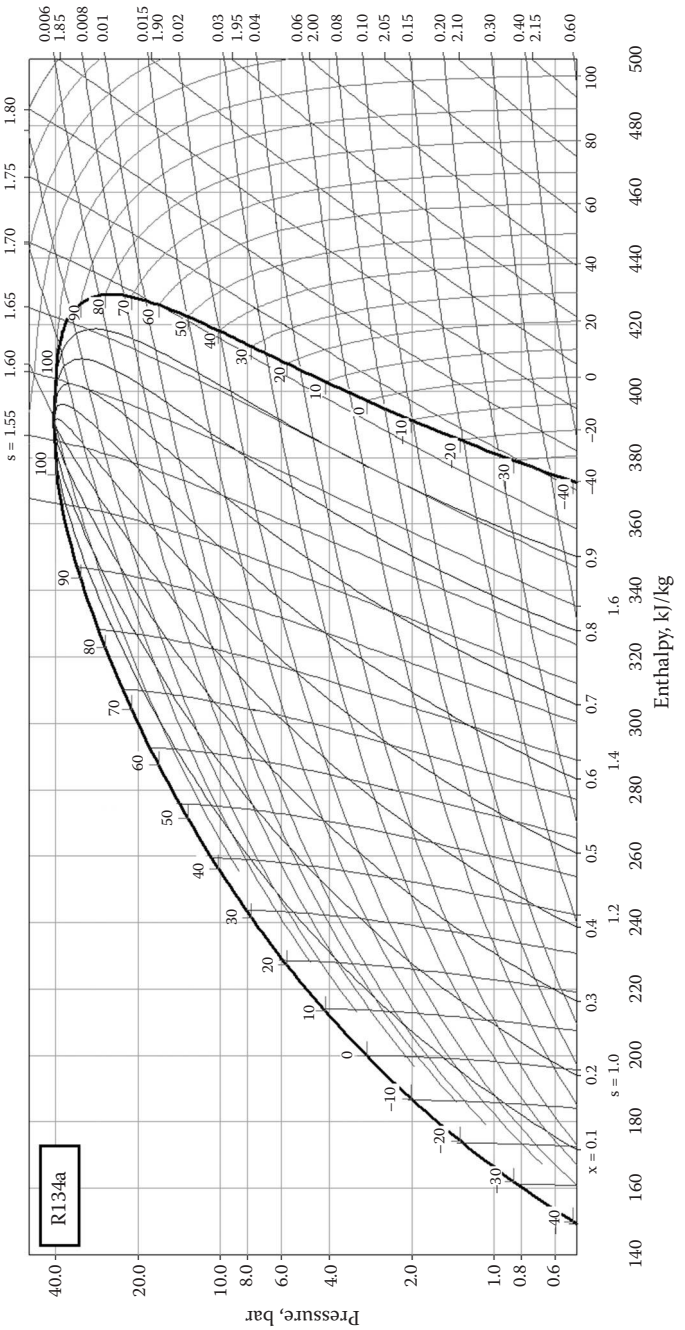

FIGURE 7.14
Pressure–enthalpy diagram for refrigerant R134a.

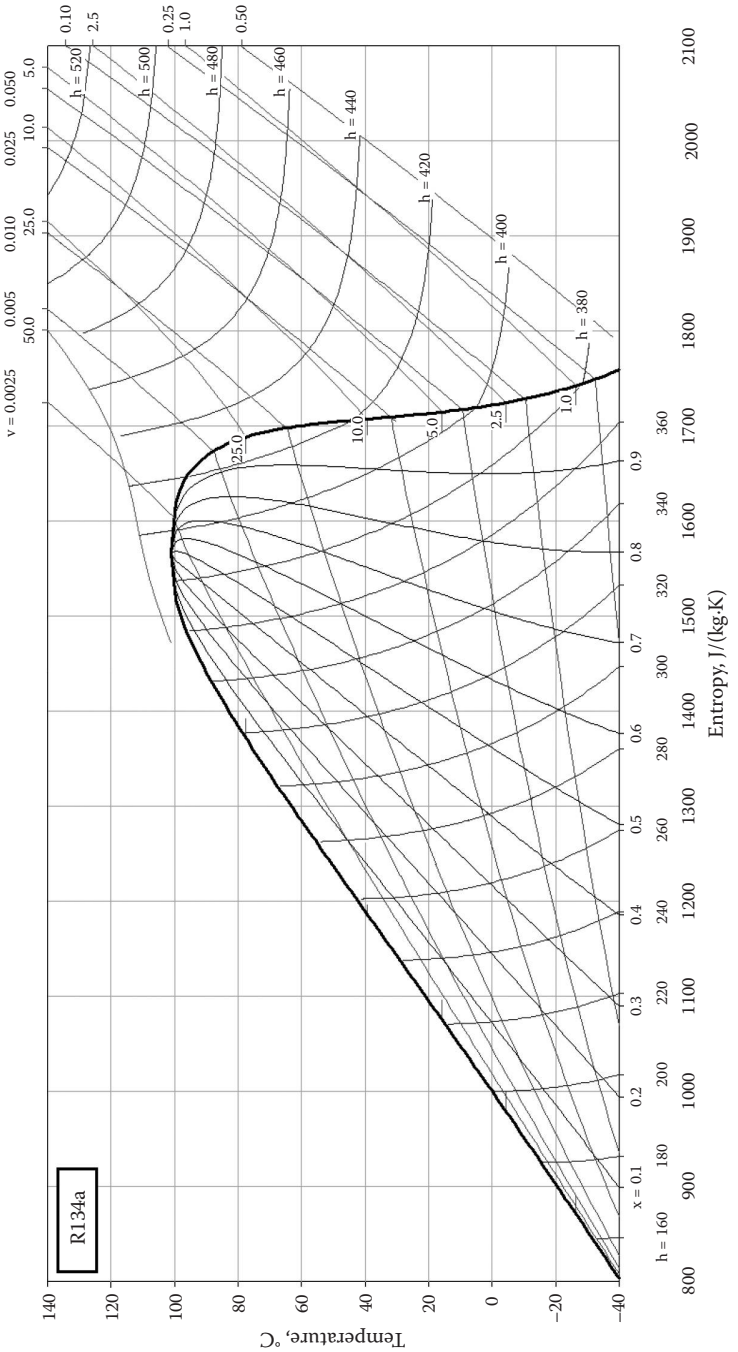

FIGURE 7.15
Temperature–entropy diagram for refrigerant R134a.

TABLE 7.10

Properties of Superheated Vapour for R134a

t, °C	s, kJ/kgK	h, kJ/kg	v, m³/kg	ρ, kg/m³
State Points at P = 1.01 bar				
Saturated Liquid at Bubble Point				
−26.21	0.8718	166.53	0.0007	1369.86
Saturated Vapour at Dew Point				
−26.21	1.7422	381.46	0.1899	5.27
Superheated Vapour				
−20	1.7623	386.47	0.1957	5.11
−10	1.7939	394.64	0.2047	4.88
0	1.8248	402.94	0.2137	4.68
10	1.8552	411.38	0.2224	4.50
20	1.8850	419.97	0.2311	4.33
30	1.9143	428.71	0.2397	4.17
40	1.9432	437.61	0.2482	4.03
50	1.9717	446.67	0.2567	3.90
60	1.9998	455.90	0.2651	3.77
70	2.0275	465.28	0.2735	3.66
80	2.0550	474.82	0.2818	3.55
90	2.0821	484.53	0.2901	3.45
100	2.1089	494.39	0.2984	3.35
110	2.1354	504.42	0.3066	3.26
120	2.1616	514.59	0.3148	3.18
130	2.1875	524.92	0.3231	3.10
State Points at P = 5 bar				
Saturated Liquid at Bubble Point				
15.74	1.0753	221.32	0.0008	1234.57
Saturated Vapour at Dew Point				
15.74	1.7147	406.04	0.0409	24.47
Superheated Vapour				
20	1.7294	410.31	0.0419	23.88
30	1.7627	420.25	0.0442	22.65
40	1.7948	430.13	0.0463	21.58
50	1.8258	440.01	0.0484	20.66
60	1.8560	449.92	0.0504	19.83
70	1.8855	459.89	0.0524	19.09
80	1.9144	469.93	0.0543	18.41
90	1.9427	480.07	0.0562	17.79
100	1.9705	490.30	0.0580	17.23
110	1.9978	500.65	0.0599	16.70
120	2.0248	511.11	0.0617	16.21
130	2.0514	521.69	0.0635	15.76

(Continued)

TABLE 7.10 ***(Continued)***

Properties of Superheated Vapour for R134a

t, °C	s, kJ/kgK	h, kJ/kg	v, m³/kg	ρ, kg/m³
140	2.0776	532.39	0.0652	15.33
150	2.1035	543.21	0.0670	14.92
160	2.1290	554.15	0.0688	14.55
State Points at P = 10 bar				
Saturated Liquid at Bubble Point				
39.39	1.1868	255.26	0.0009	1149.43
Saturated Vapour at Dew Point				
39.39	1.7073	417.94	0.0202	49.50
Superheated Vapour				
40	1.7095	418.65	0.0203	49.28
50	1.7457	430.16	0.0217	46.06
60	1.7798	441.33	0.0230	43.45
70	1.8122	452.30	0.0242	41.28
80	1.8434	463.17	0.0254	39.40
90	1.8736	473.98	0.0265	37.76
100	1.9030	484.79	0.0275	36.30
110	1.9316	495.62	0.0286	34.99
120	1.9596	506.49	0.0296	33.80
130	1.9871	517.43	0.0306	32.71
140	2.0141	528.43	0.0315	31.70
150	2.0406	539.53	0.0325	30.77
160	2.0667	550.71	0.0334	29.91
170	2.0925	561.99	0.0344	29.10
180	2.1179	573.37	0.0353	28.34
190	2.1429	584.85	0.0362	27.63
State Points at P = 15 bar				
Saturated Liquid at Bubble Point				
55.24	1.2616	279.69	0.0009	1075.27
Saturated Vapour at Dew Point				
55.24	1.7022	424.39	0.0130	76.92
Superheated Vapour				
60	1.7213	430.71	0.0136	73.72
70	1.7587	443.34	0.0146	68.34
80	1.7934	455.42	0.0156	64.14
90	1.8262	467.17	0.0165	60.70
100	1.8576	478.72	0.0173	57.79
110	1.8878	490.16	0.0181	55.28
120	1.9171	501.54	0.0188	53.06
130	1.9457	512.90	0.0196	51.09
140	1.9735	524.27	0.0203	49.30

(Continued)

TABLE 7.10 ***(Continued)***

Properties of Superheated Vapour for R134a

t, °C	s, kJ/kgK	h, kJ/kg	v, m³/kg	ρ, kg/m³
150	2.0008	535.68	0.0210	47.68
160	2.0276	547.13	0.0216	46.19
170	2.0539	558.65	0.0223	44.82
180	2.0797	570.23	0.0230	43.55
190	2.1052	581.90	0.0236	42.36
200	2.1303	593.65	0.0242	41.25
210	2.1550	605.48	0.0249	40.21
State Points at P = 20 bar				
Saturated Liquid at Bubble Point				
67.49	1.3208	299.96	0.0010	1010.10
Saturated Vapour at Dew Point				
67.49	1.6964	427.91	0.0093	107.87
Superheated Vapour				
70	1.7077	431.78	0.0095	104.74
80	1.7488	446.09	0.0105	95.03
90	1.7857	459.30	0.0114	88.05
100	1.8200	471.91	0.0121	82.62
110	1.8523	484.16	0.0128	78.17
120	1.8833	496.18	0.0134	74.43
130	1.9132	508.06	0.0140	71.19
140	1.9421	519.86	0.0146	68.35
150	1.9702	531.63	0.0152	65.81
160	1.9977	543.39	0.0157	63.52
170	2.0246	555.17	0.0163	61.44
180	2.0510	566.99	0.0168	59.53
190	2.0769	578.86	0.0173	57.77
200	2.1023	590.79	0.0178	56.14
210	2.1274	602.78	0.0183	54.62
220	2.1521	614.85	0.0188	53.20
State Points at P = 25 bar				
Saturated Liquid at Bubble Point				
77.59	1.3717	318.08	0.0011	943.40
Saturated Vapour at Dew Point				
77.59	1.6883	429.14	0.0069	144.30
Superheated Vapour				
80	1.7009	433.56	0.0072	138.74
90	1.7460	449.71	0.0081	122.84
100	1.7849	464.03	0.0089	112.42
110	1.8204	477.44	0.0096	104.67
120	1.8535	490.31	0.0102	98.52

(Continued)

TABLE 7.10 ***(Continued)***

Properties of Superheated Vapour for R134a

t, °C	s, kJ/kgK	h, kJ/kg	v, m³/kg	ρ, kg/m³
130	1.8850	502.85	0.0107	93.43
140	1.9152	515.17	0.0112	89.10
150	1.9444	527.37	0.0117	85.34
160	1.9727	539.49	0.0122	82.02
170	2.0003	551.57	0.0126	79.05
180	2.0272	563.65	0.0131	76.37
190	2.0536	575.74	0.0135	73.92
200	2.0795	587.86	0.0140	71.67
210	2.1050	600.03	0.0144	69.59
220	2.1300	612.25	0.0148	67.66
State Points at P = 30 bar				
Saturated Liquid at Bubble Point				
86.22	1.4185	335.27	0.0011	877.19
Saturated Vapour at Dew Point				
86.22	1.6765	427.98	0.0053	189.39
Superheated Vapour				
90	1.7000	436.47	0.0057	174.04
100	1.7488	454.41	0.0066	150.61
110	1.7892	469.69	0.0073	136.44
120	1.8255	483.77	0.0079	126.28
130	1.8592	497.17	0.0084	118.39
140	1.8910	510.15	0.0089	111.96
150	1.9213	522.86	0.0094	106.54
160	1.9506	535.39	0.0098	101.87
170	1.9790	547.82	0.0102	97.77
180	2.0066	560.19	0.0106	94.12
190	2.0335	572.53	0.0110	90.85
200	2.0599	584.86	0.0114	87.87
210	2.0857	597.22	0.0117	85.14
220	2.1111	609.60	0.0121	82.63
230	2.1360	622.03	0.0125	80.30
240	2.1606	634.50	0.0128	78.14
State Points at P = 35 bar				
Saturated Liquid at Bubble Point				
93.73	1.4653	352.85	0.0013	787.40
Saturated Vapour at Dew Point				
93.73	1.6573	423.31	0.0040	251.89
Superheated Vapour				
100	1.7057	441.18	0.0048	207.04
110	1.7564	460.35	0.0057	176.83

(Continued)

TABLE 7.10 ***(Continued)***

Properties of Superheated Vapour for R134a

t, °C	s, kJ/kgK	h, kJ/kg	v, m³/kg	ρ, kg/m³
120	1.7976	476.33	0.0063	159.26
130	1.8342	490.92	0.0068	146.89
140	1.8681	504.73	0.0073	137.39
150	1.9000	518.07	0.0077	129.70
160	1.9304	531.10	0.0081	123.26
170	1.9597	543.92	0.0085	117.73
180	1.9880	556.61	0.0089	112.90
190	2.0155	569.23	0.0092	108.62
200	2.0424	581.79	0.0095	104.78
210	2.0686	594.35	0.0099	101.30
220	2.0944	606.91	0.0102	98.11
230	2.1196	619.49	0.0105	95.19
240	2.1444	632.10	0.0108	92.48
State Points at P = 40 bar				
Saturated Liquid at Bubble Point				
100.32	1.5279	376.74	0.0016	632.91
Saturated Vapour at Dew Point				
100.32	1.6092	407.10	0.0026	389.11
Superheated Vapour				
110	1.7178	448.03	0.0043	234.25
120	1.7682	467.57	0.0050	200.24
130	1.8093	483.93	0.0055	180.19
140	1.8458	498.85	0.0060	166.05
150	1.8796	512.96	0.0064	155.19
160	1.9114	526.57	0.0068	146.42
170	1.9417	539.85	0.0072	139.09
180	1.9708	552.91	0.0075	132.80
190	1.9990	565.83	0.0079	127.30
200	2.0264	578.66	0.0082	122.44
210	2.0531	591.43	0.0085	118.07
220	2.0793	604.18	0.0088	114.14
230	2.1048	616.92	0.0090	110.53
240	2.1299	629.68	0.0093	107.22
250	2.1546	642.46	0.0096	104.16
260	2.1789	655.28	0.0099	101.32
270	2.2028	668.14	0.0101	98.67

7.4.4 Refrigerant R170

This fluid is from ethane series with chemical name ethane and formula CH_3CH_3 (see Table 7.11, Figure 7.16, Figure 7.17, and Table 7.12).

Critical point: $t_c = 32.73°C$ and $p_c = 50.10$ bar

TABLE 7.11

Saturated Liquid and Saturated Vapour Properties for R170

t, °C	p, bar	v_{vap}, m³/kg	h_{liq}, kJ/kg	h_{vap}, kJ/kg	s_{liq}, kJ/kgK	s_{vap}, kJ/kgK
−120	0.125	3.35204	−129.82	404.51	−0.5554	2.9336
−118	0.148	2.88022	−124.37	406.91	−0.5200	2.9043
−116	0.173	2.48626	−118.96	409.30	−0.4854	2.8761
−114	0.202	2.15565	−113.58	411.68	−0.4514	2.8490
−112	0.234	1.87686	−108.23	414.06	−0.4180	2.8230
−110	0.271	1.64067	−102.90	416.42	−0.3852	2.7979
−108	0.312	1.43970	−97.61	418.78	−0.3530	2.7738
−106	0.358	1.26795	−92.33	421.12	−0.3213	2.7505
−104	0.409	1.12060	−87.08	423.45	−0.2901	2.7281
−102	0.466	0.99367	−81.85	425.76	−0.2594	2.7065
−100	0.529	0.88392	−76.63	428.06	−0.2292	2.6856
−98	0.599	0.78869	−71.43	430.35	−0.1994	2.6655
−96	0.675	0.70577	−66.24	432.62	−0.1700	2.6460
−94	0.759	0.63334	−61.05	434.87	−0.1410	2.6272
−92	0.851	0.56985	−55.87	437.11	−0.1123	2.6091
−90	0.951	0.51404	−50.69	439.32	−0.0840	2.5915
−88	1.060	0.46483	−45.52	441.52	−0.0560	2.5745
−86	1.178	0.42132	−40.34	443.70	−0.0283	2.5581
−84	1.306	0.38274	−35.16	445.85	−0.0009	2.5421
−82	1.445	0.34844	−29.97	447.98	0.0262	2.5267
−80	1.595	0.31788	−24.79	450.09	0.0531	2.5117
−78	1.757	0.29057	−19.59	452.18	0.0797	2.4972
−76	1.930	0.26611	−14.39	454.24	0.1061	2.4831
−74	2.117	0.24415	−9.18	456.28	0.1322	2.4694
−72	2.317	0.22440	−3.96	458.29	0.1580	2.4561
−70	2.530	0.20660	1.27	460.28	0.1837	2.4432
−68	2.758	0.19051	6.50	462.24	0.2091	2.4306
−66	3.002	0.17595	11.75	464.16	0.2343	2.4183
−64	3.261	0.16274	17.00	466.06	0.2593	2.4064
−62	3.536	0.15073	22.27	467.93	0.2841	2.3948
−60	3.828	0.13980	27.54	469.77	0.3087	2.3834
−58	4.138	0.12984	32.83	471.58	0.3331	2.3724
−56	4.467	0.12073	38.12	473.35	0.3573	2.3616
−54	4.814	0.11240	43.43	475.09	0.3813	2.3510
−52	5.181	0.10476	48.75	476.79	0.4051	2.3406
−50	5.568	0.09774	54.08	478.46	0.4288	2.3305
−48	5.976	0.09129	59.43	480.09	0.4523	2.3206
−46	6.405	0.08535	64.79	481.67	0.4756	2.3108
−44	6.857	0.07987	70.18	483.22	0.4988	2.3013

(Continued)

TABLE 7.11 ***(Continued)***

Saturated Liquid and Saturated Vapour Properties for R170

t, °C	p, bar	v_{vap}, m^3/kg	h_{liq}, kJ/kg	h_{vap}, kJ/kg	s_{liq}, kJ/kgK	s_{vap}, kJ/kgK
–42	7.332	0.07482	75.53	484.73	0.5216	2.2919
–40	7.831	0.07014	80.95	486.20	0.5445	2.2826
–38	8.354	0.06581	86.40	487.61	0.5673	2.2735
–36	8.903	0.06179	91.88	488.98	0.5900	2.2645
–34	9.477	0.05806	97.39	490.30	0.6126	2.2556
–32	10.078	0.05459	102.93	491.57	0.6352	2.2468
–30	10.707	0.05136	108.51	492.79	0.6577	2.2381
–28	11.364	0.04835	114.14	493.94	0.6802	2.2294
–26	12.050	0.04554	119.82	495.04	0.7026	2.2208
–24	12.765	0.04291	125.55	496.08	0.7250	2.2122
–22	13.512	0.04046	131.33	497.05	0.7475	2.2037
–20	14.289	0.03816	137.18	497.95	0.7700	2.1951
–18	15.099	0.03600	143.09	498.78	0.7926	2.1866
–16	15.942	0.03398	149.08	499.53	0.8152	2.1780
–14	16.819	0.03208	155.13	500.19	0.8379	2.1694
–12	17.731	0.03029	161.27	500.77	0.8606	2.1607
–10	18.679	0.02861	167.49	501.26	0.8835	2.1519
–8	19.663	0.02702	173.80	501.64	0.9065	2.1430
–6	20.685	0.02552	180.20	501.91	0.9297	2.1339
–4	21.745	0.02410	186.70	502.07	0.9530	2.1247
–2	22.845	0.02276	193.30	502.10	0.9764	2.1153
0	23.986	0.02149	200.00	501.99	1.0000	2.1056
2	25.168	0.02029	206.81	501.72	1.0238	2.0956
4	26.394	0.01914	213.75	501.28	1.0478	2.0853
6	27.664	0.01805	220.81	500.66	1.0720	2.0745
8	28.981	0.01700	228.01	499.81	1.0965	2.0633
10	30.345	0.01600	235.38	498.72	1.1214	2.0514
12	31.759	0.01505	242.92	497.35	1.1466	2.0389
14	33.225	0.01412	250.71	495.64	1.1725	2.0254
16	34.745	0.01323	258.70	493.56	1.1988	2.0110
18	36.322	0.01236	267.08	490.97	1.2262	1.9951
20	37.959	0.01151	275.87	487.79	1.2547	1.9776
22	39.661	0.01067	285.24	483.85	1.2848	1.9578
24	41.431	0.00983	295.40	478.88	1.3174	1.9348
26	43.274	0.00898	306.71	472.44	1.3534	1.9074
28	45.197	0.00808	319.82	463.69	1.3951	1.8728
30	47.206	0.00708	336.06	450.64	1.4466	1.8246
32	49.309	0.00572	360.36	425.24	1.5241	1.7367

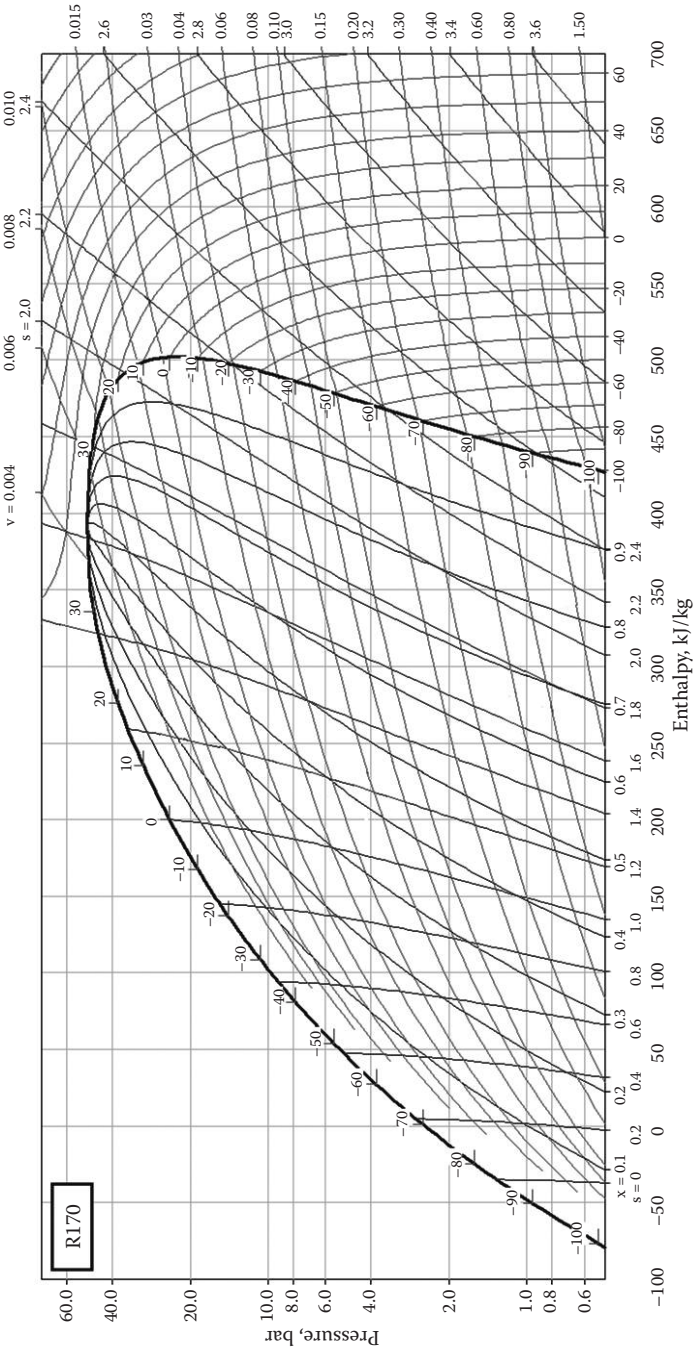

FIGURE 7.16
Pressure–enthalpy diagram for refrigerant R170.

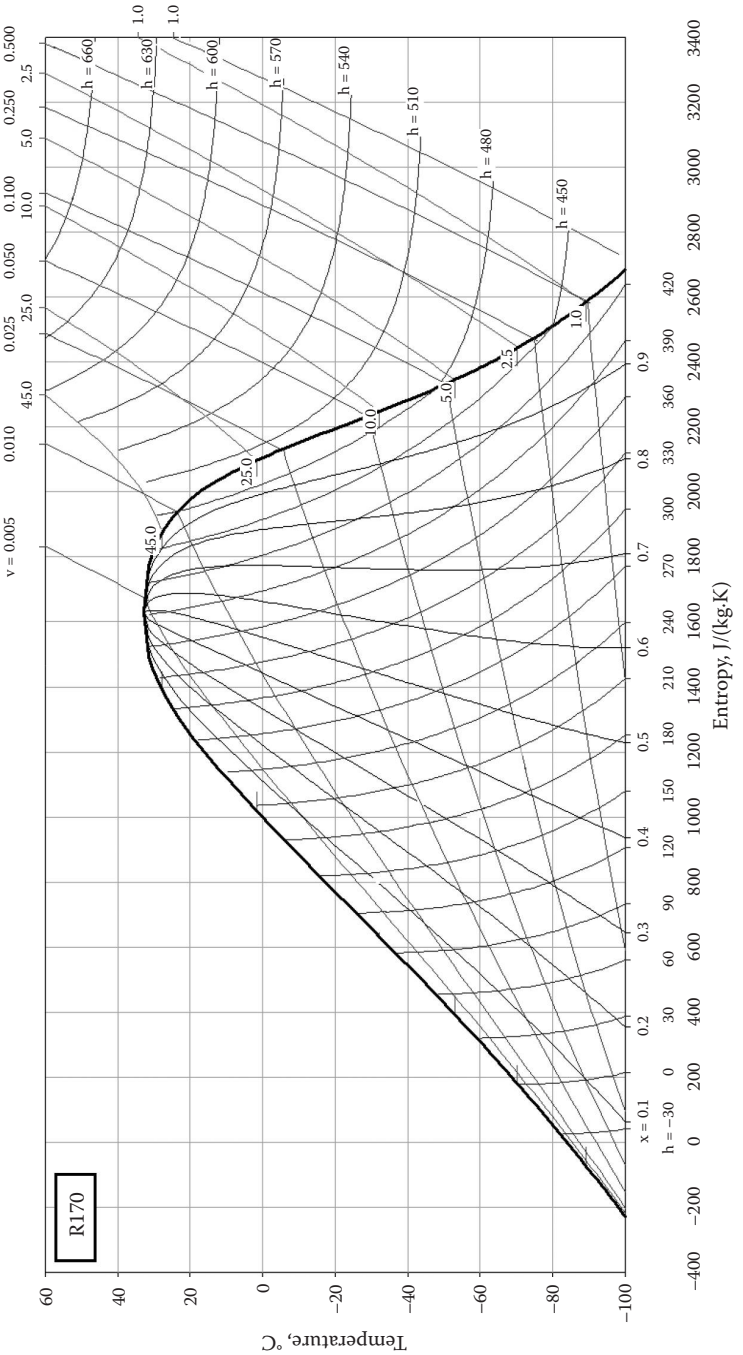

FIGURE 7.17
Temperature–entropy diagram for refrigerant R170.

TABLE 7.12

Properties of Superheated Vapour for R170

t, °C	s, kJ/kgK	h, kJ/kg	v, m³/kg	ρ, kg/m³
State Points at P = 1.01 bar				
Saturated Liquid at Bubble Point				
−88.89	−0.0684	−47.82	0.0018	543.48
Saturated Vapour at Dew Point				
−88.89	2.5820	440.55	0.4860	2.06
Superheated Vapour				
−80	2.6506	453.49	0.5123	1.95
−70	2.7250	468.22	0.5416	1.85
−60	2.7967	483.16	0.5706	1.75
−50	2.8663	498.34	0.5994	1.67
−40	2.9340	513.78	0.6279	1.59
−30	3.0001	529.52	0.6563	1.52
−20	3.0648	545.57	0.6846	1.46
−10	3.1282	561.95	0.7128	1.40
0	3.1906	578.66	0.7408	1.35
10	3.2519	595.72	0.7688	1.30
20	3.3123	613.13	0.7968	1.26
30	3.3720	630.91	0.8246	1.21
40	3.4309	649.06	0.8525	1.17
50	3.4891	667.59	0.8803	1.14
60	3.5467	686.50	0.9080	1.10
70	3.6038	705.80	0.9357	1.07
State Points at P = 5 bar				
Saturated Liquid at Bubble Point				
−52.97	0.3936	46.16	0.0020	495.05
Saturated Vapour at Dew Point				
−52.97	2.3457	475.97	0.1084	9.23
Superheated Vapour				
−50	2.3690	481.15	0.1105	9.05
−40	2.4452	498.52	0.1174	8.52
−30	2.5179	515.84	0.1241	8.06
−20	2.5880	533.22	0.1306	7.66
−10	2.6558	550.73	0.1370	7.30
0	2.7217	568.41	0.1433	6.98
10	2.7861	586.31	0.1495	6.69
20	2.8491	604.46	0.1556	6.43
30	2.9109	622.89	0.1616	6.19
40	2.9717	641.61	0.1676	5.97
50	3.0315	660.65	0.1735	5.76
60	3.0905	680.02	0.1794	5.57

(Continued)

TABLE 7.12 ***(Continued)***

Properties of Superheated Vapour for R170

t, °C	s, kJ/kgK	h, kJ/kg	v, m³/kg	ρ, kg/m³
70	3.1488	699.73	0.1853	5.40
80	3.2064	719.79	0.1911	5.23
90	3.2635	740.21	0.1969	5.08
100	3.3199	760.99	0.2027	4.93
State Points at P = 10 bar				
Saturated Liquid at Bubble Point				
−32.26	0.6323	102.22	0.0022	465.12
Saturated Vapour at Dew Point				
−32.26	2.2479	491.41	0.0550	18.18
Superheated Vapour				
−30	2.2667	495.95	0.0560	17.87
−20	2.3464	515.73	0.0599	16.68
−10	2.4216	535.15	0.0637	15.70
0	2.4934	554.40	0.0673	14.86
10	2.5625	573.61	0.0708	14.12
20	2.6294	592.87	0.0742	13.48
30	2.6944	612.26	0.0775	12.90
40	2.7578	631.81	0.0808	12.38
50	2.8200	651.58	0.0840	11.91
60	2.8809	671.58	0.0871	11.48
70	2.9409	691.86	0.0902	11.08
80	3.0000	712.43	0.0933	10.72
90	3.0583	733.31	0.0964	10.38
100	3.1159	754.50	0.0994	10.06
110	3.1728	776.03	0.1024	9.77
120	3.2292	797.91	0.1054	9.49
State Points at P = 15 bar				
Saturated Liquid at Bubble Point				
−18.24	0.7898	142.38	0.0023	442.48
Saturated Vapour at Dew Point				
−18.24	2.1876	498.68	0.0363	27.59
Superheated Vapour				
−10	2.2587	517.11	0.0388	25.77
0	2.3390	538.62	0.0417	24.00
10	2.4145	559.60	0.0444	22.55
20	2.4862	580.29	0.0469	21.32
30	2.5552	600.85	0.0494	20.26
40	2.6219	621.40	0.0517	19.33
50	2.6867	642.01	0.0540	18.51
60	2.7499	662.75	0.0563	17.76

(Continued)

TABLE 7.12 ***(Continued)***

Properties of Superheated Vapour for R170

t, °C	s, kJ/kgK	h, kJ/kg	v, m³/kg	ρ, kg/m³
70	2.8118	683.67	0.0585	17.09
80	2.8725	704.81	0.0607	16.48
90	2.9322	726.19	0.0628	15.92
100	2.9910	747.83	0.0649	15.40
110	3.0490	769.77	0.0670	14.92
120	3.1063	792.01	0.0691	14.47
130	3.1629	814.56	0.0712	14.05
140	3.2190	837.45	0.0732	13.66
State Points at P = 20 bar				
Saturated Liquid at Bubble Point				
−7.33	0.9143	175.93	0.0024	421.94
Saturated Vapour at Dew Point				
−7.33	2.1400	501.74	0.0265	37.72
Superheated Vapour				
0	2.2082	520.12	0.0285	35.13
10	2.2931	543.74	0.0309	32.39
20	2.3717	566.39	0.0331	30.23
30	2.4458	588.47	0.0351	28.45
40	2.5165	610.25	0.0371	26.94
50	2.5844	631.87	0.0390	25.64
60	2.6503	653.47	0.0408	24.49
70	2.7143	675.12	0.0426	23.47
80	2.7768	696.89	0.0443	22.56
90	2.8381	718.83	0.0460	21.73
100	2.8982	740.97	0.0477	20.97
110	2.9574	763.34	0.0493	20.27
120	3.0157	785.97	0.0510	19.63
130	3.0732	808.88	0.0525	19.03
140	3.1301	832.09	0.0541	18.47
State Points at P = 25 bar				
Saturated Liquid at Bubble Point				
1.72	1.0205	205.85	0.0025	403.23
Saturated Vapour at Dew Point				
1.72	2.0970	501.77	0.0205	48.90
Superheated Vapour				
10	2.1803	525.00	0.0225	44.50
20	2.2693	550.63	0.0246	40.67
30	2.3504	574.82	0.0265	37.75
40	2.4262	598.17	0.0283	35.39
50	2.4982	621.05	0.0299	33.42

(Continued)

TABLE 7.12 ***(Continued)***

Properties of Superheated Vapour for R170

t, °C	s, kJ/kgK	h, kJ/kg	v, m³/kg	ρ, kg/m³
60	2.5671	643.67	0.0315	31.74
70	2.6336	666.17	0.0330	30.28
80	2.6982	688.66	0.0345	28.99
90	2.7612	711.21	0.0359	27.83
100	2.8228	733.89	0.0373	26.79
110	2.8832	756.74	0.0387	25.84
120	2.9426	779.80	0.0401	24.97
130	3.0011	803.08	0.0414	24.17
140	3.0588	826.63	0.0427	23.43
150	3.1158	850.45	0.0440	22.74
160	3.1721	874.57	0.0453	22.09
State Points at P = 30 bar				
Saturated Liquid at Bubble Point				
9.50	1.1152	205.85	0.0026	384.62
Saturated Vapour at Dew Point				
9.50	2.0545	499.02	0.0163	61.54
Superheated Vapour				
10	2.0606	500.76	0.0164	61.04
20	2.1691	531.99	0.0187	53.54
30	2.2610	559.39	0.0206	48.61
40	2.3438	584.92	0.0223	44.94
50	2.4208	609.39	0.0238	42.02
60	2.4935	633.25	0.0252	39.62
70	2.5630	656.75	0.0266	37.58
80	2.6300	680.07	0.0279	35.81
90	2.6949	703.32	0.0292	34.26
100	2.7581	726.60	0.0304	32.88
110	2.8199	749.96	0.0316	31.63
120	2.8805	773.48	0.0328	30.50
130	2.9400	797.17	0.0339	29.47
140	2.9986	821.08	0.0351	28.52
150	3.0564	845.23	0.0362	27.64
State Points at P = 35 bar				
Saturated Liquid at Bubble Point				
16.33	1.2032	260.04	0.0028	363.64
Saturated Vapour at Dew Point				
16.33	2.0085	493.17	0.0131	76.39
Superheated Vapour				
20	2.0592	507.95	0.0141	71.12
30	2.1711	541.29	0.0162	61.90

(Continued)

TABLE 7.12 ***(Continued)***

Properties of Superheated Vapour for R170

t, °C	s, kJ/kgK	h, kJ/kg	v, m³/kg	ρ, kg/m³
40	2.2646	570.06	0.0179	56.00
50	2.3482	596.68	0.0194	51.67
60	2.4257	622.10	0.0207	48.26
70	2.4988	646.80	0.0220	45.46
80	2.5685	671.08	0.0232	43.10
90	2.6356	695.12	0.0244	41.06
100	2.7007	719.07	0.0255	39.26
110	2.7640	743.00	0.0265	37.68
120	2.8258	767.01	0.0276	36.25
130	2.8864	791.14	0.0286	34.95
140	2.9460	815.43	0.0296	33.77
150	3.0045	839.92	0.0306	32.68
160	3.0623	864.64	0.0316	31.68
State Points at P = 40 bar				
Saturated Liquid at Bubble Point				
22.39	1.2910	287.15	0.0029	341.30
Saturated Vapour at Dew Point				
22.39	1.9536	482.97	0.0105	95.15
Superheated Vapour				
30	2.0723	518.48	0.0126	79.64
40	2.1841	552.92	0.0144	69.32
50	2.2775	582.62	0.0159	62.71
60	2.3612	610.06	0.0173	57.85
70	2.4386	636.23	0.0185	54.04
80	2.5116	661.64	0.0196	50.91
90	2.5812	686.59	0.0207	48.26
100	2.6483	711.28	0.0217	45.98
110	2.7133	735.85	0.0227	43.98
120	2.7765	760.39	0.0237	42.21
130	2.8383	784.98	0.0246	40.61
140	2.8988	809.68	0.0255	39.17
150	2.9582	834.54	0.0264	37.85
160	3.0167	859.58	0.0273	36.64
170	3.0744	884.84	0.0282	35.52
180	3.1313	910.34	0.0290	34.49
190	3.1875	936.10	0.0298	33.52
State Points at P = 45 bar				
Saturated Liquid at Bubble Point				
27.80	1.3906	318.39	0.0032	312.50
Saturated Vapour at Dew Point				
27.80	1.8767	464.71	0.0082	122.25

(Continued)

TABLE 7.12 ***(Continued)***

Properties of Superheated Vapour for R170

t, °C	s, kJ/kgK	h, kJ/kg	v, m³/kg	ρ, kg/m³
Superheated Vapour				
30	1.9396	483.69	0.0091	109.30
40	2.0970	532.11	0.0116	86.38
50	2.2059	566.73	0.0132	75.69
60	2.2979	596.94	0.0146	68.66
70	2.3808	624.95	0.0158	63.44
80	2.4577	651.71	0.0169	59.32
90	2.5303	677.70	0.0179	55.93
100	2.5996	703.23	0.0188	53.06
110	2.6664	728.49	0.0198	50.58
120	2.7311	753.62	0.0207	48.40
130	2.7941	778.70	0.0215	46.47
140	2.8557	803.84	0.0224	44.73
150	2.9161	829.08	0.0232	43.15
160	2.9754	854.46	0.0240	41.72
170	3.0337	880.03	0.0248	40.39
180	3.0913	905.80	0.0255	39.17
190	3.1480	931.81	0.0263	38.04
State Points at P = 50 bar				
Saturated Liquid at Bubble Point				
32.64	1.5783	377.21	0.0041	242.72
Saturated Vapour at Dew Point				
32.64	1.6650	403.72	0.0049	203.67
Superheated Vapour				
40	1.9920	504.38	0.0090	110.99
50	2.1300	548.25	0.0109	91.57
60	2.2343	582.44	0.0123	81.04
70	2.3242	612.84	0.0135	73.85
80	2.4058	641.23	0.0146	68.43
90	2.4817	668.43	0.0156	64.11
100	2.5536	694.90	0.0165	60.53
110	2.6225	720.92	0.0174	57.48
120	2.6888	746.68	0.0182	54.84
130	2.7532	772.31	0.0190	52.52
140	2.8159	797.91	0.0198	50.46
150	2.8772	823.55	0.0206	48.60
160	2.9374	849.29	0.0213	46.91
170	2.9964	875.17	0.0220	45.37
180	3.0546	901.23	0.0228	43.95
190	3.1119	927.49	0.0235	42.64
200	3.1685	953.99	0.0241	41.42

7.4.5 Refrigerant R290

This fluid is from propane series with chemical name propane and formula $CH_3CH_2CH_3$ (see Table 7.13, Figure 7.18, Figure 7.19, and Table 7.14).

Critical point: t_c = 96.67°C and p_c = 42.36 bar

TABLE 7.13

Saturated Liquid and Saturated Vapour Properties for R290

t, °C	p, bar	v_{vap}, m^3/kg	h_{liq}, kJ/kg	h_{vap}, kJ/kg	s_{liq}, kJ/kgK	s_{vap}, kJ/kgK
–58	0.469	0.84401	65.87	507.13	0.4522	2.5031
–56	0.520	0.76728	70.29	509.50	0.4726	2.4952
–54	0.575	0.69889	74.73	511.86	0.4929	2.4875
–52	0.635	0.63780	79.18	514.22	0.5130	2.4802
–50	0.699	0.58311	83.64	516.57	0.5331	2.4732
–48	0.768	0.53405	88.13	518.92	0.5530	2.4664
–46	0.843	0.48996	92.62	521.27	0.5729	2.4599
–44	0.923	0.45024	97.13	523.62	0.5926	2.4537
–42	1.009	0.41440	101.66	525.96	0.6122	2.4478
–40	1.101	0.38201	106.20	528.29	0.6316	2.4420
–38	1.199	0.35266	110.75	530.62	0.6510	2.4366
–36	1.305	0.32604	115.31	532.95	0.6702	2.4313
–34	1.417	0.30185	119.88	535.26	0.6894	2.4263
–32	1.536	0.27983	124.47	537.58	0.7084	2.4214
–30	1.663	0.25975	129.07	539.88	0.7273	2.4168
–28	1.798	0.24141	133.68	542.18	0.7461	2.4124
–26	1.942	0.22464	138.30	544.47	0.7647	2.4081
–24	2.093	0.20928	142.94	546.75	0.7833	2.4041
–22	2.254	0.19518	147.59	549.03	0.8018	2.4002
–20	2.424	0.18224	152.26	551.30	0.8202	2.3965
–18	2.604	0.17033	156.94	553.55	0.8385	2.3929
–16	2.793	0.15936	161.64	555.80	0.8567	2.3895
–14	2.993	0.14925	166.36	558.04	0.8748	2.3862
–12	3.204	0.13991	171.10	560.27	0.8929	2.3831
–10	3.425	0.13127	175.85	562.48	0.9109	2.3801
–8	3.658	0.12327	180.63	564.69	0.9288	2.3772
–6	3.902	0.11586	185.44	566.88	0.9467	2.3745
–4	4.159	0.10899	190.26	569.06	0.9645	2.3719
–2	4.428	0.10260	195.12	571.23	0.9823	2.3694
0	4.710	0.09666	200.00	573.38	1.0000	2.3669
2	5.005	0.09113	204.91	575.52	1.0177	2.3646
4	5.314	0.08598	209.85	577.64	1.0354	2.3624
6	5.637	0.08117	214.82	579.75	1.0530	2.3603
8	5.974	0.07669	219.83	581.84	1.0707	2.3583
10	6.326	0.07250	224.83	583.92	1.0881	2.3564
12	6.694	0.06858	229.90	585.97	1.1057	2.3545
14	7.076	0.06490	235.00	588.01	1.1233	2.3527
16	7.475	0.06146	240.15	590.03	1.1409	2.3509
18	7.890	0.05823	245.33	592.02	1.1585	2.3492
20	8.322	0.05520	250.55	593.99	1.1760	2.3476

(Continued)

TABLE 7.13 ***(Continued)***

Saturated Liquid and Saturated Vapour Properties for R290

t, °C	p, bar	v_{vap}, m^3/kg	h_{liq}, kJ/kg	h_{vap}, kJ/kg	s_{liq}, kJ/kgK	s_{vap}, kJ/kgK
22	8.771	0.05235	255.81	595.94	1.1936	2.3460
24	9.238	0.04967	261.10	597.87	1.2112	2.3445
26	9.723	0.04715	266.44	599.76	1.2287	2.3430
28	10.226	0.04477	271.82	601.63	1.2463	2.3415
30	10.749	0.04253	277.23	603.47	1.2639	2.3401
32	11.290	0.04042	282.69	605.28	1.2815	2.3386
34	11.852	0.03842	288.19	607.06	1.2990	2.3372
36	12.433	0.03653	293.74	608.80	1.3166	2.3358
38	13.036	0.03475	299.33	610.51	1.3343	2.3344
40	13.659	0.03305	304.96	612.17	1.3519	2.3329
42	14.305	0.03145	310.65	613.80	1.3695	2.3315
44	14.973	0.02993	316.38	615.37	1.3872	2.3300
46	15.663	0.02849	322.18	616.90	1.4050	2.3284
48	16.377	0.02712	328.02	618.38	1.4228	2.3269
50	17.114	0.02581	333.94	619.80	1.4406	2.3252
52	17.876	0.02457	339.92	621.16	1.4585	2.3235
54	18.663	0.02339	345.97	622.45	1.4766	2.3217
56	19.475	0.02226	352.11	623.67	1.4947	2.3197
58	20.313	0.02118	358.35	624.81	1.5130	2.3177
60	21.179	0.02016	364.68	625.87	1.5315	2.3155
62	22.071	0.01917	371.14	626.83	1.5502	2.3131
64	22.992	0.01823	377.72	627.68	1.5691	2.3105
66	23.941	0.01732	384.46	628.43	1.5884	2.3077
68	24.919	0.01645	391.36	629.04	1.6080	2.3047
70	25.927	0.01562	398.45	629.50	1.6280	2.3013
72	26.965	0.01481	405.76	629.81	1.6485	2.2976
74	28.034	0.01403	413.34	629.92	1.6696	2.2935
76	29.134	0.01329	421.16	629.85	1.6913	2.2890
78	30.266	0.01256	429.34	629.51	1.7138	2.2838
80	31.430	0.01185	437.90	628.89	1.7372	2.2780
82	32.626	0.01115	446.91	627.93	1.7617	2.2714
84	33.854	0.01047	456.47	626.56	1.7876	2.2638
86	35.115	0.00980	466.70	624.66	1.8152	2.2550
88	36.407	0.00913	477.79	622.09	1.8449	2.2445
90	37.731	0.00845	490.06	618.60	1.8776	2.2316
92	39.085	0.00775	504.15	613.67	1.9151	2.2151
94	40.469	0.00697	521.52	606.27	1.9612	2.1921

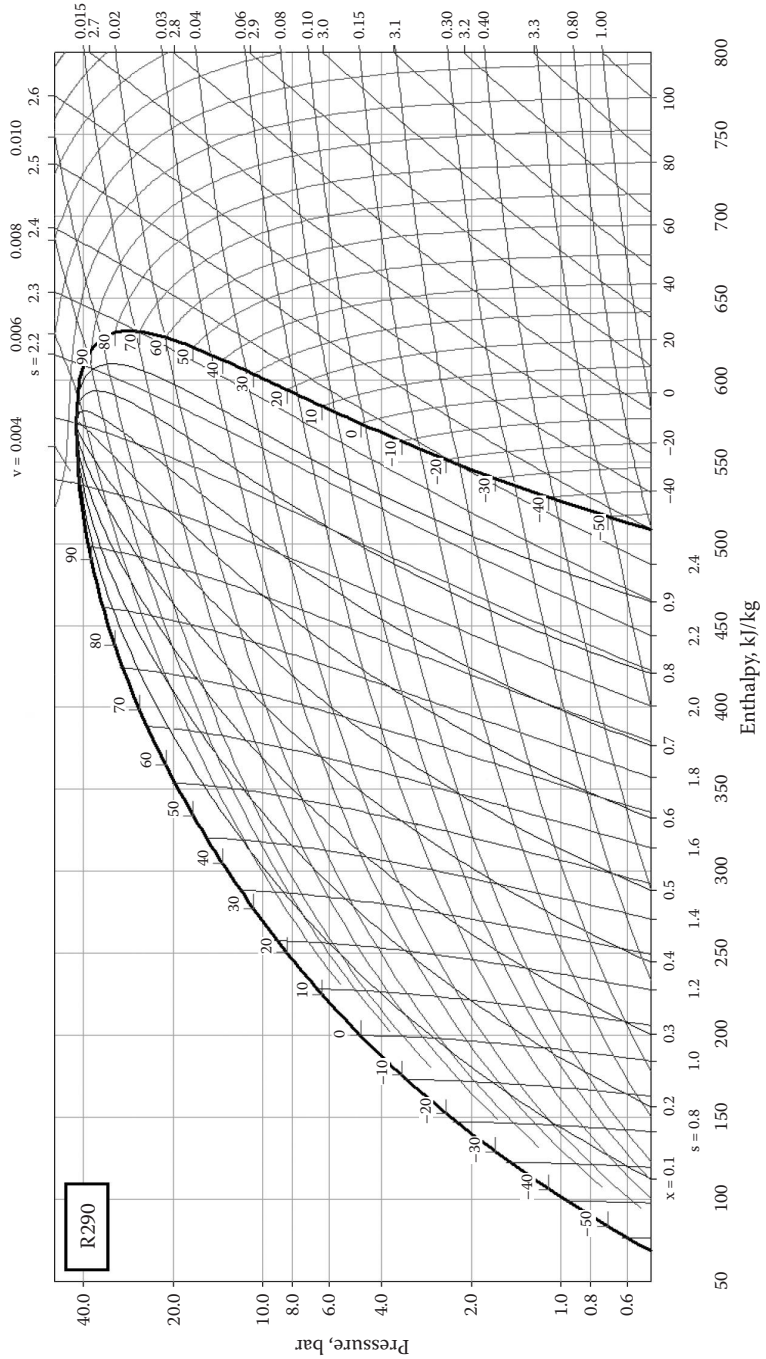

FIGURE 7.18
Pressure–enthalpy diagram for refrigerant R290.

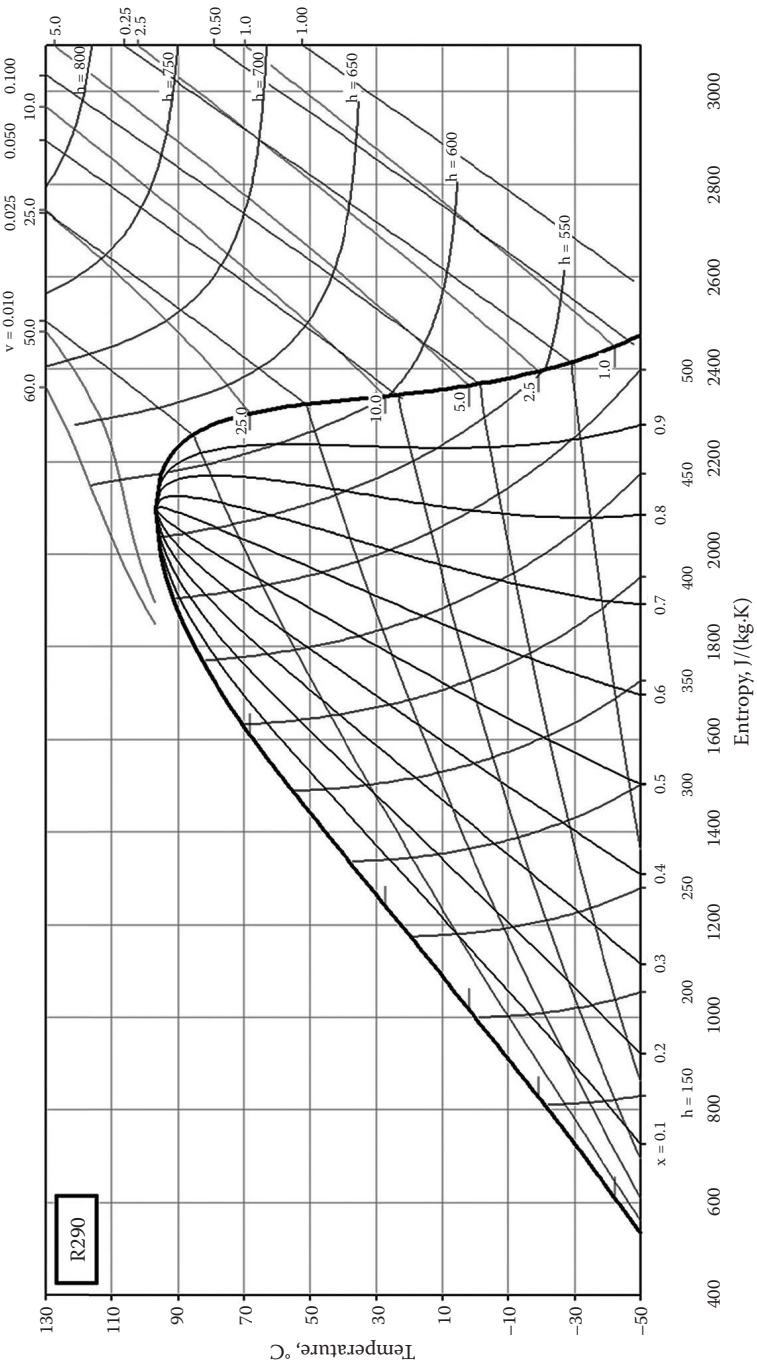

FIGURE 7.19
Temperature–entropy diagram for refrigerant R290.

TABLE 7.14

Properties of Superheated Vapour for R290

t, °C	s, kJ/kgK	h, kJ/kg	v, m^3/kg	ρ, kg/m^3
State Points at P = 1.01 bar				
Saturated Liquid at Bubble Point				
–41.97	0.6124	101.72	0.0018	571.43
Saturated Vapour at Dew Point				
–41.97	2.4477	525.99	0.4139	2.42
Superheated Vapour				
–40	2.4601	528.87	0.4180	2.39
–30	2.5222	543.66	0.4385	2.28
–20	2.5831	558.76	0.4588	2.18
–10	2.6429	574.20	0.4788	2.09
0	2.7019	590.02	0.4986	2.01
10	2.7601	606.22	0.5183	1.93
20	2.8178	622.84	0.5379	1.86
30	2.8749	639.87	0.5574	1.79
40	2.9316	657.32	0.5767	1.73
50	2.9878	675.21	0.5960	1.68
60	3.0436	693.54	0.6153	1.63
70	3.0992	712.31	0.6345	1.58
80	3.1543	731.53	0.6536	1.53
90	3.2092	751.18	0.6727	1.49
100	3.2638	771.28	0.6918	1.45
State Points at P = 5 bar				
Saturated Liquid at Bubble Point				
1.96	1.0174	204.82	0.0019	520.83
Saturated Vapour at Dew Point				
1.96	2.3647	575.48	0.0912	10.96
Superheated Vapour				
10	2.4168	590.02	0.0953	10.50
20	2.4799	608.20	0.1001	9.99
30	2.5415	626.57	0.1048	9.54
40	2.6019	645.18	0.1094	9.14
50	2.6612	664.07	0.1138	8.78
60	2.7198	683.27	0.1182	8.46
70	2.7776	702.81	0.1226	8.16
80	2.8347	722.71	0.1268	7.89
90	2.8913	742.97	0.1310	7.63
100	2.9474	763.62	0.1352	7.40
110	3.0030	784.65	0.1393	7.18
120	3.0582	806.08	0.1434	6.97
130	3.1130	827.90	0.1475	6.78

(Continued)

TABLE 7.14 ***(Continued)***

Properties of Superheated Vapour for R290

t, °C	s, kJ/kgK	h, kJ/kg	v, m³/kg	ρ, kg/m³
140	3.1675	850.12	0.1516	6.60
150	3.2216	872.75	0.1556	6.43
160	3.2753	895.77	0.1596	6.27
State Points at P = 10 bar				
Saturated Liquid at Bubble Point				
27.11	1.2385	269.42	0.0021	487.80
Saturated Vapour at Dew Point				
27.11	2.3422	600.80	0.0458	21.83
Superheated Vapour				
30	2.3622	606.86	0.0467	21.42
40	2.4297	627.65	0.0496	20.16
50	2.4947	648.31	0.0523	19.11
60	2.5576	668.99	0.0549	18.20
70	2.6191	689.78	0.0575	17.40
80	2.6794	710.74	0.0599	16.69
90	2.7385	731.94	0.0623	16.05
100	2.7968	753.40	0.0646	15.48
110	2.8544	775.15	0.0669	14.95
120	2.9112	797.22	0.0691	14.47
130	2.9675	819.61	0.0713	14.02
140	3.0232	842.35	0.0735	13.60
150	3.0784	865.43	0.0757	13.22
160	3.1331	888.88	0.0778	12.85
170	3.1875	912.68	0.0799	12.51
180	3.2414	936.85	0.0820	12.19
State Points at P = 15 bar				
Saturated Liquid at Bubble Point				
44.08	1.3880	316.62	0.0022	462.96
Saturated Vapour at Dew Point				
44.08	2.3299	615.44	0.0299	33.48
Superheated Vapour				
50	2.3735	629.40	0.0313	31.98
60	2.4437	652.41	0.0334	29.90
70	2.5105	675.02	0.0355	28.19
80	2.5750	697.45	0.0374	26.75
90	2.6375	719.86	0.0392	25.51
100	2.6986	742.34	0.0409	24.43
110	2.7584	764.97	0.0426	23.46
120	2.8173	787.80	0.0443	22.59
130	2.8752	810.86	0.0459	21.80

(Continued)

TABLE 7.14 ***(Continued)***

Properties of Superheated Vapour for R290

t, °C	s, kJ/kgK	h, kJ/kg	v, m³/kg	ρ, kg/m³
140	2.9323	834.19	0.0474	21.08
150	2.9888	857.80	0.0490	20.41
160	3.0447	881.72	0.0505	19.80
170	3.1000	905.95	0.0520	19.23
180	3.1548	930.50	0.0535	18.70
190	3.2091	955.39	0.0549	18.21
200	3.2630	980.61	0.0564	17.74
State Points at P = 20 bar				
Saturated Liquid at Bubble Point				
57.26	1.5062	356.03	0.0023	438.60
Saturated Vapour at Dew Point				
57.26	2.3285	624.40	0.0216	46.34
Superheated Vapour				
60	2.3407	631.77	0.0222	45.11
70	2.4169	657.54	0.0241	41.45
80	2.4878	682.23	0.0259	38.66
90	2.5552	706.36	0.0275	36.40
100	2.6200	730.21	0.0290	34.51
110	2.6828	753.96	0.0304	32.89
120	2.7440	777.72	0.0318	31.48
130	2.8039	801.58	0.0331	30.23
140	2.8628	825.60	0.0344	29.10
150	2.9207	849.82	0.0356	28.09
160	2.9778	874.26	0.0368	27.16
170	3.0342	898.97	0.0380	26.31
180	3.0899	923.95	0.0392	25.52
190	3.1451	949.21	0.0403	24.80
200	3.1997	974.78	0.0415	24.12
210	3.2538	1000.66	0.0426	23.48
State Points at P = 25 bar				
Saturated Liquid at Bubble Point				
68.16	1.6096	391.93	0.0024	413.22
Saturated Vapour at Dew Point				
68.16	2.3044	629.08	0.0164	61.05
Superheated Vapour				
70	2.3212	634.83	0.0168	59.60
80	2.4046	663.87	0.0186	53.63
90	2.4798	690.77	0.0202	49.42
100	2.5499	716.59	0.0217	46.18
110	2.6167	741.85	0.0230	43.54

(Continued)

TABLE 7.14 ***(Continued)***

Properties of Superheated Vapour for R290

t, °C	s, kJ/kgK	h, kJ/kg	v, m³/kg	ρ, kg/m³
120	2.6810	766.82	0.0242	41.33
130	2.7435	791.66	0.0254	39.43
140	2.8043	816.51	0.0265	37.77
150	2.8639	841.43	0.0276	36.30
160	2.9224	866.48	0.0286	34.98
170	2.9800	891.72	0.0296	33.78
180	3.0368	917.17	0.0306	32.68
190	3.0929	942.85	0.0316	31.68
200	3.1483	968.80	0.0325	30.75
210	3.2032	995.02	0.0335	29.89
220	3.2574	1021.52	0.0344	29.09
State Points at P = 30 bar				
Saturated Liquid at Bubble Point				
77.53	1.7085	427.41	0.0026	383.14
Saturated Vapour at Dew Point				
77.53	2.2851	629.61	0.0127	78.62
Superheated Vapour				
80	2.3114	638.89	0.0133	75.28
90	2.4031	671.70	0.0151	66.12
100	2.4822	700.82	0.0166	60.23
110	2.5548	728.28	0.0179	55.89
120	2.6233	754.87	0.0191	52.45
130	2.6889	780.97	0.0202	49.62
140	2.7522	806.82	0.0212	47.22
150	2.8138	832.57	0.0222	45.15
160	2.8740	858.33	0.0231	43.32
170	2.9330	884.18	0.0240	41.69
180	2.9909	910.15	0.0249	40.22
190	3.0480	936.30	0.0257	38.89
200	3.1043	962.66	0.0265	37.67
210	3.1599	989.24	0.0274	36.54
220	3.2149	1016.07	0.0282	35.50
230	3.2693	1043.17	0.0290	34.54
State Points at P = 35 bar				
Saturated Liquid at Bubble Point				
85.82	1.8126	465.75	0.0029	344.83
Saturated Vapour at Dew Point				
85.82	2.2559	624.86	0.0099	101.42
Superheated Vapour				
90	2.3113	644.88	0.0110	91.26
100	2.4107	681.44	0.0128	78.38

(Continued)

TABLE 7.14 ***(Continued)***

Properties of Superheated Vapour for R290

t, °C	s, kJ/kgK	h, kJ/kg	v, m³/kg	ρ, kg/m³
110	2.4931	712.60	0.0141	70.74
120	2.5677	741.53	0.0153	65.29
130	2.6374	769.30	0.0164	61.07
140	2.7039	796.42	0.0174	57.63
150	2.7679	823.19	0.0183	54.75
160	2.8300	849.78	0.0191	52.26
170	2.8906	876.31	0.0200	50.09
180	2.9498	902.88	0.0208	48.17
190	3.0080	929.54	0.0215	46.44
200	3.0653	956.35	0.0223	44.88
210	3.1217	983.33	0.0230	43.45
220	3.1774	1010.52	0.0237	42.14
230	3.2324	1037.93	0.0244	40.93
240	3.2869	1065.58	0.0251	39.80
State Points at P = 40 bar				
Saturated Liquid at Bubble Point				
93.33	1.9443	515.13	0.0036	281.69
Saturated Vapour at Dew Point				
93.33	2.2009	609.17	0.0072	138.12
Superheated Vapour				
100	2.3229	654.24	0.0094	105.85
110	2.4269	693.53	0.0111	89.77
120	2.5113	726.28	0.0124	80.59
130	2.5870	756.41	0.0135	74.16
140	2.6575	785.18	0.0144	69.22
150	2.7245	813.19	0.0153	65.24
160	2.7889	840.76	0.0162	61.91
170	2.8513	868.10	0.0169	59.06
180	2.9121	895.34	0.0177	56.57
190	2.9715	922.57	0.0184	54.37
200	3.0298	949.87	0.0191	52.40
210	3.0871	977.28	0.0198	50.62
220	3.1436	1004.85	0.0204	49.00
230	3.1993	1032.60	0.0210	47.51
240	3.2543	1060.56	0.0217	46.14
250	3.3087	1088.74	0.0223	44.87

7.4.6 Refrigerant R404A

This fluid is a ZEB of R125/143a/134a with composition of 44/52/4 in percent by mass (see Table 7.15, Figure 7.20, Figure 7.21, and Table 7.16).

Critical point: t_c = 72.07°C and p_c = 37.32 bar

TABLE 7.15

Saturated Liquid and Saturated Vapour Properties for R404A

t, °C	p, bar	v_{vap}, m³/kg	h_{liq}, kJ/kg	h_{vap}, kJ/kg	s_{liq}, kJ/kgK	s_{vap}, kJ/kgK
–78	0.160	1.02797	99.31	319.07	0.5721	1.6982
–76	0.184	0.90607	101.60	320.35	0.5837	1.6933
–74	0.210	0.80104	103.90	321.65	0.5953	1.6887
–72	0.239	0.71026	106.21	322.94	0.6068	1.6842
–70	0.271	0.63153	108.53	324.24	0.6182	1.6800
–68	0.306	0.56305	110.86	325.54	0.6296	1.6761
–66	0.345	0.50330	113.21	326.84	0.6410	1.6723
–64	0.388	0.45103	115.55	328.15	0.6522	1.6687
–62	0.436	0.40516	117.92	329.45	0.6634	1.6652
–60	0.488	0.36481	120.30	330.76	0.6746	1.6620
–58	0.544	0.32922	122.69	332.07	0.6858	1.6589
–56	0.606	0.29774	125.10	333.38	0.6969	1.6560
–54	0.674	0.26984	127.52	334.69	0.7079	1.6533
–52	0.747	0.24504	129.95	336.00	0.7189	1.6507
–50	0.827	0.22296	132.39	337.30	0.7299	1.6482
–48	0.913	0.20324	134.85	338.61	0.7409	1.6458
–46	1.006	0.18561	137.33	339.91	0.7518	1.6436
–44	1.106	0.16980	139.81	341.22	0.7626	1.6415
–42	1.214	0.15559	142.31	342.52	0.7735	1.6396
–40	1.330	0.14281	144.83	343.81	0.7843	1.6377
–38	1.454	0.13128	147.36	345.11	0.7950	1.6360
–36	1.587	0.12086	149.91	346.40	0.8058	1.6343
–34	1.730	0.11142	152.92	347.69	0.8184	1.6328
–32	1.882	0.10287	155.48	348.97	0.8290	1.6313
–30	2.045	0.09510	159.17	350.26	0.8441	1.6300
–28	2.218	0.08803	161.72	351.52	0.8545	1.6287
–26	2.402	0.08158	164.28	352.79	0.8648	1.6275
–24	2.598	0.07570	166.86	354.04	0.8751	1.6264
–22	2.806	0.07032	169.47	355.29	0.8854	1.6253
–20	3.027	0.06540	172.08	356.52	0.8957	1.6243
–18	3.260	0.06088	174.72	357.75	0.9060	1.6233
–16	3.507	0.05673	177.38	358.97	0.9162	1.6224
–14	3.767	0.05292	180.06	360.18	0.9265	1.6215
–12	4.043	0.04941	182.75	361.38	0.9367	1.6207
–10	4.333	0.04617	185.48	362.56	0.9470	1.6200
–8	4.639	0.04318	188.22	363.74	0.9573	1.6192
–6	4.961	0.04041	190.98	364.90	0.9676	1.6186
–4	5.299	0.03785	193.77	366.04	0.9778	1.6179
–2	5.655	0.03548	196.57	367.17	0.9881	1.6172

(Continued)

TABLE 7.15 ***(Continued)***

Saturated Liquid and Saturated Vapour Properties for R404A

t, °C	p, bar	v_{vap}, m^3/kg	h_{liq}, kJ/kg	h_{vap}, kJ/kg	s_{liq}, kJ/kgK	s_{vap}, kJ/kgK
0	6.028	0.03328	199.41	368.28	0.9984	1.6166
2	6.420	0.03124	202.26	369.38	1.0086	1.6160
4	6.830	0.02934	205.15	370.46	1.0189	1.6154
6	7.260	0.02757	208.06	371.52	1.0293	1.6148
8	7.710	0.02592	211.00	372.56	1.0396	1.6143
10	8.180	0.02438	213.96	373.58	1.0500	1.6137
12	8.672	0.02295	216.96	374.57	1.0604	1.6131
14	9.186	0.02160	219.99	375.54	1.0708	1.6125
16	9.722	0.02035	223.06	376.48	1.0812	1.6118
18	10.281	0.01917	226.16	377.40	1.0917	1.6112
20	10.864	0.01806	229.29	378.29	1.1023	1.6105
22	11.472	0.01703	232.47	379.14	1.1129	1.6098
24	12.104	0.01605	235.68	379.97	1.1235	1.6091
26	12.763	0.01514	238.94	380.75	1.1342	1.6083
28	13.448	0.01427	242.24	381.50	1.1450	1.6074
30	14.160	0.01346	245.60	382.21	1.1558	1.6065
32	14.900	0.01269	249.00	382.87	1.1668	1.6055
34	15.669	0.01197	252.46	383.49	1.1778	1.6044
36	16.468	0.01128	255.97	384.06	1.1889	1.6032
38	17.297	0.01064	259.55	384.56	1.2001	1.6019
40	18.157	0.01002	263.20	385.01	1.2115	1.6005
42	19.049	0.00944	266.92	385.39	1.2230	1.5990
44	19.974	0.00889	270.72	385.70	1.2347	1.5972
46	20.932	0.00836	274.61	385.92	1.2466	1.5953
48	21.925	0.00786	278.60	386.05	1.2587	1.5932
50	22.953	0.00738	282.69	386.08	1.2710	1.5909
52	24.018	0.00692	286.91	385.99	1.2836	1.5883
54	25.120	0.00648	291.27	385.77	1.2965	1.5853
56	26.260	0.00606	295.79	385.39	1.3098	1.5820
58	27.440	0.00565	300.49	384.83	1.3235	1.5782
60	28.660	0.00525	305.42	384.03	1.3379	1.5738
62	29.921	0.00487	310.63	382.96	1.3529	1.5687
64	31.225	0.00449	316.19	381.51	1.3688	1.5626
66	32.572	0.00410	322.23	379.54	1.3861	1.5550
68	33.964	0.00371	328.96	376.77	1.4052	1.5453
70	35.402	0.00327	336.84	372.43	1.4274	1.5312
72	36.887	0.00209	344.87	347.34	1.4500	1.4571

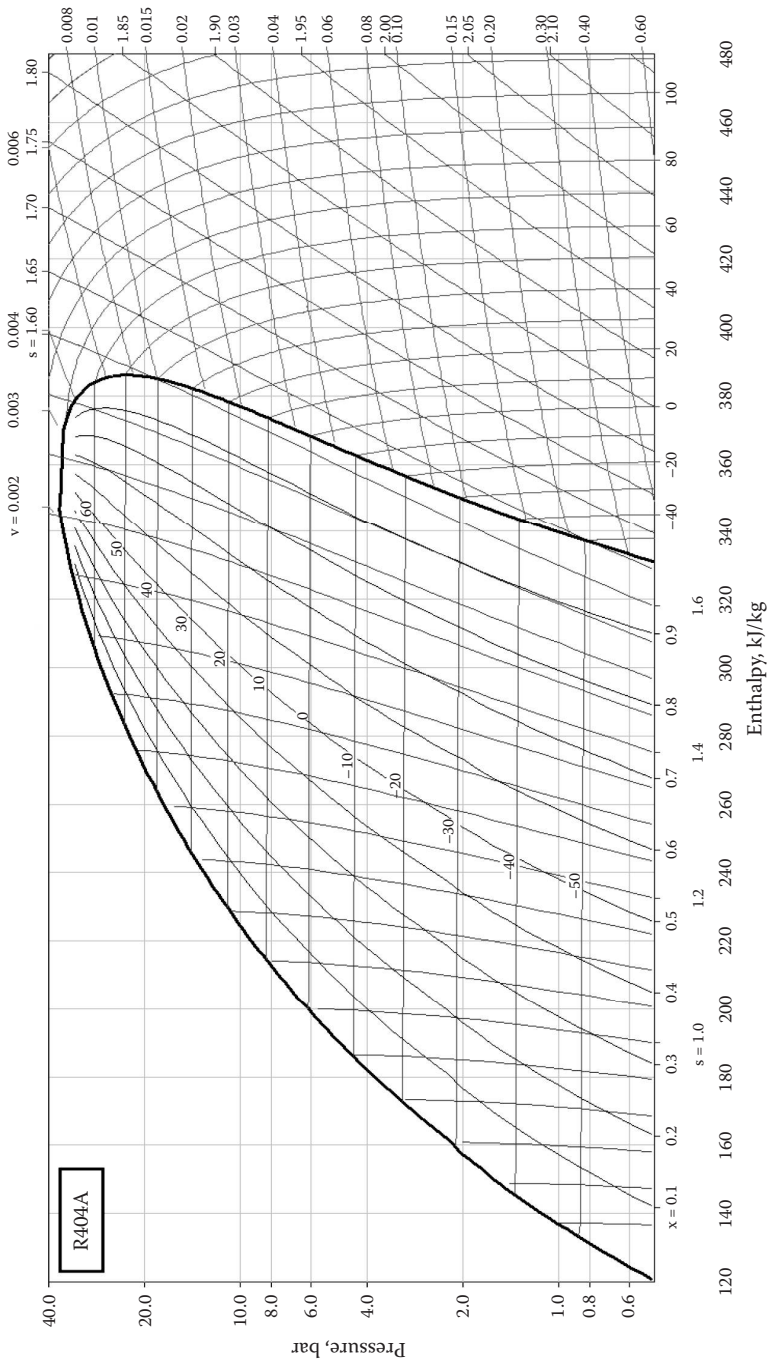

FIGURE 7.20
Pressure–enthalpy diagram for refrigerant R404A.

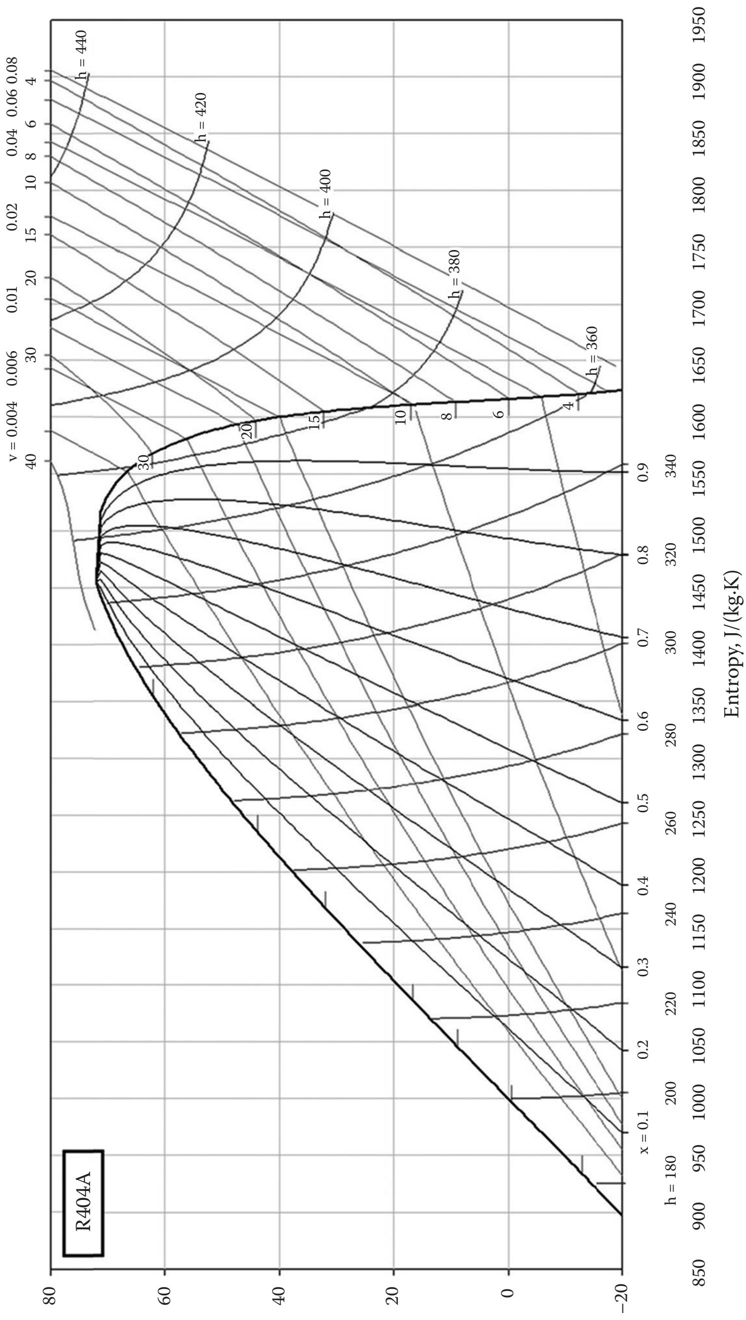

FIGURE 7.21
Temperature–entropy diagram for refrigerant R404A.

TABLE 7.16

Properties of Superheated Vapour for R404A

t, °C	s, kJ/kgK	h, kJ/kg	v, m^3/kg	ρ, kg/m^3
State Points at P = 1.01 bar				
Saturated Liquid at Bubble Point				
−46.52	0.7509	137.44	0.0008	1282.05
Saturated Vapour at Dew Point				
−45.80	1.6439	340.06	0.1849	5.41
Superheated Vapour				
−40	1.6628	344.41	0.1901	5.26
−30	1.6950	352.07	0.1990	5.02
−20	1.7266	359.91	0.2079	4.81
−10	1.7577	367.94	0.2167	4.61
0	1.7883	376.15	0.2255	4.43
10	1.8185	384.56	0.2343	4.27
20	1.8483	393.14	0.2430	4.11
30	1.8777	401.91	0.2517	3.97
40	1.9068	410.86	0.2604	3.84
50	1.9354	419.98	0.2691	3.72
60	1.9638	429.28	0.2777	3.60
70	1.9918	438.76	0.2864	3.49
80	2.0195	448.40	0.2950	3.39
90	2.0469	458.21	0.3036	3.29
100	2.0740	468.18	0.3122	3.20
110	2.1008	478.31	0.3208	3.12
120	2.1273	488.60	0.3293	3.04
130	2.1535	499.04	0.3379	2.96
State Points at P = 5 bar				
Saturated Liquid at Bubble Point				
−6.20	0.9682	191.31	0.0009	1136.36
Saturated Vapour at Dew Point				
−5.67	1.6188	365.11	0.0401	24.93
Superheated Vapour				
0	1.6370	370.05	0.0413	24.19
10	1.6687	378.86	0.0434	23.02
20	1.6998	387.81	0.0455	21.98
30	1.7303	396.90	0.0475	21.05
40	1.7603	406.14	0.0495	20.20
50	1.7898	415.53	0.0515	19.43
60	1.8189	425.08	0.0534	18.72
70	1.8475	434.77	0.0553	18.07
80	1.8758	444.61	0.0572	17.47
90	1.9037	454.61	0.0591	16.91

(Continued)

TABLE 7.16 ***(Continued)***

Properties of Superheated Vapour for R404A

t, °C	s, kJ/kgK	h, kJ/kg	v, m³/kg	ρ, kg/m³
100	1.9313	464.76	0.0610	16.39
110	1.9585	475.05	0.0629	15.91
120	1.9854	485.49	0.0647	15.45
130	2.0120	496.08	0.0666	15.02
140	2.0383	506.80	0.0684	14.62
150	2.0643	517.67	0.0702	14.24
160	2.0900	528.67	0.0720	13.88
170	2.1154	539.81	0.0739	13.54
State Points at P = 10 bar				
Saturated Liquid at Bubble Point				
16.63	1.0861	224.61	0.0010	1030.93
Saturated Vapour at Dew Point				
17.06	1.6117	377.00	0.0198	50.63
Superheated Vapour				
20	1.6216	379.88	0.0201	49.66
30	1.6544	389.65	0.0214	46.73
40	1.6862	399.46	0.0226	44.23
50	1.7172	409.34	0.0238	42.06
60	1.7476	419.30	0.0249	40.16
70	1.7774	429.37	0.0260	38.46
80	1.8066	439.54	0.0271	36.93
90	1.8353	449.83	0.0281	35.54
100	1.8636	460.25	0.0292	34.28
110	1.8915	470.79	0.0302	33.11
120	1.9190	481.45	0.0312	32.04
130	1.9461	492.24	0.0322	31.05
140	1.9728	503.15	0.0332	30.12
150	1.9992	514.19	0.0342	29.26
160	2.0253	525.36	0.0351	28.45
170	2.0510	536.64	0.0361	27.70
180	2.0765	548.05	0.0371	26.98
190	2.1016	559.57	0.0380	26.31
200	2.1265	571.21	0.0390	25.67
State Points at P = 15 bar				
Saturated Liquid at Bubble Point				
31.93	1.1679	249.45	0.0011	943.40
Saturated Vapour at Dew Point				
32.29	1.6054	382.99	0.0126	79.37
Superheated Vapour				
40	1.6326	391.40	0.0134	74.59
50	1.6664	402.13	0.0144	69.56

(Continued)

TABLE 7.16 ***(Continued)***

Properties of Superheated Vapour for R404A

t, °C	s, kJ/kgK	h, kJ/kg	v, m³/kg	ρ, kg/m³
60	1.6988	412.76	0.0153	65.43
70	1.7302	423.38	0.0161	61.95
80	1.7607	434.01	0.0170	58.94
90	1.7905	444.69	0.0178	56.29
100	1.8198	455.45	0.0185	53.95
110	1.8484	466.29	0.0193	51.84
120	1.8766	477.22	0.0200	49.93
130	1.9043	488.25	0.0207	48.19
140	1.9316	499.38	0.0215	46.60
150	1.9584	510.62	0.0222	45.13
160	1.9849	521.97	0.0228	43.76
170	2.0111	533.42	0.0235	42.50
180	2.0369	544.98	0.0242	41.31
190	2.0624	556.65	0.0249	40.21
200	2.0875	568.43	0.0255	39.16
210	2.1123	580.30	0.0262	38.18
220	2.1369	592.28	0.0268	37.26
State Points at P = 20 bar				
Saturated Liquid at Bubble Point				
43.77	1.2349	270.83	0.0012	854.70
Saturated Vapour at Dew Point				
44.08	1.5973	385.73	0.0089	112.74
Superheated Vapour				
50	1.6204	393.13	0.0095	105.72
60	1.6567	405.03	0.0103	96.75
70	1.6907	416.55	0.0111	89.90
80	1.7232	427.87	0.0119	84.38
90	1.7546	439.10	0.0125	79.76
100	1.7850	450.31	0.0132	75.81
110	1.8147	461.53	0.0138	72.37
120	1.8437	472.79	0.0144	69.32
130	1.8722	484.10	0.0150	66.60
140	1.9001	495.49	0.0156	64.14
150	1.9275	506.96	0.0162	61.90
160	1.9545	518.51	0.0167	59.86
170	1.9810	530.15	0.0172	57.97
180	2.0072	541.88	0.0178	56.23
190	2.0330	553.70	0.0183	54.61
200	2.0585	565.62	0.0188	53.10
210	2.0836	577.63	0.0193	51.69
220	2.1084	589.73	0.0199	50.37

(Continued)

TABLE 7.16 ***(Continued)***

Properties of Superheated Vapour for R404A

t, °C	s, kJ/kgK	h, kJ/kg	v, m³/kg	ρ, kg/m³
State Points at P = 25 bar				
Saturated Liquid at Bubble Point				
53.57	1.2950	290.80	0.0013	769.23
Saturated Vapour at Dew Point				
53.82	1.5859	385.86	0.0065	153.14
Superheated Vapour				
60	1.6137	395.06	0.0072	139.58
70	1.6532	408.39	0.0080	125.00
80	1.6890	420.86	0.0087	114.73
90	1.7226	432.91	0.0094	106.83
100	1.7548	444.74	0.0100	100.42
110	1.7858	456.45	0.0105	95.04
120	1.8158	468.12	0.0111	90.43
130	1.8451	479.78	0.0116	86.41
140	1.8737	491.47	0.0121	82.84
150	1.9018	503.19	0.0126	79.65
160	1.9293	514.97	0.0130	76.77
170	1.9563	526.82	0.0135	74.15
180	1.9829	538.73	0.0139	71.75
190	2.0091	550.72	0.0144	69.54
200	2.0349	562.79	0.0148	67.49
210	2.0603	574.95	0.0152	65.59
220	2.0853	587.18	0.0157	63.82
230	2.1101	599.49	0.0161	62.15
240	2.1345	611.88	0.0165	60.59
State Points at P = 30 bar				
Saturated Liquid at Bubble Point				
62.00	1.3538	310.96	0.0015	675.68
Saturated Vapour at Dew Point				
62.19	1.5688	383.03	0.0049	206.19
Superheated Vapour				
70	1.6121	397.69	0.0057	174.11
80	1.6547	412.52	0.0065	152.84
90	1.6920	425.91	0.0072	138.90
100	1.7266	438.63	0.0078	128.55
110	1.7593	451.01	0.0083	120.34
120	1.7907	463.19	0.0088	113.56
130	1.8211	475.27	0.0093	107.81
140	1.8506	487.31	0.0097	102.83
150	1.8793	499.33	0.0102	98.45

(Continued)

TABLE 7.16 ***(Continued)***

Properties of Superheated Vapour for R404A

t, °C	s, kJ/kgK	h, kJ/kg	v, m³/kg	ρ, kg/m³
160	1.9074	511.37	0.0106	94.56
170	1.9350	523.44	0.0110	91.06
180	1.9620	535.55	0.0114	87.88
190	1.9886	547.73	0.0118	84.98
200	2.0147	559.96	0.0121	82.32
210	2.0404	572.26	0.0125	79.87
220	2.0658	584.63	0.0129	77.59
230	2.0908	597.06	0.0133	75.47
240	2.1154	609.57	0.0136	73.49
250	2.1397	622.15	0.0140	71.63
State Points at P = 35 bar				
Saturated Liquid at Bubble Point				
69.44	1.4208	334.51	0.0018	552.49
Saturated Vapour at Dew Point				
68.62	1.4053	329.17	0.0017	584.80
Superheated Vapour				
70	1.5452	377.12	0.0036	279.35
80	1.6162	401.76	0.0049	205.43
90	1.6608	417.73	0.0056	178.46
100	1.6991	431.85	0.0062	161.34
110	1.7343	445.13	0.0067	148.83
120	1.7674	457.98	0.0072	139.02
130	1.7990	470.57	0.0076	130.98
140	1.8295	483.01	0.0081	124.20
150	1.8590	495.37	0.0084	118.36
160	1.8878	507.69	0.0088	113.24
170	1.9159	520.01	0.0092	108.70
180	1.9434	532.35	0.0096	104.63
190	1.9704	544.71	0.0099	100.95
200	1.9969	557.12	0.0102	97.59
210	2.0230	569.57	0.0106	94.52
220	2.0486	582.08	0.0109	91.68
230	2.0738	594.65	0.0112	89.06
240	2.0987	607.28	0.0115	86.62
250	2.1232	619.97	0.0119	84.34

7.4.7 Refrigerant R407C

This fluid is a ZEB of R32/125/134a with composition of 23/25/52 in percent by mass (see Table 7.17, Figure 7.22, Figure 7.23, and Table 7.18).

Critical point: t_c = 86.74°C and p_c = 46.19 bar

TABLE 7.17

Saturated Liquid and Saturated Vapour Properties for R407C

t, °C	p, bar	v_{vap}, m³/kg	h_{liq}, kJ/kg	h_{vap}, kJ/kg	s_{liq}, kJ/kgK	s_{vap}, kJ/kgK
–64	0.217	0.92165	107.57	373.24	0.6358	1.9060
–62	0.247	0.81803	109.95	374.54	0.6469	1.9000
–60	0.279	0.72800	112.34	375.84	0.6579	1.8942
–58	0.316	0.64955	114.74	377.14	0.6689	1.8886
–56	0.356	0.58099	117.16	378.45	0.6799	1.8832
–54	0.400	0.52091	119.58	379.75	0.6909	1.8780
–52	0.449	0.46813	122.01	381.05	0.7017	1.8731
–50	0.502	0.42164	124.46	382.35	0.7126	1.8683
–48	0.560	0.38058	126.91	383.66	0.7234	1.8637
–46	0.624	0.34424	129.38	384.96	0.7342	1.8593
–44	0.693	0.31199	131.87	386.26	0.7449	1.8550
–42	0.768	0.28332	134.36	387.55	0.7556	1.8510
–40	0.850	0.25776	136.87	388.85	0.7663	1.8470
–38	0.938	0.23493	139.39	390.14	0.7769	1.8432
–36	1.034	0.21450	141.93	391.43	0.7875	1.8396
–34	1.138	0.19617	144.48	392.72	0.7981	1.8361
–32	1.249	0.17971	147.05	394.00	0.8087	1.8327
–30	1.369	0.16488	149.63	395.28	0.8192	1.8295
–28	1.498	0.15150	152.53	396.55	0.8309	1.8264
–26	1.636	0.13942	155.13	397.82	0.8414	1.8233
–24	1.785	0.12848	157.75	399.08	0.8518	1.8204
–22	1.943	0.11855	160.38	400.34	0.8622	1.8176
–20	2.113	0.10954	162.63	401.58	0.8710	1.8149
–18	2.293	0.10134	165.32	402.82	0.8815	1.8123
–16	2.486	0.09387	168.02	404.06	0.8919	1.8098
–14	2.691	0.08705	170.72	405.28	0.9023	1.8073
–12	2.909	0.08082	173.47	406.49	0.9127	1.8050
–10	3.140	0.07511	176.23	407.69	0.9231	1.8027
–8	3.386	0.06988	179.01	408.89	0.9335	1.8005
–6	3.646	0.06508	181.81	410.07	0.9439	1.7983
–4	3.921	0.06066	184.50	411.24	0.9538	1.7962
–2	4.213	0.05660	187.38	412.40	0.9643	1.7942
0	4.520	0.05286	190.25	413.54	0.9748	1.7922
2	4.845	0.04940	193.15	414.67	0.9852	1.7903
4	5.187	0.04621	196.06	415.78	0.9956	1.7884
6	5.548	0.04326	199.01	416.88	1.0061	1.7866
8	5.927	0.04053	201.99	417.96	1.0166	1.7847
10	6.327	0.03799	204.99	419.03	1.0271	1.7830
12	6.746	0.03564	208.02	420.07	1.0376	1.7812

(Continued)

TABLE 7.17 ***(Continued)***

Saturated Liquid and Saturated Vapour Properties for R407C

t, °C	p, bar	v_{vap}, m^3/kg	h_{liq}, kJ/kg	h_{vap}, kJ/kg	s_{liq}, kJ/kgK	s_{vap}, kJ/kgK
14	7.187	0.03345	211.09	421.09	1.0481	1.7795
16	7.649	0.03142	214.18	422.10	1.0587	1.7777
18	8.134	0.02953	217.31	423.08	1.0693	1.7760
20	8.642	0.02776	220.46	424.04	1.0799	1.7743
22	9.174	0.02612	223.66	424.97	1.0906	1.7726
24	9.731	0.02458	226.89	425.88	1.1013	1.7709
26	10.313	0.02314	230.15	426.76	1.1120	1.7692
28	10.921	0.02179	233.46	427.61	1.1228	1.7675
30	11.557	0.02053	236.80	428.43	1.1337	1.7658
32	12.220	0.01935	240.19	429.21	1.1446	1.7640
34	12.913	0.01824	243.63	429.96	1.1556	1.7622
36	13.635	0.01720	247.11	430.68	1.1666	1.7604
38	14.387	0.01622	250.64	431.35	1.1777	1.7585
40	15.171	0.01530	254.23	431.98	1.1889	1.7566
42	15.988	0.01443	257.87	432.57	1.2002	1.7546
44	16.838	0.01361	261.57	433.11	1.2117	1.7525
46	17.722	0.01284	265.33	433.60	1.2232	1.7504
48	18.641	0.01211	269.16	434.03	1.2348	1.7482
50	19.597	0.01142	273.07	434.40	1.2466	1.7458
52	20.590	0.01076	277.05	434.71	1.2585	1.7434
54	21.622	0.01014	281.11	434.95	1.2706	1.7408
56	22.693	0.00956	285.26	435.11	1.2828	1.7381
58	23.806	0.00900	289.52	435.18	1.2953	1.7352
60	24.959	0.00847	293.88	435.17	1.3080	1.7321
62	26.156	0.00796	298.36	435.05	1.3210	1.7288
64	27.398	0.00748	302.97	434.82	1.3342	1.7253
66	28.684	0.00703	307.73	434.46	1.3478	1.7215
68	30.018	0.00659	312.65	433.96	1.3617	1.7173
70	31.400	0.00617	317.77	433.29	1.3761	1.7128
72	32.831	0.00576	323.11	432.44	1.3911	1.7078
74	34.313	0.00537	328.72	431.36	1.4067	1.7023
76	35.848	0.00500	334.65	430.03	1.4230	1.6962
78	37.436	0.00463	340.98	428.37	1.4404	1.6893
80	39.080	0.00428	347.84	426.33	1.4592	1.6814
82	40.781	0.00393	355.43	423.80	1.4798	1.6723
84	42.540	0.00358	364.10	420.66	1.5033	1.6617
86	44.360	0.00325	395.33	416.83	1.5894	1.6492

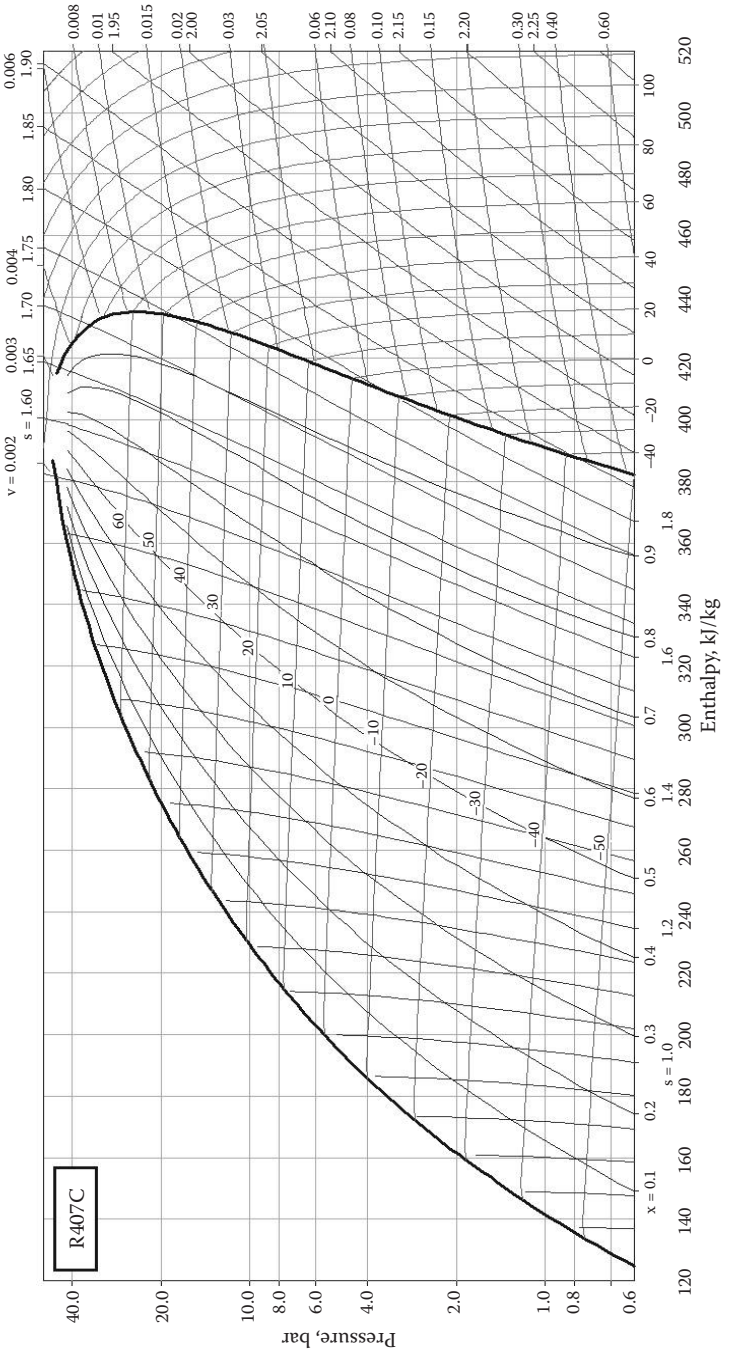

FIGURE 7.22
Pressure–enthalpy diagram for refrigerant R407C.

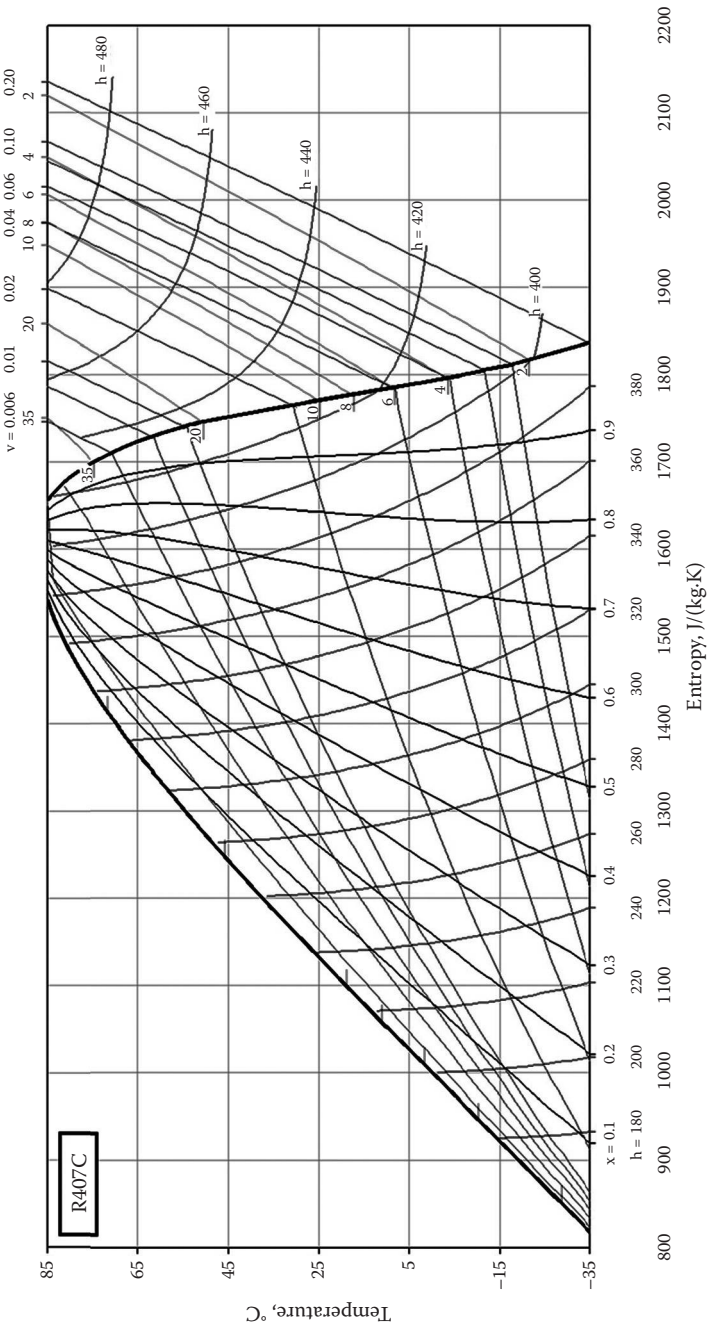

FIGURE 7.23
Temperature–entropy diagram for refrigerant R407C.

TABLE 7.18

Properties of Superheated Vapour for R407C

t, °C	s, kJ/kgK	h, kJ/kg	v, m^3/kg	ρ, kg/m^3
State Points at P = 1.01 bar				
Saturated Liquid at Bubble Point				
–43.96	0.7676	141.30	0.0007	1388.89
Saturated Vapour at Dew Point				
–36.61	1.8401	391.03	0.2192	4.56
Superheated Vapour				
–30	1.8606	395.93	0.2258	4.43
–20	1.8910	403.48	0.2358	4.24
–10	1.9209	411.20	0.2458	4.07
0	1.9504	419.11	0.2557	3.91
10	1.9794	427.19	0.2656	3.76
20	2.0081	435.45	0.2755	3.63
30	2.0364	443.89	0.2853	3.50
40	2.0645	452.53	0.2951	3.39
50	2.0922	461.35	0.3049	3.28
60	2.1197	470.37	0.3147	3.18
70	2.1469	479.59	0.3245	3.08
80	2.1740	489.01	0.3342	2.99
90	2.2008	498.63	0.3439	2.91
100	2.2275	508.46	0.3537	2.83
110	2.2541	518.50	0.3634	2.75
120	2.2805	528.76	0.3731	2.68
130	2.3069	539.24	0.3828	2.61
140	2.3331	549.96	0.3924	2.55
State Points at P = 5 bar				
Saturated Liquid at Bubble Point				
–3.82	0.9799	194.50	0.0008	1250.00
Saturated Vapour at Dew Point				
2.76	1.7889	415.05	0.0479	20.89
Superheated Vapour				
10	1.8110	421.22	0.0496	20.18
20	1.8410	429.85	0.0519	19.28
30	1.8704	438.64	0.0541	18.48
40	1.8994	447.57	0.0563	17.75
50	1.9280	456.68	0.0585	17.08
60	1.9563	465.95	0.0607	16.47
70	1.9842	475.39	0.0629	15.90
80	2.0119	485.02	0.0650	15.38
90	2.0393	494.84	0.0671	14.89
100	2.0665	504.85	0.0693	14.44

(Continued)

TABLE 7.18 ***(Continued)***

Properties of Superheated Vapour for R407C

t, °C	s, kJ/kgK	h, kJ/kg	v, m³/kg	ρ, kg/m³
110	2.0935	515.07	0.0714	14.01
120	2.1204	525.49	0.0734	13.62
130	2.1471	536.12	0.0755	13.24
140	2.1737	546.97	0.0776	12.89
150	2.2001	558.05	0.0796	12.56
160	2.2266	569.36	0.0817	12.24
170	2.2530	580.92	0.0837	11.94
State Points at P = 10 bar				
Saturated Liquid at Bubble Point				
18.78	1.0992	228.41	0.0009	1162.79
Saturated Vapour at Dew Point				
24.74	1.7695	426.11	0.0239	41.91
Superheated Vapour				
30	1.7861	431.09	0.0246	40.67
40	1.8170	440.60	0.0259	38.59
50	1.8471	450.20	0.0272	36.76
60	1.8767	459.90	0.0285	35.14
70	1.9058	469.73	0.0297	33.69
80	1.9344	479.70	0.0309	32.38
90	1.9627	489.82	0.0321	31.19
100	1.9906	500.11	0.0332	30.10
110	2.0183	510.57	0.0344	29.10
120	2.0457	521.23	0.0355	28.17
130	2.0730	532.07	0.0366	27.31
140	2.1001	543.12	0.0377	26.51
150	2.1270	554.38	0.0388	25.76
160	2.1538	565.87	0.0399	25.06
170	2.1805	577.58	0.0410	24.40
180	2.2072	589.54	0.0421	23.78
State Points at P = 15 bar				
Saturated Liquid at Bubble Point				
33.97	1.1813	253.45	0.0009	1098.90
Saturated Vapour at Dew Point				
39.36	1.7563	431.63	0.0155	64.64
Superheated Vapour				
40	1.7585	432.30	0.0155	64.36
50	1.7912	442.73	0.0166	60.29
60	1.8228	453.09	0.0176	56.89
70	1.8535	463.47	0.0185	53.99
80	1.8835	473.90	0.0194	51.46

(Continued)

TABLE 7.18 ***(Continued)***

Properties of Superheated Vapour for R407C

t, °C	s, kJ/kgK	h, kJ/kg	v, m³/kg	ρ, kg/m³
90	1.9128	484.43	0.0203	49.23
100	1.9418	495.07	0.0212	47.24
110	1.9702	505.84	0.0220	45.44
120	1.9984	516.77	0.0228	43.81
130	2.0263	527.87	0.0236	42.31
140	2.0539	539.14	0.0244	40.94
150	2.0813	550.61	0.0252	39.67
160	2.1086	562.29	0.0260	38.49
170	2.1357	574.18	0.0267	37.39
180	2.1628	586.30	0.0275	36.37
190	2.1898	598.66	0.0282	35.41
State Points at P = 20 bar				
Saturated Liquid at Bubble Point				
45.77	1.2475	274.69	0.0010	1041.67
Saturated Vapour at Dew Point				
50.61	1.7441	434.29	0.0111	89.93
Superheated Vapour				
60	1.7771	445.13	0.0120	83.36
70	1.8103	456.38	0.0128	77.84
80	1.8423	467.49	0.0136	73.31
90	1.8732	478.56	0.0144	69.48
100	1.9033	489.66	0.0151	66.17
110	1.9329	500.83	0.0158	63.27
120	1.9619	512.09	0.0165	60.68
130	1.9905	523.49	0.0171	58.36
140	2.0188	535.03	0.0178	56.26
150	2.0468	546.73	0.0184	54.35
160	2.0745	558.62	0.0190	52.59
170	2.1021	570.70	0.0196	50.96
180	2.1296	583.00	0.0202	49.46
190	2.1569	595.53	0.0208	48.06
200	2.1842	608.29	0.0214	46.75
210	2.2114	621.31	0.0220	45.53
220	2.2386	634.60	0.0225	44.38
State Points at P = 25 bar				
Saturated Liquid at Bubble Point				
55.57	1.3055	294.03	0.0010	990.10
Saturated Vapour at Dew Point				
59.85	1.7311	434.87	0.0084	118.62

(Continued)

TABLE 7.18 ***(Continued)***

Properties of Superheated Vapour for R407C

t, °C	s, kJ/kgK	h, kJ/kg	v, m³/kg	ρ, kg/m³
Superheated Vapour				
60	1.7317	435.07	0.0084	118.42
70	1.7699	447.99	0.0093	107.25
80	1.8050	460.21	0.0101	99.08
90	1.8382	472.08	0.0108	92.65
100	1.8700	483.81	0.0114	87.36
110	1.9009	495.48	0.0121	82.88
120	1.9310	507.16	0.0127	79.01
130	1.9605	518.91	0.0132	75.60
140	1.9895	530.76	0.0138	72.58
150	2.0182	542.73	0.0143	69.86
160	2.0465	554.86	0.0148	67.39
170	2.0746	567.16	0.0154	65.14
180	2.1025	579.66	0.0159	63.07
190	2.1302	592.36	0.0163	61.16
200	2.1578	605.28	0.0168	59.39
210	2.1853	618.45	0.0173	57.75
220	2.2128	631.88	0.0178	56.21
230	2.2403	645.57	0.0183	54.76
State Points at P = 30 bar				
Saturated Liquid at Bubble Point				
64.06	1.3595	312.59	0.0011	943.40
Saturated Vapour at Dew Point				
67.73	1.7162	433.58	0.0066	152.21
Superheated Vapour				
70	1.7267	437.17	0.0068	147.25
80	1.7681	451.58	0.0076	131.02
90	1.8049	464.76	0.0083	119.92
100	1.8392	477.38	0.0090	111.48
110	1.8719	489.72	0.0096	104.70
120	1.9033	501.94	0.0101	99.04
130	1.9339	514.12	0.0106	94.20
140	1.9639	526.33	0.0111	89.99
150	1.9932	538.62	0.0116	86.27
160	2.0222	551.02	0.0121	82.94
170	2.0508	563.55	0.0125	79.95
180	2.0792	576.26	0.0130	77.22
190	2.1073	589.15	0.0134	74.72
200	2.1353	602.25	0.0138	72.43
210	2.1632	615.58	0.0142	70.31
220	2.1910	629.15	0.0146	68.33
230	2.2187	642.98	0.0150	66.49

(Continued)

TABLE 7.18 ***(Continued)***

Properties of Superheated Vapour for R407C

t, °C	s, kJ/kgK	h, kJ/kg	v, m³/kg	ρ, kg/m³
State Points at P = 35 bar				
Saturated Liquid at Bubble Point				
71.60	1.4126	331.35	0.0011	892.86
Saturated Vapour at Dew Point				
74.61	1.6979	430.18	0.0052	193.42
Superheated Vapour				
80	1.7272	440.43	0.0057	174.62
90	1.7711	456.15	0.0065	153.43
100	1.8092	470.19	0.0072	139.57
110	1.8443	483.47	0.0077	129.27
120	1.8776	496.37	0.0083	121.10
130	1.9095	509.08	0.0087	114.35
140	1.9405	521.73	0.0092	108.63
150	1.9707	534.37	0.0096	103.66
160	2.0004	547.08	0.0101	99.30
170	2.0296	559.88	0.0105	95.42
180	2.0585	572.81	0.0109	91.92
190	2.0871	585.91	0.0113	88.75
200	2.1154	599.20	0.0116	85.86
210	2.1437	612.69	0.0120	83.20
220	2.1718	626.41	0.0124	80.75
230	2.1998	640.38	0.0127	78.47
240	2.2278	654.62	0.0131	76.35
State Points at P = 40 bar				
Saturated Liquid at Bubble Point				
78.48	1.4694	351.87	0.0012	826.45
Saturated Vapour at Dew Point				
80.67	1.6727	423.61	0.0040	249.38
Superheated Vapour				
90	1.7334	445.35	0.0051	197.97
100	1.7784	461.92	0.0058	173.38
110	1.8172	476.59	0.0064	157.41
120	1.8528	490.40	0.0069	145.61
130	1.8864	503.78	0.0073	136.29
140	1.9187	516.94	0.0078	128.61
150	1.9499	530.00	0.0082	122.12
160	1.9804	543.04	0.0086	116.50
170	2.0102	556.14	0.0090	111.57
180	2.0397	569.33	0.0093	107.19
190	2.0687	582.64	0.0097	103.25

(Continued)

TABLE 7.18 *(Continued)*

Properties of Superheated Vapour for R407C

t, °C	s, kJ/kgK	h, kJ/kg	v, m³/kg	ρ, kg/m³
200	2.0975	596.12	0.0100	99.69
210	2.1261	609.79	0.0104	96.43
220	2.1546	623.67	0.0107	93.45
230	2.1829	637.78	0.0110	90.69
240	2.2112	652.16	0.0113	88.14
250	2.2394	666.81	0.0117	85.76
State Points at P = 43 bar				
Saturated Liquid at Bubble Point				
82.40	1.5095	366.56	0.0013	775.19
Saturated Vapour at Dew Point				
83.94	1.6499	416.60	0.0034	297.62
Superheated Vapour				
90	1.7061	436.83	0.0043	235.15
100	1.7588	456.23	0.0051	197.64
110	1.8008	472.09	0.0057	176.47
120	1.8382	486.60	0.0062	161.70
130	1.8730	500.46	0.0066	150.41
140	1.9061	513.97	0.0071	141.32
150	1.9380	527.31	0.0075	133.73
160	1.9690	540.58	0.0079	127.25
170	1.9993	553.86	0.0082	121.61
180	2.0291	567.21	0.0086	116.63
190	2.0585	580.67	0.0089	112.18
200	2.0875	594.27	0.0092	108.17
210	2.1163	608.05	0.0096	104.53
220	2.1450	622.03	0.0099	101.20
230	2.1735	636.23	0.0102	98.14
240	2.2019	650.68	0.0105	95.31
250	2.2303	665.41	0.0108	92.68

7.4.8 Refrigerant R410A

This fluid is a ZEB of R32/125 with composition of 50/50 in percent by mass (see Table 7.19, Figure 7.24, Figure 7.25, and Table 7.20).

Critical point: t_c = 74.67°C and p_c = 51.74 bar

TABLE 7.19

Saturated Liquid and Saturated Vapour Properties for R410A

t, °C	p, bar	v_{vap}, m³/kg	h_{liq}, kJ/kg	h_{vap}, kJ/kg	s_{liq}, kJ/kgK	s_{vap}, kJ/kgK
–80	0.202	1.08368	93.07	379.69	0.5427	2.0266
–78	0.231	0.95696	95.47	380.94	0.5551	2.0179
–76	0.264	0.84752	97.87	382.19	0.5673	2.0095
–74	0.300	0.75270	100.28	383.45	0.5795	2.0013

(Continued)

TABLE 7.19 ***(Continued)***

Saturated Liquid and Saturated Vapour Properties for R410A

t, °C	p, bar	v_{vap}, m³/kg	h_{liq}, kJ/kg	h_{vap}, kJ/kg	s_{liq}, kJ/kgK	s_{vap}, kJ/kgK
–72	0.339	0.67030	102.70	384.70	0.5916	1.9935
–70	0.383	0.59849	105.14	385.95	0.6036	1.9859
–68	0.432	0.53571	107.58	387.20	0.6155	1.9785
–66	0.485	0.48068	110.03	388.44	0.6274	1.9714
–64	0.544	0.43231	112.50	389.69	0.6393	1.9646
–62	0.608	0.38969	114.98	390.93	0.6510	1.9579
–60	0.679	0.35203	117.47	392.16	0.6628	1.9515
–58	0.755	0.31868	119.97	393.40	0.6744	1.9453
–56	0.839	0.28907	122.48	394.63	0.6860	1.9393
–54	0.929	0.26272	125.01	395.85	0.6976	1.9335
–52	1.027	0.23922	127.55	397.07	0.7091	1.9278
–50	1.134	0.21819	130.11	398.28	0.7206	1.9223
–48	1.248	0.19938	132.68	399.49	0.7320	1.9170
–46	1.372	0.18250	135.26	400.68	0.7434	1.9119
–44	1.506	0.16731	137.86	401.87	0.7547	1.9069
–42	1.649	0.15363	140.47	403.06	0.7661	1.9020
–40	1.803	0.14128	143.10	404.23	0.7773	1.8973
–38	1.968	0.13011	145.75	405.39	0.7886	1.8928
–36	2.144	0.11999	148.41	406.54	0.7998	1.8883
–34	2.333	0.11081	151.08	407.69	0.8110	1.8840
–32	2.534	0.10246	153.78	408.82	0.8222	1.8798
–30	2.749	0.09485	156.49	409.93	0.8333	1.8756
–28	2.977	0.08792	159.22	411.04	0.8444	1.8716
–26	3.220	0.08158	161.97	412.13	0.8555	1.8677
–24	3.478	0.07579	164.74	413.21	0.8666	1.8639
–22	3.751	0.07048	167.53	414.27	0.8777	1.8601
–20	4.041	0.06561	170.35	415.31	0.8888	1.8564
–18	4.348	0.06113	173.18	416.34	0.8998	1.8528
–16	4.673	0.05702	176.03	417.35	0.9109	1.8493
–14	5.016	0.05322	178.91	418.34	0.9219	1.8458
–12	5.378	0.04972	181.81	419.32	0.9330	1.8424
–10	5.759	0.04649	184.74	420.27	0.9440	1.8390
–8	6.161	0.04350	187.69	421.20	0.9551	1.8357
–6	6.584	0.04074	190.67	422.10	0.9661	1.8324
–4	7.029	0.03817	193.68	422.99	0.9772	1.8292
–2	7.496	0.03579	196.71	423.84	0.9883	1.8260
0	7.986	0.03358	199.77	424.67	0.9994	1.8228
2	8.501	0.03153	202.87	425.48	1.0106	1.8196
4	9.041	0.02961	205.99	426.25	1.0217	1.8164
6	9.606	0.02783	209.15	427.00	1.0329	1.8133
8	10.198	0.02616	212.35	427.71	1.0441	1.8101
10	10.817	0.02461	215.60	428.38	1.0555	1.8070
12	11.464	0.02316	218.87	429.03	1.0668	1.8038
14	12.140	0.02180	222.18	429.63	1.0781	1.8006

(Continued)

TABLE 7.19 ***(Continued)***

Saturated Liquid and Saturated Vapour Properties for R410A

t, °C	p, bar	v_{vap}, m^3/kg	h_{liq}, kJ/kg	h_{vap}, kJ/kg	s_{liq}, kJ/kgK	s_{vap}, kJ/kgK
16	12.846	0.02052	225.53	430.20	1.0895	1.7974
18	13.582	0.01933	228.92	430.72	1.1010	1.7941
20	14.350	0.01821	232.36	431.20	1.1126	1.7908
22	15.151	0.01716	235.85	431.63	1.1242	1.7875
24	15.985	0.01617	239.39	432.01	1.1359	1.7841
26	16.854	0.01524	242.99	432.34	1.1476	1.7806
28	17.758	0.01436	246.64	432.61	1.1595	1.7770
30	18.698	0.01353	250.36	432.82	1.1715	1.7734
32	19.676	0.01275	254.14	432.97	1.1836	1.7697
34	20.692	0.01201	257.99	433.04	1.1959	1.7658
36	21.747	0.01132	261.91	433.05	1.2083	1.7618
38	22.843	0.01066	265.92	432.97	1.2208	1.7577
40	23.981	0.01003	270.02	432.80	1.2336	1.7534
42	25.161	0.00944	274.21	432.54	1.2465	1.7489
44	26.385	0.00887	278.51	432.17	1.2597	1.7442
46	27.654	0.00834	282.93	431.69	1.2731	1.7392
48	28.970	0.00782	287.47	431.07	1.2869	1.7340
50	30.333	0.00734	292.16	430.32	1.3009	1.7285
52	31.745	0.00687	297.02	429.40	1.3154	1.7225
54	33.207	0.00642	302.06	428.29	1.3303	1.7161
56	34.720	0.00599	307.32	426.96	1.3457	1.7092
58	36.287	0.00558	312.83	425.38	1.3618	1.7017
60	37.908	0.00518	318.64	423.48	1.3787	1.6934
62	39.585	0.00478	324.86	421.20	1.3966	1.6840
64	41.320	0.00440	331.58	418.41	1.4158	1.6734
66	43.114	0.00401	339.00	414.93	1.4370	1.6609
68	44.971	0.00362	414.91	410.39	1.6587	1.6454

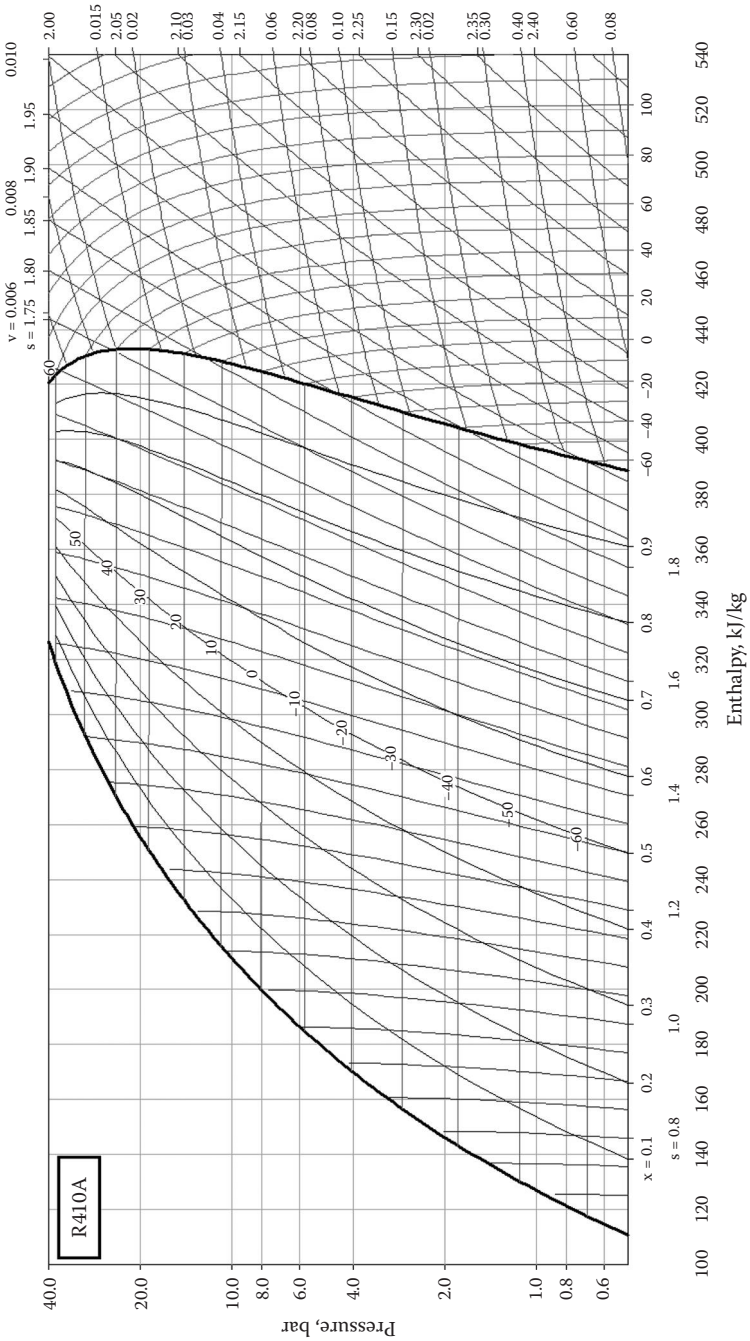

FIGURE 7.24
Pressure–enthalpy diagram for refrigerant R410A.

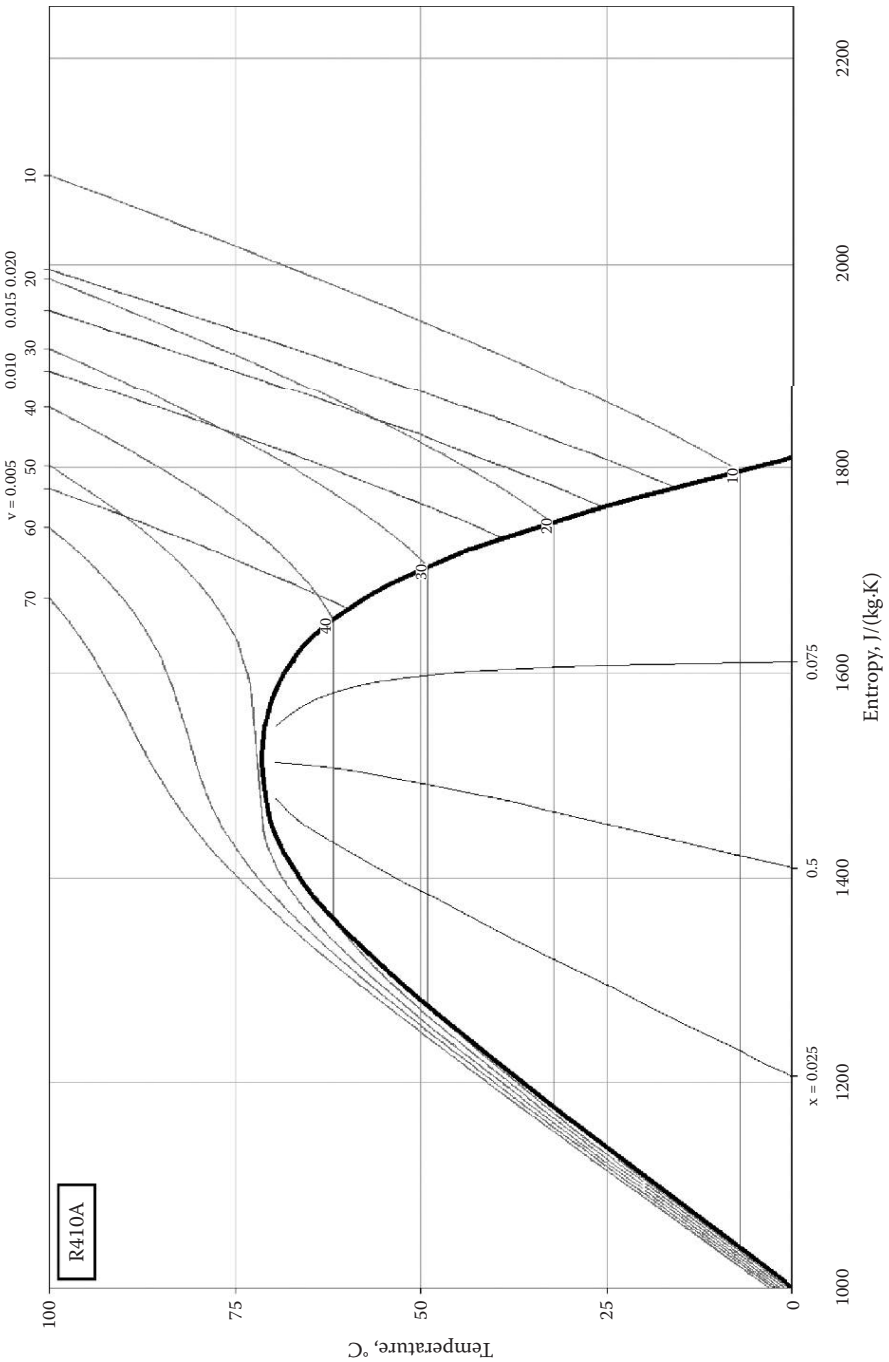

FIGURE 7.25
Temperature–entropy diagram for refrigerant R410A.

TABLE 7.20

Properties of Superheated Vapour for R410A

t, °C	s, kJ/kgK	h, kJ/kg	v, m^3/kg	ρ, kg/m^3
State Points at P = 1.01 bar				
Saturated Liquid at Bubble Point				
–52.41	0.7069	127.12	0.0007	1388.89
Saturated Vapour at Dew Point				
–52.33	1.9288	396.87	0.2430	4.11
Superheated Vapour				
–50	1.9362	398.52	0.2458	4.07
–40	1.9677	405.71	0.2577	3.88
–30	1.9985	413.03	0.2695	3.71
–20	2.0285	420.49	0.2813	3.56
–10	2.0580	428.08	0.2930	3.41
0	2.0868	435.83	0.3047	3.28
10	2.1152	443.71	0.3163	3.16
20	2.1431	451.74	0.3280	3.05
30	2.1705	459.92	0.3396	2.94
40	2.1975	468.24	0.3512	2.85
50	2.2241	476.70	0.3628	2.76
60	2.2504	485.32	0.3743	2.67
70	2.2763	494.08	0.3859	2.59
80	2.3019	503.00	0.3974	2.52
90	2.3272	512.06	0.4089	2.45
State Points at P = 5 bar				
Saturated Liquid at Bubble Point				
–14.21	0.9212	178.78	0.0008	1250.00
Saturated Vapour at Dew Point				
–14.08	1.8460	418.31	0.0534	18.73
Superheated Vapour				
–10	1.8587	421.61	0.0545	18.35
0	1.8891	429.77	0.0572	17.48
10	1.9188	438.02	0.0599	16.70
20	1.9478	446.39	0.0625	16.00
30	1.9762	454.86	0.0651	15.36
40	2.0041	463.46	0.0677	14.78
50	2.0315	472.18	0.0702	14.24
60	2.0585	481.02	0.0727	13.75
70	2.0850	490.00	0.0753	13.29
80	2.1112	499.11	0.0777	12.86
90	2.1370	508.35	0.0802	12.47
100	2.1625	517.73	0.0827	12.09
110	2.1877	527.25	0.0851	11.75

(Continued)

TABLE 7.20 ***(Continued)***

Properties of Superheated Vapour for R410A

t, °C	s, kJ/kgK	h, kJ/kg	v, m³/kg	ρ, kg/m³
120	2.2126	536.92	0.0876	11.42
130	2.2372	546.72	0.0900	11.11
140	2.2616	556.67	0.0924	10.82
State Points at P = 10 bar				
Saturated Liquid at Bubble Point				
7.18	1.0402	211.29	0.0009	1149.43
Saturated Vapour at Dew Point				
7.35	1.8112	427.49	0.0267	37.45
Superheated Vapour				
10	1.8196	429.87	0.0271	36.87
20	1.8509	438.86	0.0287	34.86
30	1.8811	447.88	0.0302	33.12
40	1.9105	456.94	0.0317	31.59
50	1.9392	466.07	0.0331	30.22
60	1.9673	475.28	0.0345	28.99
70	1.9948	484.59	0.0359	27.87
80	2.0218	493.99	0.0372	26.85
90	2.0484	503.51	0.0386	25.92
100	2.0745	513.14	0.0399	25.05
110	2.1003	522.89	0.0412	24.26
120	2.1258	532.76	0.0425	23.51
130	2.1509	542.75	0.0438	22.82
140	2.1757	552.88	0.0451	22.17
150	2.2002	563.14	0.0464	21.56
160	2.2245	573.54	0.0476	20.99
State Points at P = 15 bar				
Saturated Liquid at Bubble Point				
21.47	1.1218	235.20	0.0009	1075.27
Saturated Vapour at Dew Point				
21.64	1.7881	431.56	0.0174	57.64
Superheated Vapour				
30	1.8158	439.84	0.0184	54.45
40	1.8476	449.62	0.0195	51.24
50	1.8781	459.35	0.0206	48.51
60	1.9077	469.06	0.0217	46.14
70	1.9365	478.79	0.0227	44.05
80	1.9646	488.57	0.0237	42.19
90	1.9921	498.42	0.0247	40.52
100	2.0191	508.34	0.0256	39.00
110	2.0455	518.35	0.0266	37.62

(Continued)

TABLE 7.20 ***(Continued)***

Properties of Superheated Vapour for R410A

t, °C	s, kJ/kgK	h, kJ/kg	v, m³/kg	ρ, kg/m³
120	2.0716	528.47	0.0275	36.35
130	2.0973	538.68	0.0284	35.18
140	2.1226	549.01	0.0293	34.10
150	2.1475	559.46	0.0302	33.09
160	2.1722	570.02	0.0311	32.15
170	2.1966	580.71	0.0320	31.26
180	2.2208	591.53	0.0329	30.43
State Points at P = 20 bar				
Saturated Liquid at Bubble Point				
32.47	1.1874	255.37	0.0010	1000.00
Saturated Vapour at Dew Point				
32.65	1.7685	433.01	0.0125	79.94
Superheated Vapour				
40	1.7946	441.08	0.0133	75.25
50	1.8281	451.75	0.0143	70.07
60	1.8599	462.18	0.0152	65.83
70	1.8904	472.50	0.0161	62.26
80	1.9199	482.77	0.0169	59.18
90	1.9486	493.03	0.0177	56.49
100	1.9765	503.31	0.0185	54.10
110	2.0038	513.64	0.0192	51.96
120	2.0306	524.03	0.0200	50.02
130	2.0569	534.50	0.0207	48.26
140	2.0827	545.05	0.0214	46.64
150	2.1082	555.70	0.0221	45.15
160	2.1333	566.46	0.0228	43.77
170	2.1581	577.32	0.0235	42.49
180	2.1826	588.30	0.0242	41.29
190	2.2068	599.39	0.0249	40.17
State Points at P = 25 bar				
Saturated Liquid at Bubble Point				
41.56	1.2446	273.64	0.0011	934.58
Saturated Vapour at Dew Point				
41.74	1.7495	432.59	0.0095	105.15
Superheated Vapour				
50	1.7815	442.78	0.0103	96.75
60	1.8169	454.40	0.0112	89.14
70	1.8500	465.57	0.0120	83.16
80	1.8814	476.50	0.0128	78.26
90	1.9115	487.30	0.0135	74.11

(Continued)

TABLE 7.20 ***(Continued)***

Properties of Superheated Vapour for R410A

t, °C	s, kJ/kgK	h, kJ/kg	v, m³/kg	ρ, kg/m³
100	1.9406	498.02	0.0142	70.53
110	1.9689	508.72	0.0148	67.40
120	1.9965	519.44	0.0155	64.61
130	2.0236	530.19	0.0161	62.11
140	2.0500	541.00	0.0167	59.84
150	2.0760	551.88	0.0173	57.78
160	2.1016	562.83	0.0179	55.88
170	2.1269	573.88	0.0185	54.14
180	2.1517	585.03	0.0190	52.52
190	2.1763	596.28	0.0196	51.02
200	2.2006	607.65	0.0202	49.61
State Points at P = 30 bar				
Saturated Liquid at Bubble Point				
49.35	1.2974	291.02	0.0012	862.07
Saturated Vapour at Dew Point				
49.52	1.7298	430.52	0.0075	134.23
Superheated Vapour				
50	1.7321	431.25	0.0075	133.25
60	1.7746	445.20	0.0085	118.13
70	1.8118	457.75	0.0093	107.84
80	1.8459	469.63	0.0100	100.03
90	1.8780	481.14	0.0107	93.77
100	1.9087	492.42	0.0113	88.55
110	1.9382	503.58	0.0119	84.10
120	1.9668	514.68	0.0125	80.22
130	1.9946	525.76	0.0130	76.81
140	2.0218	536.85	0.0136	73.76
150	2.0484	547.98	0.0141	71.01
160	2.0745	559.16	0.0146	68.51
170	2.1002	570.41	0.0151	66.23
180	2.1255	581.74	0.0156	64.13
190	2.1504	593.16	0.0161	62.19
200	2.1750	604.67	0.0166	60.39
State Points at P = 35 bar				
Saturated Liquid at Bubble Point				
56.21	1.3485	308.29	0.0013	787.40
Saturated Vapour at Dew Point				
56.37	1.7080	426.70	0.0059	168.92
Superheated Vapour				
60	1.7279	433.31	0.0063	158.02
70	1.7731	448.58	0.0072	138.32

(Continued)

TABLE 7.20 ***(Continued)***

Properties of Superheated Vapour for R410A

t, °C	s, kJ/kgK	h, kJ/kg	v, m³/kg	ρ, kg/m³
80	1.8115	461.96	0.0080	125.50
90	1.8464	474.46	0.0086	115.99
100	1.8790	486.46	0.0092	108.46
110	1.9100	498.19	0.0098	102.25
120	1.9398	509.74	0.0103	96.99
130	1.9686	521.19	0.0108	92.43
140	1.9965	532.61	0.0113	88.43
150	2.0238	544.01	0.0118	84.87
160	2.0505	555.44	0.0122	81.67
170	2.0767	566.90	0.0127	78.77
180	2.1024	578.42	0.0131	76.13
190	2.1277	590.02	0.0136	73.70
200	2.1526	601.69	0.0140	71.46
210	2.1772	613.46	0.0144	69.38
State Points at P = 40 bar				
Saturated Liquid at Bubble Point				
62.35	1.4011	326.43	0.0014	704.23
Saturated Vapour at Dew Point				
62.49	1.6816	420.59	0.0047	213.22
Superheated Vapour				
70	1.7301	437.01	0.0056	179.30
80	1.7764	453.13	0.0064	156.36
90	1.8154	467.10	0.0071	141.57
100	1.8507	480.08	0.0077	130.68
110	1.8835	492.50	0.0082	122.09
120	1.9147	504.60	0.0087	115.04
130	1.9446	516.49	0.0092	109.07
140	1.9734	528.26	0.0096	103.91
150	2.0014	539.97	0.0101	99.39
160	2.0287	551.66	0.0105	95.38
170	2.0554	563.36	0.0109	91.77
180	2.0816	575.09	0.0113	88.51
190	2.1073	586.87	0.0117	85.54
200	2.1326	598.71	0.0121	82.81
210	2.1575	610.62	0.0125	80.30
220	2.1821	622.62	0.0128	77.97

7.4.9 Refrigerant R507A

This fluid is an AZB of R125/143a with composition of 50/50 in percent by mass (see Table 7.21, Figure 7.26, Figure 7.27, and Table 7.22).

Critical point: t_c = 70.9°C and p_c = 37.94 bar

TABLE 7.21

Saturated Liquid and Saturated Vapour Properties for R507A

t, °C	p, bar	v_{vap}, m³/kg	h_{liq}, kJ/kg	h_{vap}, kJ/kg	s_{liq}, kJ/kgK	s_{vap}, kJ/kgK
–80	0.139	1.15764	101.34	327.20	0.5747	1.7441
–78	0.160	1.01174	103.76	328.15	0.5872	1.7370
–76	0.184	0.88728	106.18	329.09	0.5995	1.7302
–74	0.211	0.78072	108.60	330.03	0.6117	1.7236
–72	0.241	0.68916	111.04	330.98	0.6239	1.7173
–70	0.275	0.61021	113.48	331.93	0.6360	1.7113
–68	0.312	0.54192	115.93	332.87	0.6479	1.7054
–66	0.353	0.48264	118.38	333.82	0.6598	1.6998
–64	0.399	0.43104	120.84	334.76	0.6716	1.6944
–62	0.448	0.38598	123.31	335.71	0.6833	1.6893
–60	0.503	0.34652	125.78	336.65	0.6950	1.6843
–58	0.563	0.31186	128.25	337.60	0.7065	1.6795
–56	0.628	0.28133	130.73	338.54	0.7179	1.6749
–54	0.699	0.25438	133.21	339.48	0.7293	1.6705
–52	0.777	0.23051	135.69	340.41	0.7405	1.6662
–50	0.861	0.20933	138.18	341.35	0.7517	1.6622
–48	0.952	0.19049	140.66	342.28	0.7628	1.6582
–46	1.050	0.17369	143.15	343.21	0.7737	1.6544
–44	1.155	0.15867	145.64	344.13	0.7846	1.6508
–42	1.269	0.14521	148.13	345.06	0.7954	1.6473
–40	1.391	0.13314	150.62	345.97	0.8061	1.6439
–38	1.523	0.12227	153.11	346.89	0.8166	1.6407
–36	1.663	0.11248	155.59	347.80	0.8271	1.6376
–34	1.813	0.10363	158.08	348.70	0.8375	1.6346
–32	1.973	0.09563	160.56	349.60	0.8478	1.6317
–30	2.144	0.08837	163.05	350.50	0.8580	1.6289
–28	2.325	0.08178	165.53	351.39	0.8681	1.6263
–26	2.518	0.07578	168.01	352.28	0.8781	1.6237
–24	2.723	0.07032	170.48	353.15	0.8880	1.6212
–22	2.940	0.06533	172.95	354.03	0.8978	1.6188
–20	3.170	0.06076	175.42	354.90	0.9075	1.6165
–18	3.414	0.05658	177.89	355.76	0.9172	1.6143
–16	3.671	0.05275	180.36	356.61	0.9267	1.6121
–14	3.942	0.04923	182.82	357.46	0.9362	1.6101
–12	4.228	0.04599	185.28	358.30	0.9455	1.6081
–10	4.529	0.04300	187.74	359.13	0.9548	1.6061
–8	4.846	0.04025	190.20	359.96	0.9640	1.6043
–6	5.179	0.03770	192.65	360.77	0.9731	1.6025
–4	5.529	0.03535	195.11	361.58	0.9822	1.6007

(Continued)

TABLE 7.21 ***(Continued)***

Saturated Liquid and Saturated Vapour Properties for R507A

t, °C	p, bar	v_{vap}, m³/kg	h_{liq}, kJ/kg	h_{vap}, kJ/kg	s_{liq}, kJ/kgK	s_{vap}, kJ/kgK
–2	5.896	0.03317	197.54	362.38	0.9911	1.5990
0	6.282	0.03115	200.00	363.17	1.0000	1.5974
2	6.686	0.02927	202.46	363.94	1.0088	1.5957
4	7.108	0.02752	204.92	364.71	1.0176	1.5942
6	7.551	0.02590	207.38	365.47	1.0263	1.5926
8	8.014	0.02438	209.85	366.21	1.0350	1.5911
10	8.498	0.02297	212.33	366.94	1.0436	1.5897
12	9.004	0.02165	214.81	367.65	1.0522	1.5882
14	9.532	0.02041	217.31	368.35	1.0608	1.5868
16	10.084	0.01925	219.81	369.04	1.0693	1.5854
18	10.659	0.01817	222.34	369.71	1.0778	1.5840
20	11.258	0.01715	224.87	370.36	1.0863	1.5826
22	11.883	0.01619	227.43	370.99	1.0948	1.5812
24	12.534	0.01529	230.02	371.60	1.1033	1.5798
26	13.212	0.01444	232.62	372.19	1.1118	1.5784
28	13.919	0.01365	235.26	372.75	1.1204	1.5770
30	14.653	0.01289	237.94	373.29	1.1290	1.5755
32	15.418	0.01218	240.65	373.81	1.1377	1.5740
34	16.213	0.01151	243.41	374.29	1.1464	1.5725
36	17.041	0.01087	246.23	374.74	1.1553	1.5710
38	17.901	0.01026	249.10	375.15	1.1643	1.5694
40	18.795	0.00969	252.04	375.53	1.1734	1.5678
42	19.724	0.00914	255.06	375.86	1.1827	1.5660
44	20.689	0.00862	258.17	376.15	1.1922	1.5642
46	21.692	0.00813	261.39	376.38	1.2020	1.5623
48	22.734	0.00765	264.73	376.56	1.2121	1.5603
50	23.816	0.00720	268.21	376.67	1.2225	1.5582
52	24.940	0.00676	271.86	376.71	1.2334	1.5559
54	26.107	0.00634	275.71	376.66	1.2448	1.5534
56	27.319	0.00594	279.80	376.52	1.2568	1.5507
58	28.578	0.00554	284.20	376.25	1.2697	1.5477
60	29.884	0.00515	288.98	375.84	1.2836	1.5443
62	31.241	0.00477	294.26	375.24	1.2989	1.5405
64	32.649	0.00439	300.26	374.40	1.3162	1.5361
66	34.112	0.00399	307.34	373.19	1.3365	1.5307
68	35.630	0.00355	316.37	371.35	1.3625	1.5236
70	37.207	0.00297	330.84	367.90	1.4040	1.5120

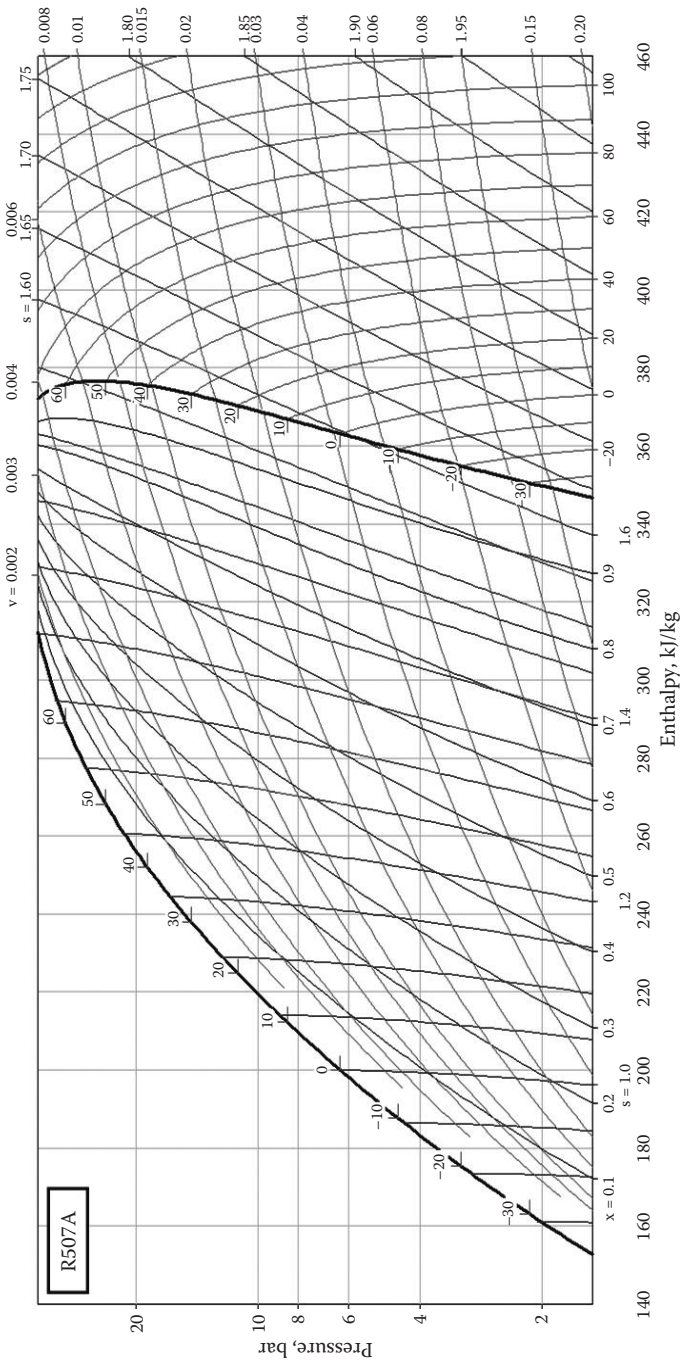

FIGURE 7.26
Pressure–enthalpy diagram for refrigerant R507A.

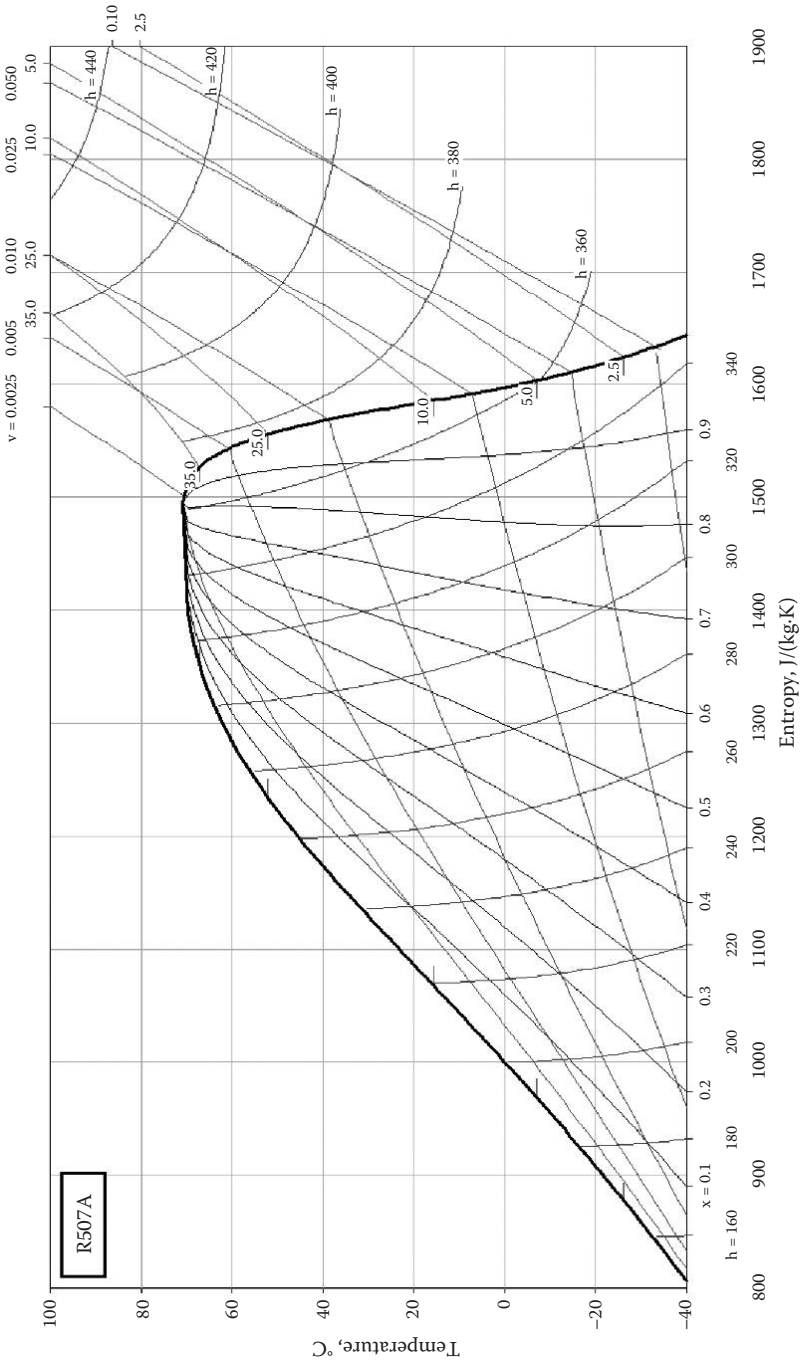

FIGURE 7.27
Temperature–entropy diagram for refrigerant R507A.

TABLE 7.22

Properties of Superheated Vapour for R507A

t, °C	s, kJ/kgK	h, kJ/kg	v, m^3/kg	ρ, kg/m^3
State Points at P = 1.01 bar				
Saturated Liquid at Bubble Point				
–46.79	0.7694	142.17	0.0008	1315.79
Saturated Vapour at Dew Point				
–46.79	1.6559	342.84	0.1801	5.55
Superheated Vapour				
–40	1.6747	347.15	0.1865	5.36
–30	1.7019	353.63	0.1957	5.11
–20	1.7286	360.25	0.2048	4.88
–10	1.7548	367.03	0.2137	4.68
0	1.7807	373.97	0.2226	4.49
10	1.8063	381.09	0.2314	4.32
20	1.8316	388.37	0.2401	4.17
30	1.8566	395.82	0.2487	4.02
40	1.8813	403.45	0.2574	3.89
50	1.9058	411.24	0.2659	3.76
60	1.9301	419.21	0.2745	3.64
70	1.9542	427.35	0.2830	3.53
80	1.9780	435.65	0.2915	3.43
90	2.0017	444.12	0.3000	3.33
100	2.0251	452.75	0.3085	3.24
110	2.0484	461.54	0.3170	3.15
120	2.0714	470.49	0.3254	3.07
State Points at P = 5 bar				
Saturated Liquid at Bubble Point				
–7.06	0.9683	191.35	0.0009	1176.47
Saturated Vapour at Dew Point				
–7.06	1.6034	360.34	0.0390	25.62
Superheated Vapour				
0	1.6246	366.06	0.0407	24.58
10	1.6536	374.11	0.0429	23.31
20	1.6815	382.17	0.0450	22.20
30	1.7087	390.26	0.0471	21.22
40	1.7352	398.43	0.0491	20.35
50	1.7612	406.69	0.0511	19.57
60	1.7866	415.05	0.0530	18.86
70	1.8117	423.52	0.0549	18.20
80	1.8364	432.12	0.0568	17.60
90	1.8607	440.84	0.0587	17.05
100	1.8848	449.69	0.0605	16.53

(Continued)

TABLE 7.22 ***(Continued)***

Properties of Superheated Vapour for R507A

t, °C	s, kJ/kgK	h, kJ/kg	v, m³/kg	ρ, kg/m³
110	1.9085	458.68	0.0623	16.04
120	1.9320	467.80	0.0641	15.59
130	1.9553	477.06	0.0659	15.17
140	1.9783	486.45	0.0677	14.76
150	2.0011	495.98	0.0695	14.39
160	2.0237	505.64	0.0713	14.03
170	2.0460	515.44	0.0731	13.69
State Points at P = 10 bar				
Saturated Liquid at Bubble Point				
15.70	1.0680	219.44	0.0009	1086.96
Saturated Vapour at Dew Point				
15.70	1.5856	368.94	0.0194	51.49
Superheated Vapour				
20	1.5996	373.02	0.0200	49.94
30	1.6308	382.31	0.0214	46.84
40	1.6603	391.41	0.0226	44.27
50	1.6886	400.42	0.0238	42.09
60	1.7160	409.40	0.0249	40.19
70	1.7426	418.39	0.0260	38.51
80	1.7685	427.42	0.0270	37.00
90	1.7939	436.51	0.0281	35.65
100	1.8188	445.68	0.0291	34.41
110	1.8433	454.95	0.0301	33.27
120	1.8674	464.31	0.0310	32.23
130	1.8912	473.78	0.0320	31.26
140	1.9147	483.36	0.0329	30.35
150	1.9379	493.06	0.0339	29.50
160	1.9608	502.87	0.0348	28.71
170	1.9835	512.80	0.0358	27.96
180	2.0059	522.85	0.0367	27.26
190	2.0281	533.02	0.0376	26.59
200	2.0501	543.30	0.0385	25.96
210	2.0718	553.70	0.0394	25.36
State Points at P = 15 bar				
Saturated Liquid at Bubble Point				
30.92	1.1330	239.18	0.0010	1020.41
Saturated Vapour at Dew Point				
30.92	1.5748	373.53	0.0126	79.62
Superheated Vapour				
40	1.6061	383.17	0.0135	73.90
50	1.6379	393.29	0.0145	68.97

(Continued)

TABLE 7.22 ***(Continued)***

Properties of Superheated Vapour for R507A

t, °C	s, kJ/kgK	h, kJ/kg	v, m³/kg	ρ, kg/m³
60	1.6678	403.12	0.0154	64.98
70	1.6964	412.78	0.0162	61.62
80	1.7239	422.36	0.0170	58.73
90	1.7506	431.90	0.0178	56.21
100	1.7765	441.45	0.0185	53.96
110	1.8019	451.03	0.0193	51.94
120	1.8267	460.67	0.0200	50.10
130	1.8511	470.38	0.0206	48.43
140	1.8751	480.17	0.0213	46.89
150	1.8987	490.05	0.0220	45.46
160	1.9220	500.03	0.0227	44.14
170	1.9450	510.11	0.0233	42.90
180	1.9677	520.28	0.0240	41.74
190	1.9902	530.57	0.0246	40.66
200	2.0124	540.96	0.0252	39.63
210	2.0343	551.46	0.0259	38.67
220	2.0560	562.06	0.0265	37.75
State Points at P = 20 bar				
Saturated Liquid at Bubble Point				
42.58	1.1855	255.96	0.0011	952.38
Saturated Vapour at Dew Point				
42.58	1.5655	375.95	0.0090	111.23
Superheated Vapour				
50	1.5932	384.80	0.0097	103.21
60	1.6272	395.93	0.0105	95.06
70	1.6585	406.53	0.0113	88.75
80	1.6881	416.82	0.0120	83.62
90	1.7163	426.93	0.0126	79.32
100	1.7435	436.94	0.0132	75.61
110	1.7698	446.91	0.0138	72.36
120	1.7955	456.86	0.0144	69.49
130	1.8206	466.84	0.0149	66.90
140	1.8451	476.87	0.0155	64.54
150	1.8692	486.95	0.0160	62.40
160	1.8930	497.10	0.0165	60.42
170	1.9163	507.34	0.0171	58.60
180	1.9393	517.66	0.0176	56.90
190	1.9621	528.07	0.0181	55.32
200	1.9845	538.57	0.0186	53.84
210	2.0067	549.17	0.0191	52.45
220	2.0286	559.87	0.0196	51.14

(Continued)

TABLE 7.22 ***(Continued)***

Properties of Superheated Vapour for R507A

t, °C	s, kJ/kgK	h, kJ/kg	v, m³/kg	ρ, kg/m³
State Points at P = 25 bar				
Saturated Liquid at Bubble Point				
52.10	1.2340	272.05	0.0011	884.96
Saturated Vapour at Dew Point				
52.10	1.5557	376.71	0.0067	148.37
Superheated Vapour				
60	1.5878	387.26	0.0074	134.44
70	1.6235	399.34	0.0082	122.18
80	1.6560	410.65	0.0088	113.11
90	1.6863	421.50	0.0094	105.95
100	1.7151	432.09	0.0100	100.05
110	1.7426	442.51	0.0105	95.06
120	1.7693	452.84	0.0110	90.74
130	1.7951	463.13	0.0115	86.93
140	1.8203	473.42	0.0120	83.54
150	1.8450	483.73	0.0124	80.50
160	1.8692	494.08	0.0129	77.72
170	1.8929	504.49	0.0133	75.18
180	1.9163	514.96	0.0137	72.84
190	1.9393	525.51	0.0141	70.67
200	1.9620	536.14	0.0146	68.66
210	1.9844	546.85	0.0150	66.78
220	2.0065	557.65	0.0154	65.02
230	2.0284	568.53	0.0158	63.37
State Points at P = 30 bar				
Saturated Liquid at Bubble Point				
60.17	1.2849	289.42	0.0012	806.45
Saturated Vapour at Dew Point				
60.17	1.5440	375.79	0.0051	195.31
Superheated Vapour				
70	1.5877	390.57	0.0060	167.30
80	1.6249	403.51	0.0067	150.06
90	1.6582	415.43	0.0073	137.83
100	1.6890	426.77	0.0078	128.42
110	1.7181	437.77	0.0083	120.80
120	1.7459	448.56	0.0087	114.44
130	1.7727	459.22	0.0092	108.98
140	1.7986	469.81	0.0096	104.22
150	1.8239	480.38	0.0100	100.00
160	1.8486	490.95	0.0104	96.22

(Continued)

TABLE 7.22 ***(Continued)***

Properties of Superheated Vapour for R507A

t, °C	s, kJ/kgK	h, kJ/kg	v, m³/kg	ρ, kg/m³
170	1.8728	501.55	0.0108	92.81
180	1.8965	512.19	0.0111	89.69
190	1.9199	522.88	0.0115	86.83
200	1.9428	533.64	0.0119	84.19
210	1.9655	544.47	0.0122	81.74
220	1.9878	555.37	0.0126	79.46
230	2.0099	566.35	0.0129	77.33
240	2.0316	577.42	0.0133	75.34
250	2.0532	588.57	0.0136	73.46
State Points at P = 35 bar				
Saturated Liquid at Bubble Point				
67.18	1.3509	312.32	0.0014	699.30
Saturated Vapour at Dew Point				
67.18	1.5268	372.21	0.0037	267.38
Superheated Vapour				
70	1.5440	378.09	0.0041	245.20
80	1.5916	394.64	0.0049	202.04
90	1.6299	408.34	0.0056	178.68
100	1.6637	420.79	0.0061	162.85
110	1.6948	432.56	0.0066	150.96
120	1.7241	443.92	0.0071	141.51
130	1.7520	455.04	0.0075	133.69
140	1.7789	465.99	0.0079	127.05
150	1.8048	476.86	0.0082	121.29
160	1.8301	487.68	0.0086	116.22
170	1.8548	498.49	0.0090	111.70
180	1.8789	509.31	0.0093	107.63
190	1.9026	520.17	0.0096	103.94
200	1.9259	531.07	0.0099	100.56
210	1.9488	542.02	0.0103	97.44
220	1.9714	553.04	0.0106	94.56
230	1.9937	564.13	0.0109	91.88
240	2.0156	575.28	0.0112	89.38
250	2.0373	586.52	0.0115	87.04
260	2.0587	597.83	0.0118	84.85

7.4.10 Refrigerant R600a

This fluid is from miscellaneous organic compounds with chemical name 2-methyl propane (isobutane) and formula $CH(CH_3)_3$ (see Table 7.23, Figure 7.28, Figure 7.29, and Table 7.24).

Critical point: t_c = 135.92°C and p_c = 36.85 bar

TABLE 7.23

Saturated Liquid and Saturated Vapour Properties for R600a

t, °C	p, bar	v_{vap}, m³/kg	h_{liq}, kJ/kg	h_{vap}, kJ/kg	s_{liq}, kJ/kgK	s_{vap}, kJ/kgK
–64	0.071	4.18089	59.96	472.30	0.4172	2.3887
–61	0.087	3.48480	66.57	476.01	0.4486	2.3785
–58	0.105	2.92289	73.15	479.74	0.4793	2.3691
–55	0.125	2.46620	79.68	483.49	0.5095	2.3605
–52	0.150	2.09261	86.19	487.26	0.5391	2.3527
–49	0.178	1.78512	92.69	491.06	0.5683	2.3455
–46	0.210	1.53054	99.17	494.88	0.5970	2.3390
–43	0.246	1.31859	105.64	498.72	0.6253	2.3332
–40	0.288	1.14119	112.12	502.58	0.6532	2.3279
–37	0.334	0.99195	118.59	506.46	0.6807	2.3232
–34	0.387	0.86580	125.07	510.36	0.7080	2.3190
–31	0.447	0.75866	131.57	514.28	0.7349	2.3154
–28	0.513	0.66726	138.07	518.21	0.7616	2.3122
–25	0.586	0.58897	144.60	522.16	0.7880	2.3095
–22	0.668	0.52163	151.14	526.13	0.8141	2.3072
–19	0.759	0.46348	157.71	530.11	0.8401	2.3054
–16	0.859	0.41308	164.30	534.10	0.8658	2.3039
–13	0.969	0.36924	170.92	538.11	0.8913	2.3028
–10	1.090	0.33098	177.57	542.13	0.9167	2.3020
–7	1.222	0.29747	184.26	546.16	0.9419	2.3016
–4	1.366	0.26803	190.98	550.20	0.9669	2.3015
–1	1.522	0.24209	197.74	554.25	0.9917	2.3017
2	1.693	0.21917	204.54	558.31	1.0165	2.3022
5	1.878	0.19886	211.38	562.37	1.0411	2.3030
8	2.077	0.18080	218.26	566.44	1.0656	2.3040
11	2.293	0.16472	225.20	570.51	1.0900	2.3052
14	2.525	0.15035	232.18	574.59	1.1143	2.3067
17	2.775	0.13748	239.22	578.67	1.1385	2.3084
20	3.042	0.12594	246.31	582.75	1.1627	2.3103
23	3.329	0.11555	253.46	586.83	1.1867	2.3124
26	3.636	0.10618	260.67	590.90	1.2108	2.3147
29	3.964	0.09772	267.94	594.97	1.2348	2.3171
32	4.314	0.09006	275.28	599.03	1.2587	2.3197
35	4.686	0.08312	282.68	603.09	1.2826	2.3224
38	5.082	0.07680	290.16	607.13	1.3065	2.3253
41	5.502	0.07105	297.71	611.17	1.3304	2.3283
44	5.948	0.06580	305.34	615.19	1.3543	2.3313
47	6.420	0.06102	313.01	619.19	1.3781	2.3345

(Continued)

TABLE 7.23 ***(Continued)***

Saturated Liquid and Saturated Vapour Properties for R600a

t, °C	p, bar	v_{vap}, m³/kg	h_{liq}, kJ/kg	h_{vap}, kJ/kg	s_{liq}, kJ/kgK	s_{vap}, kJ/kgK
50	6.919	0.05663	320.80	623.17	1.4021	2.3378
53	7.446	0.05261	328.67	627.14	1.4260	2.3411
56	8.003	0.04891	336.64	631.07	1.4500	2.3445
59	8.589	0.04551	344.71	634.98	1.4741	2.3480
62	9.207	0.04238	352.88	638.85	1.4982	2.3514
65	9.857	0.03949	361.15	642.69	1.5224	2.3549
68	10.541	0.03681	369.54	646.48	1.5467	2.3584
71	11.258	0.03434	378.05	650.23	1.5711	2.3619
74	12.011	0.03205	386.69	653.93	1.5956	2.3654
77	12.800	0.02992	395.47	657.56	1.6203	2.3688
80	13.626	0.02794	404.39	661.14	1.6452	2.3722
83	14.490	0.02609	413.48	664.64	1.6703	2.3755
86	15.394	0.02437	422.75	668.05	1.6957	2.3787
89	16.338	0.02276	432.21	671.38	1.7213	2.3817
92	17.324	0.02126	441.88	674.60	1.7473	2.3846
95	18.352	0.01985	451.79	677.69	1.7737	2.3873
98	19.423	0.01852	461.95	680.66	1.8005	2.3898
101	20.538	0.01728	472.40	683.46	1.8278	2.3919
104	21.697	0.01610	483.18	686.09	1.8558	2.3938
107	22.902	0.01499	494.32	688.50	1.8844	2.3952
110	24.153	0.01394	505.87	690.67	1.9138	2.3961
113	25.451	0.01293	517.90	692.54	1.9442	2.3965
116	26.794	0.01198	530.50	694.05	1.9758	2.3961
119	28.184	0.01105	543.76	695.11	2.0087	2.3947
122	29.620	0.01016	557.87	695.59	2.0435	2.3920
125	31.101	0.00929	573.06	695.29	2.0807	2.3877
128	32.625	0.00841	589.82	693.85	2.1213	2.3807
131	34.192	0.00751	609.14	690.48	2.1680	2.3692
134	35.798	0.00646	634.10	682.85	2.2279	2.3476

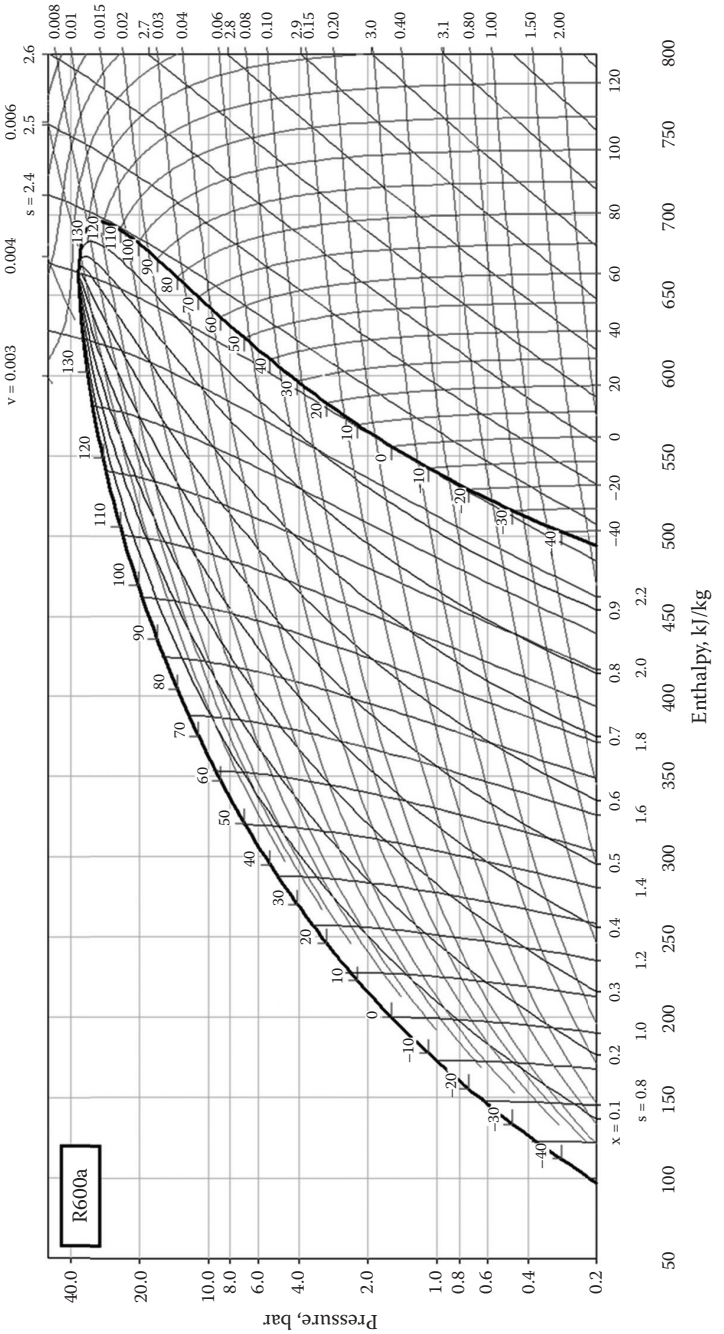

FIGURE 7.28
Pressure–enthalpy diagram for refrigerant R600a.

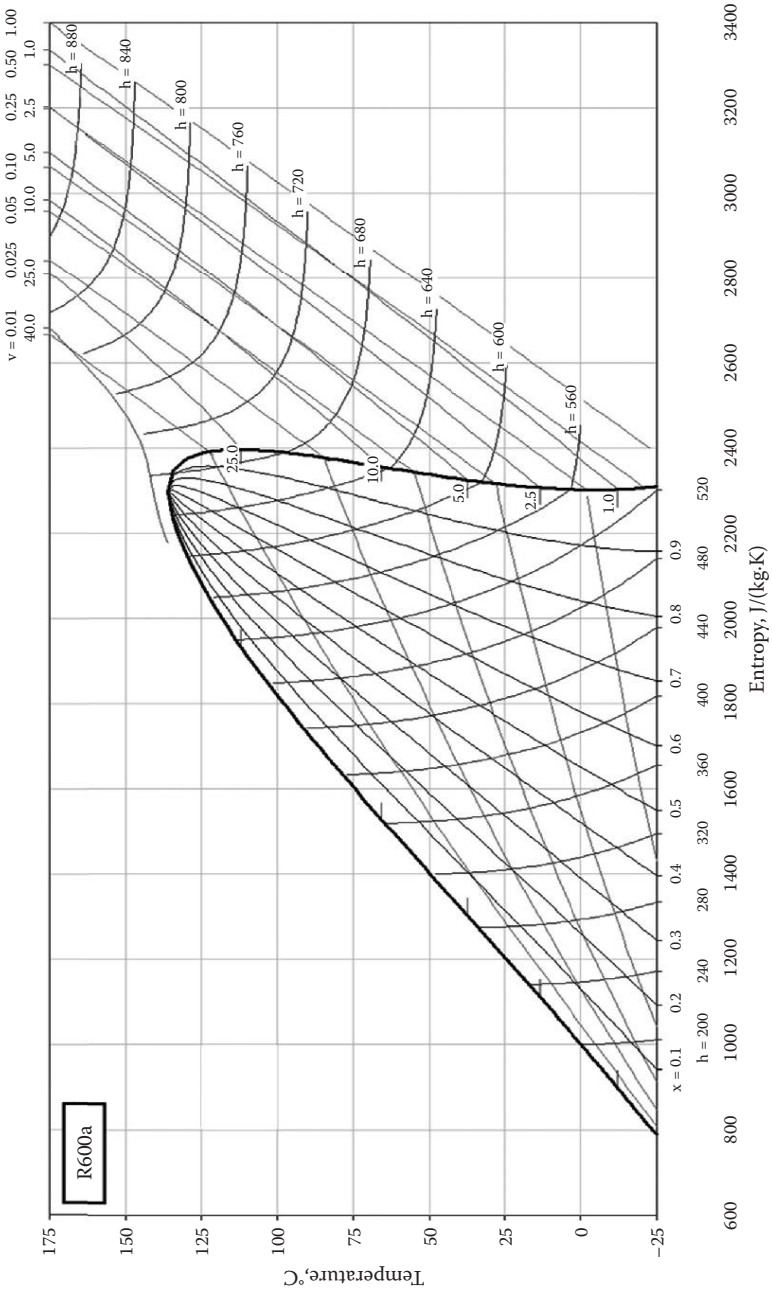

FIGURE 7.29
Temperature–entropy diagram for refrigerant R600a.

TABLE 7.24

Properties of Superheated Vapour for R600a

t, °C	s, kJ/kgK	h, kJ/kg	v, m^3/kg	ρ, kg/m^3
State Points at P = 1.01 bar				
Saturated Liquid at Bubble Point				
–11.95	0.9003	173.25	0.0017	595.24
Saturated Vapour at Dew Point				
–11.95	2.3025	539.52	0.3553	2.82
Superheated Vapour				
–10	2.3139	542.52	0.3582	2.79
0	2.3723	558.18	0.3736	2.68
10	2.4301	574.25	0.3889	2.57
20	2.4874	590.75	0.4040	2.48
30	2.5442	607.70	0.4190	2.39
40	2.6006	625.09	0.4339	2.30
50	2.6567	642.93	0.4487	2.23
60	2.7125	661.23	0.4635	2.16
70	2.7679	679.98	0.4782	2.09
80	2.8231	699.19	0.4928	2.03
90	2.8780	718.85	0.5075	1.97
100	2.9326	738.96	0.5220	1.92
110	2.9870	759.53	0.5366	1.86
120	3.0412	780.54	0.5511	1.81
130	3.0950	801.99	0.5656	1.77
140	3.1487	823.88	0.5800	1.72
150	3.2021	846.21	0.5945	1.68
State Points at P = 5 bar				
Saturated Liquid at Bubble Point				
37.39	1.3017	288.64	0.0019	537.63
Saturated Vapour at Dew Point				
37.39	2.3247	606.32	0.0780	12.82
Superheated Vapour				
40	2.3404	611.22	0.0790	12.66
50	2.4001	630.21	0.0827	12.09
60	2.4589	649.49	0.0863	11.59
70	2.5169	669.10	0.0898	11.14
80	2.5742	689.07	0.0932	10.73
90	2.6310	709.41	0.0966	10.35
100	2.6873	730.12	0.0999	10.01
110	2.7431	751.23	0.1032	9.69
120	2.7985	772.72	0.1065	9.39
130	2.8535	794.62	0.1097	9.12
140	2.9081	816.91	0.1128	8.86
150	2.9624	839.60	0.1160	8.62

(Continued)

TABLE 7.24 ***(Continued)***

Properties of Superheated Vapour for R600a

t, °C	s, kJ/kgK	h, kJ/kg	v, m³/kg	ρ, kg/m³
160	3.0163	862.70	0.1191	8.39
170	3.0699	886.19	0.1222	8.18
180	3.1232	910.07	0.1253	7.98
190	3.1762	934.35	0.1284	7.79
200	3.2289	959.03	0.1315	7.61
210	3.2813	984.08	0.1345	7.43
State Points at P = 10 bar				
Saturated Liquid at Bubble Point				
65.64	1.5275	362.93	0.0020	495.05
Saturated Vapour at Dew Point				
65.64	2.3557	643.50	0.0389	25.71
Superheated Vapour				
70	2.3831	652.84	0.0399	25.07
80	2.4447	674.30	0.0421	23.77
90	2.5050	695.89	0.0441	22.66
100	2.5641	717.66	0.0461	21.68
110	2.6224	739.68	0.0480	20.81
120	2.6798	761.98	0.0499	20.03
130	2.7366	784.58	0.0517	19.32
140	2.7927	807.50	0.0535	18.68
150	2.8484	830.75	0.0553	18.08
160	2.9035	854.35	0.0570	17.54
170	2.9581	878.30	0.0587	17.03
180	3.0124	902.60	0.0604	16.55
190	3.0662	927.26	0.0621	16.11
200	3.1196	952.28	0.0637	15.69
210	3.1727	977.65	0.0654	15.30
220	3.2254	1003.39	0.0670	14.93
230	3.2778	1029.48	0.0686	14.58
240	3.3299	1055.93	0.0702	14.25
250	3.3816	1082.74	0.0718	13.93
260	3.4330	1109.89	0.0733	13.64
State Points at P = 15 bar				
Saturated Liquid at Bubble Point				
84.71	1.6847	418.74	0.0022	458.72
Saturated Vapour at Dew Point				
84.71	2.3773	666.59	0.0251	39.84
Superheated Vapour				
90	2.4124	679.23	0.0261	38.37
100	2.4765	702.83	0.0278	36.03
110	2.5386	726.30	0.0293	34.09

(Continued)

TABLE 7.24 ***(Continued)***

Properties of Superheated Vapour for R600a

t, °C	s, kJ/kgK	h, kJ/kg	v, m³/kg	ρ, kg/m³
120	2.5990	749.78	0.0308	32.44
130	2.6583	773.36	0.0322	31.01
140	2.7165	797.12	0.0336	29.75
150	2.7738	821.10	0.0349	28.63
160	2.8304	845.34	0.0362	27.61
170	2.8864	869.85	0.0375	26.68
180	2.9417	894.65	0.0387	25.84
190	2.9965	919.76	0.0399	25.06
200	3.0508	945.18	0.0411	24.33
210	3.1047	970.93	0.0423	23.66
220	3.1581	997.00	0.0434	23.03
230	3.2111	1023.40	0.0446	22.44
240	3.2637	1050.13	0.0457	21.89
250	3.3159	1077.20	0.0468	21.37
260	3.3678	1104.59	0.0479	20.88
270	3.4193	1132.32	0.0490	20.41
State Points at P = 20 bar				
Saturated Liquid at Bubble Point				
99.57	1.8147	467.38	0.0024	421.94
Saturated Vapour at Dew Point				
99.57	2.3909	682.14	0.0179	55.99
Superheated Vapour				
100	2.3941	683.32	0.0179	55.74
110	2.4640	709.75	0.0196	51.13
120	2.5298	735.29	0.0210	47.67
130	2.5930	760.43	0.0223	44.89
140	2.6542	785.43	0.0235	42.57
150	2.7140	810.41	0.0246	40.59
160	2.7725	835.49	0.0257	38.87
170	2.8301	860.72	0.0268	37.34
180	2.8868	886.14	0.0278	35.97
190	2.9428	911.79	0.0288	34.74
200	2.9982	937.70	0.0298	33.61
210	3.0529	963.88	0.0307	32.58
220	3.1071	990.33	0.0316	31.62
230	3.1608	1017.09	0.0325	30.74
240	3.2140	1044.14	0.0334	29.92
250	3.2668	1071.49	0.0343	29.15
260	3.3192	1099.15	0.0352	28.42
270	3.3712	1127.12	0.0360	27.74

(Continued)

TABLE 7.24 ***(Continued)***

Properties of Superheated Vapour for R600a

t, °C	s, kJ/kgK	h, kJ/kg	v, m³/kg	ρ, kg/m³
State Points at P = 25 bar				
Saturated Liquid at Bubble Point				
111.97	1.9337	513.72	0.0026	380.23
Saturated Vapour at Dew Point				
111.97	2.3964	691.93	0.0133	75.36
Superheated Vapour				
120	2.4595	716.47	0.0146	68.35
130	2.5304	744.70	0.0160	62.42
140	2.5968	771.77	0.0172	58.05
150	2.6602	798.28	0.0183	54.58
160	2.7215	824.55	0.0193	51.72
170	2.7813	850.73	0.0203	49.28
180	2.8398	876.96	0.0212	47.17
190	2.8973	903.29	0.0221	45.30
200	2.9539	929.78	0.0229	43.64
210	3.0097	956.46	0.0237	42.13
220	3.0648	983.36	0.0245	40.77
230	3.1193	1010.52	0.0253	39.52
240	3.1732	1037.92	0.0261	38.36
250	3.2266	1065.60	0.0268	37.29
260	3.2796	1093.56	0.0276	36.30
270	3.3320	1121.79	0.0283	35.37
280	3.3841	1150.32	0.0290	34.50
290	3.4357	1179.13	0.0297	33.68
State Points at P = 30 bar				
Saturated Liquid at Bubble Point				
122.78	2.0529	561.69	0.0030	330.03
Saturated Vapour at Dew Point				
122.78	2.3911	695.60	0.0099	100.70
Superheated Vapour				
130	2.4598	723.03	0.0114	87.92
140	2.5376	754.77	0.0128	78.16
150	2.6075	783.99	0.0140	71.68
160	2.6731	812.10	0.0150	66.81
170	2.7360	839.65	0.0159	62.93
180	2.7969	866.94	0.0168	59.70
190	2.8563	894.13	0.0176	56.94
200	2.9144	921.34	0.0183	54.54
210	2.9715	948.63	0.0191	52.42

(Continued)

TABLE 7.24 ***(Continued)***

Properties of Superheated Vapour for R600a

t, °C	s, kJ/kgK	h, kJ/kg	v, m³/kg	ρ, kg/m³
220	3.0277	976.07	0.0198	50.53
230	3.0831	1003.68	0.0205	48.82
240	3.1378	1031.49	0.0212	47.26
250	3.1919	1059.53	0.0218	45.83
260	3.2455	1087.81	0.0225	44.51
270	3.2985	1116.34	0.0231	43.29
280	3.3510	1145.14	0.0237	42.15
290	3.4031	1174.20	0.0243	41.09
300	3.4547	1203.53	0.0249	40.10
310	3.5059	1233.14	0.0255	39.16
State Points at P = 35 bar				
Saturated Liquid at Bubble Point				
132.52	2.1956	620.65	0.0039	254.45
Saturated Vapour at Dew Point				
132.52	2.3604	687.48	0.0070	142.65
Superheated Vapour				
140	2.4647	730.14	0.0092	109.27
150	2.5505	766.02	0.0106	94.25
160	2.6240	797.44	0.0117	85.31
170	2.6917	827.10	0.0127	78.92
180	2.7559	855.88	0.0135	73.95
190	2.8177	884.21	0.0143	69.90
200	2.8778	912.32	0.0150	66.50
210	2.9364	940.36	0.0157	63.56
220	2.9939	968.41	0.0164	60.99
230	3.0504	996.56	0.0170	58.70
240	3.1060	1024.83	0.0177	56.65
250	3.1609	1053.28	0.0183	54.79
260	3.2152	1081.92	0.0188	53.09
270	3.2688	1110.77	0.0194	51.53
280	3.3218	1139.85	0.0200	50.09
290	3.3744	1169.18	0.0205	48.75
300	3.4264	1198.75	0.0211	47.50
310	3.4780	1228.58	0.0216	46.33
320	3.5292	1258.66	0.0221	45.23
330	3.5799	1289.01	0.0226	44.20

7.4.11 Refrigerant R717

This natural fluid is from inorganic compounds with chemical name ammonia and formula NH_3 (see Table 7.25, Figure 7.30, Figure 7.31, and Table 7.26).

Critical point: t_c = 132.35°C and p_c = 113.53 bar

TABLE 7.25

Saturated Liquid and Saturated Vapour Properties for R717

t, °C	p, bar	v_{vap}, m³/kg	h_{liq}, kJ/kg	h_{vap}, kJ/kg	s_{liq}, kJ/kgK	s_{vap}, kJ/kgK
–70	0.109	9.00587	–110.78	1356.08	–0.3102	6.9103
–67	0.136	7.35392	–97.81	1361.49	–0.2468	6.8320
–64	0.167	6.04553	–84.81	1366.85	–0.1843	6.7565
–61	0.205	5.00187	–71.78	1372.16	–0.1225	6.6838
–58	0.249	4.16371	–58.73	1377.40	–0.0614	6.6136
–55	0.302	3.48621	–45.65	1382.57	–0.0010	6.5459
–52	0.362	2.93517	–32.53	1387.66	0.0587	6.4805
–49	0.433	2.48431	–19.38	1392.68	0.1177	6.4173
–46	0.515	2.11333	–6.20	1397.63	0.1760	6.3562
–43	0.609	1.80641	7.01	1402.48	0.2338	6.2971
–40	0.717	1.55117	20.25	1407.25	0.2909	6.2398
–37	0.840	1.33783	33.53	1411.93	0.3474	6.1843
–34	0.980	1.15868	46.84	1416.51	0.4033	6.1305
–31	1.138	1.00753	60.19	1420.99	0.4587	6.0783
–28	1.315	0.87945	73.57	1425.36	0.5135	6.0277
–25	1.515	0.77046	86.98	1429.64	0.5677	5.9784
–22	1.738	0.67733	100.42	1433.80	0.6214	5.9305
–19	1.987	0.59744	113.89	1437.85	0.6746	5.8840
–16	2.263	0.52866	127.40	1441.78	0.7273	5.8386
–13	2.570	0.46923	140.94	1445.59	0.7795	5.7945
–10	2.908	0.41769	154.52	1449.29	0.8312	5.7514
–7	3.280	0.37285	168.12	1452.85	0.8824	5.7094
–4	3.688	0.33371	181.76	1456.29	0.9331	5.6685
–1	4.136	0.29944	195.43	1459.59	0.9833	5.6284
2	4.625	0.26935	209.14	1462.76	1.0332	5.5893
5	5.158	0.24284	222.89	1465.79	1.0825	5.5510
8	5.737	0.21943	236.67	1468.68	1.1315	5.5135
11	6.365	0.19870	250.48	1471.42	1.1800	5.4768
14	7.046	0.18029	264.34	1474.02	1.2281	5.4408
17	7.781	0.16391	278.24	1476.46	1.2759	5.4055
20	8.574	0.14929	292.19	1478.74	1.3232	5.3708
23	9.427	0.13621	306.18	1480.86	1.3703	5.3368
26	10.343	0.12449	320.23	1482.82	1.4169	5.3033
29	11.326	0.11396	334.32	1484.60	1.4633	5.2703
32	12.379	0.10447	348.48	1486.21	1.5093	5.2377
35	13.504	0.09593	362.58	1487.65	1.5547	5.2058
38	14.705	0.08820	376.86	1488.89	1.6002	5.1741
41	15.985	0.08119	391.22	1489.94	1.6454	5.1428
44	17.347	0.07483	405.66	1490.79	1.6904	5.1119

(Continued)

TABLE 7.25 ***(Continued)***

Saturated Liquid and Saturated Vapour Properties for R717

t, °C	p, bar	v_{vap}, m^3/kg	h_{liq}, kJ/kg	h_{vap}, kJ/kg	s_{liq}, kJ/kgK	s_{vap}, kJ/kgK
47	18.795	0.06905	420.19	1491.42	1.7352	5.0812
50	20.331	0.06378	434.82	1491.84	1.7798	5.0508
53	21.961	0.05898	449.56	1492.03	1.8243	5.0206
56	23.686	0.05458	464.42	1491.98	1.8687	4.9906
59	25.512	0.05056	479.40	1491.68	1.9131	4.9607
62	27.440	0.04687	494.54	1491.12	1.9573	4.9309
65	29.476	0.04348	509.83	1490.27	2.0016	4.9011
68	31.622	0.04036	525.29	1489.13	2.0460	4.8713
71	33.884	0.03748	540.95	1487.68	2.0905	4.8414
74	36.264	0.03482	556.83	1485.89	2.1351	4.8113
77	38.767	0.03236	572.94	1483.74	2.1799	4.7810
80	41.397	0.03009	589.32	1481.19	2.2250	4.7505
83	44.159	0.02797	606.00	1478.23	2.2705	4.7195
86	47.057	0.02601	623.00	1474.81	2.3164	4.6881
89	50.096	0.02418	640.38	1470.88	2.3628	4.6561
92	53.281	0.02247	658.18	1466.39	2.4100	4.6233
95	56.616	0.02087	676.46	1461.28	2.4579	4.5897
98	60.107	0.01937	695.29	1455.47	2.5068	4.5550
101	63.760	0.01796	714.75	1448.87	2.5569	4.5190
104	67.580	0.01663	734.94	1441.34	2.6084	4.4814
107	71.574	0.01537	756.02	1432.74	2.6616	4.4418
110	75.748	0.01418	778.14	1422.84	2.7171	4.3997
113	80.111	0.01303	801.55	1411.38	2.7752	4.3545
116	84.670	0.01193	826.59	1397.92	2.8370	4.3051
119	89.435	0.01086	853.77	1381.84	2.9035	4.2501
122	94.417	0.00979	883.92	1362.09	2.9767	4.1868
125	99.629	0.00870	918.54	1336.69	3.0604	4.1107
128	105.09	0.00752	961.21	1300.81	3.1632	4.0098
131	110.833	0.00599	1024.83	1235.28	3.3167	3.8374

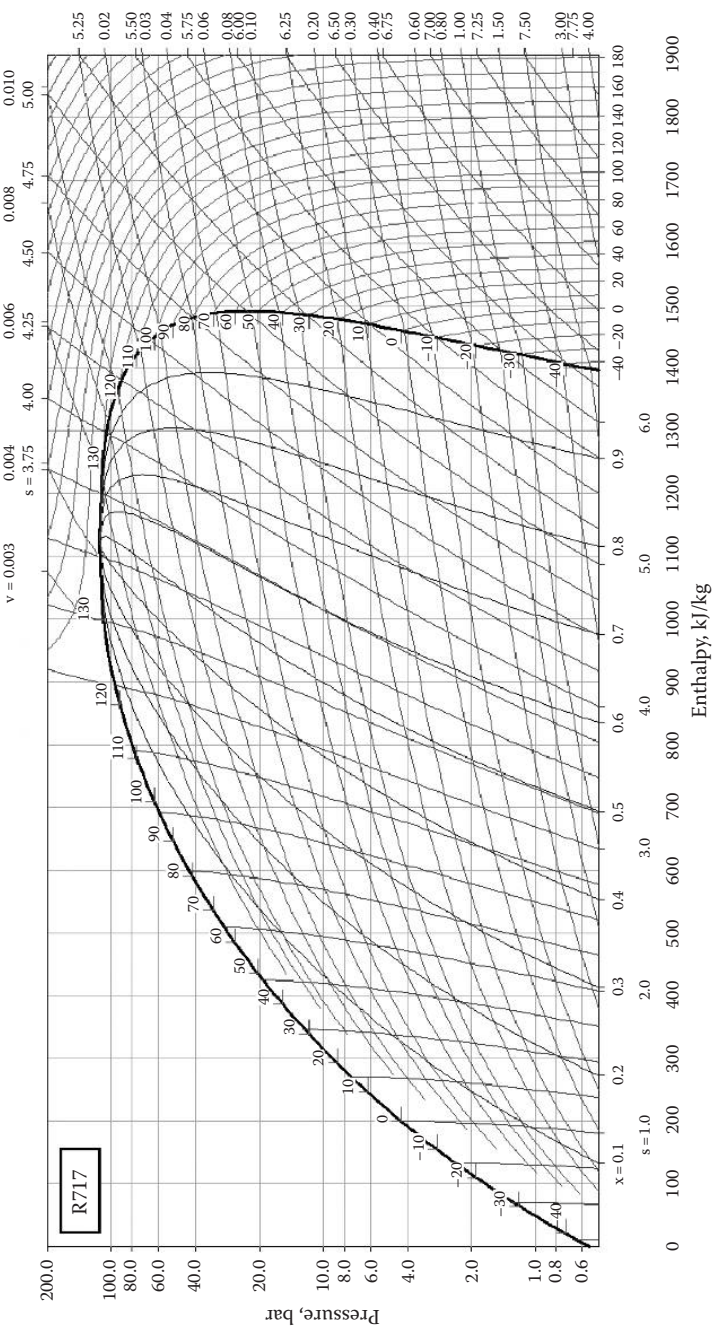

FIGURE 7.30
Pressure–enthalpy diagram for refrigerant R717.

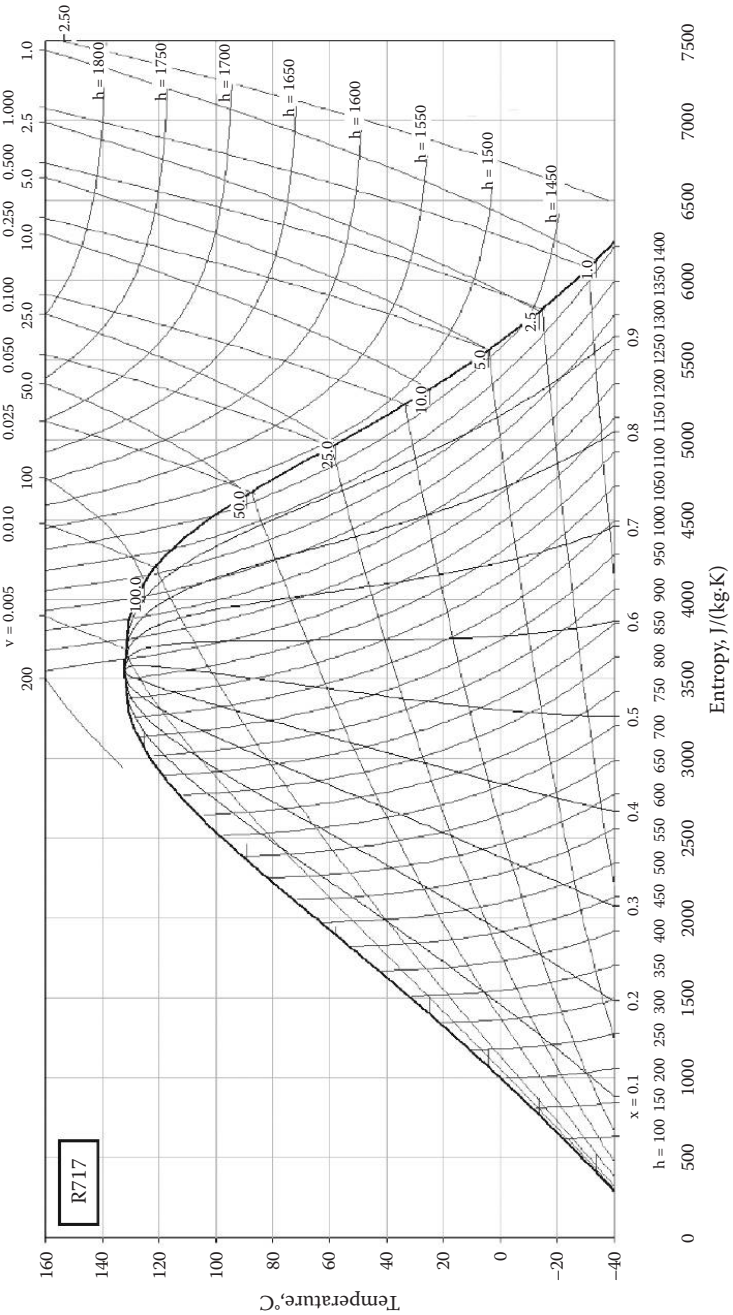

FIGURE 7.31
Temperature–entropy diagram for refrigerant R717.

TABLE 7.26

Properties of Superheated Vapour for R717

t, °C	s, kJ/kgK	h, kJ/kg	v, m^3/kg	ρ, kg/m^3
State Points at P = 1.01 bar				
Saturated Liquid at Bubble Point				
–33.40	4.1453	49.53	0.0015	680.27
Saturated Vapour at Dew Point				
–33.40	6.1199	1417.42	1.1261	0.89
Superheated Vapour				
–30	6.1519	1425.15	1.1442	0.87
–20	6.2426	1447.65	1.1968	0.84
–10	6.3286	1469.84	1.2485	0.80
0	6.4106	1491.83	1.2997	0.77
10	6.4892	1513.70	1.3503	0.74
20	6.5649	1535.50	1.4006	0.71
30	6.6379	1557.28	1.4506	0.69
40	6.7087	1579.08	1.5004	0.67
50	6.7774	1600.93	1.5499	0.65
60	6.8442	1622.85	1.5993	0.63
70	6.9093	1644.85	1.6486	0.61
80	6.9728	1666.97	1.6977	0.59
90	7.0349	1689.20	1.7468	0.57
100	7.0956	1711.56	1.7957	0.56
110	7.1551	1734.07	1.8446	0.54
State Points at P = 5 bar				
Saturated Liquid at Bubble Point				
4.14	1.0684	218.94	0.0016	632.91
Saturated Vapour at Dew Point				
4.14	5.5619	1464.94	0.2501	4.00
Superheated Vapour				
10	5.6182	1480.71	0.2573	3.89
20	5.7088	1506.80	0.2693	3.71
30	5.7936	1532.09	0.2809	3.56
40	5.8738	1556.78	0.2922	3.42
50	5.9501	1581.05	0.3032	3.30
60	6.0231	1605.01	0.3141	3.18
70	6.0933	1628.76	0.3248	3.08
80	6.1611	1652.37	0.3354	2.98
90	6.2268	1675.89	0.3459	2.89
100	6.2906	1699.38	0.3564	2.81
110	6.3527	1722.86	0.3667	2.73
120	6.4133	1746.38	0.3770	2.65
130	6.4725	1769.96	0.3872	2.58
140	6.5305	1793.62	0.3974	2.52

(Continued)

TABLE 7.26 ***(Continued)***

Properties of Superheated Vapour for R717

t, °C	s, kJ/kgK	h, kJ/kg	v, m³/kg	ρ, kg/m³
150	6.5874	1817.39	0.4076	2.45
160	6.6431	1841.27	0.4177	2.39
State Points at P = 10 bar				
Saturated Liquid at Bubble Point				
24.90	1.3999	315.07	0.0017	602.41
Saturated Vapour at Dew Point				
24.90	5.3155	1482.12	0.1286	7.77
Superheated Vapour				
30	5.3669	1497.59	0.1321	7.57
40	5.4614	1526.70	0.1387	7.21
50	5.5489	1554.54	0.1450	6.89
60	5.6309	1581.44	0.1511	6.62
70	5.7084	1607.64	0.1571	6.37
80	5.7822	1633.32	0.1628	6.14
90	5.8528	1658.61	0.1685	5.93
100	5.9208	1683.62	0.1741	5.74
110	5.9864	1708.42	0.1796	5.57
120	6.0499	1733.09	0.1850	5.41
130	6.1117	1757.68	0.1903	5.25
140	6.1719	1782.24	0.1957	5.11
150	6.2306	1806.79	0.2009	4.98
160	6.2880	1831.38	0.2062	4.85
170	6.3443	1856.03	0.2114	4.73
180	6.3995	1880.77	0.2166	4.62
State Points at P = 15 bar				
Saturated Liquid at Bubble Point				
38.71	1.6109	380.25	0.0017	581.40
Saturated Vapour at Dew Point				
38.71	5.1667	1489.16	0.0865	11.56
Superheated Vapour				
40	5.1806	1493.50	0.0871	11.48
50	5.2820	1525.78	0.0920	10.87
60	5.3748	1556.21	0.0966	10.36
70	5.4608	1585.28	0.1009	9.91
80	5.5413	1613.32	0.1052	9.51
90	5.6175	1640.59	0.1092	9.15
100	5.6899	1667.27	0.1132	8.83
110	5.7593	1693.51	0.1171	8.54
120	5.8261	1719.42	0.1209	8.27
130	5.8906	1745.09	0.1247	8.02
140	5.9531	1770.59	0.1284	7.79

(Continued)

TABLE 7.26 ***(Continued)***

Properties of Superheated Vapour for R717

t, °C	s, kJ/kgK	h, kJ/kg	v, m³/kg	ρ, kg/m³
150	6.0138	1795.98	0.1320	7.57
160	6.0730	1821.31	0.1356	7.37
170	6.1307	1846.62	0.1392	7.18
180	6.1873	1871.95	0.1428	7.00
State Points at P = 20 bar				
Saturated Liquid at Bubble Point				
49.37	1.7704	431.73	0.0018	564.97
Saturated Vapour at Dew Point				
49.37	5.0572	1491.77	0.0649	15.42
Superheated Vapour				
50	5.0643	1494.07	0.0651	15.36
60	5.1705	1528.91	0.0690	14.48
70	5.2666	1561.40	0.0727	13.75
80	5.3550	1592.18	0.0762	13.13
90	5.4374	1621.69	0.0795	12.58
100	5.5150	1650.24	0.0827	12.09
110	5.5886	1678.06	0.0858	11.65
120	5.6588	1705.31	0.0888	11.26
130	5.7262	1732.14	0.0918	10.90
140	5.7912	1758.65	0.0947	10.56
150	5.8540	1784.93	0.0975	10.25
160	5.9150	1811.04	0.1004	9.96
170	5.9743	1837.04	0.1031	9.70
180	6.0322	1862.99	0.1059	9.44
190	6.0888	1888.92	0.1086	9.21
State Points at P = 25 bar				
Saturated Liquid at Bubble Point				
58.18	1.9009	475.27	0.0018	549.45
Saturated Vapour at Dew Point				
58.18	4.9689	1491.79	0.0516	19.37
Superheated Vapour				
60	4.9902	1498.87	0.0523	19.13
70	5.0990	1535.64	0.0556	17.99
80	5.1968	1569.70	0.0587	17.05
90	5.2864	1601.79	0.0616	16.24
100	5.3697	1632.45	0.0643	15.55
110	5.4479	1662.01	0.0670	14.93
120	5.5219	1690.74	0.0695	14.38
130	5.5925	1718.82	0.0720	13.89
140	5.6601	1746.42	0.0744	13.43
150	5.7252	1773.63	0.0768	13.02

(Continued)

TABLE 7.26 ***(Continued)***

Properties of Superheated Vapour for R717

t, °C	s, kJ/kgK	h, kJ/kg	v, m³/kg	ρ, kg/m³
160	5.7881	1800.57	0.0792	12.63
170	5.8491	1827.30	0.0815	12.28
180	5.9085	1853.89	0.0837	11.94
190	5.9663	1880.39	0.0860	11.63
200	6.0228	1906.85	0.0882	11.34
State Points at P = 30 bar				
Saturated Liquid at Bubble Point				
65.75	2.0127	513.66	0.0019	534.76
Saturated Vapour at Dew Point				
65.75	4.8937	1490.02	0.0427	23.44
Superheated Vapour				
70	4.9447	1507.42	0.0440	22.73
80	5.0542	1545.53	0.0469	21.34
90	5.1524	1580.70	0.0495	20.20
100	5.2423	1613.78	0.0520	19.23
110	5.3256	1645.30	0.0544	18.40
120	5.4038	1675.65	0.0566	17.66
130	5.4778	1705.09	0.0588	17.00
140	5.5482	1733.85	0.0609	16.41
150	5.6157	1762.07	0.0630	15.87
160	5.6807	1789.87	0.0650	15.38
170	5.7435	1817.37	0.0670	14.92
180	5.8043	1844.64	0.0690	14.50
190	5.8635	1871.74	0.0709	14.11
200	5.9211	1898.74	0.0728	13.74
210	5.9775	1925.67	0.0746	13.40
State Points at P = 35 bar				
Saturated Liquid at Bubble Point				
72.43	2.1116	548.47	0.0019	520.83
Saturated Vapour at Dew Point				
72.43	4.8271	1486.87	0.0362	27.63
Superheated Vapour				
80	4.9197	1519.21	0.0383	26.12
90	5.0284	1558.15	0.0408	24.51
100	5.1260	1594.06	0.0431	23.19
110	5.2153	1627.82	0.0453	22.07
120	5.2981	1659.96	0.0474	21.11
130	5.3758	1690.91	0.0493	20.26
140	5.4494	1720.92	0.0513	19.51
150	5.5194	1750.21	0.0531	18.83
160	5.5865	1778.95	0.0549	18.21

(Continued)

TABLE 7.26 ***(Continued)***

Properties of Superheated Vapour for R717

t, °C	s, kJ/kgK	h, kJ/kg	v, m³/kg	ρ, kg/m³
170	5.6511	1807.25	0.0567	17.65
180	5.7136	1835.22	0.0584	17.13
190	5.7741	1862.96	0.0601	16.64
200	5.8330	1890.51	0.0617	16.20
210	5.8904	1917.95	0.0634	15.78
220	5.9464	1945.31	0.0650	15.38
State Points at P = 40 bar				
Saturated Liquid at Bubble Point				
78.42	2.2013	580.69	0.0020	510.20
Saturated Vapour at Dew Point				
78.42	4.7666	1482.58	0.0313	31.99
Superheated Vapour				
80	4.7877	1490.02	0.0317	31.56
90	4.9099	1533.76	0.0342	29.27
100	5.0167	1573.10	0.0364	27.47
110	5.1129	1609.44	0.0385	26.00
120	5.2010	1643.64	0.0404	24.76
130	5.2829	1676.23	0.0422	23.68
140	5.3597	1707.60	0.0440	22.74
150	5.4325	1738.05	0.0457	21.90
160	5.5019	1767.77	0.0473	21.14
170	5.5685	1796.93	0.0489	20.45
180	5.6326	1825.65	0.0505	19.82
190	5.6946	1854.03	0.0520	19.24
200	5.7547	1882.17	0.0535	18.70
210	5.8131	1910.13	0.0549	18.20
220	5.8702	1937.96	0.0564	17.73
230	5.9259	1965.72	0.0578	17.29
State Points at P = 45 bar				
Saturated Liquid at Bubble Point				
83.89	2.2840	610.98	0.0020	497.51
Saturated Vapour at Dew Point				
83.89	4.7103	1477.27	0.0274	36.52
Superheated Vapour				
90	4.7929	1506.99	0.0289	34.62
100	4.9114	1550.61	0.0311	32.16
110	5.0156	1590.02	0.0331	30.23
120	5.1097	1626.54	0.0349	28.63
130	5.1963	1660.98	0.0367	27.28
140	5.2768	1693.87	0.0383	26.11
150	5.3526	1725.55	0.0399	25.09

(Continued)

TABLE 7.26 ***(Continued)***

Properties of Superheated Vapour for R717

t, °C	s, kJ/kgK	h, kJ/kg	v, m³/kg	ρ, kg/m³
160	5.4245	1756.33	0.0414	24.17
170	5.4931	1786.39	0.0428	23.34
180	5.5589	1815.89	0.0443	22.59
190	5.6224	1844.97	0.0457	21.90
200	5.6838	1873.71	0.0470	21.26
210	5.7434	1902.20	0.0484	20.67
220	5.8014	1930.52	0.0497	20.12
230	5.8580	1958.71	0.0510	19.61
State Points at P = 50 bar				
Saturated Liquid at Bubble Point				
88.91	2.3614	639.84	0.0021	485.44
Saturated Vapour at Dew Point				
88.91	4.6571	1471.01	0.0242	41.27
Superheated Vapour				
90	4.6734	1476.92	0.0245	40.81
100	4.8072	1526.18	0.0268	37.38
110	4.9214	1569.33	0.0287	34.82
120	5.0225	1608.58	0.0305	32.78
130	5.1143	1645.10	0.0322	31.09
140	5.1989	1679.65	0.0337	29.65
150	5.2780	1712.70	0.0352	28.41
160	5.3525	1744.60	0.0366	27.31
170	5.4233	1775.62	0.0380	26.32
180	5.4910	1805.96	0.0393	25.43
190	5.5560	1835.75	0.0406	24.62
200	5.6188	1865.13	0.0419	23.88
210	5.6795	1894.18	0.0431	23.19
220	5.7386	1922.99	0.0443	22.55
230	5.7961	1951.63	0.0455	21.96
State Points at P = 75 bar				
Saturated Liquid at Bubble Point				
109.47	2.7072	774.19	0.0023	427.35
Saturated Vapour at Dew Point				
109.47	4.4073	1424.68	0.0144	69.54
Superheated Vapour				
110	4.4187	1429.03	0.0145	68.89
120	4.5961	1497.87	0.0166	60.14
130	4.7326	1552.18	0.0183	54.66
140	4.8477	1599.13	0.0197	50.68
150	4.9491	1641.53	0.0210	47.56
160	5.0408	1680.80	0.0222	45.01

(Continued)

TABLE 7.26 ***(Continued)***

Properties of Superheated Vapour for R717

t, °C	s, kJ/kgK	h, kJ/kg	v, m³/kg	ρ, kg/m³
170	5.1253	1717.82	0.0233	42.86
180	5.2042	1753.14	0.0244	41.01
190	5.2784	1787.16	0.0254	39.38
200	5.3489	1820.17	0.0264	37.93
210	5.4163	1852.37	0.0273	36.63
220	5.4810	1883.97	0.0282	35.45
230	5.5434	1915.07	0.0291	34.36
240	5.6039	1945.79	0.0300	33.37
250	5.6626	1976.21	0.0308	32.45
State Points at P = 100 bar				
Saturated Liquid at Bubble Point				
125.21	3.0668	921.18	0.0028	355.87
Saturated Vapour at Dew Point				
125.21	4.1047	1334.63	0.0086	115.87
Superheated Vapour				
130	4.2791	1404.50	0.0102	98.28
140	4.4893	1490.18	0.0121	82.48
150	4.6384	1552.53	0.0136	73.77
160	4.7606	1604.79	0.0148	67.76
170	4.8665	1651.19	0.0158	63.21
180	4.9614	1693.71	0.0168	59.57
190	5.0482	1733.49	0.0177	56.54
200	5.1288	1771.23	0.0185	53.95
210	5.2045	1807.41	0.0193	51.70
220	5.2762	1842.39	0.0201	49.72
230	5.3445	1876.43	0.0209	47.95
240	5.4100	1909.71	0.0216	46.35
250	5.4730	1942.39	0.0223	44.90
260	5.5341	1974.62	0.0230	43.57
State Points at P = 112 bar				
Saturated Liquid at Bubble Point				
131.59	3.3663	1045.29	0.0035	286.53
Saturated Vapour at Dew Point				
131.59	3.7738	1210.22	0.0055	180.51
Superheated Vapour				
140	4.2696	1412.22	0.0092	108.52
150	4.4752	1498.13	0.0109	91.36
160	4.6234	1561.53	0.0122	81.70
170	4.7450	1614.80	0.0133	75.02
180	4.8506	1662.12	0.0143	69.96
190	4.9453	1705.48	0.0152	65.90

(Continued)

TABLE 7.26 ***(Continued)***

Properties of Superheated Vapour for R717

t, °C	s, kJ/kgK	h, kJ/kg	v, m³/kg	ρ, kg/m³
200	5.0319	1746.05	0.0160	62.53
210	5.1124	1784.52	0.0168	59.65
220	5.1880	1821.41	0.0175	57.16
230	5.2596	1857.06	0.0182	54.96
240	5.3278	1891.74	0.0189	52.99
250	5.3932	1925.64	0.0195	51.22
260	5.4562	1958.91	0.0202	49.61
270	5.5172	1991.72	0.0208	48.14
280	5.5763	2024.14	0.0214	46.78

7.4.12 Refrigerant R718

This natural fluid is from inorganic compounds group known as water and chemical formula H_2O (see Table 7.27, Figure 7.32, Figure 7.33, and Table 7.28).

Critical point: $t_c = 374.14°C$ and $p_c = 220.89$ bar

TABLE 7.27

Saturated Liquid and Saturated Vapour Properties for R718

t, °C	p, bar	v_{vap}, m³/kg	h_{liq}, kJ/kg	h_{vap}, kJ/kg	s_{liq}, kJ/kgK	s_{vap}, kJ/kgK
5	0.009	147.12802	20.43	2510.22	0.0741	9.0254
10	0.012	106.38525	41.10	2519.42	0.1478	8.9005
15	0.017	77.93121	61.92	2528.59	0.2207	8.7811
20	0.023	57.79418	82.87	2537.74	0.2928	8.6669
25	0.032	43.35856	104.13	2546.85	0.3647	8.5576
30	0.043	32.89268	125.22	2555.92	0.4348	8.4530
35	0.056	25.21539	146.33	2564.96	0.5039	8.3527
40	0.074	19.52260	167.46	2573.94	0.5719	8.2566
45	0.096	15.25785	188.58	2582.87	0.6388	8.1644
50	0.124	12.03159	209.69	2591.74	0.7046	8.0759
55	0.158	9.56820	230.78	2600.54	0.7694	7.9909
60	0.199	7.67058	251.84	2609.27	0.8331	7.9092
65	0.250	6.19646	272.88	2617.92	0.8957	7.8306
70	0.312	5.04208	293.89	2626.48	0.9574	7.7550
75	0.386	4.13117	314.88	2634.96	1.0181	7.6821
80	0.474	3.40710	335.86	2643.33	1.0779	7.6119
85	0.578	2.82753	356.82	2651.61	1.1368	7.5441
90	0.701	2.36052	377.78	2659.77	1.1949	7.4787
95	0.846	1.98183	398.74	2667.81	1.2521	7.4156
100	1.014	1.67287	419.71	2675.72	1.3087	7.3546
105	1.208	1.41933	440.70	2683.51	1.3645	7.2955
110	1.433	1.21012	461.72	2691.15	1.4197	7.2384
115	1.691	1.03656	482.78	2698.64	1.4742	7.1830
120	1.985	0.89184	503.89	2705.98	1.5282	7.1293
125	2.321	0.77058	525.06	2713.14	1.5816	7.0772
130	2.701	0.66849	546.28	2720.13	1.6345	7.0266
135	3.130	0.58216	567.58	2726.94	1.6868	6.9774

(Continued)

TABLE 7.27 ***(Continued)***

Saturated Liquid and Saturated Vapour Properties for R718

t, °C	p, bar	v_{vap}, m^3/kg	h_{liq}, kJ/kg	h_{vap}, kJ/kg	s_{liq}, kJ/kgK	s_{vap}, kJ/kgK
140	3.613	0.50884	588.95	2733.54	1.7388	6.9296
145	4.154	0.44631	610.41	2739.94	1.7902	6.8830
150	4.758	0.39277	631.95	2746.12	1.8413	6.8376
155	5.431	0.34675	653.58	2752.06	1.8919	6.7932
160	6.178	0.30705	675.30	2757.76	1.9422	6.7499
165	7.005	0.27268	697.12	2763.20	1.9921	6.7075
170	7.917	0.24282	719.04	2768.37	2.0416	6.6660
175	8.920	0.21679	741.06	2773.26	2.0907	6.6254
180	10.021	0.19404	763.18	2777.84	2.1395	6.5854
185	11.227	0.17408	785.41	2782.10	2.1880	6.5462
190	12.544	0.15653	807.74	2786.04	2.2362	6.5076
195	13.978	0.14104	830.18	2789.63	2.2840	6.4695
200	15.538	0.12735	852.74	2792.85	2.3315	6.4320
205	17.230	0.11520	875.41	2795.70	2.3788	6.3949
210	19.062	0.10440	898.21	2798.15	2.4258	6.3582
215	21.042	0.09478	921.13	2800.18	2.4725	6.3218
220	23.178	0.08618	944.19	2801.78	2.5190	6.2857
225	25.477	0.07848	967.40	2802.93	2.5652	6.2499
230	27.948	0.07157	990.77	2803.61	2.6113	6.2143
235	30.600	0.06536	1014.10	2803.81	2.6568	6.1789
240	33.442	0.05976	1037.81	2803.49	2.7026	6.1434
245	36.482	0.05470	1061.72	2802.62	2.7482	6.1081
250	39.729	0.05013	1085.85	2801.20	2.7938	6.0727
255	43.194	0.04597	1110.22	2799.19	2.8393	6.0372
260	46.885	0.04220	1134.85	2796.56	2.8849	6.0017
265	50.813	0.03877	1159.78	2793.29	2.9305	5.9659
270	54.987	0.03564	1185.01	2789.33	2.9761	5.9299
275	59.417	0.03278	1210.58	2784.65	3.0219	5.8935
280	64.116	0.03017	1236.52	2779.21	3.0679	5.8568
285	69.093	0.02777	1262.87	2772.94	3.1141	5.8196
290	74.359	0.02557	1289.64	2765.80	3.1606	5.7819
295	79.927	0.02354	1316.88	2757.72	3.2074	5.7434
300	85.809	0.02167	1344.63	2748.62	3.2546	5.7042
305	92.017	0.01995	1372.94	2738.39	3.3023	5.6640
310	98.564	0.01835	1401.86	2726.94	3.3504	5.6227
315	105.46	0.01687	1431.45	2714.12	3.3992	5.5801
320	112.73	0.01549	1461.80	2699.76	3.4488	5.5359
325	120.39	0.01420	1493.02	2683.65	3.4993	5.4898
330	128.45	0.01299	1525.30	2665.49	3.5509	5.4413
335	136.93	0.01187	1558.54	2645.10	3.6036	5.3903
340	145.85	0.01080	1593.58	2621.68	3.6586	5.3354
345	155.24	0.00978	1630.38	2594.85	3.7159	5.2761
350	165.13	0.00881	1669.70	2563.58	3.7765	5.2109
355	175.54	0.00787	1712.57	2526.39	3.8420	5.1376
360	186.50	0.00695	1760.77	2480.71	3.9153	5.0523
365	198.06	0.00599	1818.19	2421.03	4.0020	4.9467
370	210.27	0.00493	1894.95	2331.81	4.1178	4.7970

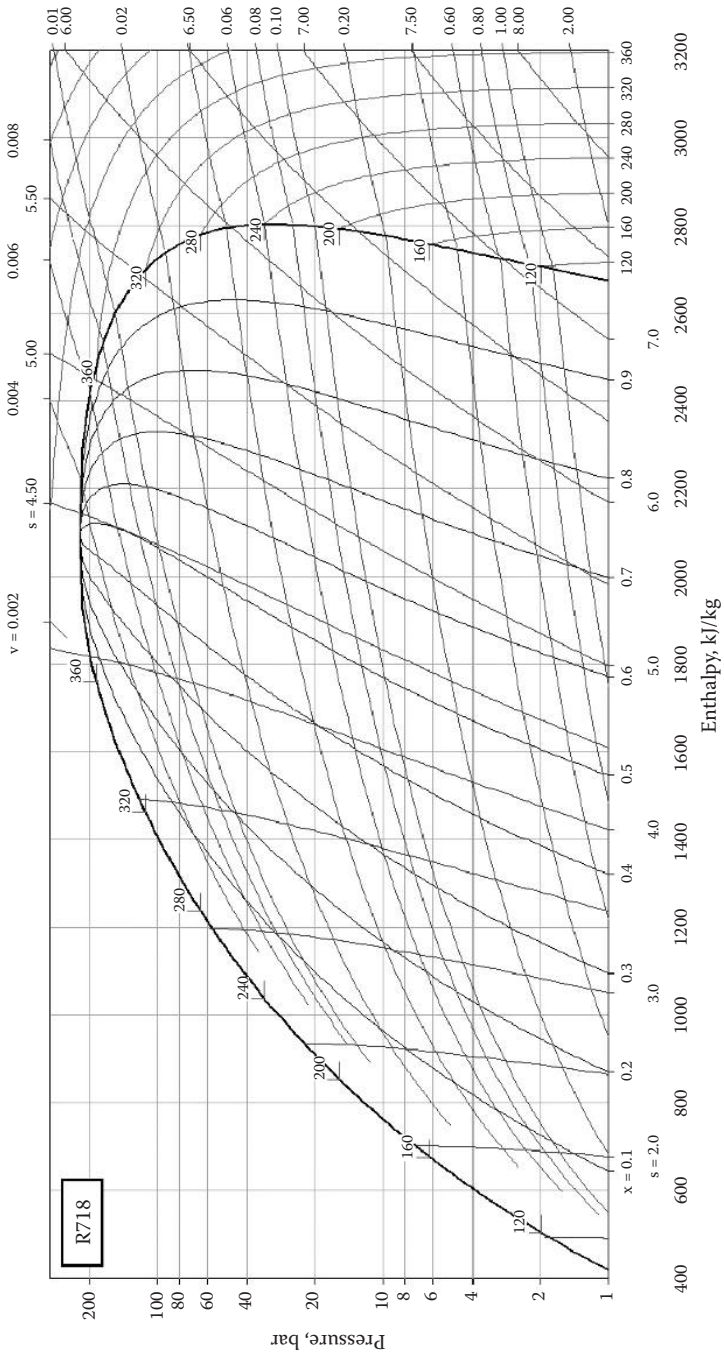

FIGURE 7.32
Pressure–enthalpy diagram for refrigerant R718.

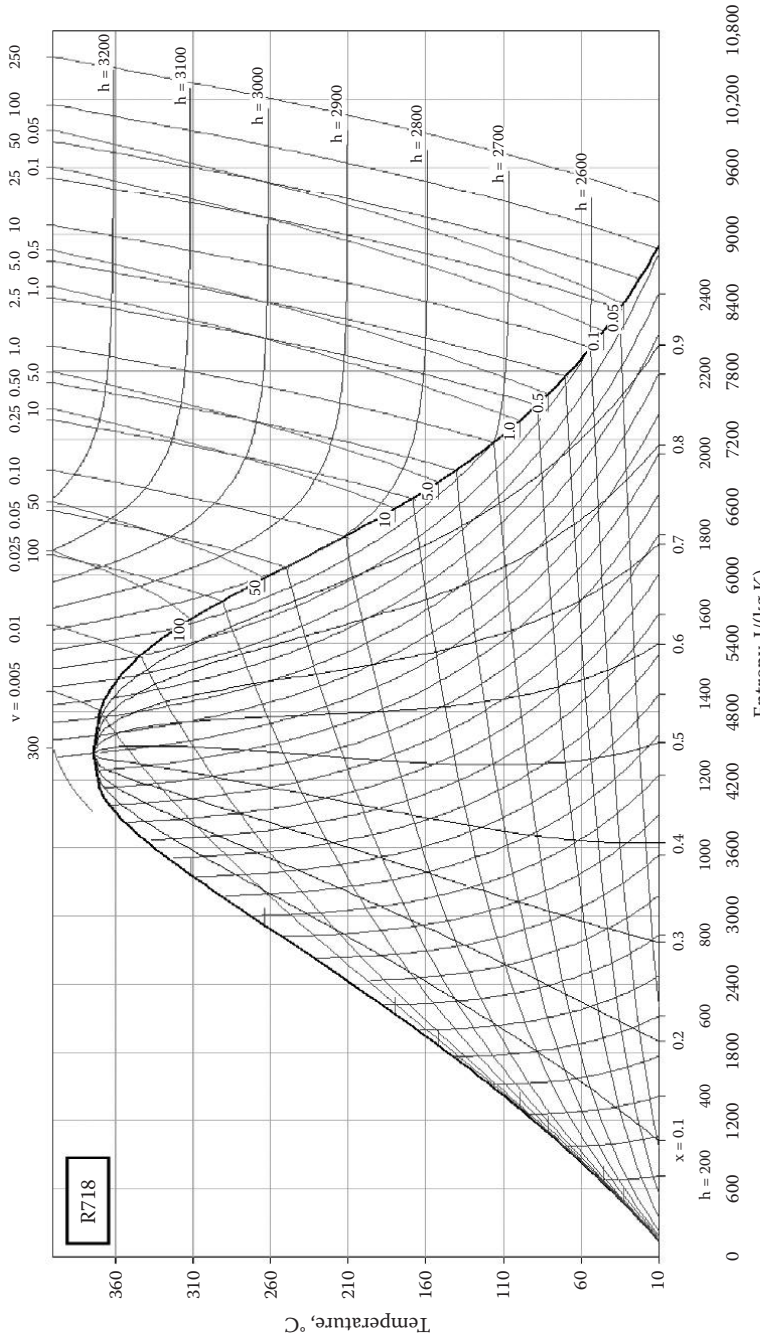

FIGURE 7.33
Temperature–entropy diagram for refrigerant R718.

TABLE 7.28

Properties of Superheated Vapour for R718

t, °C	s, kJ/kgK	h, kJ/kg	v, m^3/kg	ρ, kg/m^3
State Points at P = 1.01 bar				
Saturated Liquid at Bubble Point				
99.90	1.3076	419.30	0.0010	961.54
Saturated Vapour at Dew Point				
99.90	7.3557	2675.57	1.6783	0.60
Superheated Vapour				
100	7.3562	2675.77	1.6787	0.60
110	7.4098	2696.02	1.7269	0.58
120	7.4616	2716.15	1.7748	0.56
130	7.5119	2736.17	1.8224	0.55
140	7.5608	2756.11	1.8698	0.53
150	7.6083	2775.99	1.9170	0.52
160	7.6546	2795.81	1.9639	0.51
170	7.6998	2815.61	2.0108	0.50
180	7.7439	2835.38	2.0575	0.49
190	7.7871	2855.14	2.1041	0.48
200	7.8293	2874.90	2.1506	0.46
210	7.8706	2894.67	2.1970	0.46
220	7.9112	2914.46	2.2433	0.45
230	7.9510	2934.27	2.2896	0.44
State Points at P = 5 bar				
Saturated Liquid at Bubble Point				
151.86	1.8601	639.97	0.0011	917.43
Saturated Vapour at Dew Point				
151.86	6.8210	2748.35	0.3749	2.67
Superheated Vapour				
160	6.8645	2767.03	0.3836	2.61
170	6.9159	2789.54	0.3941	2.54
180	6.9653	2811.68	0.4045	2.47
190	7.0129	2833.49	0.4148	2.41
200	7.0590	2855.05	0.4249	2.35
210	7.1036	2876.40	0.4349	2.30
220	7.1470	2897.57	0.4449	2.25
230	7.1892	2918.60	0.4548	2.20
240	7.2304	2939.52	0.4646	2.15
250	7.2706	2960.36	0.4743	2.11
260	7.3099	2981.13	0.4841	2.07
270	7.3484	3001.85	0.4937	2.03
280	7.3862	3022.54	0.5034	1.99
290	7.4232	3043.21	0.5130	1.95
300	7.4596	3063.87	0.5225	1.91

(Continued)

TABLE 7.28 ***(Continued)***

Properties of Superheated Vapour for R718

t, °C	s, kJ/kgK	h, kJ/kg	v, m³/kg	ρ, kg/m³
State Points at P = 10 bar				
Saturated Liquid at Bubble Point				
179.91	2.1386	762.77	0.0011	884.96
Saturated Vapour at Dew Point				
179.91	6.5862	2777.76	0.1944	5.14
Superheated Vapour				
180	6.5867	2777.99	0.1945	5.14
190	6.6416	2803.13	0.2003	4.99
200	6.6937	2827.53	0.2059	4.86
210	6.7434	2851.32	0.2115	4.73
220	6.7912	2874.61	0.2169	4.61
230	6.8371	2897.48	0.2222	4.50
240	6.8814	2920.02	0.2275	4.40
250	6.9244	2942.27	0.2327	4.30
260	6.9661	2964.29	0.2378	4.21
270	7.0066	2986.12	0.2429	4.12
280	7.0462	3007.81	0.2479	4.03
290	7.0848	3029.37	0.2530	3.95
300	7.1226	3050.83	0.2579	3.88
310	7.1596	3072.22	0.2629	3.80
320	7.1959	3093.54	0.2678	3.73
State Points at P = 15 bar				
Saturated Liquid at Bubble Point				
198.32	2.3156	845.15	0.0012	869.57
Saturated Vapour at Dew Point				
198.32	6.4445	2791.81	0.1318	7.59
Superheated Vapour				
200	6.4543	2796.45	0.1325	7.55
210	6.5107	2823.39	0.1366	7.32
220	6.5639	2849.35	0.1406	7.11
230	6.6143	2874.49	0.1445	6.92
240	6.6625	2898.97	0.1482	6.75
250	6.7087	2922.91	0.1519	6.58
260	6.7532	2946.41	0.1556	6.43
270	6.7962	2969.53	0.1592	6.28
280	6.8378	2992.35	0.1627	6.15
290	6.8783	3014.92	0.1662	6.02
300	6.9176	3037.28	0.1697	5.89
310	6.9560	3059.47	0.1731	5.78
320	6.9935	3081.52	0.1765	5.67

(Continued)

TABLE 7.28 ***(Continued)***

Properties of Superheated Vapour for R718

t, °C	s, kJ/kgK	h, kJ/kg	v, m³/kg	ρ, kg/m³
330	7.0302	3103.46	0.1799	5.56
340	7.0661	3125.32	0.1832	5.46
State Points at P = 20 bar				
Saturated Liquid at Bubble Point				
212.42	2.4484	909.27	0.0012	847.46
Saturated Vapour at Dew Point				
212.42	6.3406	2799.18	0.0996	10.04
Superheated Vapour				
220	6.3858	2821.32	0.1021	9.79
230	6.4420	2849.30	0.1053	9.49
240	6.4949	2876.17	0.1084	9.22
250	6.5450	2902.14	0.1114	8.97
260	6.5928	2927.36	0.1144	8.74
270	6.6385	2951.98	0.1172	8.53
280	6.6825	2976.10	0.1200	8.33
290	6.7250	2999.81	0.1228	8.15
300	6.7661	3023.17	0.1255	7.97
310	6.8060	3046.26	0.1281	7.80
320	6.8449	3069.11	0.1308	7.65
330	6.8828	3091.76	0.1334	7.50
340	6.9198	3114.26	0.1360	7.35
350	6.9560	3136.63	0.1386	7.22
360	6.9914	3158.90	0.1411	7.09
State Points at P = 25 bar				
Saturated Liquid at Bubble Point				
223.99	2.5559	962.72	0.0012	833.33
Saturated Vapour at Dew Point				
223.99	6.2571	2802.74	0.0800	12.51
Superheated Vapour				
230	6.2946	2821.49	0.0817	12.24
240	6.3533	2851.31	0.0844	11.85
250	6.4082	2879.73	0.0870	11.49
260	6.4598	2907.01	0.0895	11.17
270	6.5088	2933.37	0.0919	10.88
280	6.5556	2958.99	0.0943	10.60
290	6.6004	2983.99	0.0966	10.35
300	6.6435	3008.48	0.0989	10.11
310	6.6851	3032.55	0.1011	9.89
320	6.7255	3056.28	0.1033	9.68
330	6.7646	3079.72	0.1055	9.48
340	6.8028	3102.91	0.1076	9.29

(Continued)

TABLE 7.28 ***(Continued)***

Properties of Superheated Vapour for R718

t, °C	s, kJ/kgK	h, kJ/kg	v, m³/kg	ρ, kg/m³
350	6.8400	3125.91	0.1098	9.11
360	6.8763	3148.74	0.1119	8.94
370	6.9119	3171.44	0.1139	8.78
380	6.9468	3194.03	0.1160	8.62
State Points at P = 30 bar				
Saturated Liquid at Bubble Point				
233.90	2.6467	1008.90	0.0012	819.67
Saturated Vapour at Dew Point				
233.90	6.1867	2803.81	0.0667	15.00
Superheated Vapour				
240	6.2262	2823.99	0.0682	14.66
250	6.2869	2855.42	0.0706	14.17
260	6.3432	2885.16	0.0728	13.73
270	6.3960	2913.58	0.0750	13.33
280	6.4459	2940.92	0.0771	12.97
290	6.4933	2967.39	0.0792	12.63
300	6.5387	2993.15	0.0811	12.32
310	6.5822	3018.32	0.0831	12.04
320	6.6242	3043.01	0.0850	11.77
330	6.6648	3067.30	0.0869	11.51
340	6.7042	3091.25	0.0887	11.27
350	6.7425	3114.92	0.0905	11.05
360	6.7798	3138.36	0.0923	10.83
370	6.8162	3161.61	0.0941	10.63
380	6.8518	3184.70	0.0959	10.43
State Points at P = 35 bar				
Saturated Liquid at Bubble Point				
242.60	2.7264	1050.23	0.0012	813.01
Saturated Vapour at Dew Point				
242.60	6.1250	2803.11	0.0571	17.53
Superheated Vapour				
250	6.1746	2828.86	0.0587	17.03
260	6.2365	2861.59	0.0608	16.44
270	6.2939	2892.43	0.0628	15.91
280	6.3474	2921.78	0.0648	15.44
290	6.3979	2949.94	0.0666	15.01
300	6.4457	2977.13	0.0684	14.62
310	6.4914	3003.53	0.0702	14.25
320	6.5352	3029.28	0.0719	13.92
330	6.5774	3054.49	0.0735	13.60
340	6.6181	3079.26	0.0752	13.30

(Continued)

TABLE 7.28 ***(Continued)***

Properties of Superheated Vapour for R718

t, °C	s, kJ/kgK	h, kJ/kg	v, m³/kg	ρ, kg/m³
350	6.6576	3103.66	0.0768	13.03
360	6.6959	3127.75	0.0784	12.76
370	6.7333	3151.58	0.0799	12.51
380	6.7697	3175.19	0.0815	12.27
390	6.8053	3198.63	0.0830	12.05
400	6.8401	3221.91	0.0845	11.83
State Points at P = 40 bar				
Saturated Liquid at Bubble Point				
250.40	2.7975	1087.80	0.0013	800.00
Saturated Vapour at Dew Point				
250.40	6.0698	2801.06	0.0498	20.09
Superheated Vapour				
260	6.1360	2835.99	0.0517	19.33
270	6.1987	2869.76	0.0537	18.64
280	6.2565	2901.45	0.0555	18.03
290	6.3104	2931.54	0.0572	17.49
300	6.3611	2960.34	0.0588	17.00
310	6.4092	2988.11	0.0604	16.55
320	6.4550	3015.04	0.0620	16.13
330	6.4988	3041.27	0.0635	15.75
340	6.5410	3066.92	0.0650	15.39
350	6.5817	3092.10	0.0664	15.05
360	6.6212	3116.89	0.0679	14.73
370	6.6595	3141.34	0.0693	14.43
380	6.6968	3165.51	0.0707	14.15
390	6.7332	3189.44	0.0720	13.88
400	6.7687	3213.19	0.0734	13.62
410	6.8035	3236.76	0.0747	13.38
State Points at P = 45 bar				
Saturated Liquid at Bubble Point				
257.49	2.8620	1122.43	0.0013	787.40
Saturated Vapour at Dew Point				
257.49	6.0196	2797.96	0.0441	22.70
Superheated Vapour				
260	6.0383	2807.91	0.0445	22.45
270	6.1077	2845.26	0.0464	21.55
280	6.1706	2879.76	0.0481	20.77
290	6.2285	2912.08	0.0498	20.09
300	6.2825	2942.73	0.0513	19.48
310	6.3332	2972.03	0.0528	18.93
320	6.3811	3000.26	0.0543	18.42

(Continued)

TABLE 7.28 ***(Continued)***

Properties of Superheated Vapour for R718

t, °C	s, kJ/kgK	h, kJ/kg	v, m³/kg	ρ, kg/m³
330	6.4269	3027.60	0.0557	17.96
340	6.4706	3054.22	0.0571	17.53
350	6.5127	3080.24	0.0584	17.13
360	6.5534	3105.76	0.0597	16.75
370	6.5927	3130.87	0.0610	16.40
380	6.6309	3155.63	0.0623	16.06
390	6.6681	3180.10	0.0635	15.75
400	6.7044	3204.32	0.0647	15.45
State Points at P = 50 bar				
Saturated Liquid at Bubble Point				
263.99	2.9213	1154.72	0.0013	775.19
Saturated Vapour at Dew Point				
263.99	5.9731	2794.00	0.0394	25.35
Superheated Vapour				
270	6.0186	2818.59	0.0405	24.67
280	6.0878	2856.47	0.0422	23.68
290	6.1504	2891.44	0.0438	22.82
300	6.2081	2924.20	0.0453	22.07
310	6.2617	2955.22	0.0467	21.40
320	6.3122	2984.89	0.0481	20.79
330	6.3599	3013.46	0.0494	20.24
340	6.4054	3041.13	0.0507	19.73
350	6.4490	3068.05	0.0519	19.25
360	6.4909	3094.37	0.0532	18.81
370	6.5314	3120.18	0.0543	18.40
380	6.5705	3145.56	0.0555	18.01
390	6.6085	3170.59	0.0567	17.65
400	6.6456	3195.31	0.0578	17.30
410	6.6816	3219.78	0.0589	16.97
State Points at P = 75 bar				
Saturated Liquid at Bubble Point				
290.59	3.1661	1292.83	0.0014	729.93
Saturated Vapour at Dew Point				
290.59	5.7774	2764.90	0.0253	39.49
Superheated Vapour				
300	5.8611	2812.51	0.0267	37.43
310	5.9381	2857.03	0.0280	35.66
320	6.0065	2897.20	0.0292	34.19
330	6.0683	2934.21	0.0304	32.93
340	6.1253	2968.82	0.0314	31.82
350	6.1782	3001.57	0.0324	30.84

(Continued)

TABLE 7.28 ***(Continued)***

Properties of Superheated Vapour for R718

t, °C	s, kJ/kgK	h, kJ/kg	v, m³/kg	ρ, kg/m³
360	6.2280	3032.84	0.0334	29.95
370	6.2751	3062.89	0.0343	29.15
380	6.3200	3092.00	0.0352	28.40
390	6.3630	3120.29	0.0361	27.71
400	6.4044	3147.92	0.0369	27.07
410	6.4443	3175.00	0.0378	26.48
420	6.4829	3201.59	0.0386	25.92
430	6.5205	3227.80	0.0394	25.39
440	6.5570	3253.66	0.0402	24.89
State Points at P = 100 bar				
Saturated Liquid at Bubble Point				
311.06	3.3607	1408.09	0.0015	689.66
Saturated Vapour at Dew Point				
311.06	5.6138	2724.34	0.0180	55.49
Superheated Vapour				
320	5.7100	2780.99	0.0193	51.94
330	5.7993	2834.35	0.0204	48.95
340	5.8760	2881.01	0.0215	46.57
350	5.9440	2923.06	0.0224	44.60
360	6.0057	2961.76	0.0233	42.91
370	6.0624	2997.93	0.0241	41.43
380	6.1151	3032.13	0.0249	40.12
390	6.1647	3064.76	0.0257	38.94
400	6.2117	3096.13	0.0264	37.87
410	6.2564	3126.46	0.0271	36.89
420	6.2992	3155.92	0.0278	35.98
430	6.3404	3184.69	0.0285	35.14
440	6.3801	3212.85	0.0291	34.35
450	6.4186	3240.50	0.0297	33.62
460	6.4560	3267.71	0.0304	32.92
State Points at P = 125 bar				
Saturated Liquid at Bubble Point				
327.89	3.5291	1511.63	0.0016	645.16
Saturated Vapour at Dew Point				
327.89	5.4620	2.6734	0.0135	74.13
Superheated Vapour				
320	5.3123	2584.05	0.0120	83.19
330	5.4932	2692.15	0.0138	72.41
340	5.6151	2766.25	0.0151	66.31
350	5.7115	2825.82	0.0161	62.01
360	5.7929	2876.94	0.0170	58.69

(Continued)

TABLE 7.28 ***(Continued)***

Properties of Superheated Vapour for R718

t, °C	s, kJ/kgK	h, kJ/kg	v, m³/kg	ρ, kg/m³
370	5.8643	2922.48	0.0179	55.99
380	5.9284	2964.05	0.0186	53.70
390	5.9871	3002.65	0.0193	51.73
400	6.0414	3038.97	0.0200	49.99
410	6.0923	3073.49	0.0206	48.44
420	6.1404	3106.56	0.0213	47.04
430	6.1861	3138.45	0.0219	45.76
440	6.2297	3169.36	0.0224	44.59
450	6.2716	3199.45	0.0230	43.51
460	6.3119	3228.83	0.0235	42.50
470	6.3510	3257.66	0.0241	41.56
State Points at P = 150 bar				
Saturated Liquid at Bubble Point				
342.24	3.6839	1609.78	0.0017	602.41
Saturated Vapour at Dew Point				
342.24	5.3095	2610.16	0.0103	96.71
Superheated Vapour				
350	5.4418	2692.07	0.0115	87.19
360	5.5650	2769.41	0.0126	79.53
370	5.6622	2831.45	0.0135	74.17
380	5.7443	2884.63	0.0143	70.06
390	5.8162	2931.95	0.0150	66.71
400	5.8808	2975.11	0.0156	63.90
410	5.9399	3015.16	0.0163	61.49
420	5.9946	3052.82	0.0168	59.36
430	6.0458	3088.58	0.0174	57.47
440	6.0942	3122.83	0.0179	55.77
450	6.1401	3155.83	0.0184	54.22
460	6.1840	3187.79	0.0189	52.80
470	6.2262	3218.89	0.0194	51.49
480	6.2668	3249.25	0.0199	50.27
490	6.3059	3278.97	0.0203	49.14
500	6.3439	3308.18	0.0208	48.08
State Points at P = 175 bar				
Saturated Liquid at Bubble Point				
354.75	3.8386	1710.28	0.0018	555.56
Saturated Vapour at Dew Point				
354.75	5.1416	2528.45	0.0079	126.26
Superheated Vapour				
360	5.2725	2610.99	0.0089	112.91
370	5.4328	2713.23	0.0101	99.31

(Continued)

TABLE 7.28 ***(Continued)***

Properties of Superheated Vapour for R718

t, °C	s, kJ/kgK	h, kJ/kg	v, m³/kg	ρ, kg/m³
380	5.5482	2787.96	0.0110	90.99
390	5.6414	2849.30	0.0118	85.01
400	5.7210	2902.49	0.0124	80.34
410	5.7913	2950.16	0.0131	76.53
420	5.8548	2993.84	0.0136	73.31
430	5.9131	3034.53	0.0142	70.53
440	5.9672	3072.87	0.0147	68.08
450	6.0181	3109.36	0.0152	65.90
460	6.0661	3144.34	0.0156	63.94
470	6.1118	3178.08	0.0161	62.16
480	6.1555	3210.78	0.0165	60.52
490	6.1975	3242.61	0.0169	59.01
500	6.2380	3273.69	0.0174	57.61
510	6.2771	3304.14	0.0178	56.31
520	6.3150	3334.01	0.0182	55.09
530	6.3518	3363.43	0.0185	53.95
State Points at P = 200 bar				
Saturated Liquid at Bubble Point				
365.81	4.0181	1828.83	0.0020	490.20
Saturated Vapour at Dew Point				
365.81	4.9266	2409.34	0.0058	171.53
Superheated Vapour				
370	5.1057	2524.08	0.0069	144.98
380	5.3155	2659.99	0.0083	121.14
390	5.4498	2748.31	0.0092	108.86
400	5.5537	2817.73	0.0099	100.59
410	5.6404	2876.54	0.0106	94.37
420	5.7159	2928.45	0.0112	89.42
430	5.7833	2975.52	0.0117	85.31
440	5.8447	3019.00	0.0122	81.82
450	5.9014	3059.73	0.0127	78.77
460	5.9544	3098.29	0.0131	76.09
470	6.0043	3135.10	0.0136	73.68
480	6.0516	3170.48	0.0140	71.51
490	6.0967	3204.67	0.0144	69.53
500	6.1399	3237.85	0.0148	67.72
510	6.1814	3270.19	0.0151	66.04
520	6.2215	3301.79	0.0155	64.48
530	6.2603	3332.76	0.0159	63.04
540	6.2980	3363.18	0.0162	61.68
State Points at P = 220 bar				
Saturated Liquid at Bubble Point				
373.80	4.2891	2007.84	0.0026	378.79

(Continued)

TABLE 7.28 *(Continued)*

Properties of Superheated Vapour for R718

t, °C	s, kJ/kgK	h, kJ/kg	v, m³/kg	ρ, kg/m³
Saturated Vapour at Dew Point				
373.80	4.5315	2164.66	0.0036	280.90
Superheated Vapour				
380	5.0519	2502.20	0.0061	163.92
390	5.2689	2644.91	0.0074	135.57
400	5.4071	2737.21	0.0083	121.17
410	5.5136	2809.43	0.0090	111.57
420	5.6022	2870.39	0.0096	104.41
430	5.6792	2924.08	0.0101	98.74
440	5.7478	2972.67	0.0106	94.06
450	5.8102	3017.49	0.0111	90.09
460	5.8678	3059.41	0.0115	86.64
470	5.9215	3099.05	0.0120	83.61
480	5.9720	3136.86	0.0124	80.91
490	6.0199	3173.16	0.0127	78.47
500	6.0655	3208.20	0.0131	76.25
510	6.1092	3242.19	0.0135	74.22
520	6.1512	3275.28	0.0138	72.35
530	6.1917	3307.59	0.0142	70.62
540	6.2308	3339.24	0.0145	69.01
550	6.2688	3370.30	0.0148	67.50
560	6.3056	3400.82	0.0151	66.10
570	6.3415	3430.91	0.0154	64.77
580	6.3765	3460.59	0.0157	63.51

7.4.13 Refrigerant R729

This natural fluid is from inorganic compounds with chemical name air (see Table 7.29, Figure 7.34, Figure 7.35, and Table 7.30).

Critical point: t_c = –140.65°C and p_c = 37.74 bar

TABLE 7.29

Saturated Liquid and Saturated Vapour Properties for R729

t, °C	p, bar	v_{vap}, m³/kg	h_{liq}, kJ/kg	h_{vap}, kJ/kg	s_{liq}, kJ/kgK	s_{vap}, kJ/kgK
–199	0.37	0.56287	81.70	300.93	–0.1366	2.8200
–198	0.43	0.49266	84.13	301.79	–0.1055	2.7908
–197	0.49	0.43301	86.53	302.64	–0.0753	2.7627
–196	0.57	0.38207	88.90	303.48	–0.0457	2.7355
–195	0.65	0.33839	91.25	304.30	–0.0169	2.7093
–194	0.73	0.30076	93.56	305.11	0.0112	2.6839
–193	0.83	0.26821	95.86	305.90	0.0387	2.6593
–192	0.94	0.23994	98.12	306.67	0.0655	2.6354
–191	1.05	0.21529	100.37	307.43	0.0917	2.6123
–190	1.18	0.19372	102.60	308.18	0.1174	2.5898
–189	1.32	0.17479	104.81	308.90	0.1426	2.5680

(Continued)

TABLE 7.29 ***(Continued)***

Saturated Liquid and Saturated Vapour Properties for R729

t, °C	p, bar	v_{vap}, m^3/kg	h_{liq}, kJ/kg	h_{vap}, kJ/kg	s_{liq}, kJ/kgK	s_{vap}, kJ/kgK
–188	1.47	0.15811	107.00	309.61	0.1673	2.5467
–187	1.63	0.14337	109.18	310.30	0.1915	2.5260
–186	1.81	0.13030	111.34	310.97	0.2153	2.5058
–185	2.00	0.11869	113.50	311.61	0.2387	2.4861
–184	2.21	0.10833	115.65	312.24	0.2617	2.4669
–183	2.43	0.09908	117.79	312.85	0.2844	2.4481
–182	2.67	0.09078	119.92	313.43	0.3067	2.4296
–181	2.92	0.08333	122.05	313.98	0.3287	2.4116
–180	3.19	0.07661	124.18	314.52	0.3505	2.3939
–179	3.48	0.07056	126.31	315.02	0.3720	2.3764
–178	3.79	0.06507	128.44	315.50	0.3933	2.3593
–177	4.12	0.06011	130.57	315.96	0.4144	2.3425
–176	4.48	0.05559	132.71	316.38	0.4352	2.3259
–175	4.85	0.05148	134.85	316.77	0.4559	2.3095
–174	5.24	0.04773	137.00	317.14	0.4765	2.2933
–173	5.66	0.04431	139.16	317.47	0.4969	2.2773
–172	6.10	0.04118	141.33	317.76	0.5172	2.2614
–171	6.57	0.03831	143.52	318.03	0.5374	2.2458
–170	7.07	0.03567	145.72	318.25	0.5575	2.2302
–169	7.59	0.03324	147.93	318.44	0.5775	2.2146
–168	8.14	0.03100	150.16	318.58	0.5975	2.1992
–167	8.71	0.02893	152.42	318.68	0.6175	2.1838
–166	9.32	0.02702	154.69	318.74	0.6374	2.1684
–165	9.96	0.02526	156.99	318.75	0.6573	2.1530
–164	10.63	0.02362	159.31	318.71	0.6773	2.1376
–163	11.33	0.02209	161.67	318.62	0.6973	2.1222
–162	12.07	0.02068	164.05	318.47	0.7173	2.1066
–161	12.83	0.01936	166.47	318.26	0.7375	2.0910
–160	13.64	0.01813	168.92	317.99	0.7577	2.0752
–159	14.48	0.01698	171.41	317.65	0.7781	2.0592
–158	15.36	0.01591	173.95	317.24	0.7986	2.0430
–157	16.28	0.01490	176.54	316.74	0.8194	2.0265
–156	17.24	0.01396	179.17	316.17	0.8403	2.0097
–155	18.24	0.01307	181.87	315.49	0.8615	1.9925
–154	19.28	0.01223	184.62	314.72	0.8831	1.9749
–153	20.36	0.01144	187.45	313.83	0.9050	1.9567
–152	21.49	0.01070	190.37	312.81	0.9273	1.9380
–151	22.66	0.00999	193.37	311.65	0.9501	1.9185
–150	23.88	0.00932	196.48	310.32	0.9736	1.8981
–149	25.15	0.00867	199.71	308.80	0.9978	1.8766
–148	26.46	0.00806	203.09	307.07	1.0230	1.8538
–147	27.83	0.00747	206.66	305.05	1.0494	1.8293
–146	29.24	0.00689	210.45	302.70	1.0772	1.8027
–145	30.71	0.00633	214.55	299.90	1.1072	1.7732
–144	32.24	0.00577	219.08	296.48	1.1401	1.7395
–143	33.81	0.00519	224.28	292.12	1.1779	1.6992
–142	35.45	0.00456	230.77	286.00	1.2252	1.6463
–141	37.14	0.00371	241.42	274.70	1.3033	1.5551

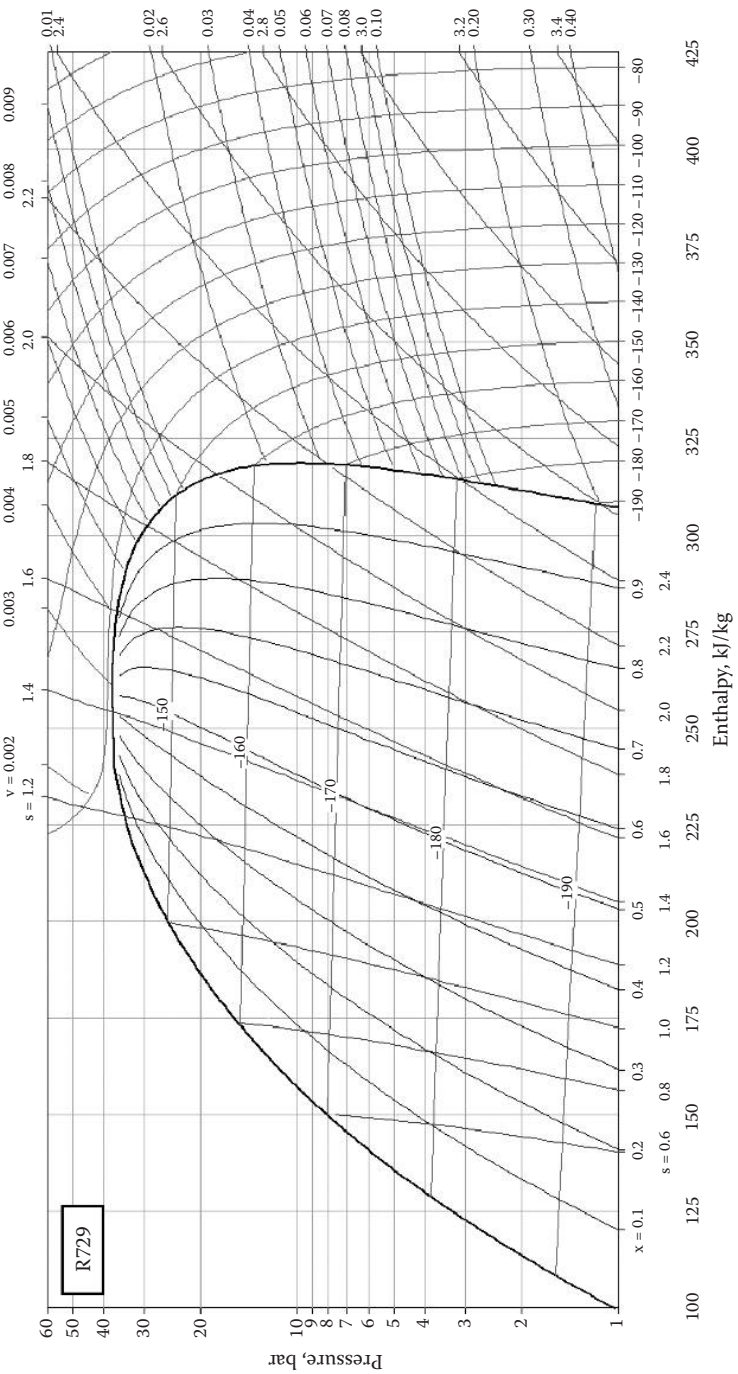

FIGURE 7.34
Pressure–enthalpy diagram for refrigerant R729.

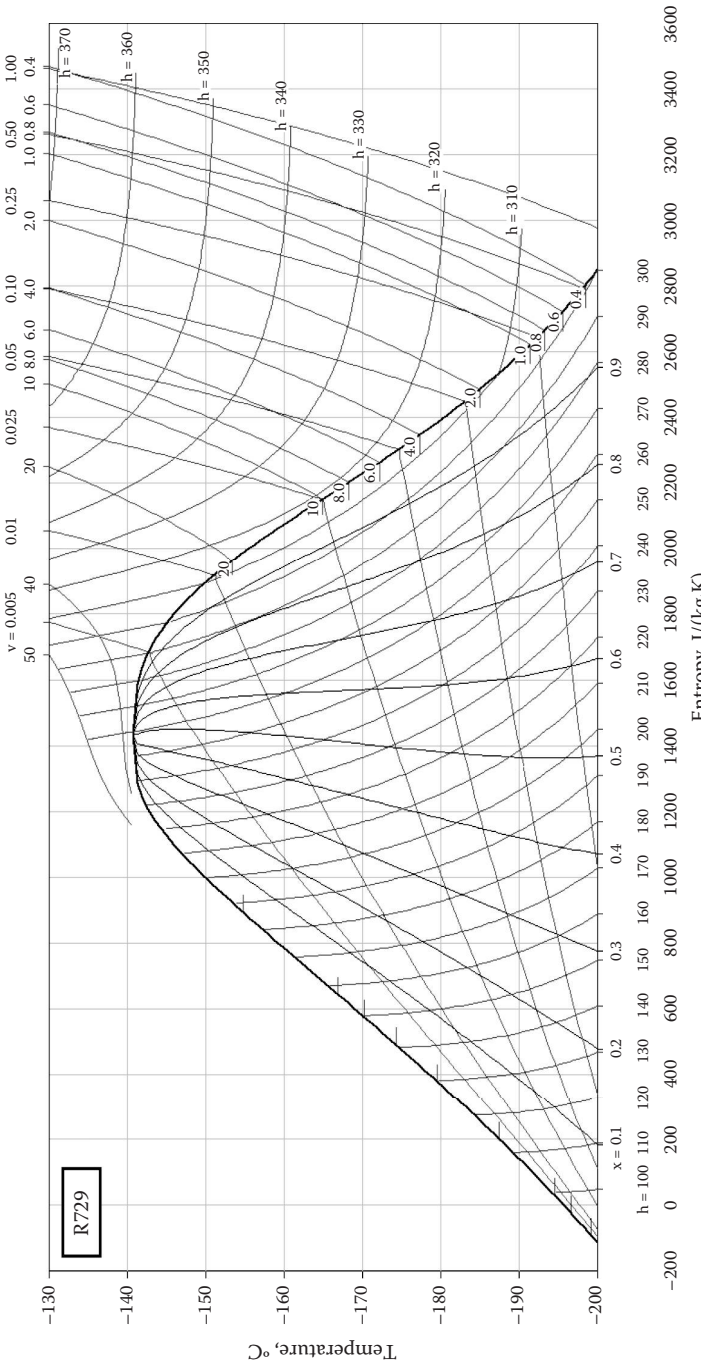

FIGURE 7.35
Temperature–entropy diagram for refrigerant R729.

TABLE 7.30

Properties of Superheated Vapour for R729

t, °C	s, kJ/kgK	h, kJ/kg	v, m^3/kg	ρ, kg/m^3
State Points at P = 1.01 bar				
Saturated Liquid at Bubble Point				
–194.41	0.0315	99.57	0.0011	877.19
Saturated Vapour at Dew Point				
–191.36	2.6205	307.16	0.2237	4.47
Superheated Vapour				
–190	2.6382	308.62	0.2279	4.39
–180	2.7584	319.21	0.2580	3.88
–170	2.8647	329.63	0.2877	3.48
–160	2.9601	339.94	0.3170	3.15
–150	3.0470	350.20	0.3461	2.89
–140	3.1266	360.40	0.3751	2.67
–130	3.2003	370.58	0.4040	2.48
–120	3.2689	380.73	0.4328	2.31
–110	3.3330	390.87	0.4615	2.17
–100	3.3932	400.99	0.4902	2.04
–90	3.4500	411.11	0.5189	1.93
–80	3.5038	421.21	0.5475	1.83
–70	3.5547	431.31	0.5761	1.74
–60	3.6032	441.41	0.6047	1.65
–50	3.6495	451.50	0.6333	1.58
–40	3.6937	461.59	0.6618	1.51
–30	3.7361	471.67	0.6904	1.45
–20	3.7768	481.76	0.7190	1.39
State Points at P = 5 bar				
Saturated Liquid at Bubble Point				
–176.67	0.4396	135.69	0.0013	787.40
Saturated Vapour at Dew Point				
–174.61	2.3031	316.92	0.0500	20.01
Superheated Vapour				
–170	2.3589	322.55	0.0533	18.77
–160	2.4668	334.20	0.0601	16.63
–150	2.5616	345.39	0.0667	15.00
–140	2.6467	356.28	0.0730	13.69
–130	2.7242	366.99	0.0793	12.62
–120	2.7956	377.57	0.0854	11.71
–110	2.8619	388.05	0.0915	10.93
–100	2.9238	398.46	0.0975	10.26
–90	2.9820	408.82	0.1035	9.66
–80	3.0368	419.13	0.1094	9.14

(Continued)

TABLE 7.30 ***(Continued)***

Properties of Superheated Vapour for R729

t, °C	s, kJ/kgK	h, kJ/kg	v, m³/kg	ρ, kg/m³
–70	3.0887	429.41	0.1154	8.67
–60	3.1380	439.66	0.1213	8.25
–50	3.1849	449.90	0.1271	7.86
–40	3.2297	460.11	0.1330	7.52
–30	3.2725	470.31	0.1389	7.20
–20	3.3136	480.50	0.1447	6.91
–10	3.3530	490.67	0.1506	6.64
0	3.3909	500.84	0.1564	6.39
State Points at P = 10 bar				
Saturated Liquid at Bubble Point				
–166.83	0.6447	157.14	0.0014	724.64
Saturated Vapour at Dew Point				
–164.94	2.1521	318.75	0.0252	39.76
Superheated Vapour				
–160	2.2150	325.72	0.0272	36.71
–150	2.3247	338.66	0.0311	32.15
–140	2.4188	350.71	0.0347	28.83
–130	2.5023	362.24	0.0381	26.25
–120	2.5780	373.44	0.0414	24.15
–110	2.6474	384.41	0.0446	22.41
–100	2.7117	395.21	0.0478	20.93
–90	2.7717	405.90	0.0509	19.64
–80	2.8280	416.49	0.0540	18.52
–70	2.8811	427.01	0.0570	17.53
–60	2.9313	437.47	0.0601	16.64
–50	2.9791	447.88	0.0631	15.85
–40	3.0246	458.26	0.0661	15.13
–30	3.0680	468.60	0.0691	14.47
–20	3.1096	478.92	0.0721	13.88
–10	3.1494	489.21	0.0750	13.33
0	3.1878	499.48	0.0780	12.82
10	3.2246	509.74	0.0809	12.36
20	3.2602	519.99	0.0839	11.92
State Points at P = 15 bar				
Saturated Liquid at Bubble Point				
–160.10	0.7822	172.92	0.0015	671.14
Saturated Vapour at Dew Point				
–158.41	2.0496	317.41	0.0163	61.24
Superheated Vapour				
–150	2.1622	330.78	0.0190	52.52
–140	2.2696	344.54	0.0218	45.86

(Continued)

TABLE 7.30 ***(Continued)***

Properties of Superheated Vapour for R729

t, °C	s, kJ/kgK	h, kJ/kg	v, m³/kg	ρ, kg/m³
−130	2.3609	357.14	0.0243	41.11
−120	2.4417	369.10	0.0267	37.45
−110	2.5147	380.64	0.0290	34.50
−100	2.5816	391.89	0.0312	32.04
−90	2.6436	402.93	0.0334	29.96
−80	2.7015	413.82	0.0355	28.16
−70	2.7559	424.59	0.0376	26.59
−60	2.8072	435.27	0.0397	25.19
−50	2.8558	445.87	0.0418	23.95
−40	2.9020	456.41	0.0438	22.83
−30	2.9460	466.89	0.0458	21.82
−20	2.9881	477.34	0.0478	20.90
−10	3.0285	487.75	0.0499	20.06
0	3.0672	498.13	0.0519	19.28
10	3.1044	508.49	0.0539	18.57
20	3.1403	518.82	0.0558	17.91
30	3.1749	529.14	0.0578	17.29
State Points at P = 20 bar				
Saturated Liquid at Bubble Point				
−154.76	0.8934	186.52	0.0016	625.00
Saturated Vapour at Dew Point				
−153.33	1.9628	314.13	0.0117	85.47
Superheated Vapour				
−150	2.0186	320.92	0.0127	78.57
−140	2.1486	337.54	0.0153	65.55
−130	2.2507	351.63	0.0174	57.50
−120	2.3378	364.52	0.0193	51.73
−110	2.4150	376.72	0.0212	47.26
−100	2.4849	388.47	0.0229	43.64
−90	2.5491	399.91	0.0246	40.63
−80	2.6087	411.12	0.0263	38.06
−70	2.6644	422.15	0.0279	35.84
−60	2.7168	433.05	0.0295	33.89
−50	2.7663	443.85	0.0311	32.17
−40	2.8132	454.56	0.0327	30.62
−30	2.8579	465.19	0.0342	29.23
−20	2.9005	475.77	0.0357	27.97
−10	2.9413	486.30	0.0373	26.83
0	2.9804	496.79	0.0388	25.77
10	3.0180	507.24	0.0403	24.80
20	3.0542	517.67	0.0418	23.91

(Continued)

TABLE 7.30 ***(Continued)***

Properties of Superheated Vapour for R729

t, °C	s, kJ/kgK	h, kJ/kg	v, m³/kg	ρ, kg/m³
State Points at P = 25 bar				
Saturated Liquid at Bubble Point				
−150.22	0.9931	199.34	0.0017	574.71
Saturated Vapour at Dew Point				
−149.11	1.8790	308.98	0.0088	114.29
Superheated Vapour				
−140	2.0375	329.30	0.0112	89.28
−130	2.1555	345.57	0.0132	75.88
−120	2.2507	359.66	0.0149	67.17
−110	2.3329	372.65	0.0165	60.77
−100	2.4061	384.96	0.0179	55.75
−90	2.4728	396.83	0.0194	51.66
−80	2.5342	408.38	0.0207	48.23
−70	2.5913	419.70	0.0221	45.30
−60	2.6448	430.83	0.0234	42.75
−50	2.6953	441.83	0.0247	40.50
−40	2.7430	452.71	0.0260	38.51
−30	2.7883	463.50	0.0272	36.72
−20	2.8315	474.21	0.0285	35.10
−10	2.8727	484.86	0.0297	33.63
0	2.9122	495.46	0.0310	32.29
10	2.9502	506.01	0.0322	31.06
20	2.9867	516.52	0.0334	29.93
30	3.0218	527.00	0.0346	28.88
40	3.0558	537.46	0.0358	27.90
State Points at P = 30 bar				
Saturated Liquid at Bubble Point				
−146.19	1.0918	212.54	0.0019	520.83
Saturated Vapour at Dew Point				
−145.48	1.7878	301.31	0.0066	151.52
Superheated Vapour				
−140	1.9232	318.93	0.0083	120.19
−130	2.0675	338.81	0.0103	96.91
−120	2.1734	354.48	0.0119	83.99
−110	2.2616	368.40	0.0133	75.12
−100	2.3386	381.36	0.0146	68.42
−90	2.4079	393.70	0.0159	63.08
−80	2.4713	405.61	0.0170	58.68
−70	2.5299	417.22	0.0182	54.95
−60	2.5846	428.60	0.0193	51.75
−50	2.6359	439.80	0.0204	48.95

(Continued)

TABLE 7.30 ***(Continued)***

Properties of Superheated Vapour for R729

t, °C	s, kJ/kgK	h, kJ/kg	v, m³/kg	ρ, kg/m³
−40	2.6844	450.86	0.0215	46.47
−30	2.7304	461.81	0.0226	44.26
−20	2.7741	472.66	0.0237	42.27
−10	2.8159	483.43	0.0247	40.47
0	2.8558	494.14	0.0258	38.83
10	2.8941	504.79	0.0268	37.33
20	2.9309	515.39	0.0278	35.95
30	2.9663	525.95	0.0288	34.68
40	3.0005	536.48	0.0299	33.49
State Points at P = 35 bar				
Saturated Liquid at Bubble Point				
−142.54	1.2109	228.83	0.0022	450.45
Saturated Vapour at Dew Point				
−142.27	1.6624	287.91	0.0047	210.97
Superheated Vapour				
−140	1.7812	303.56	0.0059	168.80
−130	1.9813	331.08	0.0082	121.68
−120	2.1019	348.91	0.0098	102.50
−110	2.1972	363.97	0.0111	90.41
−100	2.2786	377.65	0.0122	81.67
−90	2.3508	390.51	0.0134	74.90
−80	2.4163	402.82	0.0144	69.40
−70	2.4764	414.74	0.0154	64.81
−60	2.5324	426.37	0.0164	60.90
−50	2.5847	437.78	0.0174	57.50
−40	2.6340	449.03	0.0183	54.51
−30	2.6806	460.13	0.0193	51.86
−20	2.7249	471.12	0.0202	49.49
−10	2.7671	482.01	0.0211	47.35
0	2.8074	492.82	0.0220	45.40
10	2.8461	503.57	0.0229	43.62
20	2.8832	514.26	0.0238	41.99
30	2.9189	524.91	0.0247	40.48
40	2.9533	535.51	0.0256	39.09

7.4.14 Refrigerant R744

This natural fluid is from inorganic compounds with chemical name carbon dioxide and formula CO_2 (see Table 7.31, Figure 7.36, Figure 7.37, and Table 7.32).

Critical point: $t_c = 31.06°C$ and $p_c = 73.83$ bar

TABLE 7.31

Saturated Liquid and Saturated Vapour Properties for R744

t, °C	p, bar	v_{vap}, m³/kg	h_{liq}, kJ/kg	h_{vap}, kJ/kg	s_{liq}, kJ/kgK	s_{vap}, kJ/kgK
–46	8.018	0.04771	100.46	433.72	0.6121	2.0792
–45	8.336	0.04594	102.57	433.99	0.6212	2.0739
–44	8.663	0.04424	104.68	434.25	0.6303	2.0686
–43	9.000	0.04263	106.78	434.50	0.6394	2.0633
–42	9.346	0.04108	108.88	434.74	0.6483	2.0581
–41	9.701	0.03960	110.98	434.97	0.6572	2.0529
–40	10.067	0.03819	113.07	435.19	0.6661	2.0477
–39	10.442	0.03683	115.15	435.40	0.6749	2.0426
–38	10.828	0.03553	117.24	435.59	0.6836	2.0374
–37	11.224	0.03429	119.32	435.78	0.6923	2.0324
–36	11.631	0.03310	121.36	435.95	0.7007	2.0273
–35	12.048	0.03196	123.43	436.11	0.7093	2.0223
–34	12.477	0.03086	125.51	436.26	0.7179	2.0172
–33	12.916	0.02981	127.59	436.39	0.7264	2.0122
–32	13.367	0.02880	129.66	436.51	0.7348	2.0073
–31	13.829	0.02783	131.74	436.62	0.7432	2.0023
–30	14.303	0.02690	133.83	436.71	0.7516	1.9973
–29	14.788	0.02600	135.91	436.79	0.7600	1.9924
–28	15.286	0.02514	138.00	436.86	0.7684	1.9875
–27	15.796	0.02431	140.10	436.91	0.7767	1.9825
–26	16.318	0.02352	142.20	436.95	0.7850	1.9776
–25	16.852	0.02275	144.31	436.97	0.7934	1.9727
–24	17.400	0.02201	146.42	436.97	0.8016	1.9678
–23	17.960	0.02130	148.55	436.96	0.8099	1.9629
–22	18.533	0.02061	150.67	436.94	0.8182	1.9580
–21	19.120	0.01995	152.81	436.89	0.8265	1.9531
–20	19.720	0.01932	154.95	436.83	0.8347	1.9482
–19	20.334	0.01870	157.10	436.75	0.8430	1.9433
–18	20.961	0.01811	159.26	436.65	0.8512	1.9384
–17	21.603	0.01754	161.43	436.54	0.8594	1.9334
–16	22.259	0.01699	163.61	436.40	0.8677	1.9285
–15	22.929	0.01645	165.79	436.25	0.8759	1.9236
–14	23.614	0.01594	167.99	436.07	0.8841	1.9186
–13	24.313	0.01544	170.19	435.88	0.8923	1.9136
–12	25.028	0.01496	172.40	435.66	0.9005	1.9086
–11	25.758	0.01450	174.63	435.42	0.9088	1.9036
–10	26.504	0.01405	176.86	435.16	0.9170	1.8985
–9	27.265	0.01361	179.11	434.87	0.9252	1.8934
–8	28.042	0.01319	181.37	434.56	0.9335	1.8883

(Continued)

TABLE 7.31 ***(Continued)***

Saturated Liquid and Saturated Vapour Properties for R744

t, °C	p, bar	v_{vap}, m^3/kg	h_{liq}, kJ/kg	h_{vap}, kJ/kg	s_{liq}, kJ/kgK	s_{vap}, kJ/kgK
–7	28.835	0.01278	183.64	434.22	0.9417	1.8832
–6	29.644	0.01239	185.93	433.86	0.9500	1.8780
–5	30.470	0.01201	188.23	433.46	0.9582	1.8728
–4	31.313	0.01163	190.55	433.04	0.9665	1.8675
–3	32.173	0.01128	192.88	432.59	0.9749	1.8622
–2	33.050	0.01093	195.23	432.11	0.9832	1.8568
–1	33.944	0.01059	197.61	431.60	0.9916	1.8514
0	34.857	0.01026	200.00	431.05	1.0000	1.8459
1	35.787	0.00994	202.42	430.47	1.0085	1.8403
2	36.735	0.00963	204.86	429.85	1.0170	1.8347
3	37.702	0.00933	207.32	429.19	1.0255	1.8290
4	38.688	0.00904	209.82	428.49	1.0342	1.8232
5	39.693	0.00875	212.34	427.75	1.0428	1.8173
6	40.716	0.00847	214.89	426.96	1.0516	1.8113
7	41.760	0.00820	217.48	426.13	1.0604	1.8052
8	42.823	0.00794	220.11	425.24	1.0694	1.7990
9	43.906	0.00768	222.77	424.30	1.0784	1.7926
10	45.010	0.00743	225.47	423.30	1.0875	1.7861
11	46.134	0.00719	228.21	422.24	1.0967	1.7795
12	47.279	0.00695	231.03	421.09	1.1061	1.7726
13	48.446	0.00671	233.86	419.90	1.1155	1.7657
14	49.634	0.00648	236.74	418.62	1.1251	1.7585
15	50.844	0.00626	239.67	417.26	1.1348	1.7511
16	52.077	0.00604	242.70	415.79	1.1447	1.7434
17	53.332	0.00582	245.78	414.22	1.1548	1.7354
18	54.611	0.00561	248.94	412.54	1.1652	1.7271
19	55.914	0.00540	252.19	410.73	1.1757	1.7184
20	57.242	0.00519	255.53	408.76	1.1866	1.7093
21	58.594	0.00498	258.99	406.63	1.1977	1.6997
22	59.973	0.00478	262.59	404.30	1.2093	1.6895
23	61.378	0.00457	266.35	401.72	1.2214	1.6785
24	62.812	0.00436	270.32	398.86	1.2342	1.6667
25	64.274	0.00415	274.56	395.65	1.2477	1.6539
26	65.766	0.00394	279.14	391.97	1.2623	1.6395
27	67.289	0.00371	284.23	387.64	1.2786	1.6231
28	68.846	0.00348	290.02	382.42	1.2971	1.6039
29	70.437	0.00321	296.97	375.73	1.3193	1.5799
30	72.065	0.00289	306.21	366.06	1.3489	1.5464

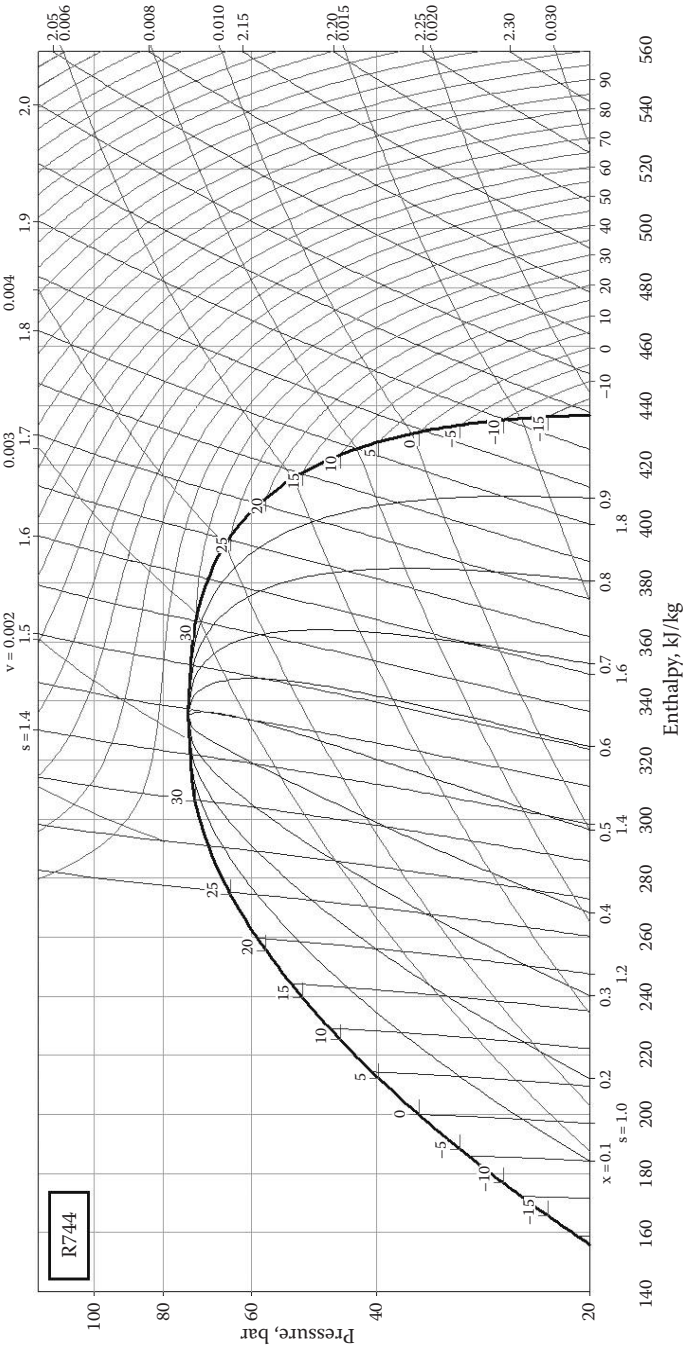

FIGURE 7.36
Pressure–enthalpy diagram for refrigerant R744.

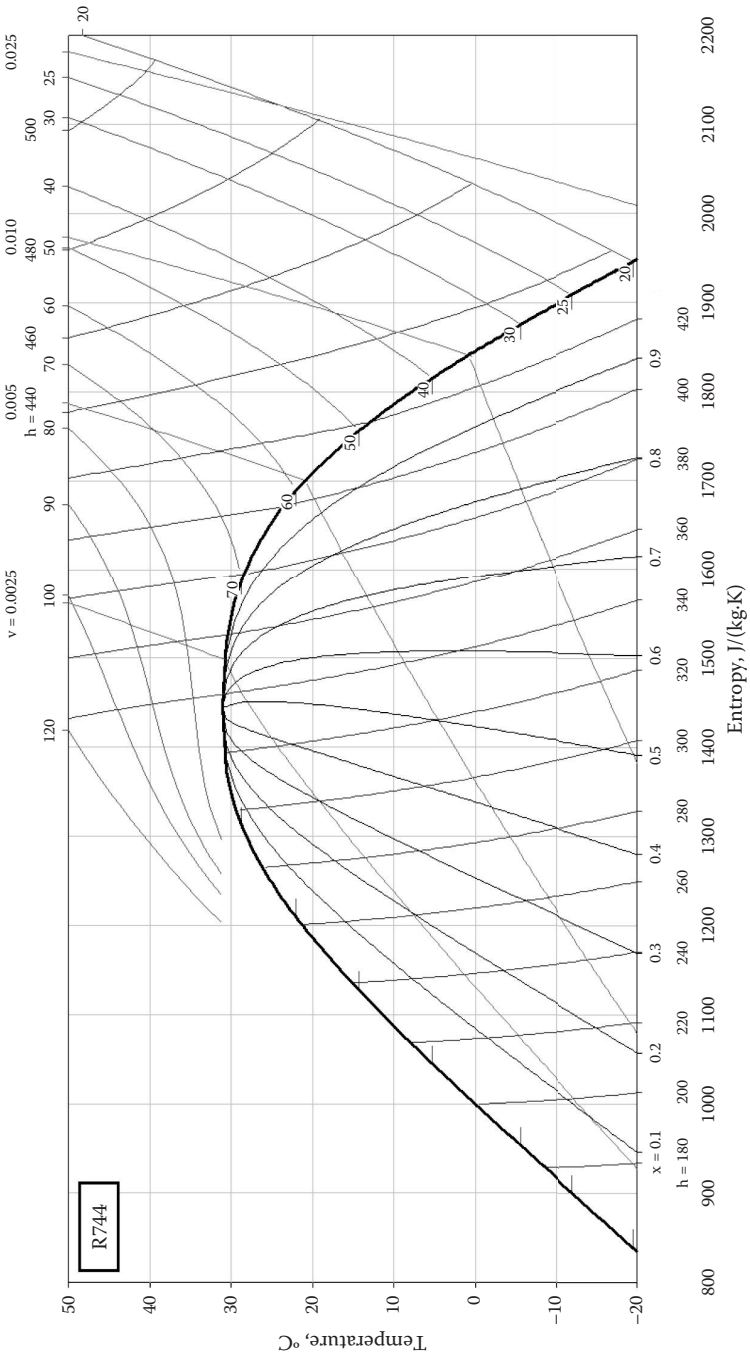

FIGURE 7.37
Temperature–entropy diagram for refrigerant R744.

TABLE 7.32

Properties of Superheated Vapour for R744

t, °C	s, kJ/kgK	h, kJ/kg	v, m^3/kg	ρ, kg/m^3
State Points at P = 10 bar				
Saturated Liquid at Bubble Point				
−40.18	0.6645	112.69	0.0009	1123.60
Saturated Vapour at Dew Point				
−40.18	2.0486	435.15	0.0384	26.01
Superheated Vapour				
−40	2.0494	435.34	0.0385	25.98
−30	2.0910	445.24	0.0410	24.40
−20	2.1297	454.85	0.0434	23.05
−10	2.1663	464.27	0.0457	21.88
0	2.2010	473.58	0.0480	20.85
10	2.2342	482.82	0.0502	19.94
20	2.2662	492.03	0.0523	19.11
30	2.2970	501.22	0.0545	18.36
40	2.3269	510.42	0.0566	17.68
50	2.3558	519.64	0.0586	17.05
60	2.3840	528.90	0.0607	16.47
70	2.4115	538.19	0.0628	15.93
80	2.4384	547.53	0.0648	15.43
90	2.4646	556.92	0.0668	14.97
State Points at P = 15 bar				
Saturated Liquid at Bubble Point				
−28.57	0.7636	136.81	0.0009	1075.27
Saturated Vapour at Dew Point				
−28.57	1.9903	436.82	0.0256	39.02
Superheated Vapour				
−20	2.0281	446.24	0.0272	36.73
−10	2.0688	456.73	0.0290	34.52
0	2.1066	466.88	0.0306	32.64
10	2.1423	476.80	0.0322	31.01
20	2.1762	486.56	0.0338	29.58
30	2.2086	496.23	0.0353	28.31
40	2.2398	505.83	0.0368	27.17
50	2.2699	515.40	0.0383	26.13
60	2.2990	524.96	0.0397	25.18
70	2.3273	534.52	0.0411	24.31
80	2.3548	544.10	0.0425	23.50
90	2.3816	553.71	0.0439	22.76
100	2.4078	563.35	0.0453	22.06
110	2.4334	573.03	0.0467	21.41
120	2.4584	582.75	0.0481	20.81

(Continued)

TABLE 7.32 ***(Continued)***

Properties of Superheated Vapour for R744

t, °C	s, kJ/kgK	h, kJ/kg	v, m³/kg	ρ, kg/m³
State Points at P = 20 bar				
Saturated Liquid at Bubble Point				
−19.54	0.8385	155.94	0.0010	1030.93
Saturated Vapour at Dew Point				
−19.54	1.9459	436.80	0.0190	52.55
Superheated Vapour				
−10	1.9904	448.27	0.0205	48.80
0	2.0324	459.54	0.0219	45.65
10	2.0712	470.32	0.0232	43.04
20	2.1074	480.77	0.0245	40.81
30	2.1417	490.99	0.0257	38.87
40	2.1744	501.05	0.0269	37.16
50	2.2057	511.02	0.0281	35.62
60	2.2359	520.91	0.0292	34.24
70	2.2650	530.77	0.0303	32.98
80	2.2933	540.61	0.0314	31.83
90	2.3207	550.44	0.0325	30.77
100	2.3475	560.28	0.0336	29.79
110	2.3735	570.14	0.0346	28.87
120	2.3990	580.03	0.0357	28.02
130	2.4239	589.95	0.0367	27.23
State Points at P = 25 bar				
Saturated Liquid at Bubble Point				
−12.04	0.9002	172.32	0.0010	990.10
Saturated Vapour at Dew Point				
−12.04	1.9088	435.67	0.0150	66.76
Superheated Vapour				
−10	1.9195	438.47	0.0153	65.49
0	1.9676	451.37	0.0166	60.31
10	2.0104	463.28	0.0178	56.26
20	2.0496	474.57	0.0189	52.94
30	2.0861	485.45	0.0199	50.14
40	2.1206	496.06	0.0210	47.72
50	2.1533	506.47	0.0219	45.58
60	2.1846	516.74	0.0229	43.68
70	2.2147	526.92	0.0238	41.98
80	2.2437	537.03	0.0247	40.43
90	2.2719	547.11	0.0256	39.01
100	2.2992	557.17	0.0265	37.71
110	2.3258	567.23	0.0274	36.51
120	2.3517	577.29	0.0283	35.39

(Continued)

TABLE 7.32 ***(Continued)***

Properties of Superheated Vapour for R744

t, °C	s, kJ/kgK	h, kJ/kg	v, m³/kg	ρ, kg/m³
State Points at P = 30 bar				
Saturated Liquid at Bubble Point				
–5.57	0.9535	186.92	0.0010	961.54
Saturated Vapour at Dew Point				
–5.57	1.8757	433.69	0.0122	81.83
Superheated Vapour				
0	1.9064	441.98	0.0129	77.33
10	1.9550	455.49	0.0141	71.06
20	1.9980	467.89	0.0151	66.20
30	2.0373	479.59	0.0161	62.25
40	2.0738	490.82	0.0170	58.93
50	2.1081	501.74	0.0178	56.07
60	2.1406	512.43	0.0187	53.55
70	2.1718	522.96	0.0195	51.32
80	2.2017	533.38	0.0203	49.31
90	2.2306	543.72	0.0211	47.50
100	2.2586	554.01	0.0218	45.84
110	2.2857	564.27	0.0226	44.32
120	2.3121	574.51	0.0233	42.91
130	2.3378	584.75	0.0240	41.61
State Points at P = 35 bar				
Saturated Liquid at Bubble Point				
0.16	1.0013	200.37	0.0011	925.93
Saturated Vapour at Dew Point				
0.16	1.8450	430.97	0.0102	97.94
Superheated Vapour				
0	1.8440	430.69	0.0102	98.15
10	1.9016	446.69	0.0114	88.03
20	1.9498	460.58	0.0124	80.90
30	1.9925	473.30	0.0133	75.38
40	2.0314	485.30	0.0141	70.90
50	2.0676	496.80	0.0149	67.13
60	2.1016	507.97	0.0157	63.89
70	2.1339	518.89	0.0164	61.04
80	2.1648	529.64	0.0171	58.51
90	2.1945	540.27	0.0178	56.24
100	2.2231	550.80	0.0185	54.19
110	2.2508	561.27	0.0191	52.31
120	2.2777	571.71	0.0198	50.59
130	2.3038	582.12	0.0204	49.00
140	2.3293	592.52	0.0210	47.52

(Continued)

TABLE 7.32 ***(Continued)***

Properties of Superheated Vapour for R744

t, °C	s, kJ/kgK	h, kJ/kg	v, m³/kg	ρ, kg/m³
State Points at P = 40 bar				
Saturated Liquid at Bubble Point				
5.30	1.0455	213.11	0.0011	892.86
Saturated Vapour at Dew Point				
5.30	1.8155	427.52	0.0087	115.34
Superheated Vapour				
10	1.8469	436.35	0.0092	108.32
20	1.9028	452.44	0.0103	97.51
30	1.9500	466.51	0.0111	89.78
40	1.9920	479.44	0.0119	83.77
50	2.0304	491.64	0.0127	78.87
60	2.0660	503.35	0.0134	74.73
70	2.0996	514.70	0.0140	71.18
80	2.1315	525.81	0.0147	68.05
90	2.1620	536.74	0.0153	65.26
100	2.1914	547.54	0.0159	62.76
110	2.2197	558.24	0.0165	60.49
120	2.2471	568.87	0.0171	58.42
130	2.2737	579.46	0.0177	56.52
140	2.2995	590.02	0.0183	54.77
150	2.3248	600.57	0.0188	53.14
State Points at P = 45 bar				
Saturated Liquid at Bubble Point				
9.99	1.0874	225.45	0.0012	862.07
Saturated Vapour at Dew Point				
9.99	1.7862	423.31	0.0074	134.59
Superheated Vapour				
10	1.7863	423.33	0.0074	134.52
20	1.8551	443.15	0.0086	116.86
30	1.9086	459.08	0.0095	105.80
40	1.9544	473.18	0.0102	97.73
50	1.9953	486.21	0.0109	91.38
60	2.0329	498.54	0.0116	86.17
70	2.0679	510.38	0.0122	81.75
80	2.1010	521.89	0.0128	77.94
90	2.1324	533.14	0.0134	74.57
100	2.1625	544.22	0.0140	71.58
110	2.1914	555.16	0.0145	68.88
120	2.2194	566.01	0.0151	66.43
130	2.2464	576.78	0.0156	64.19
140	2.2727	587.51	0.0161	62.14

(Continued)

TABLE 7.32 ***(Continued)***

Properties of Superheated Vapour for R744

t, °C	s, kJ/kgK	h, kJ/kg	v, m³/kg	ρ, kg/m³
150	2.2983	598.20	0.0166	60.23
160	2.3232	608.87	0.0171	58.47
State Points at P = 50 bar				
Saturated Liquid at Bubble Point				
14.30	1.1280	237.62	0.0012	826.45
Saturated Vapour at Dew Point				
14.30	1.7563	418.22	0.0064	155.76
Superheated Vapour				
20	1.8039	432.05	0.0071	140.53
30	1.8669	450.80	0.0081	124.00
40	1.9176	466.44	0.0088	113.02
50	1.9618	480.47	0.0095	104.81
60	2.0015	493.52	0.0102	98.26
70	2.0382	505.92	0.0108	92.83
80	2.0725	517.86	0.0113	88.20
90	2.1049	529.47	0.0119	84.19
100	2.1358	540.85	0.0124	80.64
110	2.1654	552.05	0.0129	77.47
120	2.1940	563.11	0.0134	74.61
130	2.2215	574.08	0.0139	72.01
140	2.2482	584.97	0.0144	69.63
150	2.2741	595.82	0.0148	67.43
160	2.2994	606.63	0.0153	65.40
State Points at P = 55 bar				
Saturated Liquid at Bubble Point				
18.30	1.1683	249.91	0.0013	793.65
Saturated Vapour at Dew Point				
18.30	1.7245	412.01	0.0055	180.51
Superheated Vapour				
20	1.7436	417.58	0.0058	172.48
30	1.8233	441.34	0.0069	145.29
40	1.8810	459.09	0.0077	130.00
50	1.9290	474.37	0.0084	119.30
60	1.9714	488.27	0.0090	111.09
70	2.0099	501.29	0.0096	104.46
80	2.0456	513.72	0.0101	98.90
90	2.0791	525.72	0.0106	94.13
100	2.1109	537.41	0.0111	89.97
110	2.1412	548.88	0.0116	86.27
120	2.1703	560.18	0.0121	82.96
130	2.1984	571.35	0.0125	79.97

(Continued)

TABLE 7.32 ***(Continued)***

Properties of Superheated Vapour for R744

t, °C	s, kJ/kgK	h, kJ/kg	v, m³/kg	ρ, kg/m³
140	2.2255	582.42	0.0129	77.24
150	2.2518	593.43	0.0134	74.74
160	2.2774	604.38	0.0138	72.43
170	2.3023	615.29	0.0142	70.29
State Points at P = 60 bar				
Saturated Liquid at Bubble Point				
22.02	1.2096	262.66	0.0013	751.88
Saturated Vapour at Dew Point				
22.02	1.6893	404.25	0.0048	209.64
Superheated Vapour				
30	1.7756	430.04	0.0058	171.49
40	1.8436	450.96	0.0067	149.20
50	1.8967	467.85	0.0074	135.10
60	1.9421	482.76	0.0080	124.79
70	1.9827	496.49	0.0086	116.69
80	2.0200	509.46	0.0091	110.04
90	2.0547	521.88	0.0096	104.42
100	2.0874	533.92	0.0100	99.56
110	2.1185	545.68	0.0105	95.30
120	2.1482	557.22	0.0109	91.50
130	2.1768	568.60	0.0114	88.08
140	2.2044	579.85	0.0118	84.98
150	2.2311	591.02	0.0122	82.15
160	2.2570	602.12	0.0126	79.55
170	2.2822	613.16	0.0130	77.14
State Points at P = 65 bar				
Saturated Liquid at Bubble Point				
25.49	1.2547	276.75	0.0014	704.23
Saturated Vapour at Dew Point				
25.49	1.6471	393.91	0.0041	246.91
Superheated Vapour				
30	1.7187	415.44	0.0048	206.85
40	1.8042	441.78	0.0058	171.48
50	1.8641	460.80	0.0066	152.50
60	1.9133	476.94	0.0072	139.48
70	1.9563	491.50	0.0077	129.61
80	1.9953	505.07	0.0082	121.68
90	2.0313	517.96	0.0087	115.09
100	2.0650	530.37	0.0091	109.45
110	2.0969	542.43	0.0096	104.55
120	2.1273	554.22	0.0100	100.23

(Continued)

TABLE 7.32 ***(Continued)***

Properties of Superheated Vapour for R744

t, °C	s, kJ/kgK	h, kJ/kg	v, m³/kg	ρ, kg/m³
130	2.1564	565.82	0.0104	96.35
140	2.1845	577.27	0.0108	92.85
150	2.2116	588.60	0.0112	89.67
160	2.2379	599.85	0.0115	86.76
170	2.2634	611.03	0.0119	84.07
State Points at P = 70 bar				
Saturated Liquid at Bubble Point				
28.73	1.3128	294.92	0.0016	636.94
Saturated Vapour at Dew Point				
28.73	1.5871	377.75	0.0033	303.95
Superheated Vapour				
30	1.6335	391.78	0.0037	268.95
40	1.7614	431.09	0.0050	198.31
50	1.8308	453.12	0.0058	171.92
60	1.8846	470.78	0.0064	155.34
70	1.9305	486.30	0.0070	143.29
80	1.9714	500.54	0.0075	133.86
90	2.0088	513.94	0.0079	126.15
100	2.0436	526.75	0.0084	119.65
110	2.0764	539.13	0.0088	114.05
120	2.1075	551.20	0.0092	109.13
130	2.1371	563.02	0.0095	104.78
140	2.1657	574.67	0.0099	100.85
150	2.1932	586.17	0.0103	97.30
160	2.2198	597.57	0.0106	94.06
170	2.2457	608.89	0.0110	91.08
180	2.2708	620.14	0.0113	88.33
State Points at P = 73 bar				
Saturated Liquid at Bubble Point				
30.56	1.3738	313.91	0.0018	558.66
Saturated Vapour at Dew Point				
30.56	1.5168	357.34	0.0026	378.79
Superheated Vapour				
40	1.7330	423.62	0.0046	217.71
50	1.8101	448.14	0.0054	184.79
60	1.8673	466.90	0.0060	165.50
70	1.9152	483.07	0.0066	151.90
80	1.9573	497.75	0.0071	141.45
90	1.9957	511.48	0.0075	133.00
100	2.0312	524.54	0.0079	125.93

(Continued)

TABLE 7.32 ***(Continued)***

Properties of Superheated Vapour for R744

t, °C	s, kJ/kgK	h, kJ/kg	v, m^3/kg	ρ, kg/m^3
110	2.0644	537.13	0.0083	119.87
120	2.0960	549.36	0.0087	114.58
130	2.1260	561.33	0.0091	109.91
140	2.1549	573.10	0.0095	105.71
150	2.1826	584.71	0.0098	101.93
160	2.2095	596.20	0.0102	98.48
170	2.2355	607.60	0.0105	95.32
180	2.2608	618.93	0.0108	92.40
190	2.2854	630.21	0.0111	89.70
200	2.3094	641.45	0.0115	87.19

References and Additional Readings

Alves-Filho, O. (1996), *Heat Pump Drying of Fruit and Roots – The Influence of Heat and Mass Transfer on Dryer Characteristics*, PhD thesis, Norwegian University of Science and Technology, Trondheim.

Alves-Filho, O. (2002), Combined innovative heat pump drying technologies and new cold extrusion techniques for production of instant foods, *Drying Technology*, Vol. 20(8), pp. 1541–1557.

Alves-Filho, O. (2011), Heat pump drying engineering modeling for evolving from lab tests to commercial plants, *CD-ROM Proceedings of the Fifth International Conference on Advanced Computational Methods in Enginieering (ACOMEN 2011)*, Liège, Belgium, 14–17 November.

Alves-Filho, O. and Eikevik, T. (2008), Heat pump kinetics of Spanish cheese, *International Journal of Food Engineering*, Vol. 4(6), Article 6.

Alves-Filho, O. and Eikevik, T. (2008), Single- and multistage heat pump drying of protein, *Drying Technololgy*, Vol. 26(4), pp. 470–475.

Alves-Filho, O., Eikevik, T. and Goncharova-Alves, S.V. (2007), Single and multistage heat pump drying of protein, *CD-ROM Proceedings of the International Institute of Refrigeration "New Ventures in Freeze-Drying*," Strasbourg, France, 7–9 November.

Alves-Filho, O., Eikevik, T. and Goncharova-Alves, S. (2009), Fish protein atmospheric freeze and evaporation drying, *Proceedings of the 8th World Congress of Chemical Engineering*, Montreal, Quebec, Canada, 23–27 August, pp. 622–628.

Alves-Filho, O., Lystad, T., Eikevik, T. and Strommen, I. (2000), A new carbon dioxide heat pump dryers – An approach for better product quality, energy use and environment friendly technology, *CD-ROM Proceedings of the 12th International Drying Symposium (IDS'00)*, Noordwijkerhout, The Netherlands, 28–31 August.

Alves-Filho, O. and Mujumdar, A.S. (2002), An examination of emerging drying technologies from the energy standpoint (Plenary lecture), *Proceedings of the 1st International Conference "Energy-Saving Technologies for Drying and Hygrothermal Processing*," Moscow, Russia, 28–30 May, Vol. 1, pp. 36–51.

Alves-Filho, O. and Mujumdar, A.S. (2005), Novel drying technologies for energy savings and high product quality – Model based case studies (Plenary lecture), *Proceedings of the 2nd International Conference "Energy-Saving Technologies for Drying and Hygrothermal Processing" (DHTP-2005)*, Moscow, Russia, 11–14 October, Vol. 1, pp. 29–47.

Alves-Filho, O., Rainuzzo, J. and Aasen, I.M. (2003), Freeze-granulation and two stages heat pump drying of thraustochytrids for enrichment of rotifers, *CD-ROM Proceedings of the Second Nordic Drying Conference (NDC'03)*, Copenhagen, Denmark, 25–27 June.

Alves-Filho, O. and Roos, Y.H. (2006), Advances in multi-purpose drying operations with phase and state transitions, *Drying Technology*, Vol. 24(3), pp. 383–396.

Alves-Filho, O. and Strømmen, I. (1996), Performance and improvements in heat pump dryers, *Proceedings of the 10th International Drying Symposium (IDS'96)*, Krakow, Poland, 30 July–2 August, Vol. A, pp. 405–416.

Owen, M.S., ed., *ASHRAE Handbook of Fundamentals*. (2009), American Society of Heating, Refrigeration and Air-Conditioning Engineer, New York.

Owen, M.S., ed., *ASHRAE Handbook of HVAC Applications*. (2011), American Society of Heating, Refrigeration and Air-Conditioning Engineer, New York.

Owen, M.S., ed., *ASHRAE Handbook of HVAC Systems and Equipment*. (2012), American Society of Heating, Refrigeration and Air-Conditioning Engineer, New York.

Owen, M.S., ed., *ASHRAE Handbook of Refrigeration*. (2010), American Society of Heating, Refrigeration and Air-Conditioning Engineer, New York.

Bejan, A., Tsatsaronis, G. and Moran, M. (1996), *Thermal Design and Optimization*, Wiley, New York, 542 pp.

Colak, N. and Hepbasli, A. (2009), A review of heat pump drying. Part 2—Applications and performance assessments, *Energy Conversion and Management*, Vol. 50(9), pp. 2187–2199.

Dossat, R.J. (1981), *Principles of Refrigeration*, 2nd ed., Wiley, New York, 612 pp.

Eikevik, T., Alves-Filho, O. and Strommen, I. (2001), Potential applications for a new CO_2 heat pump dryer, *CD-ROM Proceedings of the 1st Nordic Drying Conference*, Trondheim, Norway, 27–29 June.

Fellows, P.J. (2005), *Food Processing Technology: Principles and Practice*, 2nd ed., Woodhead Publishing Limited, Cambridge, UK, 575 pp.

Gosney, W.B. (1982), *Principles of Refrigeration*, Cambridge University Press, Cambridge, UK, 666 pp.

Granryd, E., Ekroth, I., Lundqvist, P., Melinder, Å., Palm, B. and Rohlin, P. (2009), *Refrigerating Engineering*, KTH Energy Technology, Stockholm.

Heldman, D.R. and Lund, D.B., Eds. (1992), *Handbook of Food Engineering*, Marcel Dekker, New York, 756 pp.

Holman, J.P. (1988), *Thermodynamics*, 4th ed., McGraw-Hill Book Company, Singapore, 780 pp.

IEA (International Energy Agency, France). (2013), *Energy Efficiency*, Market Report, IEA, Paris.

Islam, M.R. and Mujumdar, A.S. (2004), Heat pump assisted drying, in *Guide to Industrial Drying*, A.S. Mujumdar, Ed., pp. 187–210, Colour Publication, Mumbai.

Kays, W.M. and Crawford, M.E. (1993), *Convective Heat and Mass Transfer*, 3rd ed., McGraw-Hill Book Company, San Francisco, CA, 601 pp.

Keey, R.B. (1972), *Drying – Principles and Practice*, Pergamon Press, Toronto, 358 pp.

Lock, G.S.H. (1996), *Latent Heat Transfer – An Introduction to Fundamentals*, Oxford University Press, Oxford, 288 pp.

Mujumdar, A.S. (2007), *Handbook of Industrial Drying*, Taylor & Francis, Boca Raton, FL, 1318 pp.

Mujumdar, A.S. (2004), *Guide to Industrial Drying: Principles, Equipment and New Developments*, Colour Publications Pvt. Ltd., Mumbai, India, 349 pp.

Pronyk, C., Cenkowski, S. and Muir, W.E. (2004), Drying foodstuffs with superheated steam, *Drying Technology*, Vol. 22, pp. 899–916.

Senadeera, W., Alves-Filho, O. and Eikevik, T. (2012), Influence of atmospheric sublimation and evaporation on the heat pump fluid bed drying of bovine intestines, *Drying Technology*, Vol. 30, pp. 1583–1591.

Skelland, A.H.P. (1985), *Diffusional Mass Transfer*, Krieger Publishing Company, Malabar, FL, 510 pp.

Skovrup, M.J. (2001), *CoolPack, Version 1.50*, IPU Refrigeration and Energy Technology, Lyngby, Denmark.

Stoecker, W.F. (1989), *Design of Thermal Systems*, McGraw-Hill Book Company, San Francisco, CA, 565 pp.

Strømmen, I., Eikevik, T. and Alves-Filho, O. (2003), Operational modes for heat pump drying – New technologies and production of a new generation of high quality dried fish products, *CD-ROM Proceedings of 21st IIR International Congress of Refrigeration*, Washington, DC, 17–22 August.

Strømmen, I., Eikevik, E. and Claussen, I.C. (2007), Atmospheric freeze drying with heat pumps – New possibilities in drying of biological materials, *CD-ROM Proceedings of the 5th Asia – Pacific Drying Conference*, Hong Kong, 13–15 August.

Strømmen, I. and Kramer, J. (1994), New applications of heat pumps in drying process, *Drying Technology*, Vol. 12, pp. 889–901.

Index

Note: Page numbers ending in "f" refer to figures. Page numbers ending in "t" refer to tables.